2020

The human intermediate prolactin receptor: a breast cancer proto-oncogene

Jacqueline M. Grible
Virginia Commonwealth University

THE HUMAN INTERMEDIATE PROLACTIN RECEPTOR: A BREAST CANCER PROTO-ONCOGENE

A dissertation submitted in partial fulfillment of the requirements for the degree of Doctor of Philosophy at Virginia Commonwealth University.

by

JACQUELINE M. GRIBLE

B.S., Molecular Genetics

The Ohio State University, 2015

Committee Chair: Charles V. Clevenger, M.D., Ph.D.,

Chair, Department of Pathology

Virginia Commonwealth University

Richmond, Virginia

August, 2020

Acknowledgements

First and foremost, I would like to thank my advisor Dr. Charles V. Clevenger. The dedication and passion he exhibits for his lab's research has been a true source of inspiration. His commitment to the field, as well as his support of my own scientific curiosity, is genuinely what made this dissertation possible. I am incredibly grateful for the opportunity I was given in his lab, to not only grow as a scientist, but as a person as well. I would like to thank him for being a constant source of scientific guidance, professional counsel, and sourdough recipes.

I would like to thank the members of my doctoral committee: Dr. J. Chuck Harrell, Dr. Jolene Windle, Dr. Paula Bos, and Dr. Senthil Radhakrishnan. Their guidance, support, and critical analyses of my work have helped shaped my academic career to gain the most from this experience as possible. I would like to thank them for their open-door policies as I made my way through the oftentimes choppy waters of graduate school.

To my program advisor, Dr. Rita Shiang, my first VCU mentor, Dr. Mike Grotewiel, and the Graduate Programs Coordinator Extraordinaire, Harold Greenwald, thank you for your unceasing guidance throughout the doctoral training process. To my labmates, current and former (Alicia, Justin, Shannon, Madhavi, Shawn, and Fiona), thank you for fostering such a supportive environment. Most especially, Alicia Woock, thank you for being the greatest lab wife I could have ever hope for. As a colleague, a friend, and personal baker, thank you for your honesty and encouragement, and for showing me more fun things to do in Richmond than I would have been able to discover on my own.

To my cohort family, Dr. Dana Lapato, Dr. Mike Kammerman, Dr. Naren Gajenthra

Kumar, and Tanya Puccio, there are no greater scientists and friends with whom I would have wanted to share this experience. You have been my favorite people with whom to both celebrate the little scientific victories and commiserate the scientific setbacks.

To my parents, Linda and Andy Grible, I am incredibly and indefinably lucky to have been born your daughter. I have never once questioned your pride in me, and I will always be grateful of the sacrifices you made in raising your children. To my siblings, especially my sister Kate Wei and her family, for quite literally opening up her home to me when I was in most need of a place to rest. To my closest friends, Dr. Casey Mazzotti, Nettie Yanko, and Clare Casey, for always providing an ear to listen, a shoulder to cry on, and for over a decade's worth of wonderful memories and embarrassing stories.

And finally, to my fiancé, Daniel O'Connell. You have been at my side, unwavering, for every win and every loss for the last seven years, and I can confidently assert that I would not have been able to reach this finish line without you. Thank you for always being there to listen, for the home-cooked meals, and for consistently putting my needs far ahead of your own. When I count my blessings, I count you twice.

TABLE OF CONTENTS

LIST OF TABLES

LIST OF FIGURES

Abstract

THE HUMAN INTERMEDIATE PROLACTIN RECEPTOR:
A BREAST CANCER PROTO-ONCOGENE

By Jacqueline M. Grible

A dissertation submitted in partial fulfillment of the requirements for the degree of Doctor of Philosophy at Virginia Commonwealth University.

Virginia Commonwealth University, 2020.

Committee Chair: Charles V. Clevenger, M.D., Ph.D.,
Chair, Department of Pathology

Epidemiological, cellular, and genetic analyses indicate the hormone prolactin (PRL) and its cognate receptor in humans (hPRLr) are significantly involved in breast cancer pathogenesis. Recent evidence demonstrated that a truncated mouse PRLr (mPRLrT) is oncogenic when expressed alongside its canonical long form counterpart (mPRLrL). mPRLrT shares significant sequence homology with a naturally-occurring and widely-expressed hPRLr splice variant, the intermediate hPRLr (hPRLrI). To confirm the oncogenic potential of hPRLrI, isoform-specific hPRLrI knock-down (KD) was performed in breast cancer cell line MCF7. hPRLrI KD resulted in a significant decrease in proliferation, migration, and anchorage-independent growth. Next, given the homology between mPRLrT and hPRLrI, we hypothesized hPRLrI may similarly induce transformation, when expressed alongside wild-type long hPRLr (hPRLrL). Like the mPRLrT, hPRLrI co-expression with hPRLrL in the immortalized but minimally transformed human breast cell line MCF10AT resulted in a significant increase in proliferation, migration, and anchorage-independent growth. These results were

not observed following overexpression of either isoform alone, demonstrating that hPRLrL+I co-expression is necessary to induce transformation of mammary epithelia. To test our hypothesis in vivo, we established MCF10AT xenografts using female NSG mice. Following intraductal injection, we observed rapid tumor growth in the hPRLrL+I co-expression cohort, significantly over that of the cohorts harboring either isoform alone. To determine mechanisms of transformation, we examined both differential protein stability and altered signaling events. In analyzing receptor degradation, a cycloheximide assay revealed hPRLrL stability is increased when heterodimerized with hPRLrI. hPRLrL turnover has been reported to be impaired in human breast cancer, indicating this phenomenon may be involved in the observed hPRLrI-mediated transformation. In regards to differential signaling, we examined the Jak2/Stat5a pathway. Jak2 is a promiscuous kinase whose significant oncogenic actions are well-characterized, while Stat5a is a transcription factor whose activities are critical in attenuating the oncogenicity of Jak2. Following PRL stimulation, it was observed that hPRLrL+I co-expression induced approximately two-fold greater Jak2-Y1007/1008 phosphorylation (pJak2), compared to that induced by hPRLrL expression alone. A significant elevation in p-Erk1/2 and p-Mek1/2 were also observed following stimulation of hPRLrL+I heterodimers. Further, it was observed that hPRLrL+I co-expression induced ten-fold less Stat5a-Y694 phosphorylation (pY-Stat5a) than hPRLrL expression alone. These data indicate unchecked pJak2 activity may also be a contributing mechanism in the observed transformation. We last assessed the clinical relevance of hPRLrI in breast cancer, using both a breast cancer tissue microarray (TMA) to examine hPRLrI protein expression, as well as The Cancer Genome Atlas (TCGA) data to investigate relevance at the transcript level. In both approaches, a significant association was found between hPRLrI expression and greater disease malignancy, with significant enrichment in KRAS activity. Overall,

these results demonstrate that hPRLrI, alongside hPRLrL, contributes to mammary transformation.

This dissertation is dedicated in multiplicity:

to my family, my friends, and my fiancé,

for their unrelenting support and feigned comprehension of what I do in the lab.

Data obtained during the course of these studies and presented in Chapters 6 through 8 are incorporated into the following publication:

Grible JM, Zot P, Olex AL, Hedrick SE, Harrell JC, Woock AE, Idowu MO, and Clevenger CV. "The human intermediate prolactin receptor is a mammary proto-oncogene". *Manuscript in submission.*

Data presented in Chapters 5 through 8 is incorporated into the following provisional patent filing:

Clevenger CV, **Grible JM** (2019). "The human intermediate prolactin receptor as a mammary oncogene", VCU Invention No. CLE-19-013 (2019-009).

The most exciting phrase to hear in science, the one that heralds new discoveries, is not, 'Eureka!' but, 'That's funny...'

Isaac Asimov

CHAPTER 1

GLOBAL INTRODUCTION TO BREAST CANCER

1.1 Statistics

Breast cancer is the most commonly diagnosed cancer in women in the United States, and the second most deadly. In 2020, an estimated 276,480 cases of invasive carcinoma are predicted to be diagnosed in women and 2,620 in men[8]. Further, it is estimated that 42,170 women and 500 men will succumb to the disease in 2020[8]. Inasmuch, 1 in 8 women and 1 in 1000 men will be diagnosed with breast cancer at some point of her or his lifetime, respectively. Further, it is estimated that 1 in 39 women will die from complications of breast cancer, namely that of distant metastases[8].

Breast cancer incidence rates increase with age, and both disease occurrence and outcome vary significantly between different ethnic populations and races. Breast cancer is most commonly diagnosed in women 50 years and older, with a plateau observed around 55-60 years of age[8]. Breast cancer is most common amongst non-Hispanic white women, while breast cancer mortality is highest in African-American women. Critically, advances in screening and early detection have significantly improved survival outcomes of breast cancer patients. While the incidence rates of breast cancer have increased slightly (0.3%) from 2007 to 2016, overall mortality has decreased significantly. Current survival statistics indicate that the 5-year average survival rate for women with invasive breast cancer is 91%, and the 10-year average survival rate is 84%[8]. Due to the aforementioned advances in early detection, 62% of all breast cancers are diagnosed prior to invasion (i.e. during the localized stage,

wherein the tumor is confined to the breast tissue), and it is during this early stage that 5-year survival rates are 99% on average[8].

1.2 Signs, symptoms, and screening recommendations

During the early stages of disease progression, when the tumor would be most easily treated, it is critical for an individual to be aware of changes to the breast (e.g. discovering a new mass, breast swelling or pain, skin dimpling, nipple discharge, swollen lymph nodes) in order to identify early warning signs[8]. Other symptoms of possible malignant and/or pre-malignant disease include a general change in the size/shape/appearance of a breast, an abnormal rash-type of skin lesion over the aerola or breast skin, or abnormal discharge from the nipple[8]. Monthly self-examinations are critical, as are adhering to Centers for Disease Control and Prevention (CDC) and American Cancer Society (ACS) guidelines for preemptive screening. Current recommendations stipulate that all women of average risk (e.g. those in the general population, with none of the risk factors enumerated in Section 1.3) should start receiving biennial mammograms at the age of 50[8]. Women who are higher than average risk (e.g. those who have a first degree relative with breast cancer) are recommended to start receiving annual mammograms in their 40s, or potentially earlier. If any of the aforementioned signs and symptoms are found, an individual is encouraged to see a physician for evaluation.

1.3 Risk factors

The two greatest breast cancer risk factors are 1) being born genetically female, and 2) being of advanced age[8]. Additional significant contributing factors include having a prior breast cancer diagnosis, having a family history of malignant breast disease, and carrying a pathogenic BRCA allele[8]. However, there are also certain

lifestyle-driven factors that are modifiable, which if addressed early enough, can lower an individual's risk for developing the disease. For example, obesity in premenopausal women has consistently been shown to be a significant risk factor in breast cancer development, with incidence rates increasing regardless of subtype and hormone receptor status[17,180,201,297]. Furthermore, adherence to a "Western diet" (i.e. intake of high levels of red and processed meat, refined grains, high-sugar, etc.) has been shown to significantly increase ones risk for breast cancer, while a higher intake of fruits and vegetables can decrease breast cancer risk[92,93,265]. Additionally, numerous studies have indicated that exercise and moderate physical activity may help to mitigate an individual's risk[35,165,203]. Other risk factors include smoking, heavy drinking, birth control use, though admittedly the effect size of these factors is relatively small[64]. Pregnancy, in addition, carries a well-known yet poorly understood dichotomous effect on a woman's risk for breast cancer, as is discussed below.

While long-term there is a parity-protective effect against breast cancer, in the short term, pregnancy is significantly associated with malignancy. This specific subset of breast cancer is termed pregnancy-associated breast cancer (PABC). PABC represents a transient increased risk for breast cancer during pregnancy and the subsequent 5-15 years after birth, compared to women who are nulliparous[6,164]. PABC becomes a greater concern as maternal age increases[164]. Uniparous and multiparous women who are 25 years old and younger have a minimal increase in breast cancer risk, while this risk linearly increase with age[164]. The more children a woman has does not appear to increase her risk beyond that which is observed with uniparity[164]. However, the effect of pregnancy on breast cancer risk is dichotomous. There is a well-document long-term protective effect for women who have given birth, especially if conception happens while a woman is in her early 20s[143]. While these two seemingly opposed effects of pregnancy on breast cancer risk present a unique dichotomy

for investigators, one relatively simple explanation may lie in the biological significance of prolactin (PRL) on breast cancer pathogenesis. PRL levels increase up to 20-fold above baseline during pregnancy and remain high after birth for an extended period of time. After this spike in PRL levels, subsequent baseline PRL serum concentrations drop below pre-conception levels, following the trend of the association observed between pregnancy and breast cancer risk.

1.4 Diagnosis

If and/or when a suspicious area of the breast is uncovered, either during mammographic or patient self-examination, additional procedures will be performed to determine if the area of interest is malignant or not. This will typically involve a breast biopsy, which provides critical information for diagnosing the stage and subtype of the malignancy, which will ultimately be used to inform treatment options.

1.4.1 Staging

Breast cancers are staged by the size and invasiveness of the primary tumor, presence of infiltrate in the local (e.g. mammary and/or axillary) nodes, and the presence of distant (e.g. lungs, bones, liver, etc.) metastases. When a particular breast cancer is pathologically staged, it is given a score within each of the 3 aforementioned categories: tumor (T), node (N), and metastasis (M). Details regarding the specifics on each of these staging categories can be found in Tables 1 and 2.

1.4.2 Breast cancer histological subtypes

The histological subtype of a patient's tumor is based on the size, shape, and arrangement of the breast cancer cells. The majority ($\geq$75%) of breast cancers present as invasive ductal carcinoma (IDC)[8]. The second-most common histological sub-

Table 1. Breast cancer TNM staging

Stage	**Tumor/Specimen characteristic**
T0	No evidence of tumor in the breast
T1	Primary tumor is less than 20mm wide
T2	Primary tumor is between 20mm and 50 mm wide
T3	Primary tumor is greater than 50 mm wide
T4	Primary tumor has infiltrated locally into either the chest wall, skin, or both
N0	No lymph node infiltration
N1	Infiltration is observed in 1-3 axillary lymph nodes and/or the internal mammary lymph nodes
N2	Infiltration is observed in 4-9 axillary lymph nodes and/or the internal mammary lymph nodes
N3	Infiltration is observed in greater than 10 axillary lymph nodes, or has spread to the lymph nodes beneath the clavicle and/or collarbone
M0	No distant metastasis
M1	Distant metastasis

Table 2. Breast cancer pathologic staging

Stage	Anatomic stage/prognostic group
I	T0-T1, N0-N1mi, M0
II	T0-T3, N0-N1, M0
III	T0-T4, N0-N2, M0
IV	Any T, Any N, M1

type is invasive lobular carcinoma (ILC), which represent approximately 15% of invasive breast cancers[8]. Additional histological classifications include mucinous, tubular, cribriform, and papillary carcinoma, however cases of these histologies are rare. Breast cancer histology can be further subgrouped by tumor grade, whereby a tumor is either well-differentiated (grade I), somewhat differentiated (grade II), or poorly differentiated (grade III), and an increase in tumor grade is correlated positively with worse overall prognosis. Once a patient's tumor has become invasive, clinicians will examine certain molecular features of the tumor, namely its hormone receptor (HR) status, which specifically examines the protein and/or copy number status of the estrogen receptor (ER), progesterone receptor (PR), and the human epidermal growth factor receptor 2 (Her2). These markers serve as guides for treatment options and prognostic factors.

1.4.3 Breast cancer molecular subtypes

In addition to the histological parsing of breast cancers, breast tumors have also been shown to stratify by differential gene expression patterns[60]. This classification system for breast tumors was first established using microarrays and hierarchical clustering analytics, which resulted in the establishment of five intrinsic molecular

subtypes based on gene expression profiling: Luminal A, Luminal B, Her2-enriched, Basal-like, and Claudin-low[60,217]. While performing a microarray on every patient tumor is not currently feasible, investigators have been able to "condense" these gene expression profiles into a 50-gene signature, which has a comparable level of effectiveness as a full microarray at differentiating intrinsic subtype. This panel has been termed the PAM50 system.

Generally speaking, there is an association with these gene expression patterns and HR status, as is discussed below. An additional gene that plays a significantly contribution to the diagnosing of breast cancer molecular subtypes is that of KI67, which is a commonly-used marker for active proliferation. This subtype stratification is critical when discussing the clinical management of a patient's respective tumor/disease, as the intrinsic molecular subtype of a patient's tumor is a major, significant determinant in response to treatment and survival outcomes.

1.4.3.1 Luminal A

Luminal A represents the most commonly-diagnosed molecular subtype of breast cancer. These tumors are typically positive for both ER and PR (ER/PR+), while lacking Her2 (Her2-) and expressing low KI67 status[217]. Cases of luminal A tumors are less aggressive and easier to successfully treat in the short-term, typically being smaller in size, slower growing, and less likely to immediately metastasize. Luminal A tumors are also typically of a lower grade, and have the best overall 5-year prognosis with the lowest risk for short-term distant metastasis[8,284]. However, luminal breast cancers are at a greater risk for long-term distant relapse than the other intrinsic subtypes[8,284].

1.4.3.2 Luminal B

Luminal B breast cancers present as more aggressive tumors than those of the luminal A subtype, with worse baseline distant RFS at 5 and 10 years[228]. While these tumors are typically ER+ and may or may not express Her2, they oftentimes lack PR (PR-), with significant KI67 status[217]. Luminal B breast cancers are generally of higher grade than luminal A, and have a greater risk of distant-relapse within the first 5 years than luminal A breast cancers[8,227,284].

1.4.3.3 Her2-enriched

Her2-enriched breast cancers are defined by their significant over-expression of the Her2 oncogene, which is the driving factor in this particular subtype. These cancers have a worse prognosis than the luminal subtype, however they are often able to be successfully treated with targeted treatment aiming at Her2 (e.g. Herceptin)[8].

1.4.3.4 Basal-like

Basal-like breast cancers tend to present as triple-negative for the three aforementioned HRs (e.g. are ER/PR/Her2-, triple-negative breast cancer, TNBC), high KI67 expression, and express genes typically associated with myoepithelial/basal-epithelial cells[217]. While each subtype is molecularly distinguishable from one another, basal-like breast cancers are the most unique from each other group, and hold the most intrinsic diversity[160]. Basal-like breast cancers offer the worst short-term overall prognosis, with almost 40% of patients relapsing within 5 years of diagnosis[104]. These cancers currently lack effective therapeutic targets, contributing to the overall short-term poor outcome. However, long-term outcome survival outcome of basal-like breast cancers are significantly better, with 10-year recurrence-free survival

rates being higher than that of luminal breast cancers[227,284].

1.4.3.5 Claudin-low

An additional molecular subtype that typically presents as TNBC, although it accounts for only a minority (25-39%) of TNBC clinical cases, is that of claudin-low[226]. Claudin-low breast cancers are characterized by their relatively low expression of genes associated with tight junctions and cell-cell adhesions, including claudins, occludin, and e-cadherin[129]. This subtype characteristically is enriched for genes associated with epithelial-to-mesenchymal transition (EMT), immune response, interferon gamma (INFγ) activation, and breast stem cell signature gene expression patterns[226]. Concerning the prognosis of claudin-low tumors, these tend to fare worse than luminal A breast cancers, but have both a similar relapse-free survival (RFS) and overall survival (OS) curve to the other intrinsic subtypes[226].

1.5 Treatment

Treatment for breast cancer typically begins with tumor resection, along with some degree of removal of the surrounding normal tissue (e.g. breast-conserving therapy/lumpectomy, wherein the majority of the normal tissue remains, or mastectomy, where the entire breast is removed). The selection of which surgical resection occurs is dependent on the intrinsic characteristics of the tumor as well as patient wishes. For example, one tumor characteristic that can influence treatment options is the presence/absence of infiltration into the axillary lymph nodes, which is evaluated at the time of surgery. Additional tumor characteristics that play a role in treatment decisions are cancer stage, molecular/histologic subtype, and/or specific genetic aberrations (e.g. BRCA status, PI3K mutations, etc.), as described above.

As breast cancer represents a heterogenous group of diseases, breast tumors vary

significantly in their response to treatment. Following the advent of molecular subtyping, investigators and clinicians alike have worked diligently to ascertain those mutations and characteristics of each individual class of tumors, in order to facilitate treatment. The rationale here being that specific mutations will respond differentially to specific therapies, and therefore should only be administered to those who are predicted to have the greatest positive response. Two of the most well-characterized targeted therapies are Trastuzumab (brand name Herceptin), the anti-Her2 monoclonal antibody (mAb), and antiestrogens, such as aromatase inhibitors (e.g. Letrozole and Anastrozole) and ER inhibitors (e.g. Tamoxifen and Fulvestrant). Additional targeted therapies being utilized today include CDK4 inhibitors (e.g. Palbociclib, Ribociclib) and PI3K pathway inhibitors (e.g. Everolimus, Alpelisib)[20,85,132,142,276].

1.5.1 Breast cancer models

In order to study breast cancer in a high-throughput manner, an array of models have been developed in the field that recapitulate breast cancer biology and development. These models encompass both *in vitro* breast cell lines and *in vivo* xenograft/transgenic rodent models. For the purposes of this dissertation, we limited the scope of our *in vitro* and *in vivo* approach to include only luminal disease models (MCF7 and T47D), normal mammary gland (MCF10A), or partially-transformed basal mammary epithelia (MCF10AT).

MCF7 and T47D cells are both well-established models of ER+, luminal disease. While most studies have classified both of these cell lines as luminal A, evidence exists that one or both of these cell lines may in fact be luminal B[130]. Regardless, both cell lines are ER+ and hormone-responsive, making them excellent models for HR+ disease. Furthermore, as will be discussed in detail in Chapter 2, both of these cell lines express both the long and intermediate forms of the human prolactin

receptor, and are PRL-responsive as well. For xenograft purposes, both MCF7 and T47D xenografts require exogenous estrogen (typically in the form of a subcutaneous estrogen pellet) for primary tumor formation[130].

MCF10A cells are, for all intents and purposes, a normal mammary cell line[261]. MCF10A cells were originally derived from human fibrocystic mammary tissue, and achieved immortality following extended cultivation[261]. This cell line, being karyotypically normal, will form neither colonies in soft agar, nor tumors *in vivo*, and require at least two significant oncogenic "hits" for full transformation to be realized[81]. Within that notion, the partially-transformed MCF10AT cell line harbors oncogenic H-ras (G12V), and when xenografted into immunocompromised mice, have an invasive carcinoma rate of approximately 25%, and do not metastasize[81].

1.6 Limitations in our understanding of early transforming events

While advances in other cancers, such as colon cancer, have developed well-defined markers of early transforming events, no such markers exist for typical vs atypical breast hyperplasia. For example, women diagnosed with ductal carcinoma *in situ* (DCIS; stage 0 breast cancer) are not guaranteed to develop invasive carcinoma, and some women with DCIS do not require therapeutic intervention[202]. However, treatment is typically recommended considering the unknown outcome. While currently clinicians are able to stratify DCIS by disease grade, with low grade DCIS progressing to invasive disease at a lower frequency than that of high grade DCIS if left untreated, we are still very limited in our understanding of which lesions will progress to malignancy, and as such we lack clinically-actionable markers to facilitate our understanding of this progression[202]. Furthermore, while the risk factors enumerated in Section 1.3 provide a framework to understand which patients should begin screening at an earlier age, clinical predictive modeling still lacks a high degree of cer-

tainty regarding patient outcomes. However, one area of study that continues to give promise in the understanding of breast cancer etiology is that of PRL and its cognate receptor (hPRLr). As will be discussed in the following chapter, cellular, genetic, and epidemiologic studies have strongly implicated this hormone and its receptor in the pathogenesis of human breast cancer.

CHAPTER 2

PROLACTIN BIOLOGY AND ROLE IN NORMAL AND MALIGNANT BREAST

2.1 Prolactin

2.1.1 History

Changes to the anterior pituitary gland during pregnancy were first observed in the early 1900s. In 1928, a French group identified a factor capable of inducing lactogenesis in rabbits, and five years later, an American group made similar observations and named the factor "prolactin" (PRL)[237,262]. This factor, it was noted, was also able to stimulate growth of pigeon crop sac[237]. In searching for the hormone in humans, researchers were confounded by the significant overlap in functionality between PRL and growth hormone (GH), making efforts to disentangle the actions/expression of one from the other difficult. Finally, in 1971, human PRL was identified, isolated, and purified from human pituitary glands[140,172]. To date, every known mammal has been observed to express PRL. Further, while the primary role of the hormone is its namesake, over 300 functions for PRL are now known and appreciated[36].

2.1.2 Gene and protein structure

PRL is a member of the group I helix bundle protein hormone family, which includes other such peptide hormones as GH and placental lactogen (PL). It is believed that these genes are each derived from an ancestral duplication event, accounting for their significant degree of sequence homology[131,206]. The gene encoding PRL (in

humans, is Ensembl ID ENST00000306482.2) is located on the short arm of chromosome 6, at locus 6p22.3 on the minus strand. The gene is comprised of 5 exons and 4 introns, and is approximately 10 kilobases (kb) in length[275]. The open reading frame (ORF) of the human PRL gene is 681 nucleotides (nt) long[275]. From this DNA sequence, an immature protein product ("pre-hormone") of 227 amino acids (aa) is formed, containing a 28 residue signal peptide[72]. The signal peptide is cleaved during post-translational modification, and the resulting mature human PRL protein is comprised of 199 aa, and is approximately 23kDa in molecular mass.

Despite PRL being expressed in every mammal known to date, the PRL gene and peptide sequences are not entirely conserved between species. While primate PRL is up to 97% conserved amongst species, conservation between primates and rodents is as low as 56%[71,159,255,257]. Studies of the PRL protein secondary structure indicate that 50% of the peptide chain is organized as alpha-helices, and the remainder of the sequence forms loops[31]. Studies of the tertiary structure of PRL have concluded the three-dimensional structure of PRL is comprised of four antiparallel long alpha-helices[1,82,111,148].

PRL expression is regulated by two distinct and independent promoters, a proximal promoter and a distal promoter[29,30]. The proximal promoter region, encompassing an area of approximately 5 kb upstream of the transcription start site, regulates pituitary PRL expression. The distal promoter, lying further upstream than the proximal promoter, is approximately 2 kb in length and regulates non-pituitary expression of PRL. Additionally, a region approximately 2 kb upstream of the transcription start site contains an estrogen response element (ERE), which facilitates estrogen-driven prolactin transcript expression[3].

2.1.3 Pituitary PRL synthesis and autocrine/paracrine regulation

Prolactin is primarily made in the anterior pituitary gland by a specialized type of cell known as a lactotroph (or mammotroph)[16,127]. Lactotrophs are regulated by both positive and negative stimuli to synthesize and secrete PRL. Prolactin-releasing factors include thyrotropic-releasing hormone, estrogen, oxytocin, and neurotensin, while prolactin-inhibiting factors include dopamine (DA), somatostatin, and γ-aminobutyric acid[100,256]. PRL is also able to regulate its own release through what is known as a "short loop" negative feedback system, and it is this activity that is mainly responsible for PRL homeostasis maintenance[25]. In this manner, elevated PRL concentrations stimulate DA release, which in turn inhibits PRL by acting through the D_2 receptor (D_2R) present on lactotrophs[25]. Normal levels of serum PRL in a non-lactating female are typically between 10-20ng/mL, while that of a pregnant woman can range upwards of 200-400ng/mL[57].

2.1.4 Extrapituitary PRL

As stated above, PRL is also synthesized and secreted outside of the pituitary gland. While PRL has been found to be secreted by the hypothalamus, placenta, and uterus, among other tissues, the extrapituitary site of PRL synthesis most critical for this dissertation is that from both normal and malignant breast tissue[12,63,105,125]. The discovery of autocrine/paracrine PRL in the breast was first published on in 1995 by Clevenger *et al.*[63]. Polymerase chain reaction (PCR) of the breast cancer cell lines MDA-MB-231 and MCF7 revealed PRL expressed at the transcript level, and subsequent immunoblot (IB) and bioassay confirmed expression and activity at the protein level. Mammary-derived PRL was subsequently confirmed using both normal and malignant patient samples[63].

2.2 Prolactin receptor

2.2.1 Gene structure and transcript regulation

The hPRLr gene is located on the short arm of chromosome 5 at locus 5p13.2[13]. The full gene length is over 100kb, and is comprised of 11 alternatively-spliced exons. From the perspective of transcriptional regulation, a low concentration of PRL is known to stimulate expression of its cognate receptor[147,190]. Conversely, studies have shown that high *in vivo* PRL concentrations actually down-regulate receptor expression[83]. Furthermore, little is understood of what drives the differential splicing of this gene. hPRLr is under transcriptional control of three unique and independent tissue-specific promoters, similar to what is observed with PRL. Termed promoter I, II, and III, each promoter controls PRLr expression in a specific tissue. Promoter I drives expression in gonadal tissue, promoter II drives expression in the liver, and promoter III is utilized for PRLr expression in all other tissues where the protein is expressed, including the mammary gland[107,136].

2.2.2 Protein structure

PRLr is a member of the type I cytokine receptor superfamily, and functions as a dimer[23,24,149]. Type I cytokine receptors are single-pass transmembrane receptors that contain a conserved "WSXWS" (Tryptophan-Serine-X-Tryptophan-Serine) motif within the extracellular domain (ECD)[23,24,76,209]. Other members of this receptor superfamily include granulocyte-macrophage colony-stimulating factor receptor (GM-CSFr), interleukin receptors (ILR), erythropoietin receptor(EPOR), and growth hormone receptor (GHR)[291]. In addition to certain shared structural motifs, members of this family share an additional common aspect in that they lack any intrinsic kinase activity. Meaning, all downstream signaling events that come about following ligand

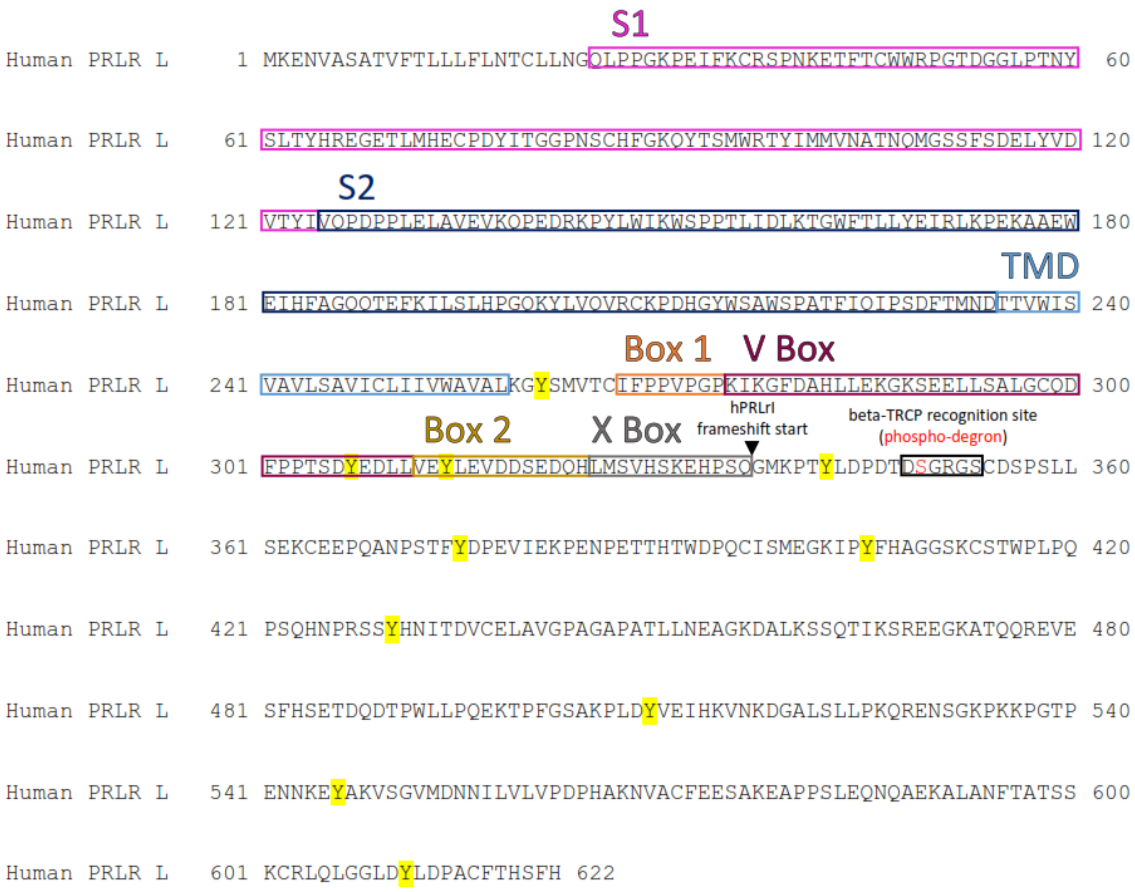

Fig. 1. Annotated hPRLr amino acid sequence. The full-length hPRLr peptide sequence with subdomains with the ECD (S1, S2), TMD, and ICD (Box 1, V Box, Box 2, and X Box) annotated. The differential splice start site that generates the hPRLrI isoform is denoted, as is the β-TrCP recognition sequence and the S349 phosphodegron. All intracellular tyrosine residues are highlighted in yellow.

interaction is through the activity of associating kinases and signaling effectors.

Regarding the molecular structure of the hPRLr, there are three distinct domains: the ECD, transmembrane domain (TMD), and intracellular domain (ICD). Both the ECD and ICD are broken down further into conserved subdomains as depicted in Figure 1 and discussed in detail below.

The hPRLr-ECD is divided into two fibronectin-like subdomains, termed S1 and S2, each of which is approximately 100 aa[24,82,258]. Each of these subdomains is com-

prised of 7 β-strands each[24]. The more N-terminal, membrane distal S1 subdomain contains four highly conserved cysteines which are critical for the formation of disulfide bonds, and are known to be necessary for ligand interaction[244]. This region also contains two tryptophans (W72 and W139, respectively) which are similarly involved in PRL/hPRLr binding[266].The hPRLr/ligand interaction occurs in a sequential manner at a 2:1 receptor:ligand ratio. PRL contains two hPRLr binding sites: a high affinity site (site 1) and a low affinity site (site 2)[74,75,116]. hPRLr first binds PRL at the high affinity site, which then allows for interaction with the lower affinity site 2 (Figure 2A). At high ligand concentrations, however, PRL supersaturates hPRLr forming a 2:2 receptor:ligand complex, antagonizing downstream signal transduction (Figure 2B). The membrane-proximal S2 subdomain contains the highly conserved WSXWS motif, which is known to be essential for proper protein folding, and, by extension, is known to also be a critical component of receptor-ligand interaction[21,76,258]. Work from our lab has also shown that the hPRLr-ECD strengthens hPRLr dimerization, with later studies confirming it is specifically the S2 domain that is critical for this function[106,182].

The hPRLr-TMD is the membrane-spanning link between the hPRL ECD and ICD. To date, the most well-characterized activity of the TMD is in its activity in the dimerization of hPRLr, which has reported on for many type I cytokine receptors[45,70,106,195]. As a full crystal structure of the hPRLr remains elusive, understanding how extracellular ligand interaction confers intracellular signaling is yet to be fully understood. However, studies with the GHR are able to provide a possible bridge in our knowledge gap. In 2014, studies with GHR provided a possible mechanism, whereby ligand stimulation results in a conformational change of the GHR-TMD dimers, subsequently altering the GHR-ICD conformation and bringing such signaling intermediaries as Jak2 within close enough proximity to dimerize and activate[43].

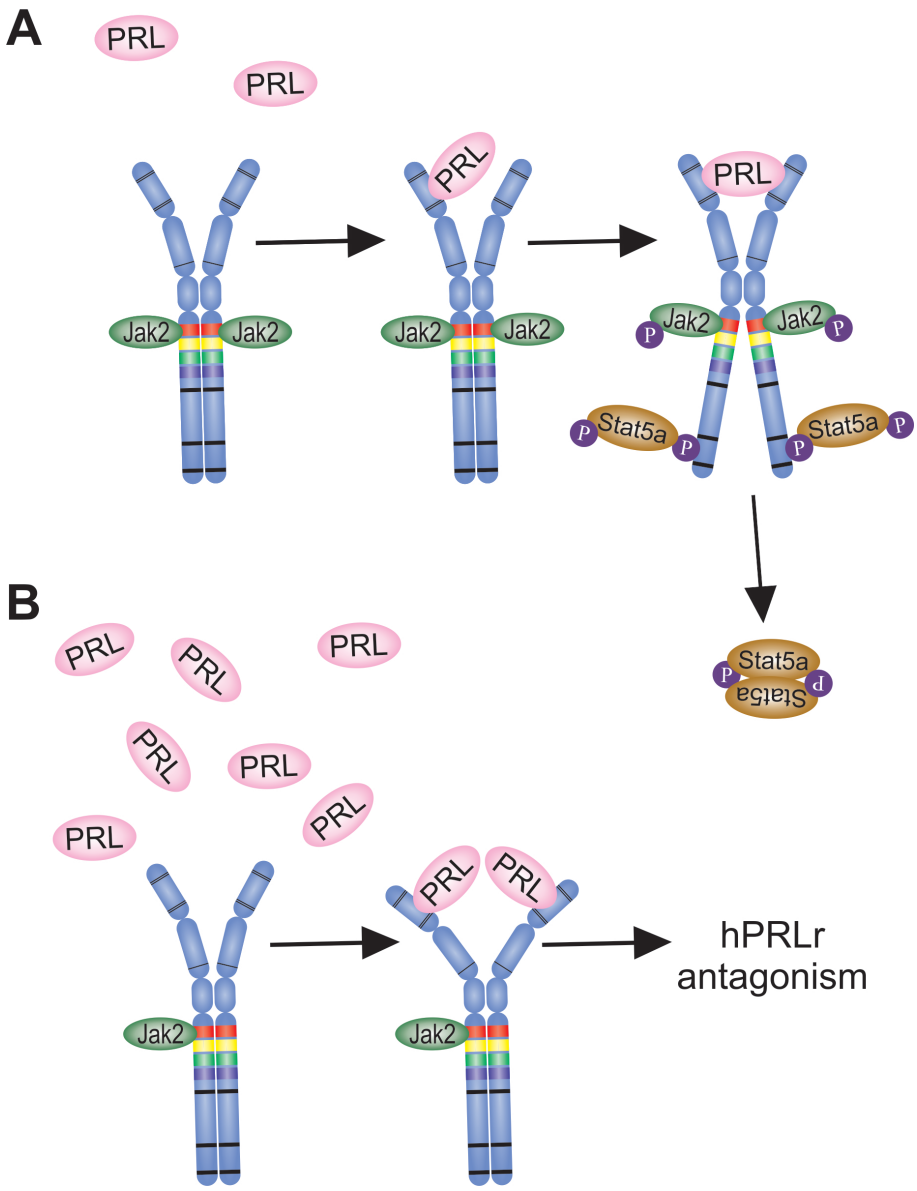

Fig. 2. PRL binding to hPRLr schematic. **A**. Pre-dimerized hPRLr binds ligand in a sequential manner, forming a 2:1 complex, resulting in downstream signal transduction. **B**. High PRL concentrations supersaturate the predimerized receptor, inhibiting signaling activity.

However, there is not complete cross-over between GHR and PRLr biology, and more research is necessary to understand the biological activities of the hPRLr-TMD.

Lastly, the hPRLr-ICD is composed of four subdomains (Box 1, V box, Box 2, and X box) and an intrinsically-disordered C-terminal tail (Figure 1)[126]. Box 1 and Box 2 are relatively conserved across mammalian species, while the V box and X box are less so[199]. The membrane-proximal Box 1 is a proline-rich region of the hPRLr-ICD that contains sites necessary for Jak2-hPRLr interaction[47,79,167,218]. The V box, V here standing for "variable", is the region between Box 1 and Box 2. Little is known of the function, if any, of the V box. Box 2 is conserved less than Box 1 across the cytokine receptors, and contains primarily hydrophobic, acidic residues. Similar to the V box, little is known regarding the function of Box 2, despite attempts using serial domain truncation deletions[56]. However, it has been speculated that Box 2 may assist with Jak2 binding[167]. The X box, X here standing for "extended", contains the residue necessary for cyclophilin A (CypA) binding to hPRLr, proline 334 (P334), which is a prolyl isomerase critical for the signaling capabilities of hPRLr and is discussed in Section 2.3[64,306]. Lastly, while both the hPRLr-ECD and TMD are considered critical in receptor dimerization, work from our lab has shown that hPRLr dimeric interaction is further strengthened by the ICD[106].

As stated above, the C-terminal cytoplasmic portion of the hPRLr-ICD is intrinsically disordered, and a full understanding of the structure/function of the globular C-terminal tail is yet to occur. However, characterization of specific residues within this region have provided critical insight into the signaling capabilities and regulation of hPRLr. First, immediately following the X box is a β-TrCP (an E3 ubiquitin ligase) recognition sequence (D348-S353; Figure 1). Within this recognition sequence lies the crucial phosphodegron residue S349 (discussed in Section 2.4)[174,175,220,267,268,285]. The C-terminal tail also contains 10 tyrosine (Y) residues, each of which may be phospho-

rylated and contribute to hPRLr actions (Figure 1). Two of these tyrosines, Y509 and Y587, have been implicated in Stat5a docking onto the receptor[192,218].

2.2.3 Dimerization of hPRLr

For decades, it was generally accepted that dimerization of hPRLr occurred in a ligand-dependent manner. It was believed that binding of hPRLr to PRL site 1 functioned to recruit the second member of the hPRLr dimer to PRL site 2, all happening in a step-wise fashion[73,110,258]. However, it was later observed that ligand-independent dimerization was able to occur with GHR and EPOR, both of whom share significant homology with hPRLr[44,109,123,183,243,270]. However, predimerization alone was not shown to be sufficient for signaling[44,70,109,162].

This trend of predimerized cytokine receptor was found to also hold true with the hPRLr, as work from our lab confirmed[106]. Immunoprecipitation (IP) and deletion studies of differentially epitope-tagged hPRLr isoforms in T47D cells further corroborated that the hPRLr-TMD is necessary for dimerization, however the hPRLr-ECD and hPRLr-ICD likely contribute strength to this interaction[106]. While the focus of the studies by Gadd *et al.* concerned the ligand-independent dimerization of hPRLr, one additional critical piece of information was established by this study: hPRLr isoforms are capable of heterodimerizing endogenously, assuming that the TMD is intact.

2.2.4 Isoforms

There is a growing body of appreciation for the unique biology of differentially-spliced isoforms in the human genome, particularly in the context of cancer[281]. There currently are 7-10 generally accepted and annotated forms of the hPRLr, all of which are formed through either differential splicing events or proteolysis. While consider-

able work has been done in characterizing the full-length form of the hPRLr transcript, there is minimal understanding regarding the biology of the shorter hPRLr isoforms. Furthermore, no studies to date have examined or provided a mechanism of action for the differential splicing events that drive unique hPRLr isoform generation. What is known, however, is discussed below.

First cloned in 1989, the hPRLrL ORF is 1869 basepairs (bps) in length, comprised of 10 exons, and the resultant protein is 622 amino acids long. When run on a sodium dodecyl sulfate polyacrylamide gel electrophoresis (SDS-PAGE) gel for IB, the full length receptor runs at 90kDa, and scatchard analyses have indicated the hPRLrL ligand affinity (dissociation constant, K_D) is $1.3x10^{-9}M$[63]. Given that the hPRLrL is the full-length form of the receptor, it retains all possible signaling capabilities intrinsic to the ICD, and the full length receptor is capable of stimulating a wide array of downstream signal transduction events. These pathways include, but by no means are limited to: Jak2/Stat5, PI3K, Src, Ras, and MAPK[64]. To date, this hPRLr isoform has been found in up to 98% of human breast cancers at the transcript level, highlighting the biological significance of this protein in malignancy[234].

The intermediate hPRLr (hPRLrI; ENST00000619676.3) was the second hPRLr isoform to be discovered[63]. Reverse transcription PCR (RT-PCR) performed on both normal and malignant breast tissues revealed expression of an hPRLr variant of a similar size to the intermediate rat PRLr (rPRLrI)[7]. Inasmuch, this new variant was termed the intermediate isoform, based on the size similarity with the rPRLrI[63]. hPRLrI was found to share 100% homology with hPRLrL up to bp 1009, followed by a 572 bp (corresponding 190 residue) interstitial deletion within the C terminal cytoplasmic domain[63]. The resultant hPRLrI protein shares said homology with hPRLrL up to residue glutamine 336 (Q336; Figure 3). This 572 bp deletion, being an out-of-frame interstitial loss, induces a frameshift, which results in a novel 13

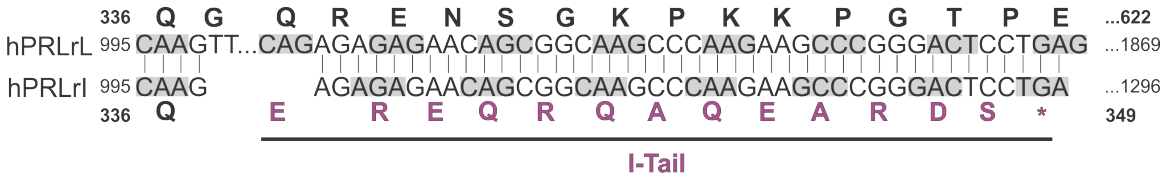

Fig. 3. hPRLrL and hPRLrI nucleotide and peptide alignment. hPRLrL and hPRLrI ORFs aligned alongside respective peptide sequences. The unique hPRLrI I-Tail sequence is highlighted in purple. Adapted from Kline *et al.* 1999.

amino acid tail ("I-Tail") and a premature stop codon (Figures 3 and 4). hPRLrI is 349 aa, 1296 bp, and runs at 50-55kDa. A full literature review of hPRLrI biology is presented in Chapter 3.

The hPRLrΔS1 isoform was originally cloned in our lab from T47D cells, and lacks the N-terminal S1 domain corresponding to bp 71-373 (exons 4-5) of the hPRLr-ECD (Figure 4)[158]. Since its initial cloning, hPRLrΔS1 has been found in the breast cancer cell line MCF7, as well as patient breast and parathyroid tumors[119]. hPRLrΔS1 has a molecular mass of approximately 70kDa, the mRNA of which was approximately 1.5kb in length[158]. Transfection of Chinese hamster ovary (CHO) cells with hPRLrΔS1 followed by surface plasmon resonance (SPR) demonstrated that this isoform binds ligand with a 94-fold and 30-fold lower affinity at PRL sites I and II, respectively[158]. Curiously, hPRLrΔS1 does not exhibit self-antagonism at high ligand concentration, in direct contrast to what is observed with hPRLrL[119,158]. From a signaling perspective, hPRLrΔS1 is capable of stimulating Jak2 phosphorylation, albeit that such a signaling response requires a much higher concentration of ligand, compared to that of hPRLrL. Indeed, this difference in ligand concentration required for hPRLrΔS1 signaling is commensurate with the elevation in serum PRL concentration observed during pregnancy[57]. This would suggest that hPRLrΔS1 may contribute to the pleiotropic effects of PRL on pregnancy-associated mammary differentiation[158].

To date, two short hPRLr isoforms have been cloned: hPRLrS1a and hPRLrS1b

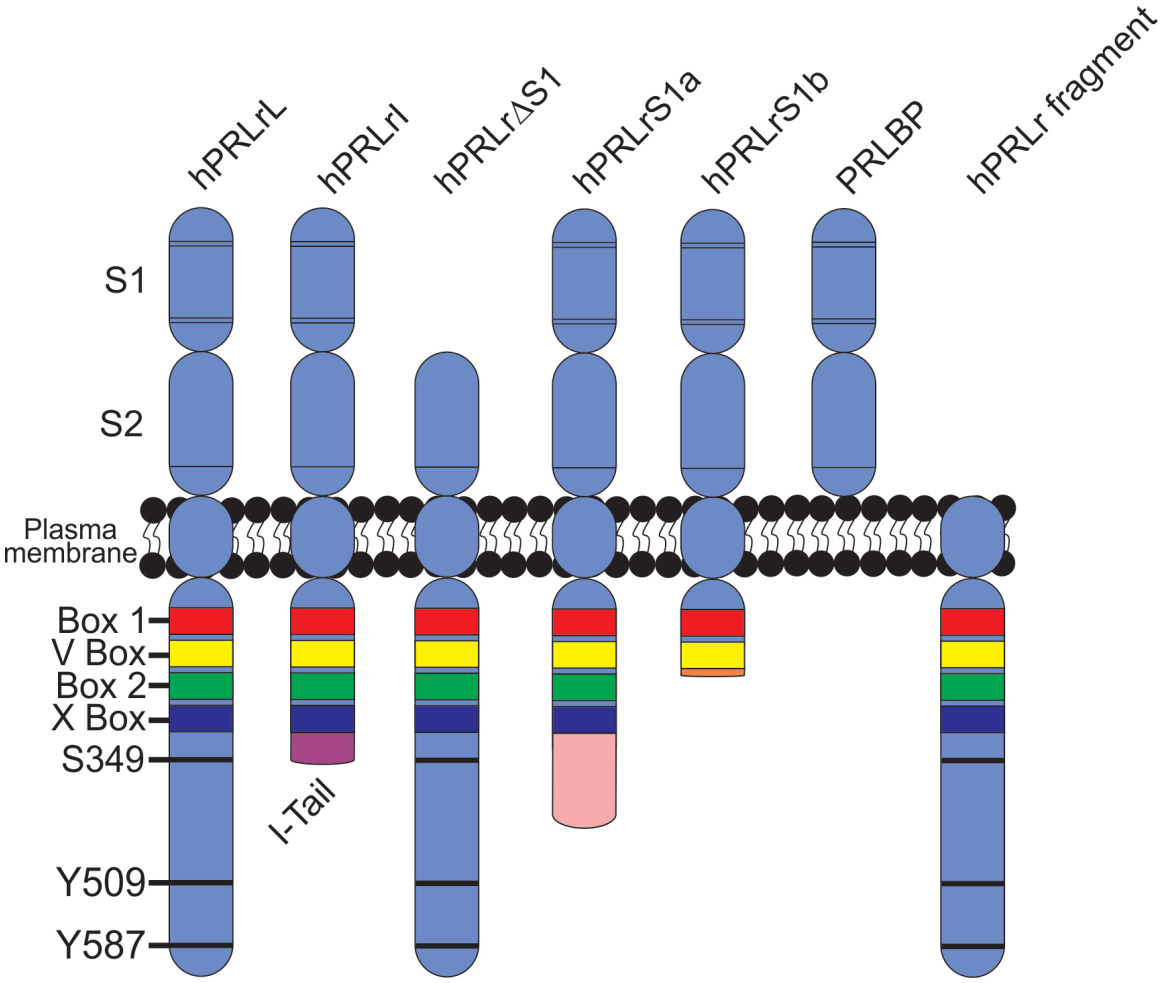

Fig. 4. hPRLr isoforms. 2-dimensional rendering of hPRLr isoforms. The conserved Box 1, V Box, Box 2, and X box subdomains are noted in red, yellow, green, and blue, respectively. The unique hPRLrI I-Tail is noted in purple, as are the unique regions of hPRLrS1a (pink) and hPRLrS1b (orange). The tyrosine residues hypothesized as being critical for Stat5a involvement, Y509 and Y587 respectively, are annotated, as is the phosphodegron S349.

(Figure 4)[135]. Discovery of a novel hPRLr exon (exon 11) led these investigators to uncover both aforementioned short isoforms in T47D cells. Both of these isoforms are generated by alternative splicing of hPRLr exons 10 and 11. The hPRLrS1a nucleotide sequence contains a portion of exon 10 in addition to exon 11, is 2.0kb long, with a mature protein of 376 aa[135]. Concomitantly, hPRLrS1b contains none of exon 10, with a small portion of exon 11, is 1.8kb long, and the hPRLrS1b protein is 288 aa in length[135]. Both of these short isoforms were found to be expressed in both normal and malignant breast tissue, with cell surface expression levels being comparable to that observed with hPRLrL[135]. Additionally, both S1a and S1b were found to bind ligand at a similar capacity of hPRLrL. Most critically, however, neither short form was able to result in the induction of β-casein transcription, a common reporter gene for PRL activity[135]. Rather, both short isoforms were found to act in a dominant negative fashion, antagonizing hPRLrL transcriptomic actions[99,135]. However, a later study was able to show that short form expression in $PRLr^{+/-}$ mice was sufficient for rescue of normal mammary gland development, indicating that these short forms are not pure antagonists[33]. Later characterization studies demonstrated that the short forms are capable of stimulating Jak2 phosphorylation, furthering the hypothesis that hPRLrS1a and hPRLrS1b may hold some functionality beyond hPRLrL inhibition[229].

The smallest hPRLr isoform known to date is the hPRL binding protein (PRLBP). The first study detailing a putative PRLBP was published in 1986, where milk samples from post-partum women was used in a PRL binding assay using column chromatography. A subset of these samples contained a factor which bound to human prolactin[61]. Subsequently, a similar PRL binding factor was later identified in the serum of patients with schizophrenia[289]. These findings were recapitulated in rabbits, rats, and other mammalian species[10,67,225]. Considering the significant homology between GH and PRL, and that GH is capable of binding to and activating hPRLr, it was

no surprise that teasing apart the actions of putative GH binding protein(s) (GHPB) from that of PRLBP proved challenging[9,194,224]. Ultimately, expression of a PRLBP in human serum was confirmed and characterized, and was found to be the product of proteolytic cleavage[156,186]. This isoform, comprised of just the hPRLr ECD (Figure 4), was found to be 32kDa, and binds hPRL in serum[156]. Up to 36% of serum hPRL is bound by PRLBP, as was discovered by co-immunoprecipitation (coIP) analyses[156]. Similar levels of PRLBP were found in the sera of men compared to nonlactating, nonpregnant women, revealing a lack of sexual dimorphism. *In vitro* competition functional analyses using the rat Nb2-11C lymphoma cell line also confirmed that PRLBP sufficiently inhibits PRL mitogenic activities, in a concentration-dependent manner[156].

Following the proteolytic cleavage event that generates the PRLBP, an additional hPRLr isoform is generated: the "hPRLr fragment", which corresponds to the hPRLr TMD-ICD (Figure 4). This fragment was found capable of ligand-independent heterodimerization with hPRLrL, and this interaction was shown to augment Stat5a transactivation in T47D cells[106]. Subcellular fractionation assays also show that the hPRLr fragment localizes primarily to the plasma membrane[106]. These preliminary results suggested the hPRLr fragment may indeed hold functional significance in malignancy, and warrants further investigation.

Additional hPRLr isoforms that have been reported on include hPRLrΔS2, hPRLrΔ7/11, hPRLrΔ4-SF1b, and hPRLrΔ4-Δ7/11[98,272,273,274]. These isoforms are hypothesized as having a wide array of unique biological activities, acting in both antagonistic and agonistic manners. However, further corroboration is necessary to validate both the occurrence and nature of these putative hPRLr isoforms, in addition to a more full characterization of their respective biological activities.

2.2.5 PRLr homologs in rodents

PRLr exists in every mammalian species studied to date. However, special interest has been given to that of rodent PRLr (specifically mouse and rat), given both their relative ease in experimental modeling as well as their conserved homology to humans (Figure 5)[26]. While there is not 100% homology and biological actions shared between rodent and human PRLr, studies that have examined PRLr rodent homologs provide insight into the biology of the receptor. To date, there have been three PRLr isoforms characterized in the rat, and four in the mouse, which are discussed below.

A receptor specific for PRL was first described in 1975, wherein it was discovered that estrogen stimulation of rat liver tissue induced expression of a factor capable of binding PRL[223]. Following a number of characterization studies that examined the regulatory effect of PRL on PRLr expression, efforts to clone the wild-type rat PRLr (rPRLr) were successful, using rat liver samples[40,83,190]. The first rPRLr isoform to be cloned was a 2.2kb species present in rat liver tissue[40]. The resultant protein product was 291 amino acids long, 40kDa, and contained an initial 19 amino acid stretch of hydrophobic residues indicative of a signal peptide sequence[40,108]. This form was found to be the dominant rPRLr species in rat liver, prostate, and ovary[40]. A longer rPRLr isoform (4kb) was observed by Northern blot analysis as being present in the kidney and mammary gland, but would not be fully elucidated until the following year[87]. The shorter, 291 amino acid rPRLr isoform would later be referred to as the short form (rPRLrS), based on size comparison to the other two isoforms that would later be characterized.

Given this preliminary indication of a 4kb long rPRLr (rPRLrL) isoform, investigators were keen on identifying and cloning this 4kb mammary rPRLr species. The full-length rPRLrL was cloned out of rat mammary tissue, and the mature pro-

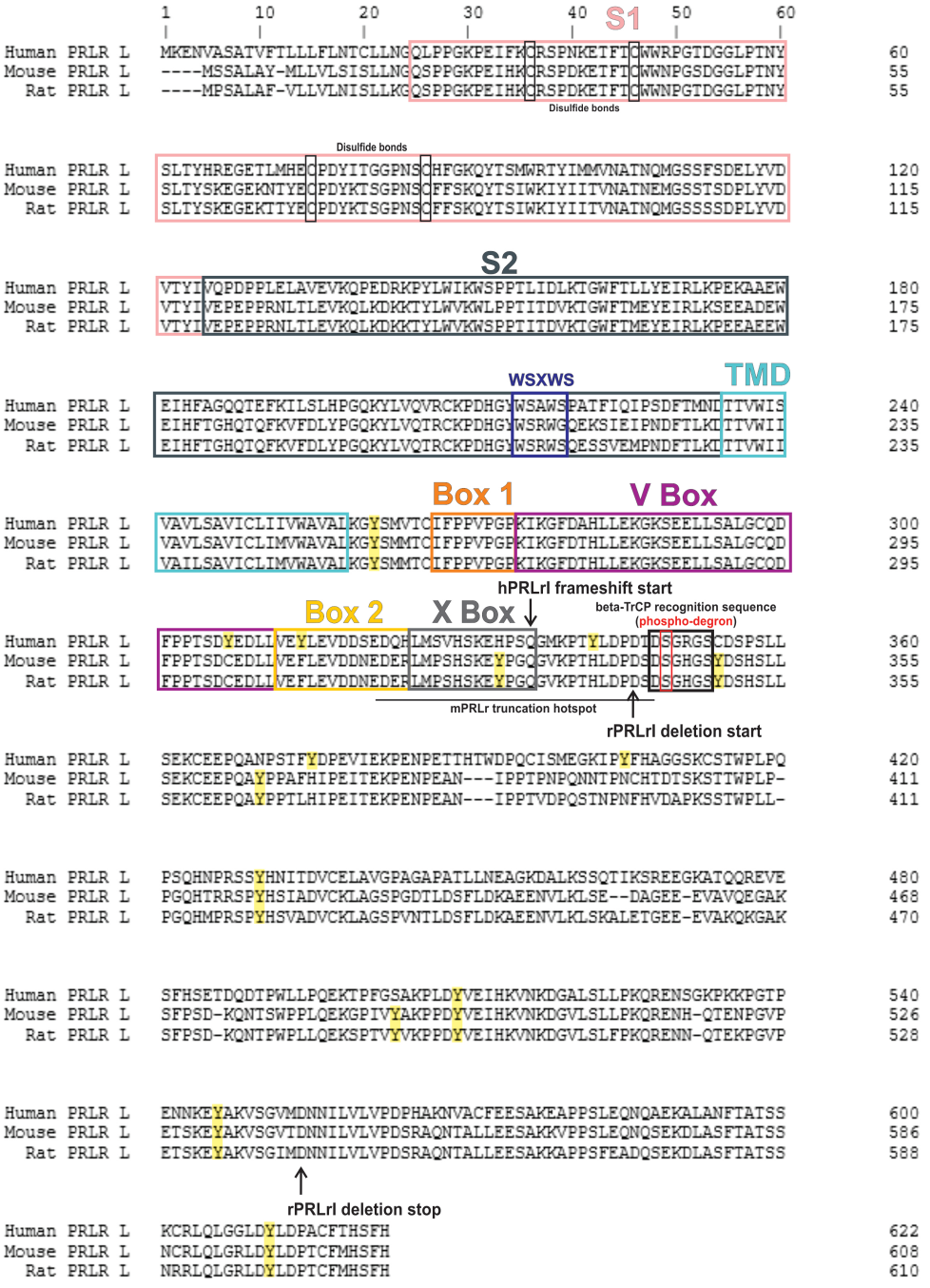

Fig. 5. hPRLr, mPRLr, and rPRLr amino acid annotated alignment. The conserved PRLr regions of the human, mouse, and rat orthologs are as indicated. The mPRLr truncation hotspot (Griffith *et al.* 2016) is underlined, and the black arrow indicates the rPRLrI deletion start site.

tein was found to be 592 amino acids long[87]. This full-length form was 66kDa, and scatchard analyses confirmed rPRLrL binds PRL with a high degree of affinity (K = $3.5x10^9M^{-1}$), and is also capable of binding GH and PL[87]. These studies were subsequently corroborated by independent investigators and rPRLrL was later also cloned from rat ovary, uterus, lung, and a variety of additional normal rat tissues[200,253,304].

The final rPRLr isoform cloned to date was discovered in the Nb2 cell line, which is a pre-T rat lymphoma model[7,112]. This transformed cell line, which was derived from a transplantable rat lymph node tumor, is dependent on lactogenic hormones for proliferation[112,236]. While studying this dependency, investigators successfully cloned a novel rPRLr isoform missing 594 nucleotides from the intracellular domain[7]. This interstitial loss of genetic material was not associated with consensus splicing sequences (e.g. intronic GT/AG), and therefore was classified as an in-frame deletion[7]. This novel isoform had a molecular mass of 62kDa, and based on its relative weight compared to rPRLrL and rPRLrS, this form was subsequently deemed the intermediate rPRLr (rPRLrI)[7]. Later characterization revealed this isoform associates with both the serine/threonine kinase Raf1 as well as the adaptor protein Cbl, and is capable of stimulating phosphorylation of both aforementioned proteins[65,137]. Cbl was also shown to facilitate the interaction between rPRLrI and PI3K, and PRL stimulation of rPRLrI was shown to result in PI3K activation[137].

Similar to that which was observed in rat tissue, investigators discovered a factor within mouse liver tissue that was capable of binding to PRL[178,179]. Following solubilization and affinity chromatography, a purified 37kDa mPRLr was recovered[179]. Scatchard analysis revealed that the binding affinity of mPRLr with PRL was highly specific (K_aPRL = $2.6x10^9M^{-1}$), and that it's affinity for GH was significantly less so[144,179]. It was subsequently shown that this same receptor was capable of binding PL in mouse liver[124]. While analyses in 1988 utilizing SDS-PAGE indicated this

mPRLr to be a 37kDa protein, actual cloning and sequencing of the receptor would not happen for another year[124]. Furthermore, the results from this study suggested there were likely more than one mPRLr isoform, similar to what had been previously established with the rat. Ultimately, studies were successful in cloning the cDNA of three unique mPRLr isoforms[80].

Similar to rPRLr, the dominant mPRLr isoform found in the liver was a short form of 303 aa and 42kDa[80]. Two other short forms were identified, with one being 292 aa long and the other having a length of 310 aa[80]. As this 1989 study was unable to identify an mPRLr that was similar in size to that of the rPRLr discovered earlier, investigators hypothesized that the full-length long form of mPRLr was yet to be discovered. Ultimately, in 1993, studies were able to confirm the existence of a fourth and final full-length mPRLr (mPRLrL), whose ORF and peptide length closely resembled that discovered in the rat[62]. The full-length mPRLrL had an ORF of 1827 nucleotides, a mature protein of 608 amino acids, and was predicted to weigh approximately 70kDa[62].

2.3 Prolactin/Prolactin receptor signaling

hPRLr localizes to the plasma membrane, predimerized, where it is activated by ligand stimulation[106]. Said stimulation induces a conformational change of the hPRLr ICD, as mediated by the peptidyl prolyl *cis/trans* isomerase CypA, which allows for transduction of downstream signaling events[269]. This intricate network of kinases, transcription factors, and adaptor proteins connects extracellular signals to intracellular transcript regulation and ultimate physiologic response. This section will discuss those signaling pathways most relevant to this dissertation (e.g. Jak2, Stat5a, MAPK, and Ras), however it should be noted that these signaling pathways represent only a small fraction of PRL signal transduction.

2.3.1 Jak2/Stat5a

Janus kinase 2 (Jak2) tyrosine (1007/1008) phosphorylation reaches its peak within 5 minutes of PRL stimulation[94,245,246]. IP studies uncovered that Jak2 is constitutively associated with hPRLr within the conserved Box 1 motif regardless of PRL binding, which likely contributes to the early and immediate signaling response from Jak2 following ligand stimulation[47,167,218]. Jak2, being the promiscuous kinase that it is, has a multitude of substrates, including the hPRLr, Stat5a, and Jak2 itself[168]. To this end, the kinase actions of Jak2 extend far beyond regulating Stat5a transcriptional activities, having functions required in the optimal activation of Src, MAPK, and PI3K pathways, and the actions of Jak2 are known in being critical for PRL-driven cellular proliferation[168,232]. Additionally, recent studies have suggested a role for Jak2 in EMT and tamoxifen-resistance[139,309]. Jak2 also stimulates its own negative regulation through Stat5a, as is discussed later in this section.

Signal transducer and activator of transcription 5a (Stat5a) is likely one of the most highly-studied pathways involved in PRL-mediated signal transduction. Following PRL stimulation, Jak2 mediates Stat5a phosphorylation on tyrosine residue 694 (pY-Stat5a)[141,213]. Stat5a subsequently self-dimerizes and retro-translocates to the nucleus where it regulates transcription of PRL-responsive genes[163,181,207]. For decades it was considered dogma that the only active form of Stat5a was that which was tyrosine phosphorylated, and unphosphorylated Stat5a (upY-Stat5a) were considered inactive[115,294]. However, recent studies have indicated that upY-Stat3 and upY-Stat5 are indeed active and function independently of their phosphorylated counterparts[86,134]. There exist also two serine residues (S726 and S780) on Stat5a whose phosphorylation statuses carry different functional consequences on Stat5a regulation[28]. While Stat5a's role in PRL-mediated signal transduction is substantial, evi-

dence for unique physiologic effects of upY- and phospho-serine (pS) Stat5a indicate this transcription factor likely has pleiotropic effects within the PRL signaling cascade.

As stated above, Stat5a down-regulates Jak2 activity through a negative feedback loop. pY-Stat5a transcriptional activity results in the expression of suppressors of cytokine signaling (SOCS) and cytokine-inducible SH2-containing (CISH) proteins, as well as peptide inhibitor of activated Stat (PIAS) proteins[59,248,271]. These proteins act in a number of ways to attenuate Jak2 activity. The SOCS/CISH mechanisms of action include both direct binding onto the activation loop of Jak2, as well as binding of phosphotyrosine motifs on activated cytokine receptors[271], while PIAS inhibits pY-Stat from binding DNA[59,248]. In these manners, Jak2 is inhibited in a variety of fashions, thereby abrogating this promiscuous kinase.

2.3.2 MAPK

PRL has been shown to stimulate the mitogen-activated protein kinase (MAPK) pathway in a variety of models, both normal and malignant[65,78,259,288,300]. The MAPK cascade represents a number of protein kinases, including Erk (p44/42), Mek, and Raf, that work in coordination to transmit surface-level signaling into the nucleus for gene-level response. In breast cancer cells stimulated with PRL, MAPK signaling is downstream of Jak2 and Ras activation[42]. Among the physiologic actions induced by MAPK activity in response to PRL stimulation, proliferation driven by cyclin D1 (CCND1) and c-Myc expression is the most well-documented[2,65,78]. Additional work has implicated a role for PRL-driven MAPK activation in migration, invasion, and survival[5,120,238].

2.3.3 RAS

Ras is both an upstream component of the MAPK pathway, and a downstream element of Jak2 signaling, and there is significant overlap between the biologies of these pathways. However, recent years have demonstrated a unique role for Ras in breast cancer. All Ras proteins (KRAS, NRAS, HRAS) are small GTPases, which are enzymes that hydrolyze guanosine triphosphate (GTP) to guanosine diphosphate (GDP), thereby acting as a kind of "molecular switch". In the context of PRL signal transduction, PRL stimulation promotes the association between Jak2 and Src Homology 2 Domain-Containing Transforming Protein 1 (SHC1), which then recruits Growth Factor Receptor Bound Protein 2 (Grb2) to associate with SHC1[64,286]. This complex then recruits the Son of Sevenless (SOS) guanine nucleotide exchange factor (GEF) which subsequently associates with and activates Ras[5,301]. While certain cancers, such as pancreatic or colon, are driven by Ras mutations, a role for Ras in breast cancer remains controversial[39]. Insofar as Ras activation by PRL, this has been observed in malignant tissue, both *in vitro* and *in vivo*[48,90]. While it would appear that Ras does not have a significant and consistent role in the development of primary breast tumors, reports indicate a critical role in metastasis, mesenchymal maintenance, and EMT[151,210,298].

2.4 Prolactin receptor stability

While there are a variety of ways by which the PRL/PRLr axis is regulated, one critical manner is through ligand-induced receptor degradation. Given that abnormal and/or hyperactive PRL signaling can result in unabated proliferation, having a ready negative feedback mechanism is crucial to mitigate this effect. PRL-induced receptor turnover was observed by our lab as early as 1997 when PRL stimulation

of malignant mammary tissue was shown to decrease hPRLr protein expression[234]. Subsequent motif analyses confirmed that the hPRLr contains a conserved recognition motif (^{348}DSGRGS^{353}) within the ICD that is utilized by the F-box protein β-TrCP (a subunit of the E3 ubiquitin ligase SCFβ-TrCP)[175]. Immunoprecipitation studies confirmed that hPRLr and β-TrCP coIP, and that this interaction was promoted by ligand stimulation[175]. A specific serine residue within this motif, S349, was theorized as being the critical residue capable of ligand-induced phosphorylation, and phospho-deficient point mutagenesis significantly impaired the hPRLr/β-TrCP interaction[175]. Ultimately, it was observed that pS349 was a true phospho-degron, in that phosphorylation at this site was sufficient for β-TrCP recruitment followed by polyubiquitination, endocytosis, and receptor turnover via the lysosomal pathway[175,285].

Once these initial studies confirmed hPRLr undergoes ligand-stimulated degradation, a number of characterization studies were carried out in order to fully elucidate the proteins involved in this activity. To this end, mutagenesis studies determined efficient hPRLr ubiquitination, internalization, and degradation requires Jak2[268]. Interestingly, phosphodeficiency mutagenesis of all hPRLr tyrosine residues almost entirely abolished hPRLr-S349 phosphorylation, indicating there may be some interplay between these residues[268]. A separate study uncovered that the recruitment of β-TrCP to hPRLr was found to be contingent upon the activity of glycogen synthase kinase 3β (GSK3β)[219]. Immunoprecipitation studies showed that GSK3β coIPs with hPRLr in a ligand-independent manner, and subsequent *in vitro* kinase studies determined that GSK3β is capable of directly phosphorylating hPRLr-S349[219]. GSK3β kinase activity is dampened by phosphorylation on serine residue 9 (S9) by Ras signaling effector Mek1, and constitutive Ras expression resulted in a more stable hPRLr[219].

Analysis of hPRLr degradation kinetics in 293T and human mammary epithelial cells (HMEC) indicated, under standard physiologic conditions in normal tissue, the

wild-type receptor had a half-life ($t_{1/2}$) of approximately 3 hours[175]. In breast cancer cells, however, hPRLr $t_{1/2}$ is much greater[174]. For example, hPRLr $t_{1/2}$ in T47D cells was found to be approximately 7 hours[174]. These results were corroborated in two additional breast cancer cell lines, MCF7 and MDA-MB-468. Phospho-deficient replacement mutagenesis (hPRLr-S349A) was sufficient to phenocopy the elevated hPRLr stability observed in breast cancer cells[175]. Levels of hPRLr-S349 phosphorylation, β-TrCP, and GSK3β were all decreased in malignant tissue compared to normal, suggesting a critical role in hPRLr stability in breast cancer[174,219]. In testing this hypothesis, expression of hPRLr-S349A in CHO cells significantly increased both the signaling capacity of hPRLr following ligand stimulation as well as cellular proliferation[175]. A later study took these analyses a step further and examined the transforming potential of degradation-resistant hPRLr, and found that hPRLr-S349A expression in the partially-transformed cell line MCF10AΔp53 contributed significantly to both 2-dimensional and 3-dimensional proliferation[220].

2.5 Epidemiological studies of prolactin in breast cancer

Clinical levels of circulating PRL have long been hypothesized as being a potential marker for breast cancer risk. Studies as early as the 1970s tested this hypothesis with mixed results, however testing sensitivity and limited sample sizes may have been factors in curbing reproducible results[68,187]. To date, the most well-defined and clear evidence for an associative link between PRL and breast cancer came from studies utilizing data obtained during the Nurses' Health Study (NHS) I and II.

The NHS began in 1976, wherein 121,700 female registered nurses from the age of 30-55 were enrolled from 11 different US states. The follow-up NHSII began in 1989 and enrolled 116,429 women (25-42 years old). These women answered a detailed health questionnaire (including questions on weight, menopause status, diet,

etc.), provided blood samples, and received biennial follow-ups. The first study to utilize this large prospective study focused on the association between plasma PRL and breast cancer risk in post-menopausal women, and found a linear increase in breast cancer risk along with higher plasma PRL levels[121]. Since this initial report, two additional nested case-control studies of NHS and NHSII with moderate sample sizes (n=377 and 235, respectively) confirmed there to be an increase in the relative risk (RR) for breast cancer with increasing plasma prolactin levels ($RR_{NHS} = 1.3$; $RR_{NHSII} = 1.5$)[277,280]. A 20-year followup study took these data a step further an examined the relevance of assessing proximal versus distant PRL levels relative to disease occurrence, discovering that PRL levels closer (<10 years) to disease onset are a much better RR predictor than those measured further out ($\geq$10 years)[278]. Additionally, these studies indicated that the effect of PRL on breast cancer is the strongest in those cases of ER+ disease, much more so than that of ER-[278].

There have been a multitude of studies that have evaluated the link between elevated PRL levels and a number of confirmed breast cancer risk factors. While not as direct and clear-cut as the studies enumerated above linking serum PRL and breast cancer risk, a consistent association between these breast cancer risk factors and high PRL concentrations would at least suggest that PRL is involved in the underlying etiological mechanism(s) of breast cancer. Those breast cancer risk factors that have a consistent positive correlation with PRL include, but are not limited to: family history of breast cancer[88,143,279]; mammographic density[113,235,305]; medication use, including oral contraceptives and antipsychotics[89,212,231]; and pregnancy (the relationship between pregnancy and breast cancer is discussed in Section 1.3).

2.6 Models of PRL in breast cancer

Considering the relevance of PRL in breast cancer, establishment of both *in vitro* and *in vivo* models is critical in understanding how this hormone is involved in malignancy. Those models are discussed below, with their appropriate strengths and weaknesses.

2.6.1 *In vitro* models

There are a number of breast cell lines, both normal and malignant, that have been shown to be PRL-responsive, and have concomitantly been shown to express hPRLr[211,254]. Considering that epidemiological studies have implicated PRL is more strongly involved in ER+ malignant etiology, the two most prominent breast cancer cell lines used in the field to study PRL actions are the luminal models MCF7 and T47D[34,38,211]. These two cell lines express multiple hPRLr isoforms, including hPRLrL and hPRLrI, and represent the majority of *in vitro* studies examining PRL actions in breast cancer. Additional cell lines that are used, albeit less frequently, are MDA-MB-231, BT-474, and SKBR3[91,204]. *In vitro* modeling includes assessing both 2-dimensional behaviors, such as proliferation and viability, and 3-dimensional cellular affects, including colony-forming potential and invasion through a matrix. *In vitro* cell-based assays are powerful in that they provide a quick and efficient means to study cellular behaviors, without the financial and temporal burden of murine studies. However, *in vitro* approaches are limited in their mimicry of disease progression and biology. For example, standard cell lines are cultured on a hard, plastic, 2D surface, which is not reflective of conditions *in vivo*. Even those approaches that attempt to mitigate this effect by culturing in a 3D matrix (e.g. soft agar and Matrigel®) are unable to fully recapitulate tissue-respective cell-type heterogeneity. To this end,

while *in vitro* approaches to studying PRL's involvement in breast cancer are certainly useful, concurrent *in vivo* studies are necessary to confirm effects ascertained *in vitro* are similarly observed in a living system.

2.6.2 *In vivo* models

Early methods of establishing rodent models for PRL over-exposure used pituitary isografts, in which pituitaries are transplanted under the kidney thereby elevating and prolonging PRL in circulation[293]. This method was successful in underscoring the involvement of PRL in spontaneous mammary tumorigenesis, in both mice and rats[176]. These initial studies paved the way for more advanced transgenic approaches.

Initial transgenic models placed the rPRL gene under the control of the metallothionein promoter, driving ubiquitous rPRL overexpression[296]. This particular model develops spontaneous mammary tumors within 11-15 months[296]. To assess mammary-specific PRL over expression, promoters including that for whey acidic protein (WAP) and rat neu-related lipocalin (NRL) have been utilized for study[188,239]. In particular, considerable headway has been made by the lab of Dr. Linda Schuler in characterizing the NRL-PRL model[239]. Two NRL-PRL mouse lines were originally generated (lineage 1655-8 and 1647-13, named for their founder mice), and while mammary-specific PRL overexpression was observed in both of these models, only NRL-PRL 1655-8 demonstrated elevated PRL in circulation (NRL-PRL 1655-8: 253±28ng/ml; NRL-PRL 1647-13: 45±13ng/ml; mean±sd)[239]. Virgin NRL-PRL 1655-8 females exhibited early alveolar development by 13 weeks, and hyperplasias were evident in both lines within 6-9 months[239]. By 17 months, 70% of NRL-PRL female mice develop carcinoma[48,239,240]. Both lines develop spontaneous ER+ and ER- mammary carcinomas, indicating these PRL-driven tumors to be independent of the integration site of the NRL-PRL transgene[239]. While early differences in mammary

pathology were noted between NRL-PRL 1655-8 and NRL-PRL 1647-13 (namely, earlier and larger epithelial hyperplasias on average), the tumor latencies between these two models are comparable[208]. Furthermore, while elevated serum PRL is noted in breast cancer patients, the Schuler group has primarily focused on NRL-PRL 1647-13 for their transgenic studies, in order to reduce the likelihood that transgenic PRL is influencing the mammary gland through secondary effects on other tissues[208].

While the long latency period is a general drawback of this transgenic line, it does more accurately reflect the biology of human disease[208]. As a noteworthy aside, mPRL does not appear to efficiently agonize hPRLr, which is a clear limitation to *in vivo* approaches[282]. However, in an attempt to overcome this particular limitation, a humanized PRL mouse model expressing only human PRL was generated in 2013[58]. Unfortunately, initial characterization of this mouse model did not examine oncogenesis, and at the time of writing this dissertation, there have been no additional studies published on this model[58,247].

2.7 PRL/hPRLr as clinical therapeutic targets

Rodent studies revealing PRL's role in mammary tumorigenesis spurred investigators to treat these rodent models with the DA agonist bromocriptine, which inhibits pituitary PRL secretion[292,293]. Inhibition of rodent pituitary PRL was sufficient for both prophylaxis against incipient mammary tumors as well as reduction in established tumors[292]. Unfortunately, clinical trials using bromocriptine on human breast cancer patients did not see any benefit in OS or RFS[11,37]. One possible rationale for the lack of observed clinical efficacy of bromocriptine is that this drug has no bearing on local, mammary (normal or malignant) PRL production, which could be sufficient to maintain tumorigenic growth in the absence of pituitary PRL. As a result, many investigators began searching and developing reagents that would alternatively

antagonize hPRLr[102,103].

Currently, a number of hPRLr antogonists have been developed with differing modalities. These have involved GH analogs acting as GHR antagonists that cross-react with hPRLr (hGH-G120R), as well as homologous molecules that recognize only hPRLr (G129R-hPRL, Δ1-9-G129R-hPRL)[102,152,184]. While studies have showed these agents are capable of blocking growth *in vitro*, residual agonism, inconsistent results, and unfavorable pharmacokinetics of these inhibitors has hampered clinical applications[66,102,152,184]. More recently, both a next generation hPRLr monoclonal antibody (mAb; LFA102) as well as an antibody-drug conjugate (ADC; ABBV-176) have been developed[77,169]. Preliminary *in vitro* and *in vivo* studies with LFA102 found this mAb to be an effective antagonist to hPRLr signaling in breast cancer cells, blocking both proliferation and tumor progression[77]. A Phase I clinical trial using LFA102 found no dose-limiting toxicities with the mAb and minimal adverse events (limited to fatigue and nausea), however it did not show antitumor activity at the doses tested[4]. Similarly, a Phase I trial using the ADC ABBV-176 in patients with advanced solid tumors did not see a positive response[169]. One critical limitation to the therapeutic approaches enumerated here is that all of these methods are pan-hPRLr inhibitors. As will be discussed in this dissertation, an isoform-specific approach may be necessary for clinical benefit to be observed.

2.8 Oncogenicity of truncated mPRLr mutants

This notion of isoform-specificity in terms of hPRLr antagonist design, and truly the source of our central hypothesis for this dissertation project, was first realized following the results of a 2016 study regarding early oncogenic events in Stat1-null mice[114]. Stat1 is a transcription factor normally expressed in the epithelial cells of the mammary gland, and is an independent prognostic indicator of prolonged progression-

free survival. Stat1 is involved in interferon (INF) signaling, and mice null for Stat1 have significant immunological defects.

In assessing the role of Stat1 in breast cancer, the Schreiber lab uncovered a subset of ER/PR+ breast neoplasias which express significantly reduced Stat1, and that this downregulation is associated with faster tumor progression[54]. Within this study, considering the relatively early stage in their breast cancer subgroup at which Stat1 is lost, these investigators established a Stat1-null mouse line[54]. This mouse model was monitored longitudinally, and spontaneous ER/PR+ mammary tumors were observed. Further, while grappling with the incomplete phenotypic penetrance inherent in this model, the investigators examined whether or not parity may play a role in the tumor development of their Stat1-null mice. Strikingly, it was observed that multiparous mice had a significantly quicker onset and faster progression, when compared to their nulliparous counterparts[54]. These data indicated that pregnancy-associated hormones, including PRL, are significantly involved in the observed tumorigenesis driven by a lack of Stat1.

As a follow-up to this study, these investigators sought additional early consequences of Stat1 loss. In specific, they wanted to assess genomic events that could be contributing to the observed tumorigenic phenotype[114]. They performed whole-genome sequencing (WGS) on the aforementioned spontaneously-arising Stat1-null ER/PR+ tumors, in addition to both adjacent normal tissue as well as DCIS samples. It was observed that 100% of tumors, and 78% of the DCIS samples, contained mutations in the mPRLr gene. The majority of these mutations were truncation events occurring in the heterozygous state (i.e. a single tumor sample would contain a truncated mPRLr allele as well as a normal mPRLr allele). Further, no mPRLr mutations were found in adjacent normal tissue, indicating these mutations to be a tumor-specific, and a likely significant-contributory, event. Additionally, genetic ex-

amination of mPRLr truncation mutants uncovered a putative mutational hotspot, encompassing residues glutamate 316 (E316) to aspartate 343 (D343) of the mPRLr peptide sequence.

Considering the heterozygous expression of these truncated mPRLr (mPRLrT) mutants, these investigators hypothesized that co-expression of mPRLrT with wild-type mPRLrL in a non-transformed cell line might contribute to cellular transformation. To this end, the investigators co-expressed both mPRLr variants in mouse embryonic fibroblasts (MEFs), and assessed for transforming potential both *in vitro*, using soft agar, and *in vivo* using nude mice. It was observed that following co-expression of both mPRLr variants, and not that of individual expression, that significant *in vitro* colony formation and *in vivo* tumor formation occurred. An accompanying mechanistic study depicted that this transformation event may be a result of increased Stat5 and/or Stat3 phosphorylation, but concluded more studies were needed to fully parse out a mechanism of action.

Lastly, the investigators probed both The Cancer Genome Atlas (TCGA) as well as the Exome Aggregation Consortium (ExAC) to assess corresponding hPRLr truncating mutations in human breast tumors. While mutations such as these do occur, they are rare, and occur on the order of $<2\%$ of breast cancers (allele frequency <0.00001). Following these results, Griffith *et al.* (2016) examined the potential relationship of hPRLr isoform skewing. Meaning, while the hPRLr exists as at least 7 differentially-spliced isoforms, they chose to focus on the short forms of hPRLr (S1a, S1b, Δ4 S1b, ΔS4-Δ7/11, Δ7/11, and ΔS1; for simplicity's sake, these forms will collectively be termed "hPRLrS" for discussion of this study; hPRLrI was not examined) as a possible surrogate for mPRLrT. They assessed a change in the hPRLrL:hPRLrS ratio, using TCGA-RNAseq data, and uncovered a decrease in this ratio (e.g. less hPRLrL relative to hPRLrS expression) in comparing Stat1-expressing to Stat1-null

primary tumors[114]. These results suggested this particular subset of patient tumors may rely preferentially on the short forms of hPRLr, over that of the full-length form.

The work of Griffith *et al.* (2016) was not without its limitations, a number of which are highlighted here:

1. First, the authors utilized MEFs for the entirety of the study. While this may be an easy-to-use and readily-transfectable cell line, it is not an appropriate model for mammary transformation. Alternatively, a mammary epithelial cell line should have been considered.

2. Second, limited mechanistic insight is presented. The authors only assess the tyrosine phosphorylation status of two transcription factors, Stats 3 and 5, without examining any other components of PRL signaling events. Additionally, all signaling events were examined at a baseline level of 0.05% FBS, rather than complete serum-starvation, rendering analyses of stimulation events tenuous at best.

3. Lastly, it is worth reiterating the scarcity of corresponding hPRLr truncating events in breast cancer, which really calls into light the biological relevance of the bioinformatics approach utilized. However, while some work was performed in comparing mPRLrT with hPRLrS, these investigators failed to note the striking similarity between mPRLrT and hPRLrI (Figure 6).

Considering these results regarding the oncogenic effect of mPRLrL+T co-expression, and in further consideration of the significant similarity observed between the mPRLr truncation hotspot and the hPRLrI differential splice junction, ***the overarching hypothesis of this dissertation is such: hPRLrI is a mammary proto-oncogene, when expressed in concert with hPRLrL***.

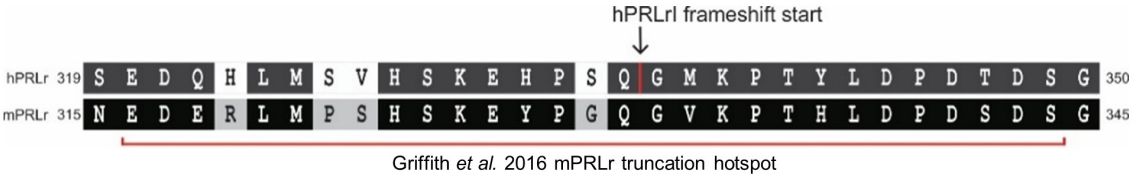

Fig. 6. hPRLrI and mPRLrT peptide alignment. The hPRLrI frameshift start site begins immediately following Q336, as indicated by the top arrow. The mPRLr truncation hotspot (E316-S344; Griffith *et al.* 2016) is denoted by the red bracket.

2.9 Dissertation aims

Aim 1: To assess the *in vitro* transforming potential of hPRLrI co-overexpression with hPRLrL.

Hypothesis: hPRLrI is transforming in normal mammary epithelia, when expressed in concert with hPRLrL, and this transformation is the result of altered hPRLrL+I heterodimer signaling and/or complex stability.

Aim 2: To correlate *in vitro* transformation findings with *in vivo* tumorigenic potential of hPRLrL+I co-overexpression

Hypothesis: hPRLrL+I co-expression contributes to mammary transformation *in vivo*, as determined by both primary tumor growth and metastatic burden.

Aim 3: To analyze the clinical relevance of hPRLrI through assessment of both patient specimens and *in silico* TCGA findings

Hypothesis: hPRLrI mRNA and protein expression correlates positively with aggressive clinicopathologic outcomes.

CHAPTER 3

LITERATURE REVIEW OF HPRLRI AND RECEPTOR HETERODIMERIZATION

3.1 Introduction

There is currently precious little literature regarding hPRLrI, its biology, and its putative role in breast cancer pathogenesis. While what is known is discussed here, the relative scarcity of information on hPRLrI means we are beholden to examining other proteins and systems (e.g. other cytokine receptors, Her2, rPRLrI, etc.) in order to guide our path in understanding this isoform. Furthermore, as our hypothesis is driven by the heterodimerization of hPRLrL+I, this literature review also examines the functional significance of receptor heterodimerization, both of PRLr and Her2.

3.2 hPRLrI

3.2.1 Initial characterization

hPRLrI was first cloned from both normal and malignant breast tissue, and at the time was only the second annotated form of the hPRLr to be discovered[63]. This isoform was termed the intermediate form based on its size similarity to the intermediate PRLr discovered in rats some years prior[7,63]. This initial study uncovered hPRLrI transcript and protein expression in both mammary epithelia and stroma, as well as a human T cell lymphoma cell line and patient-derived hepatocytes[63]. Follow-up characterization of hPRLrI in 1999 included assays examining ligand binding, cell surface expression and signal transduction, among other characteristics[157]. hPRLrL

and hPRLrI were ectopically and individually expressed in the murine myeloid cell line Ba/F3. Scatchard analysis of the resulting transfectants demonstrated that both isoforms bind radiolabeled PRL to a similar capacity: K_dhPRLrL, 1.79 ± 0.22nM; K_dhPRLrI, 1.64 ± 0.23 nM[157]. Both isoforms also showed comparable surface levels expression: hPRLrL was expressed at 6026 ± 517 receptors/cell, hPRLrI was expressed at 6300 ± 674 receptors/cell. Phenotypic studies of these Ba/F3 transfectants indicated that hPRLrI is able to induce only moderate proliferation but is able to enhance cellular viability at a level comparable to that of hPRLrL[157]. Next, studies on the proximal signaling capabilities of hPRLrI showed that, while capable of stimulating Jak2 phosphorylation, hPRLrI is able to induce Fyn activation only minimally[157]. Finally, Northern blot analyses were able to show that *hPRLrI* expression is unique and independent from that of *hPRLrL*, suggesting a unique physiological role for this isoform[157].

In addition to these two studies, only one other publication to date has directly commented on the role of hPRLrI in breast cancer pathogenesis[41]. In this brief study, a subset of examined breast cancer cases were found to express neither Stat5a nor the hPRLrL. However, IHC using polyclonal antisera generated against hPRLrI (Zymed) was able to confirm that hPRLrI was expressed in this subset. In this specific, and small (n=15), sample set, it was noted that hPRLrL and hPRLrI expression appeared almost mutually exclusive. However, several issues with this study are evident: only a small sample size was examined, the polyclonal antiserum was not shown to be validated in any sense, and the hormone receptor status of these cancers was not reported on, to name only a few[41]. However, it did provide corroborating evidence for hPRLrI expression in breast cancer, albeit weak at best.

3.2.2 hPRLrI transcript expression in normal tissue

hPRLrI variable tissue expression, unique from that of hPRLrL, is strong evidence for non-redundant physiologic function. While this dissertation is focused on the actions of hPRLrI in malignancy, functions of the isoform in normal tissue may provide insight into its actions in cancerous tissue. During the initial cloning and discovery, qRT-PCR analyses revealed *hPRLrI* transcript is found in normal human mammary epithelium[63]. Follow-up preliminary characterization of *hPRLrI* using Northern blot analysis uncovered significant variable expression in a variety of normal human tissues[157]. The normal tissues expressing the highest levels of *hPRLrI*, aside from the placenta, include the small intestine and kidney, whereas those tissues expressing the highest expression level of *hPRLrL* include the adrenal gland, pituitary gland, and the hippocampus[157]. There are a variety of functions the intermediate could have in these tissues, ranging from gut immunomodulation to electrolyte transport. Two additional studies have uncovered *hPRLrI* expression in white adipose tissue, as well as corroborated transcript expression in normal mammary epithelium[41,177]. However, validation of hPRLrI expression at the protein level would be necessary to confirm biological relevance in these respective tissues.

3.3 Prolactin receptor isoform dimerization

3.3.1 hPRLr short form heterodimerization and ratio studies

As stated prior, hPRLr isoforms are capable of heterodimerizing through the likely synergistic actions of the S2 and transmembrane domains, which adds considerable complexity toward unmasking PRL/hPRLr actions[45,182,195]. While much of the focus of study has traditionally been on hPRLrL homodimers, three studies have emerged in which have examined the importance of the hPRLr isoform ratio

in breast cancer[114,193,229]. Two of these studies, namely Qazi *et al.* 2006 and Meng *et al.* 2004, focused on the S1a and S1b forms, which are hypothesized as being dominant-negative hPRLr isoforms. In these studies, a decrease in the transcript ratio of short:long hPRLr in breast cancer compared to normal samples was found[193,229]. Conversely, Griffith *et al.* (2016) expanded their ratio analyses to include all short forms known at the time of publication (e.g. S1a, S1b, Δ4 S1b, ΔS4-Δ7/11, Δ7/11, and ΔS1. hPRLrI was not examined in this study), for expression comparison against hPRLrL. In contrast to the preceding two studies, Griffith and colleagues discovered a significant increase in the short:long ratio in Stat1-low luminal breast cancers. These studies set a clear precedent for the utility of examining hPRLr isoform ratios in breast cancer.

3.3.2 Heterodimerization modeling with rPRLr isoform chimeras

One significant limitation of studying the heterodimeric actions of cytokine receptors has been the putative frequency by which homo- versus heterodimers form. More specifically, parsing out endogenous homodimeric signaling from that of heterodimers has proven to be a challenging course of study. One way by which investigators have overcome this particular difficult has been in the utilization of receptor chimeras comprised of the rPRLr ICD and the GM-CSFr ECD[55].

GM-CSFr is a member of the growth factor receptor superfamily, similar to PRLr[22]. Many structural and peptide features of GM-CSFr are shared with PRLr, including the conserved cysteine residues in the ECD, necessary for disulfide bond formation, as well as the canonical cytokine receptor WSXWS motif[22]. GM-CSFr dimers are comprised of an α and β subunit, which pair in a 1:1 ratio[153]. The α subunit binds its ligand with a relatively low affinity, while the β subunit is entirely unable to bind GM-CSF[153]. However, upon α/β interaction, the β subunit converts

the low affinity binding sites on the α subunit into a high-affinity receptor, resulting in biological activity[153]. In this capacity, the α and β GM-CSFr ECD could be used to force a one-to-one pairing of receptor ICDs.

In utilizing this particular biological feature, investigators from our lab generated rPRLr-GM-CSFr receptor chimeras in order to study the functionality of receptor heterodimers[55]. The utilized rPRLr isoforms were the short, intermediate, and long forms, and intracellular signaling capabilities were confirmed by assessing Jak2 phosphorylation following ligand stimulation[55]. A follow-up study using these chimeras was performed to assess the functional stoichiometry of those rPRLr residues and subdomains required for certain biological activities and signaling[56]. The isoforms investigated include rPRLrI and rPRLrL, and the mutant rPRLr variants assessed included a set of serial truncation mutants as well as tyrosine replacement mutants. Constructs were transfected into Ba/F3 cells, and it was observed that, regardless of the mutation/isoform, cell surface expression was not significantly different from that of wild-type rPRLr[56]. This study uncovered that the *trans* pairing of hPRLr tyrosine residues is essential for their respective functional activities: meaning, for example, αY309βI co-transfectants were unable to activate Jak2, indicating it is the paired actions of contralateral tyrosine residues that contribute to PRLr signal transduction[56].

3.4 Heterodimer formation in other cytokine receptors

Heterodimerization of other cytokine receptors has been studied only minimally. GHR, which shares considerable homology to hPRLr, has at least 5 isoforms. These include the full-length GHR, the GH binding protein (GHBP), two short forms named for their amino acid lengths (GHR1-279, GHR1-277), and one isoform characterized by differential splicing of exon 3 (GHR-d3)[14,197,215,242]. Preliminary analyses of GHR heterodimers suggest that, similar to hPRLr, GHR short forms may act in a dominant

negative fashion, inhibiting both downstream signal transduction and ligand-induced transcription[14]. While these studies focused on GHR isoform heterodimerization, recent interest in GHR/hPRLr heterodimeric actions in breast cancer has sparked unique insight.

An early study using ovine GHR/PRLr-ICD GM-CSFr-ECD receptor chimeras suggested GHR and PRLr are capable of both heterodimerization and ligand activation by placental lactogen[128]. A follow-up study reaffirmed this hypothesis and further showed this heterodimerization is ligand-induced, occuring rapidly and transiently (peak interaction occurs within 2.5-3 minutes of stimulation)[32,299]. Analyses of signal transduction uncovered GHR/PRLr heterodimers are not only capable of stimulating the phosphorylation of Stat5, MAPK, and Jak2, but exhibit prolonged activation of Stat3 and Stat1 as well[32,166]. These results would indicate there is sufficient shared homology and reciprocity between these two receptors to have heterodimerization result in a functional complex.

This notion of cytokine receptor heterodimerization is not limited to PRLr and GHR. For example, wild-type EPOR heterodimerization with a dominant negative truncated EPOR was sufficient to inhibit EPOR ligand-stimulated autophosphorylation and Jak2 phosphorylation[19,191]. Another example is the typical heterodimerization of a number of the interleukin receptors (e.g. IL-2R, IL-31R), which is critical in modulating their functionality[95,196]. While PRLr and the interleukin receptors do not share considerable sequence homology, their respective conserved structural biologies contribute to the precedent of unique heterodimeric versus homodimeric actions.

3.5 Parallels with Her2

While the Her proteins are not members of the type 1 cytokine receptor superfamily, Her2 biology in breast cancer provides an excellent example of the unique and

malignant outcome of receptor heterodimerization. Her2, also known as ErbB2, is a receptor tyrosine kinase (RTK) with no known high-affinity ligand. On its own, Her2 actions are limited. It is not until Her2 heterodimerizes with a different Her protein that the receptor complex is capable of ligand-induced autophosphorylation within the ICD, triggering an array of pro-survival and proliferation signaling effectors. Under normal physiological conditions with limited ErbB2 expression, Her2-stimulated CCND1/CDK4/6 actions are kept in check by such cell cycle inhibitors as p21[122]. However, Her2 amplification upregulates CCND1 and subsequent G1/S progression, tipping the scale away from growth arrest to proliferation, from apoptosis to survival[122]. Given the apparent similarities between Her2 and hPRLr heterodimerization in mammary transformation, those analogous aspects will be fully examined below, with a focus on the differential stability and signaling of ErbB heterodimers.

3.5.1 Stability

Her2 is capable of heterodimerizing with all three other members of the ErbB family. Early studies realized that heterodimerization with Her2 significantly delayed receptor endocytosis and degradation[260]. Specifically, it was the truncated nature of Her2 that was found to increase the stability of ErbB1, ErbB3, and ErbB4[260]. Following this investigation, it was hypothesized that the truncated ErbB2 lacked some component or structure necessary for internalization, with immediate notions involving the clathrin coating machinery[260]. However, subsequent studies showed this delay in degradation may actually be reflective of elevated receptor recycling as a result of decreased interaction with ubiquitin-ligase machinery[170,171]. These studies demonstrated that Her2/ErbB1 heterodimerization weakens the interaction potential with the ubiquin ligase c-Cbl, thereby prolonging receptor activity[155]. Similar to what has been shown with hPRLr stabilization studies, Her2 degradation kinetics

have been shown to have a direct affect on prolonging signal transduction .

3.5.2 Signaling

Her2 homodimers are incapable is signaling on their own, owing to a lack of ligand-binding domain. Inasmuch, this proto-oncogene provides excellent framework for the malignant propensity of receptor heterodimerization. For example, the most well-characterized Her2 heterodimeric partner is Her3. While Her3 was once-believed to be either kinase-inactive or a "pseudokinase", research from the lab of Dr. Mark Lemmon has shown this not to be the case[118,252]. Indeed, this group demonstrated that ErbB3 retains its kinase activity, albeit at a 1000-fold weaker level than ErbB1[252]. However, the ErbB3 kinase domain was demonstrated to bind ATP with an affinity comparable to that of other active kinases ($K_d \approx 1.1$uM), and despite having weaker kinase activity, ErbB3 was shown to be capable of autophosphorylation[252]. These results were subsequently corroborated in patient samples harboring oncogenic ErbB3 mutants[145]. Analogous to what is observed with hPRLr isoforms, the ErbB family is capable of fine-tuning mitogenic signals through heterodimerization, the best example being Her2/Her3 heterodimers. These receptors are able to compensate for one another's shortcomings, in being capable of ligand stimulation and enhanced receptor autophosphorylation followed by MAPK, Ras, and PI3K activation[27,216]. These signaling effectors ultimately act through CCND1 to stimulate proliferation and motility[27,216].

Under standard conditions, normal cellular processes work to inactivate these proto-oncogenic pathways. However, in Her2 over-expressing cells, these safeguards are not put into place. The elevated stability incurred within the Her2/Her3 receptor complex results in prolonged signal transduction, increased receptor affinity for ligand, and delayed receptor endocytosis, as discussed above[146,154,170,260,287]. This increase in

receptor stability resulting in prolonged signaling is mirrored with hPRLr, where a stabilized hPRLr is capable of continuous ligand-stimulation[175]. These similarities between Her2 and hPRLr biologies set a framework by which we could guide our actions in studying hPRLrI oncogenicity.

3.5.3 Key differences between Her2 and hPRLr heterodimerization model

Despite the parallels between these two model systems, there are a number of discrepancies that must be addressed in order to avoid over-simplification in comparing the two genes. First and foremost, the structural biology of the two receptors are quite different: Her2 is an RTK, while hPRLr is a type I cytokine receptor lacking intrinsic kinase activity. Second, in consideration of Her2/Her3 heterodimers as the most well-characterized example, Her2 does not have a high affinity ligand whereas Her3 has limited tyrosine kinase activity[51,252]. In this manner, Her2/Her3 heterodimerization is analogous to bringing two compensatory pieces of the puzzle together, to create an oncogenic complex. While our hypothesis is that hPRLrI interaction with hPRLrL facilitates the full oncogenic potential of hPRLr, each isoform on its own is fully capable of both binding ligand as well as activating downstream signal transduction, just to differential effect. The final key difference between these two models lies in the actual receptor affinity for ligand. hPRLrL and hPRLrI homodimers bind PRL to similar capacity, and there is no evidence to date suggesting isoform heterodimerization increases ligand affinity[157]. Her2 association with Her3, on the other hand, decreases the rate of epidermal growth factor (EGF) dissociation from the dimer, allowing for a prolonged interaction that contributes to the observed unchecked signal transduction[287]. While Her2 sets the framework for the biological relevance of heterodimer formation in breast cancer oncogenesis, these differences are worth considering.

CHAPTER 4

MATERIALS AND METHODS

4.1 Cell lines and culturing conditions

All cell lines were maintained at 37°C and 5% CO_2. For general cell line maintenance, cells were grown to 70-80% confluency and then passaged at a 1:4 dilution. For long-term storage, cell lines were cryopreserved in liquid nitrogen (vapor phase) at either 5% (CHO, HEK-293T, MCF7, T47D) or 7.5% (MCF10A, MCF10AT) dimethyl sulfoxide (DMSO), per ATCC recommendations. Lines were also routinely checked for mycoplasma infection (MycoAlert Plus Detection Kit, VWR #75860-360).

4.1.1 CHO

CHO cells, PRLr-null, were maintained in Ham's F-12K (Kaighn's) media (Thermofisher Scientific #21127-022), supplemented with 10% fetal bovine serum (FBS; Corning #MT35011CV) and 1% penicillin-streptomycin (P/S; ThermoFisher Scientific #15140-122). For serum-starvation media and subsequent PRL stimulation, see Section 4.11.

4.1.2 HEK-293T

Human embryonic kidney (HEK) 239T cells were maintained in DMEM (Life Technologies #11965092), supplemented with 10% FBS and 1% P/S. 293T cells were used for viral particle production (See Section 4.2).

4.1.3 MCF10A/MCF10AT

MCF10A/MCF10AT cells were maintained in DMEM/F12 (Thermo Fisher Scientific #11330-032), supplemented with 5% horse serum (Atlanta Biologicals #S1215OH), 1% P/S, EGF (20ng/mL; ThermoFisher Scientific #PHG0311L), hydrocortisone (0.5mg/mL; Sigma-Aldrich #H0888), cholera toxin (100ng/mL; Sigma-Aldrich #C8052), and insulin (10ug/mL; Sigma-Aldrich #I0516).

4.1.4 MCF7/T47D

MCF7 and T47D cells were maintained in DMEM supplemented with 10% FBS and 1% P/S.

4.2 Viral production

4.2.1 Lentivirus

293T cells were grown to 80-90% confluence. Cells were subsequently transiently transfected using Lipofectamine 3000 (see Section 4.4) with the following constructs: 4.5ug of respective lentiviral construct, 1.5ug pMDG, and 6ug pCMVΔR8.91. Transfections were carried out on a 10cm plate. Cells were incubated in Opti-MEM/transfection reagent overnight at 37°C. The following day, the Opti-MEM was replaced with fresh growth media, and replaced in the incubator for 16-20 hours at 32°C. The viral supernatant was subsequently harvested, and either applied directly to the cells to be transfected (e.g. MCF7, etc.; supplemented with polybrene) or aliquoted and stored at -80°C.

4.2.2 Retrovirus

Regarding retrovirus production, the same procedure as in Section 4.2.1 was performed, with the following constructs at the given amounts: 12ug retroviral construct, 8ug pMLV-gag-pol, 4ug pVSVG.

4.3 Stable transduction and stable cell line generation

Cell lines to be stably transfected (e.g. MCF10A/MCF10AT over-expressors, MCF7/T47D hPRLrI KD) were grown in 6-well plates to 25% confluency and overlaid with 1mL of viral supernatant (Section 4.2). Cells were then spin-fected at 500xg for 2 hours, 32°C. Cells were then placed back in a 37°C incubator overnight, and imaged the following day for respective fluorescent reporter to confirm successful transduction as applicable. Cells were then expanded and subject to fluorescence-activated cell sorting (FACS), as carried out by the VCU Flow Cytometry Core. Alternatively, cells having retrieved transfection with a puromycin-resistance gene within the respective backbone were subject to antibiotic selection: cells were maintained at 2ug/mL puromycin for one week, followed by one week at 1ug/mL. Once stable pools were established, cells were maintained at 0.5ug/mL puromycin.

4.4 Transient transfection

For all transient transfections, Lipofectamine 3000 was used, per the manufacturer's protocol. For 12-well transfections, 1.5uL Lipofectamine 3000 Reagent, 2uL P3000, and 1ug of construct were used per well; for 10cm plate transfections, 21.7uL Lipofectamine 3000 Reagent, 28uL P3000 Reagent, and 14ug of construct were used per plate. All cells were imaged the day following transfection to confirm respective flourescent reporter expression and concomitant transfection efficiency.

4.5 Soft agar assay

The bottom layer of the soft agar assay was established by mixing 2x respective growth media with 1.2% noble agar, yielding a final solution of standard 1x concentration growth media and 0.6% noble agar. This layer was plated in a 6-well plate and allowed to polymerize for 1 hour at room temperature. Cells were then harvested from an 80% confluent plate using 1x Versene, strained using a 40um filter (ThermoFisher Scientific) to establish a single-cell suspension, and counted using a Countess Cell Counter (Invitrogen; additionally, given that this cell counting system does not account for the 1:1 dilution of sample with trypan blue, final concentration values were multiplied by 2 in order to account for this discrepancy). The top, cell-containing layer was established by mixing 2x respective growth media with 0.6% noble agar, yielding a final solution of standard 1x concentration growth media and 0.3% noble agar. For MCF7 and T47D experiments, $1x10^5$ cells were used. For MCF10A/MCF10AT, $2x10^5$ cells were used. Cells were suspended in the aforementioned 0.3% noble agar solution, overlaid atop the base layer, and allowed to polymerize for 1 hour at room temperature. Once solidified, a feeder layer comprised of 1mL standard 1x growth media was applied overtop each well, and replaced thrice weekly using gentle aspiration with a P1000 tip. Cells were cultured for 2 weeks at 37°C, 5% CO2, and stained with tetrazolium bromide (MTT) at endpoint. 10 images per well were taken at 4x on an inverted scope, and colony size and number were quantified using CellProfiler (www.cellprofiler.org). 50um diameter was used as the cut-off for colony calling.

4.6 Proliferation assay

All proliferation assays were carried out on an xCELLigence apparatus (ACEA Biosciences, Inc.), using an E-plate 16 (ACEA Biosciences, Inc. #5469830001). The

readout Cell Index (CI) reflects cell density. Cells were seeded at the following densities: MCF10A/MCF10AT, 12,500 cells/well; MCF7, 5,000 cells/well; T47D, 20,000 cells/well. For PRL-driven proliferation, cells were allowed to adhere for 16 hours followed by serum-starved (starvation media: DMEM/F-12, no phenol red Thermo Fisher Scientific #21041025 supplemented with 0.1% BSA) for 16-20 hours and subsequent PRL (250ng/mL) stimulation. CI was measured every 15 minutes until each well reached its respective CI plateau (24-48 hours following plating).

4.7 Migration assay

Migration assays were carried out on an IncuCyte apparatus (Sartorius) using a 96-well ImageLock plate (Sartorius). Respective migration efficiency was measured as "% Wound Closure". Cells were seeded at the following densities: MCF10A/MCF10AT, 50,000 cells/well; MCF7/T47D 40,000 cells/well. Cells were allowed to adhere for 8-12 hours, followed by scratch establishment using an IncuCyte®WoundMaker. Cells were washed with 1x PBS, and 100uL fresh respective complete growth media was applied to each well. Wells were imaged every 3 hours, and images were compiled once all wounds reached 100% closure. Images were then analyzed using the manufacturer's provided Incucyte®Automated Image Analysis Software.

4.8 hPRLrI isoform-specific KD

To perform hPRLrI isoform-specific KD, a pair of shRNA constructs were designed to target bp 997 to 1020 of the hPRLrI ORF, which spans the hPRLrI alternative splice junction (occurs at position 1009 in the hPRLrI ORF). The hPRLrI-targeting sequences were: 5' - CACCCAAGTCAAGAGAGAGAA - 3' and 5' - CCAAGTCAAGAGAGAGAACAG - 3'. These constructs were then cloned into the psi-U6 vector (Gene Copoeia #CS-HSH061317-LVRU6GP-01), which contains both a green

flourescent protein (GFP) reporter and a puromycin resistance cassette. Both constructs were subsequently spinfected (See Section 4.3) into both MCF7 and T47D cells, both individually and together. Cells were sorted for high GFP expression, expanded, and relative hPRLrI expression was determined via IB. A scrambled RNA (scRNA) negative control was used.

4.9 hPRLr isoform stable over-expression

MCF10A/MCF10AT cells were spinfected (Section 4.3) with either empty vector (EV), hPRLrL, hPRLrI, or hPRLrL/I (0.5:0.5) retroviral constructs (Section 4.2.2). Respective hPRLr isoform cDNA was cloned into the pBabe-GFP vector (Addgene 10668). Cells were sorted for high GFP expression, and successful isoform over-expression was confirmed via IB.

4.10 Cycloheximide assay

CHO cells were transiently transfected (Section 4.4) with either hPRLrL, hPRLrI, or hPRLrL/I (0.5:0.5; constructs were subcloned into the pTracer EF V5 HisA vector from Addgene), serum-starved for 16-20 hours, then stimulated ± PRL (250ng/mL) and cycloheximide (CHX, 100ug/mL) for 5 hours. Lysates were harvested once per hour (lysis buffer: 1x laemmli sample buffer, 5% BME, RIPA), and relative hPRLr isoform was blotted for to assess degradation kinetics. $t_{1/2}$ was approximated by determining the average slope of the rate of degradation. To this end, the following equation was used: $x = (50\% - b)/m$. The definitions of each variable are as follows: x, $t_{1/2}$; b, y-intercept as defined by the average rate of degradation; m, slope of the rate of degradation.

4.11 PRL signaling

Regarding all PRL stimulations, cells were serum-starved (using DMEM/F12 phenol red-free supplemented to 0.1% bovise serum albumin, BSA) for 16-20 hours prior to stimulation. Cells were then stimulated ± PRL (250ng/mL) at 37°C for the given time points. Cells were then washed with ice-cold 1x phosphate-buffered saline (PBS), and harvested on ice using the aforementioned lysis buffer (Section 4.10). Lysates were then subject to 3 rounds of sonication by pulsing on a ThermoScientific probe sonicator at power setting 4, and eluted at 90C for 10 minutes. Protein concentration was assessed via BCA assay, per the manufacturer's protocol. Downstream signaling activation events were then assessed via IB, using the antibodies listed in Table 3.

4.12 Immunoblot

All IB experiments were carried out as such: 50-200 ug of protein (protein of interest-dependent) were loaded onto a 7% SDS-PAGE gel. Samples were run for a sufficient length of time to allow for resolving between respective proteins of interest (on average, 45 min - 2 hours). Samples were then transferred to a polyvinylidene difluoride (PVDF) membrane using the Trans-Blot Turbo System (BioRad) using an appropriate transfer setting (as determined by the molecular weight(s) of the protein(s) of interest). Membranes were then blocked for one hour at room temperature. Regarding blocking buffers, 5% BSA was used for phospho-protein IBs; 5% milk was used for all other IBs. Membranes were then incubated with primary antibody for either one hour and room temperature or overnight (14-18 hours) at 4°C. Membranes were then washed 3x with 1x tris-buffered saline with Tween20 (TBST) for 5 min., followed by incubation with secondary antibody for one hour at room temperature.

Membranes were then subject to a second round of 3x washes with 1x TBST for 5 min., and all subsequent imaging was performed using an ImageQuant apparatus (GE). All band intensity and densitometry quantifications were carried out using the manufacturer-provided ImageQuant TL (GE) general image analysis software. Band intensities were normalized to the loading control unless otherwise stated.

4.13 Generation of a custom hPRLrI polyclonal antibody

An hPRLrI-specific polyclonal antibody (pAb) was generated by and purchased from New England Peptide (NEP; Gardner, MA). New Zealand White SPF rabbits were thrice immunized with a peptide corresponding to residues 331-346, located on the C-terminus of hPRLrI (Ac-C^{331}KEHPSQEREQRQAQEA^{346}-amide). Pre-immunization/first bleed samples from two different rabbits were provided, to test the preliminary efficacy of this antibody. Unpurified sera was additionally sent, as a further quality control measure. Once efficacy was confirmed, affinity purification of antibody from sera was performed by NEP to yield the purified hPRLrI antibody. The antibody was diluted by the manufacturer in PBS (pH 7.4), to yield a final concentration of 1mg/mL. Upon arrival, the antibody was thawed on ice, aliquoted (200uL and 20uL), and stored at -80°C.

4.14 Immunohistochemistry

Tissues were subject to formalin fixation and paraffin embedding (FFPE) by the VCU Mouse Model Core Facility and sectioned at 0.5uM sections using a Kedee KD2258 microtome (Harrell Lab). Sections were adhered to Superfrost(R) Plus Micro Slides (VWR, #48311-703), and allowed to dry overnight at room temperature. The following day, the paraffin was melted at 60°C for 30 minutes, using a slide warmer (C&A Scientific, Premiere XH-2002; Harrell Lab). Tissue deparaffinization

and rehydration were carried out as such, and all steps were performed at room temperature (rt): 3x 10" xylene immersions, 2x 5" 100% ethanol immersions, 2x 5" 95% immersions, 5" in 80%, and a final 5" immersion in ddH_2O. For the stringent fixation protocol (i.e. that which was used for the hPRLrI polyclonal ab), an extra 30" fixation step using 10% formalin (Sigma-Aldrich, #HT501640-19L). Antigen retrieval was carried out as such: 20x citrate buffer (pH 6.0, Thermo Fisher Scientific, #005000) was diluted to 1x in ddH_2O, and chilled to 4°C. Slides were then immersed in this 1x citrate buffer solution. 500mL dH_2O was used to fill the bottom of the pressure cooker (Pascal DakoCytomation), in which the chilled coplin jar was placed, the lid was secured, and the pressure valve was closed. The cycling protocol used was: 20" temperature and pressure increase to eventual 125C and 18-20 psi for 30 seconds, and then gradually cooled to 90C while the pressure was also slowly released. The slides were then immediately immersed in ddH_2O for 5". Antigen retrieval buffer was reused up to a single time before disposal. Endogenous peroxidase activity was inactivated for 20" in 3% (in 1x PBS) H_2O_2, followed by a 5" immersion in ddH_2O and 5" in 1x PBST. Slides were then placed into a humidity chamber, excess PBST was removed using a KimWipe (KimTech), and a circle was drawn around each section using a liquid blocker mini pap pen (Life Technologies, #008877). Slides were then blocked with 250-300uL 10% NGS (Thermo Fisher Scientific #50-062Z) for 1 hr at room temperature in said humidity chamber. Slides were then immersed in PBST for 5". hPRLrI primary antibody was used at 1:12,500 in 10% normal goat serum (NGS) and incubated overnight (18-20 hours) at 4°C in the humidity chamber. 250-300uL of secondary antibody (Signal Stain Boost HRP-Rabbit secondary, CST #8114P or S) was incubated for 1 hr at room temperature in a humidity chamber. Slides were then incubated in PBST for 5". Peroxidase substrate incubation (SignalStain DAB Substrate Kit, CST #8059P, 3:7 substrate to diluent; 100-200uL) was

performed at room temperature for 1 minute, and slides were stained in a stepwise fashion (e.g. performed one at a time to ensure individual timing accuracy). Slides were then dipped in ddH_2O and incubated in fresh ddH_2O for 5", being careful to minimize exposure to light. Intensity and efficacy of DAB staining was assessed using a light microscope before proceeding. Slides were then hematoxylin (Gill #3) counter-stained by immersing in the dye for 5 seconds, then incubating in tap water for 5". Slides were then dehydrated using the following procedure: 3" in 80% ethanol, 3" in 95% ethanol, 2 5" incubations in 100% ethanol, and 2 10" incubations in xylene. Slides were mounted using Permount (Fisher #SP15-100), and cured overnight at room temperature before slide cleaning with xylene and scanning by the VCU Mouse Model Core Facility utilizing the Vectra®Polaris™ slide scanner and imaging system.

4.15 Hematoxylin and eosin

The hematoxylin and eosin (H&E) protocol used was adapted from that of Shannon E. Hedrick. Tissue deparaffinization and rehydration was carried out as such, in the given immersions for the designated amount of time (all procedural steps were carried out at room temperature): 10" in xylene, 5" in xylene, 5" in xylene, 3" in 100% ethanol, 3" in 100% ethanol, 3" in 95% ethanol, 3" in 80% ethanol, and 5" in dH_2O. For hematoxylin (Gill #3, Sigma #GHS316) staining and blueing, slides were immersed for 5", followed by 5" immersion in tap water. An appropriate level of staining was confirmed under a light microscope before proceeding to eosin staining. For the eosin (Eosin Y, 5% weight in water, Sigma #318906) counterstain, slides were immersed for 2", followed by 2" immersion in tap water. Again, an appropriate level of staining was confirmed under a light microscope. For tissue rehydration, slides were immersed in 95% ethanol for 1", 100% ethanol for 1", 100% ethanol for 1", xylene

for 3", and a final xylene immersion for 10". Slides were mounted using Permount (Fisher #SP15-100), and allowed to cure overnight in the fume hood. Slides were then cleaned using xylene and scanned by the VCU Mouse Model Core Facility using the aforementioned scanner.

4.16 Immunoprecipitation

Adherent cells were first rinsed in ice-cold 1x PBS, and scraped in ice-cold co-immunoprecipitation buffer (Tris-HCl pH 7.4, 150 mM NaCl, 1 mM EDTA, 0.1% Triton X-100, 5% glycerol, 1% Phosphatase Inhibitor Cocktail 2, and 1x Protease Inhibitor). Cells were lysed and pelleted at 12,000 g for 10 min at 4°C. Supernatants were transferred to a new tube. In all cases, 5% input was saved for IB analysis before 4 μg of hPRLrI pAb was added and incubated overnight. Anti-IgG2a antibody was utilized as a control. 50 μl of Dynabead protein G magnetic beads (Thermo Fisher Scientific, Waltham, MA) were added for 1 h at 4°C and samples were collected on a magnetic particle concentrator (DynaMag-2 Magnet, Themo Fisher Scientific) and washed three times in fresh IP buffer. Bound proteins were recovered in 2x Laemmli buffer and run on a 7% SDS-PAGE gel followed by WB analysis.

4.17 Normal tissue microarray generation

A list of potential organs was created based on *Kline et al.* 1999, wherein expression of hPRLrI across a variety of normal tissues was assessed via Northern blot[157]. An APBU (VCU pathology database beginning in the 1990s) search was performed to identify benign representations of each relevant organ, choosing both male (M) and female (F) cases. All cases were arbitrarily chosen from 2005. Once cases were chosen, slides and blocks were examined by Patricija Zot, M.D. (VCU) to ensure each was the best representation of normal tissue for that respective tissue. From those selections,

a custom tissue microarray (TMA) was generated, each sample in triplicate.

4.18 Breast cancer tissue microarray scoring

A breast cancer TMA (n=250) was obtained from the VCU Department of Pathology. Slides were stained using the custom hPRLrI pAb, following the protocol enumerated in Section 4.14. Stained tissue samples were scored using the Allred scoring system (% positive x staining intensity) by Patricija Zot, M.D. (VCU).

4.19 Mice

NOD.Cg-*Prkdc*^{scid} *Il2rg*^{tm1Wjl}/Szj (NSG) were preliminarily purchased from the VCU Cancer Mouse Model Core Facility. All additional NSG mice required for *in vivo* studies were provided as a generous gift from J. Chuck Harrell, Ph.D. (VCU).

4.20 Xenograft studies

All *in vivo* studies were carried out using 5-7 week old female NSG mice (Section 4.19). Cell numbers used were as follows: 2x10^6 MCF10A/MCF10AT hPRLr isoform over-expressing cells, 1.5X10^6 MCF7 scRNA/hPRLrI KD cells. Cells were suspended in 1x PBS and subsequently mixed with Matrigel, to reach a final PBS/cell:Matrigel ratio of 1:2, with a final volume of 100uL/injection. Mice were anesthesized using isofluorane, and cells were injected bilaterally into the fourth set of mammary glands. For MCF7 xenografts, an estrogen pellet was concurrently implanted subcutaneously, between the scapulae. Following injection, tumors were palpated daily until a volume of approximately 10mm^3 was reached. Tumors were then measured via caliper thrice weekly, alongside thrice weekly mouse weighs. Endpoint was as dictated in the approved Institutional Animal Care and Use Committee (IACUC) protocol (total tumor burden $\leq$ 2cm^3, $\geq$ 10% reduction in body weight, or obvious moribund

behavior). At endpoint, mice were euthanized via CO_2 asphyxiation followed by cervical dislocation. All tumors were harvested following euthanasia: one full tumor was subject to FFPE, while the contralateral tumor was bisected, and one half was snap frozen in liquid nitrogen while the other was placed in RNA later for potential future studies. All visceral organs, brain, femur, and axillary lymph nodes were additionally harvested for FFPE and microscopic examination for micrometastases.

4.21 Estrogen pellet implantation survival surgery

All surgical procedures were performed in accordance with VCU IACUC Care and Use Guidelines. All surgical tools were autoclaved prior to use, and estrogen pellets were submerged in 1x PBS at 37°C overnight prior to implantation. Mice were induced under 5% isoflourane with oxygen set to 1-2 L/min. Toe pinch was used to confirm lack of responsiveness. Mice were maintained at 2% isoflourane, and ophthalmic lubricant was applied. The mid-scapular incision site was shaved, and Meloxicam SR (4mg/kg) was administered subcutaneously. The incision site was cleaned using three cycles of betadine followed by ethanol. An additional toe pinch was administered to confirm lack of responsiveness. The operating surgeon was then scrubbed in, and a sterile drape was placed over the mouse with a 1 inch x 1 inch window cut in the center of the drape. A small incision was made posterior to the scapulae using a scalpel, just larger than the diameter of the estrogen pellet. Within the incision, a small pocket was made using a hemostat. The pellet was inserted into the pocket using forceps, and the incision was closed using a wound clip. Each mouse was then monitored for 30 minutes, and once fully recovered (BAR; bright, allert, responsive) the mouse was placed back in its cage. Wound clips were removed 10-14 days post-surgery.

4.22 TCGA RNAseq analysis for hPRLr isoform-specific expression

Access to controlled TCGA data was obtained through dbGap in September 2019, by providing a brief Research Use Statement (RUS), describing the intended scientific use. RNAseq BAM files were downloaded from the Genomic Data Commons (GDC) TCGA-BRCA project on 10/28/2019[117]. To expedite processing, BAM files were first filtered for all reads aligned to chromosome 5 then this subset was converted to FASTQ format using SamTools v1.9[173]. Reads were aligned to the GRCh38 version of the human transcriptome using STAR v2.7.3a[84]. The Salmon v0.12.0 quant mode was used to obtain read counts and transcripts per million reads (TPM) measures for each transcript[214]. Patients with expression of the target transcripts hPRLrL (ENST00000618457.5) and hPRLrI (ENST00000619676.4) were verified visually using Integrated Genome Browser based on read alignment covering or spanning, respectively, the documented differential splice junction (corresponding to bp 1010-1581 of the hPRLrL ORF).

4.23 Global differentially-expressed genes analysis

The pre-processed RNAseq HT-Seq-count gene expression values were downloaded from the GDC TCGA-BRCA project on 2/26/2020. Cases were grouped by their ratio of hPRLrI:hPRLrL expression, stratifying by tertile, whereby the top (n=67) and bottom (n=67) tertiles were compared to obtain relevant differentially expressed genes (DEGs). Values were imported into R v3.6.0 for analysis with DESeq2[185,230]. Genes with a total read count across all conditions of 10 or less were removed prior to analysis due to low expression. DESeq2 results were filtered by removing genes with an adjusted p value (padj) > 0.01, an average normalized read count across all conditions (baseMean) < 10, and a log2 fold change > 1.5 or < -1.5.

DEG signatures were determined via Gene Set Enrichment Analysis (GSEA; Broad Institute)[263].

4.24 Statistical analyses

Statistical tests (t-tests, ANOVAs) were carried out using PRISM (GraphPad, San Diego, CA). For the z-tests used in the TCGA demographics data (Table 10), the following equation was used:

$$\frac{\bar{x} - \mu}{\frac{\sigma}{\sqrt{n}}}$$

These variables defined are: $\bar{x}$, sample average; μ, population average; σ, standard deviation; n, sample size.

4.25 Primer design and Tm optimization (gradient PCR)

The gene sequence of interest was input into ApE(M. Wayne Davis, The University of Utah) as a first line approach to obtain % GC content, sequence length, and Tm. OligoAnalyzer (IDT, Coralville, IA) was used to assess for primer dimers, hairpin loops, and specific melting temperatures (Tms) given unique salt concentrations. The parameters for primer design included:

1. Tm >50°C minimum, >60°C ideally
2. Tms of the forward and reverse primer should be within 5°C of each other
3. 15-40 nucleotides in length, ideally 18-24
4. % GC should be between 50-75%, but should be >60%

5. Primers should begin/end with 2-4 GCs, and all care should be taken to avoid starting with a T

6. For sequencing primers, one primer/kb is necessary

4.26 RNA extraction and purification

All work spaces and gloves were treated with RNase Zap (ThermoFisher Scientific, #AM9780), and unless specifically stated, all steps were carried out at room temperature. Cells were at 90-95% confluence at the time of harvest. Growth media was aspirated, and cells were washed with 1x PBS. 1mL of TRIzol^{TM} reagent (ThermoFisher Scientific, #15596026) was used per 10cm^2 of culture dish surface area (i.e. 1mL for a 35mm dish, 3mL for a 60mm dish, and 8mL for a 100mm dish). Samples were homogenized by pipetting the mixture up and down 1-2 dozen times. This homogenized sample was then incubated at room temperature for 5 minutes, and then transferred to a 15mL conical. 0.2mL chloroform/1mL TRIzol^{TM} was added to the homogenized sample, shook vigorously for 15 seconds, and incubated at room temperature for 3 minutes. Samples were then centrifuged for 20 minutes at 10,000xg, 4°C. The top, clear (aqueous) phase was carefully pipetted off into a new, clean 15mL conical. 0.5mL isopropanol/1mL TRIzol^{T}M was added to this aqueous phase, incubated at room temperature for 10 minutes, and centrifuged at 10,000xg for 15 minutes, 4°C. Following this centrifugation, RNA was pelleted at the bottom with the appearance of a small, semi-opaque white mass. The supernatant was aspirated off, being careful to avoid the pellet. The RNA pellet was washed with 75% ethanol, and the sample was centrifuged at 7,500xg for 5 minutes at 4°C. The ethanol was carefully aspirated off, and the sample was let to airdry for 5-10 minutes at room temperature. The final RNA pellet was resuspended in RNase-free water.

4.27 Cloning

PCR was used to amplify the insert, based on the appropriate respective Tm (Table 22). Band extraction, isolation, and purification was performed using the E.Z.N.A. Gel Extraction Kit (Omega Bio-tek, VWR, #101318-970). Amplicons were subject to a secondary round of purification using a Qiagen PCR purification kit (#28104). Purified amplicons were sent to Eurofins (Luxembourg) for sequencing. Both insert and vector were double-digested, per the respective protocol(s) of the appropriate restriction enzyme The vector was then subject to treatment with recombinant shrimp alkaline phosphatase (rSAP, #M0371S; New England Biolabs, NEB) per the manufacturer's specifications, followed by heat inactivation. Both the digested insert and vector were run on a 2% agarose gel, and bands were isolated and purified in the same manner enumerated above. Insert and vector were ligated at room temperature using T4 DNA ligase (NEB, #M0202S), and immediately transformed into competent cells (discussed below). All cloning results were confirmed by final sequencing analysis, and sequencing reads were mapped against the respective gene of interest for manual confirmation using Geneious software (Biomatters, Aukland, New Zealand).

4.28 Bacterial transformation and Mini/Maxiprep

Agar plates were made using 15g of agar mixed with 25g of LB in ddH_2O. This solution was autoclaved, subsequently cooled to 60°C, and carbenicillin (50ug/mL) was introduced. This solution was poured into petri dishes (10-20mL/dish), allowed to solidify at room temperature, parafilmed, and then stored at 4°C for up to 12 weeks. For bacterial transformations, either DH5α (ThermoFisher Scientific) or XL10 Gold (Agilent) competent cells were used, per the manufacturer's instructions. Bacterial plates were incoculated, colonies were grown at 37°C for 16-20 hours, and individual

colonies were selected for subsequent mini-prep. Mini- and/or maxiprep (Qiagen) was/were performed in accordance with the manufacturer's instructions. Once DNA was purified, samples were sent to Eurofins Scientific (Luxembourg) for DNA sequencing confirmation. Purified DNA was stored long-term at -80°C. Transformed bacterial inoculants were homogenized 1:1 with glycerol, and stored at -80°C as well.

4.29 Hand-casting gels

For all IB applications, either 7.5% SDS-PAGE gels were either purchased (Bio-Rad, #4561026) or 7% gels were hand-cast. For hand-casting gels, 5.1mL ddH_2O, 2.3mL acrylimide/bis, 2.5mL resolving gel buffer, and 100uL SDS were mixed and degassed for 15 min. 50uL 10% APS and 5uL TEMED were added, and the solution was poured into the gel mold. The gel polymerized at room temperature for 1 hr. Overtop the stacking layer (5.1mL ddH_2O, 2.3mL acrylimide/bis, 2.5mL stacking gel buffer, 100uL SDS, 50uL 10% APS and 10uL TEMED) was laid, using the same method as listed above. Gels were wrapped in running buffer-soaked paper towels, and stored at 4°C for up to 2 weeks.

4.30 Antibodies

Table 3. Primary antibodies

Antibody target	Manufacturer	Catalog #	IB concentration	IHC concentration
hPRLr ECD	Invitrogen	35-9200	1:1000	NA
hPRLr (total)	Santa Cruz Biotechnology	sc-377098	1:1000	NA
pY694-Stat5a	Cell Signaling	9359S	1:1000	NA
Stat5a	Santa Cruz Biotechnology	sc-1081	1:1000	NA
pY1007/1008-Jak2	Cell Signaling	3776S	1:500	NA
Jak2	Cell Signaling	3230S	1:500	NA
pY202/204-p44/42	Cell Signaling	9101S	1:1000	NA
p44/42	Cell Signaling	9102S	1:1000	NA
Vinculin	Abcam	ab129002	1:1000	NA
Vinculin	Bio-Rad	MCA465GA	1:1000	NA
hPRLrI pAb	New England Peptide	NA	1:5000	1:12500
Src	Cell Signaling	2108S	1:1000	NA
pT180/pY182-p38	Cell Signaling	9211S	1:1000	NA
p38	Cell Signaling	9212S	1:1000	NA
pS217/221-MEK1/2	Cell Signaling	9121S	1:1000	NA
MEK1/2	Cell Signaling	9122S	1:1000	NA
KRAS	Cell Signaling	53270	1:1000	NA
V5 tag	ThermoFisher Scientific	R960-25	1:1000	NA

Table 4. Secondary antibodies

Product name	Manufacturer	Catalog #	IB concentration	IHC concentration
Anti-mouse IgG	Cell Signaling	7076S	1:2500	NA
Anti-rabbit IgG	Cell Signaling	7074S	1:2500	NA
SignalStain Boost IHC Detection Reagent	Cell Signaling	8114P	NA	1x

4.31 Tissue Culture Reagents

Table 5. Tissue Culture Reagents.

Reagent	**Manufacturer**	Catalog number	**Stock solution**	Storage temperature
DMEM	Life Technologies	11965092	NA	4°C
DMEM/F12	ThermoFisher Scientific	11330-032	NA	4°C
Ham's F-12K	ThermoFisher Scientific	21127-022	NA	4°C
Opti-MEM	ThermoFisher Scientific	31985070	NA	4°C
DMEM/F12 phenol red free	ThermoFisher Scientific	21041025	NA	4°C
PBS pH7.4	Quality Biological	119-069-491	10x	rt
Fetal bovine serum	Corning	MT35011CV	1x	-20°C
Horse serum	Atlanta Biologicals	S1215OH	1x	-20°C
Penicillin/streptomycin	ThermoFisher Scientific	15140-122	1x	-20°C
Hydrocortisone	Sigma-Aldrich	H0888	1mg/mL	-20°C
Epidermal growth factor	ThermoFisher Scientific	PHG0311L	100ug/mL	-20°C
Cholera toxin	Sigma-Aldrich	C8052	1mg/mL	4°C
Insulin	Sigma-Aldrich	10516	NA	4°C
Versene	ThermoFisher Scientific	15040-066	1x	4°C
Trypsin	Quality Biological	118-086-721	10x	-20°C
Lipofectamine	ThermoFisher Scientific	L3000015	NA	4°C
Polybrene	Sigma-Aldrich	TR-1003-G	1mg/mL	-20°C
Prolactin	Gift of Anthony Kossiakoff Ph.D. (University of Chicago)	NA	250ng/uL	-80°C
Bovine serum albumin	Sigma-Aldrich	10735078001	1%	4°C
MTT	ThermoFisher Scientific	AC15899-0010	5mg/mL	4°C
DMSO	ThermoFisher Scientfici	MT-25-950-CQC	NA	rt
Cycloheximide	Sigma-Aldrich	C7698-1G	100ug/uL	-20°C
Puromycin	Gemini Bio-Products	400-128P	1mg/mL	-20°C
Noble agar	Sigma-Aldrich	9002-18-0	NA	rt

CHAPTER 5

GENERATION AND CHARACTERIZATION OF A NOVEL POLYCLONAL HPRLRI ANTIBODY

5.1 Limitations of currently available hPRLr antibodies

While considerable research and progress has been made regarding human prolactin receptor biology since its initial cloning in 1989, the majority of research performed to date has been focused on the full-length, long form of the receptor (hPRLrL)[149]. hPRLrL retains all necessary extracellular domains for ligand interaction, in addition to all necessary intracellular components for downstream signaling events. Inasmuch, characterization of the different hPRLr isoforms has been limited, for it has long been dogma that the only truly fully active form of the receptor is the long form, and that the other isoforms are either inert, significantly reduced in activity, or dominant negative (Section 2.2.4)[63,135,156,157,158]. As a result, reagents to study the differentially-spliced hPRLr isoforms are incredibly limited. To date, all commercially-available hPRLr antibodies recognize portions of either the hPRLr ECD or ICD, respectively, which are recognized by most if not all receptor isoforms. While these antibodies may by used for IB purposes to examine individual isoform expression (isoforms may be parsed by respective molecular weight), they are insufficient for isoform-specific IHC.

The similarities between receptor isoforms represent an additional limitation to studying their respective biologies. While differential splicing events can introduce novel coding sequence unique from the wild-type form which would invariably assist in the development of isoform-specific reagents, many of the annotated hPRLr isoforms

are characterized only by a loss of genetic material. Those variants include the $\Delta S1$ form as well as the PRLBP[156,158]. Fortunately for the purposes of this dissertation project, the differential splicing event that generates hPRLrI creates a unique 13 amino acid tail, the I-Tail, which was adequate in length to create a pAb specific against this region (Section 4.13).

5.2 Antibody efficacy, specificity, and characterization

Our lab worked with New England Peptide (NEP; Gardner, MA) to generate this hPRLrI antibody. Two separate rabbits, J8088 and J8084, were inoculated with the antigen-containing peptide enumerated in Section 4.13. Pre-immune serum and and 1st bleeds were sent of both rabbits, and used to probe lysates of CHO-EV transfectants (negative control) and T47D (Figure 7). The pre-immune serum was used to assess the background level of signal and non-specific binding (Figure 7A, B). The black arrow in Figure 7A represents the presumed band of interest, running at approximately 50kDa. The first bleed obtained from rabbit J8088 had significantly less background, and an easier distinction of the band of interest. Rabbit J8084 did not have a clearly discernible band of interest at the appropriate molecular weight, thus rabbit J8088 was selected for downstream applications.

In order to confirm that the band of interest demonstrated in Figure 7A was in fact hPRLrI, a blocking peptide experiment was performed. The blocking peptide is comprised of the antigenic sequence used to hPRLrI pAb, and if this antibody has high specificity, the band of interest should diminish in intensity following pAb/blocking peptide co-incubation (the blocking peptide would sequester the antibody from interacting with membrane-bound protein). As is observed in Figure 7C, co-incubation with the blocking peptide was sufficient to completely ablate signal of the band of interest, confirming the specificity of this approach. Additionally, no cross-reactivity

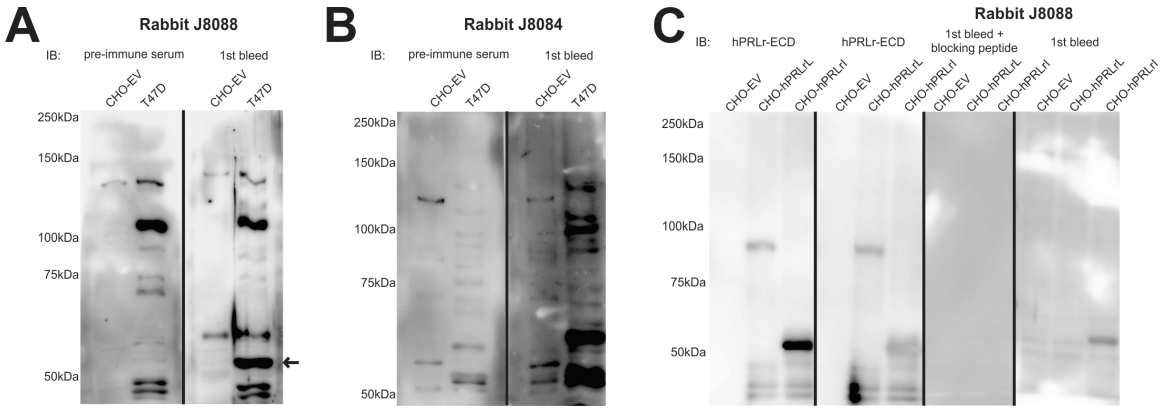

Fig. 7. Confirmation of hPRLrI pAb approach. Pre-immune serum and first bleeds of two different inoculated mice (**A**. and **B**.) were provided by NEP. These were used as preliminary confirmation of approach for IB purposes. CHO-EV was utilizes as the negative control, T47D as the positive control. The band of interest at 50-55kDa in the positive control lane, and not that of the negative control, was observed using only the first bleed from Rabbit J8088 (black arrow). **C**. A blocking peptide experiment was performed (third blot from the left) using J8088 first bleed. No cross-reactivity was observed with hPRLrL.

with hPRLrL was observed.

Once the band of interest was confirmed to be hPRLrI, the antibody was purified by NEP using affinity chromatography, and sent to our lab for downstream applications. Using the affinity-purified hPRLrI pAb, we optimized working concentration for both IB (1:5000 primary; Figure 8A) and IHC (1:12,500 primary; Figure 9) purposes. Additionally, the same blocking peptide assay as above was performed, to confirm specificity of the antibody following affinity purification, for both IB (Figure 8B) and IHC (Figure 9) utilities.

After confirming our hPRLrI polyclonal antibody could be used for both IB and IHC purposes, we were interested in examining its use in IP studies. Considering the initial studies that examined both hPRLrI signaling as well as hPRLrI structure, we hypothesized that hPRLrI would retain the ability to bind both Jak2 and Src, while being unable to interact with Stat5a[157]. Indeed, IP studies using CHO-hPRLrI transfectants grown in complete media confirmed this hypothesis (Figure 10). How-

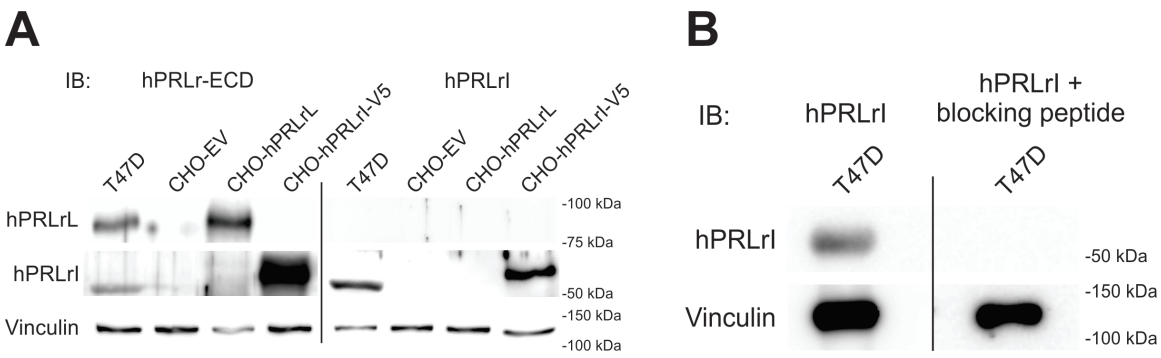

Fig. 8. Specificity of a pAb generated against hPRLrI I-Tail, assessed by IB. An anti-hPRLrI antibody, recognizing the unique hPRLrI I-Tail, was generated and specificity was determined through **A**. IB of T47D and CHO transfectant lysates and **B**. IB of T47D lysates in the presence/absence of an hPRLrI antibody blocking peptide.

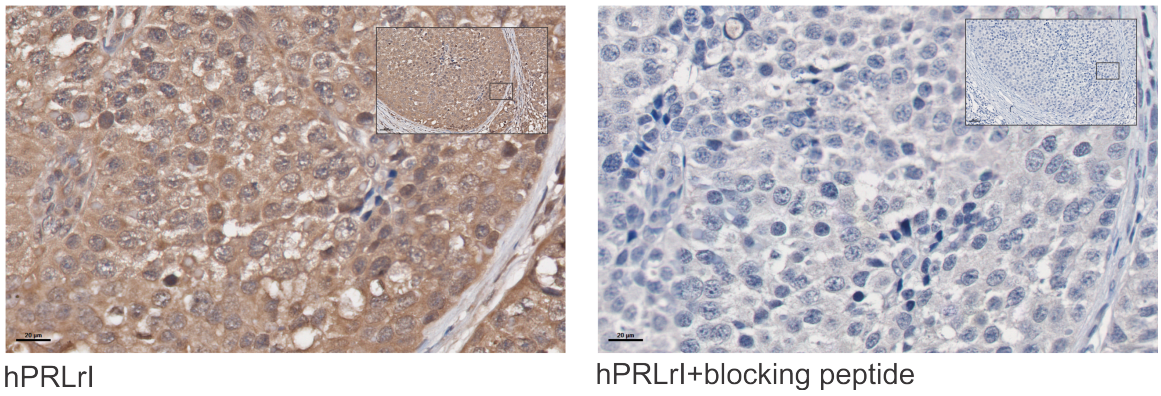

Fig. 9. Specificity of a pAb generated against hPRLrI I-Tail, assessed by IHC. IHC of a human breast cancer tissue sample, in the presence/absence of the blocking peptide.

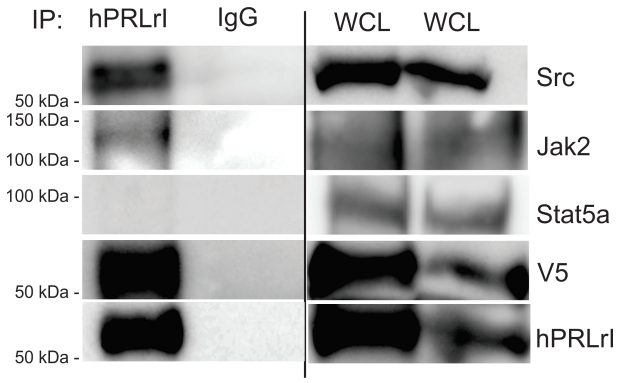

Fig. 10. hPRLrI IP. Our hPRLrI pAb was used to IP for Src, Jak2, and Stat5a interaction with hPRLrI. The hPRLrI construct was linked to a V5 tag, and overexpressed in CHO cells cultured in complete media. n=2.

ever, these results represent only a small subset of the known proteins which bind to and/or interact with hPRLr (e.g. Nek3, Vav2, PI3K, etc.). Therefore additional studies are needed to gain a full understanding of those proteins that interact with this specific splice variant.

5.2.1 Expression in an array of normal tissues

Northern blot analyses have indicated that differential tissue expression of hPRLrI is independent and distinct from hPRLrL, suggesting a unique biological role for the splice variant[157]. Considering that mRNA and protein expression levels rarely have a strong correlation, we were interested to uncover hPRLrI protein expression in an array of normal tissue. To this end, a custom normal TMA was generated (courtesy of Patricija Zot, M.D.), and our pAb was used for IHC. Furthermore, as sex is a biological factor, tissues from both males and females were obtained to assess sex-specific differences. Using this TMA, we found the highest hPRLrI expression in the female kidney, male and female pancreas, male stomach, female liver, female thymus, and uterus (Figure 11). From these data, we were also able to establish a *bona fide* negative control (female bladder) for downstream IHC purposes. This preliminary

characterization of our hPRLrI-specific polyclonal antibody was sufficient to indicate this antibody could be used for subsequent analyses of hPRLrI protein expression, as is discussed in Chapter 8 of this dissertation.

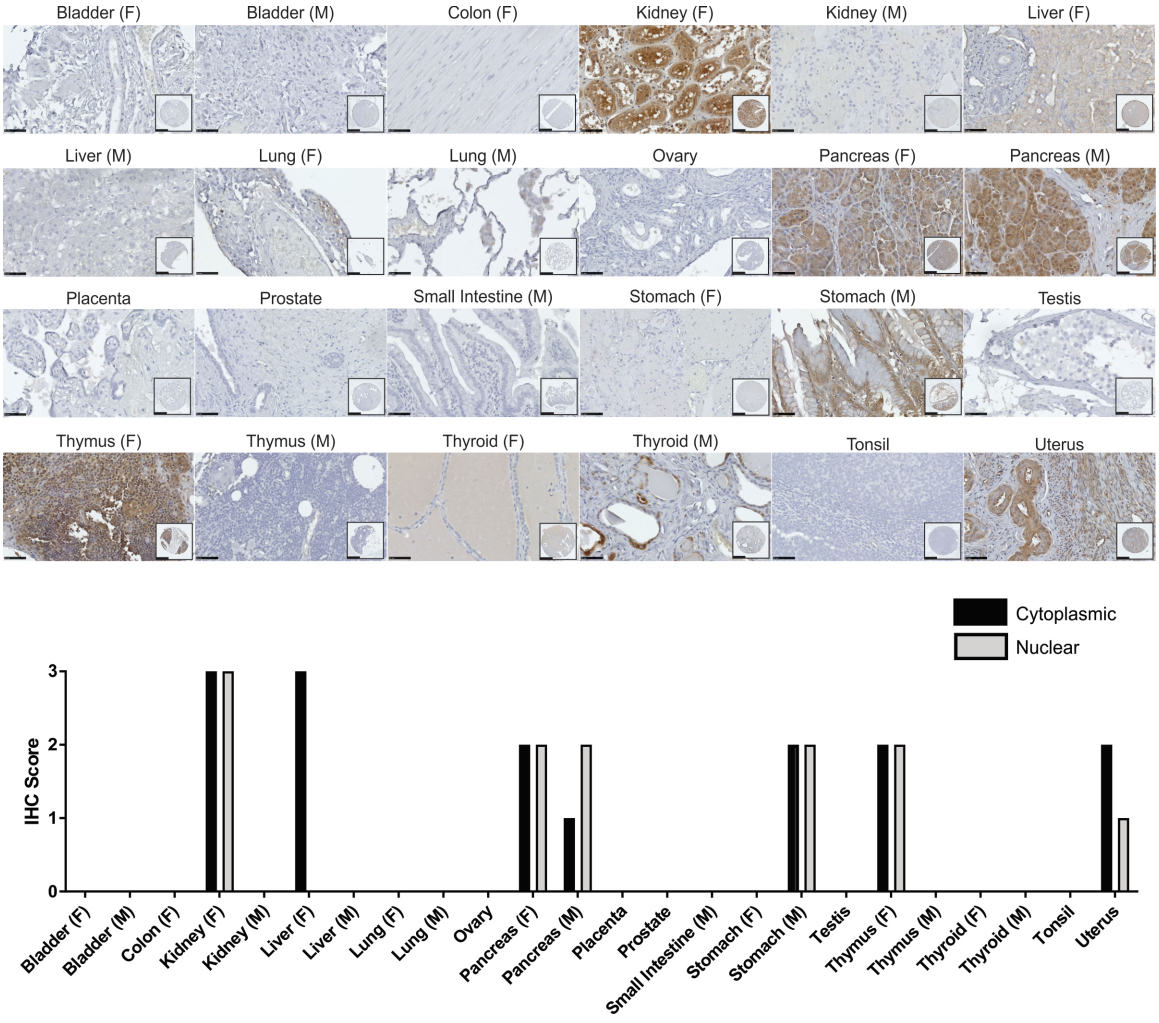

Fig. 11. hPRLrI protein expression in normal tissue. A variety of normal tissues, obtained from both men (M) and women (F), were obtained and used to assess hPRLrI protein expression through IHC. Both cytoplasmic and nuclear staining were assessed.

CHAPTER 6

AIM 1: TO ASSESS THE *IN VITRO* TRANSFORMING POTENTIAL OF HPRLRI CO-OVEREXPRESSION WITH HPRLRL

6.1 Hypothesis

hPRLrI is transforming in normal mammary epithelia, when expressed in concert with hPRLrL, and this transformation is the result of altered hPRLrL+I heterodimer signaling and/or complex stability.

6.2 Results

While a dramatic transforming effect was observed by Griffith *et al.* (2016) with the co-expression of mPRLrT and mPRLrL in MEFs, an examination into both ExAC and TCGA-reposited human breast cancer (BRCA) cohort data indicated there are corresponding hPRLr truncating mutations in less than 2% of human breast tumors. However, the authors failed to realize the homology between mPRLrT and hPRLrI (Figure 6). Specifically, the hPRLrI frameshift start-site aligned in the center of the mPRLrT mutational hotspot, resulting in 90% shared peptide homology and 74% nucleotide homology. Considering this significant degree of similarity between mPRLrT and hPRLrI, we hypothesized that hPRLrI may act in a similarly oncogenic nature in human breast cancer.

In order to assess the role of hPRLrI in breast cancer, respective expression levels of both hPRLrL and hPRLrI were first assessed via IB, in a panel of both breast cancer cell lines as well as patient-derived xenograft (PDX) samples (Figure 12). It was observed that, while the normal basal epithelial breast cell line MCF10A

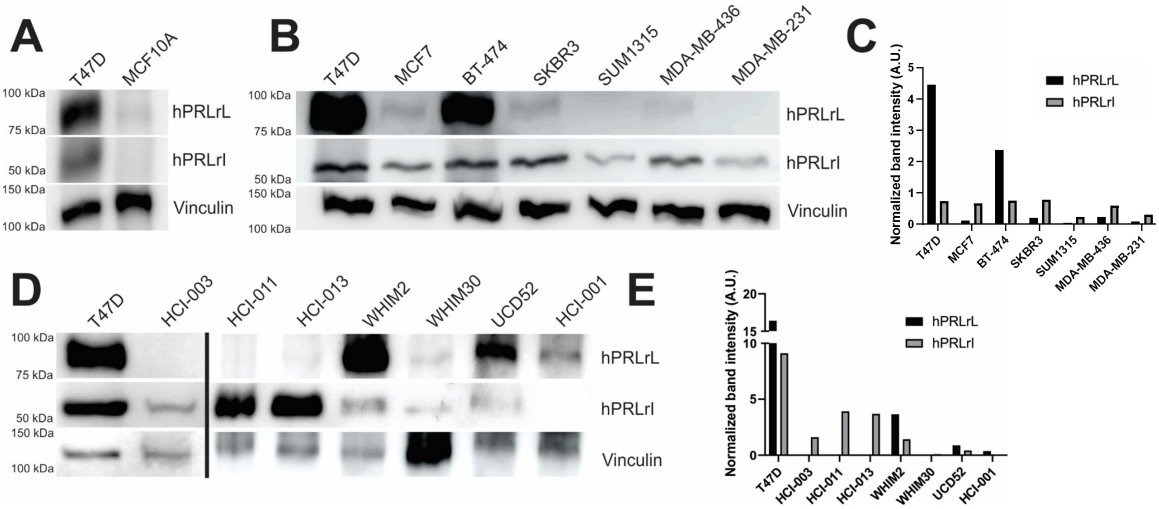

Fig. 12. Expression of hPRLrI in normal and malignant breast cancer cell lines and PDX samples. Protein samples from **A**. luminal breast cell line T47D, normal human breast cell line MCF10A, as well as a panel of both **B, C** breast cancer cell lines and **D, E** PDXs were probed for hPRLrL and hPRLrI protein expression via IB. Respective hPRLr isoform identification was determined by assessing molecular mass (hPRLrL: 90kDa; hPRLrI: 55kDa), as compared to T47D positive control cells.

expresses a low level of hPRLrL, there is little to no hPRLrI expressed. In comparison, there is a significant amount of both isoforms expressed in the luminal breast cancer cell line T47D. Further, while expression of hPRLrL was confined primarily to the luminal breast cancer cell lines, hPRLrI was expressed across all breast cancer cell lines assayed, irrespective of intrinsic subtype (Table 6). Within the PDX panel, a similar trend was observed (Table 7).

Once expression of hPRLrI was confirmed in breast cancer cells, the next reasonable step was to assess if hPRLrI carries a critical function in breast cancer pathogenesis. To this end, we performed isoform-specific known-down (KD) of hPRLrI using two luminal cell lines, MCF7 and T47D. We obtained two shRNA constructs that were designed to span the hPRLrI differential splice junction, and these constructs were introduced into both of these cell lines either individually or in combination (Figure 13; the α-hPRLrI pAb used to this end is characterized in Chapter 5). Using

Table 6. Breast cancer cell line subtypes

Cell line	hPRLrL	hPRLrI	ER	PR	Her2	Molecular subtype
MCF10A	+	-	-	-	-	Normal breast
T47D	+	+	+	+	-	Luminal A/B
MCF7	+	+	+	+	-	Luminal A/B
BT-474	+	+	+	+	+	Luminal B
SKBR3	+	+	-	-	+	Her2-enriched
SUM1315	-	+	-	-	-	Basal-like
MDA-MB-436	+	+	-	-	-	Basal-like
MDA-MB-231	-	+	-	-	-	Basal-like

Table 7. Patient-derived xenograft (PDX) subtypes

PDX ID	hPRLrL	hPRLrI	ER	PR	Her2	Molecular subtype
HCI-003	-	+	+	+	-	Luminal B
HCI-011	-	+	+	+	-	Luminal B
HCI-013	+	+	+	+	-	Luminal B
WHIM2	+	+	-	-	-	Basal-like
WHIM30	+	+	-	-	-	Basal-like
UCD52	+	+	-	-	-	Basal-like
HCI-001	+	-	-	-	-	Basal-like

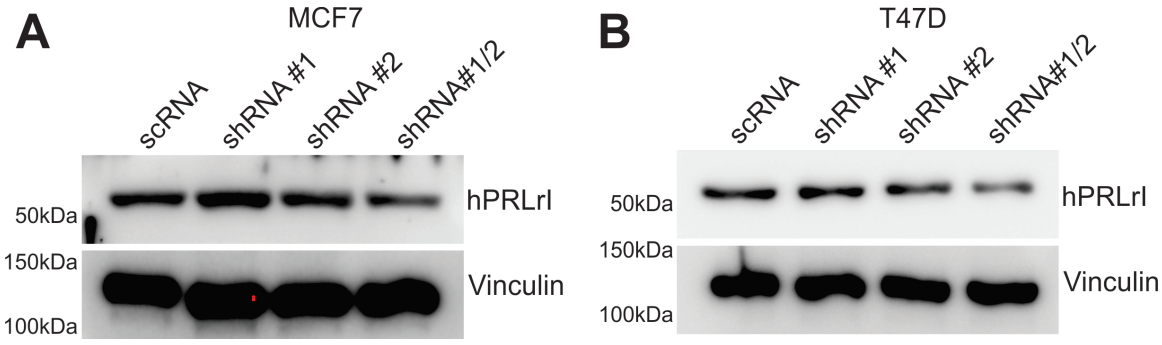

Fig. 13. hPRLrI isoform-specific KD optimization using two different shRNAs constructs. hPRLrI KD was optimized in both **A**. MCF7 and **B**. T47D cells. Two different shRNA constructs were introduced either individually or concurrently, and KD efficiency was determined via IB using our hPRLrI pAb.

both constructs concurrently resulted in the greatest degree of KD, and that approach was utilized moving forward.

Following confirmation that hPRLrI protein expression was inhibited by our shRNA constructs (Figure 14A, B), we moved forward with assessing differential malignant potential. Our first approach examined if hPRLrI loss effected anchorange-independent growth. Following hPRLrI KD, MCF7 cells formed significantly less colonies in soft agar (Figure 14C), and the colonies that did form were slightly but statistically significantly smaller (Figure 14D) than the scRNA control MCF7 cells. We also examined differential proliferation and migration, uncovering that MCF7 hPRLrI KD cells both grew significantly slower (Figure 14E) and migrated less readily (Figure 14F) than the scRNA control. These results indicate that hPRLrI-specific loss is sufficient to reduce malignant phenoypic potential of MCF7 cells *in vitro*.

As a corollary to our hPRLrI KD approach, we also performed hPRLrI overexpression (OE) in an attempt to rescue the phenotype (Figure 15A, B). hPRLrI OE was sufficient to rescue both proliferation (Figure 15C) and anchorage-independent growth (Figure 15D, E), confirming that any unlikely putative off-target effects of our hPRLrI KD were not the cause of the observed change in phenotype.

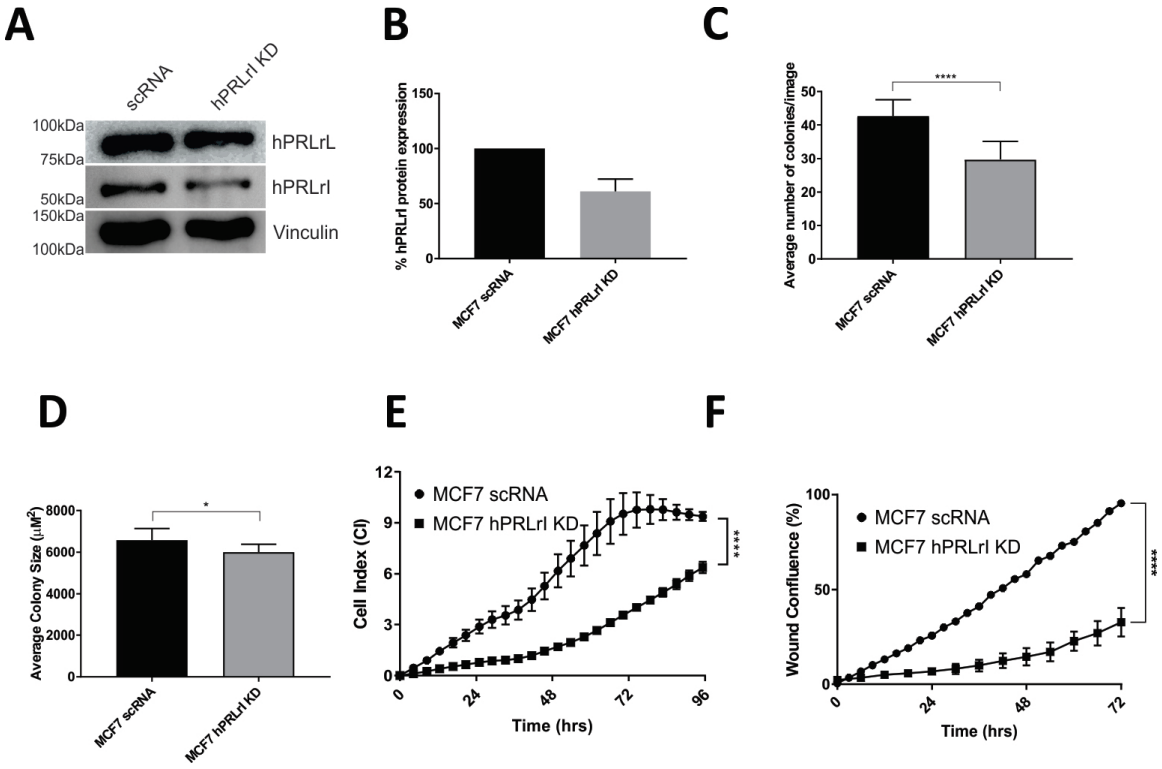

Fig. 14. MCF7 hPRLrI KD *in vitro*. **A**. MCF7 cells were stably transfected with either scrambled RNA (scRNA) negative control or shRNA targeting the hPRLrI splice site. **B**. hPRLrI protein expression was quantified by densitometry. These transfectants were analyzed for differential anchorage-independent growth via soft agar assay, quantifying both **C**. colony number and **D**. colony size, using CellProfiler. Transfectants were further assessed for **E**. proliferative potential and **F**. ability to migrate. *$p < 0.05$, ****$p < 0.001$, n=3.

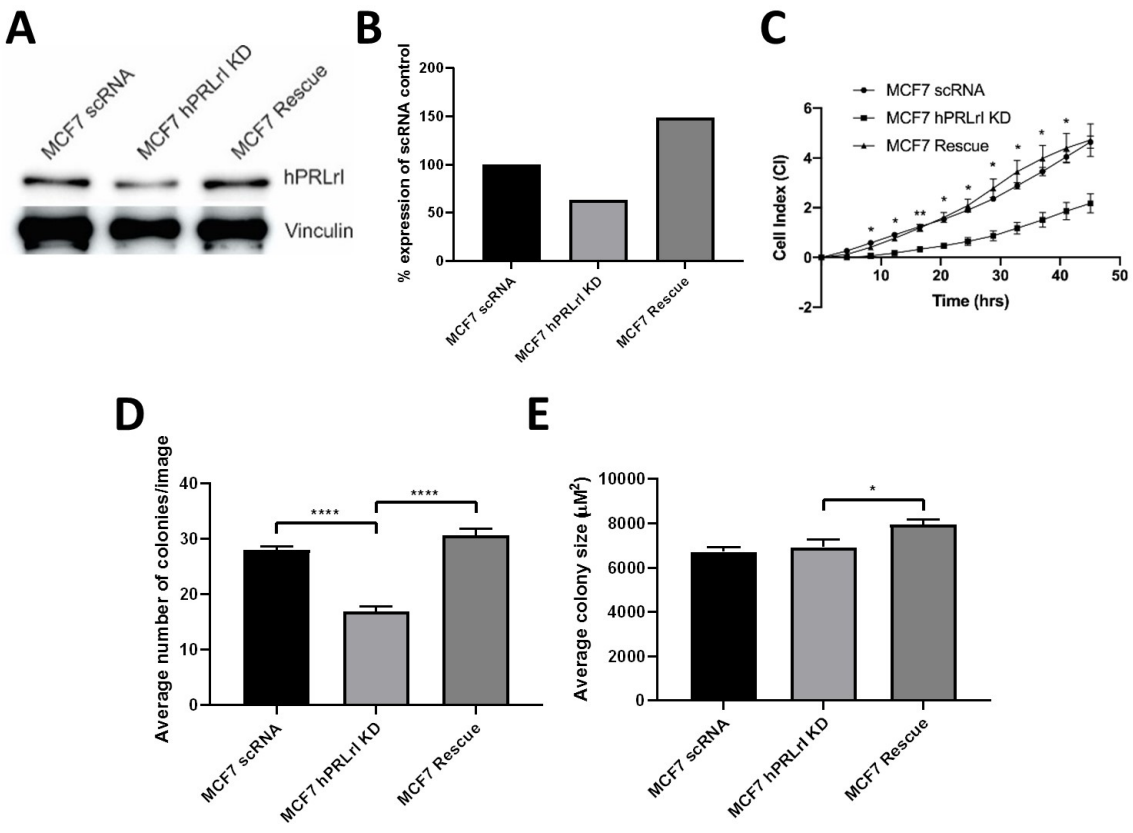

Fig. 15. MCF7 hPRLrI over-expression rescue of KD cells *in vitro*. MCF7 hPRLrI KD cells were stably transfected with hPRLrI cDNA. **A**. Protein expression was evaluated by IB and **B**. quantified by densitometry. **C**. Proliferation was assessed using an xCELLigence apparatus, and rescue of anchorage-independent colony formation was assessed by soft agar, quantifying both D. colony number and **E**. colony size. *$p < 0.05$, **$p < 0.01$, ****$p < 0.001$. n=3.

These assays were repeated using the luminal cell line T47D, in which we also were able to confirm our shRNA constructs did not target hPRLrL (Figure 16A, B). While hPRLrI KD was able to significantly reduce the average number of T47D colony number (Figure 16C), there was no significant difference in colony size (Figure 16D). In examining proliferation and migration, hPRLrI KD significantly mitigated T47D proliferation (Figure 16E), but there was no difference in migration (Figure 16F). Similar to what was observed with MCF7, hPRLrI OE in T47D hPRLrI KD cells was sufficient to rescue the phenotype (Figure 17). However, it should be noted that hPRLrI KD in T47D cells was not entirely sufficient to abrogate the malignant phenotype, as no difference in wound closure was observed (Figure 16F).

Given our *in vitro* hPRLrI KD results, we were interested to examine the effect of hPRLr isoform over-expression in normal human mammary epithelial cells. For our preliminary approach, we utilized the mammary basal epithelial cell line MCF10AT. MCF10AT cells are a partially transformed human breast basal epithelial cell line expressing oncogenic HRAS (G12V), which when xenografted into immunocompromised mice have an invasive carcinoma rate of approximately 25%, and do not metastasize[81]. Furthermore, given the data presented by Griffith *et al.* 2016 suggesting that full-length PRLr co-expression with the truncated form is necessary for the observed transformation, we were most interested in examining the effect of hPRLrL+I co-overexpression in said MCF10AT cells[114]. To this end, MFC10AT cells were stably transfected with either isoform on its own (MCF10AT-hPRLrL, MCF10AT-hPRLrI, respectively), both together (0.5:0.5, MCF10AT-hPRLrL+I), or empty vector (MCF10AT-EV) as a negative control, and protein expression was confirmed by IB (Figure 18A). Following confirmation of overexpression, our MCF10AT transfectants were assessed for their ability to grow in soft agar. Individual hPRLr isoform overexpression slightly yet insignificantly elevated MCF10AT colony forming

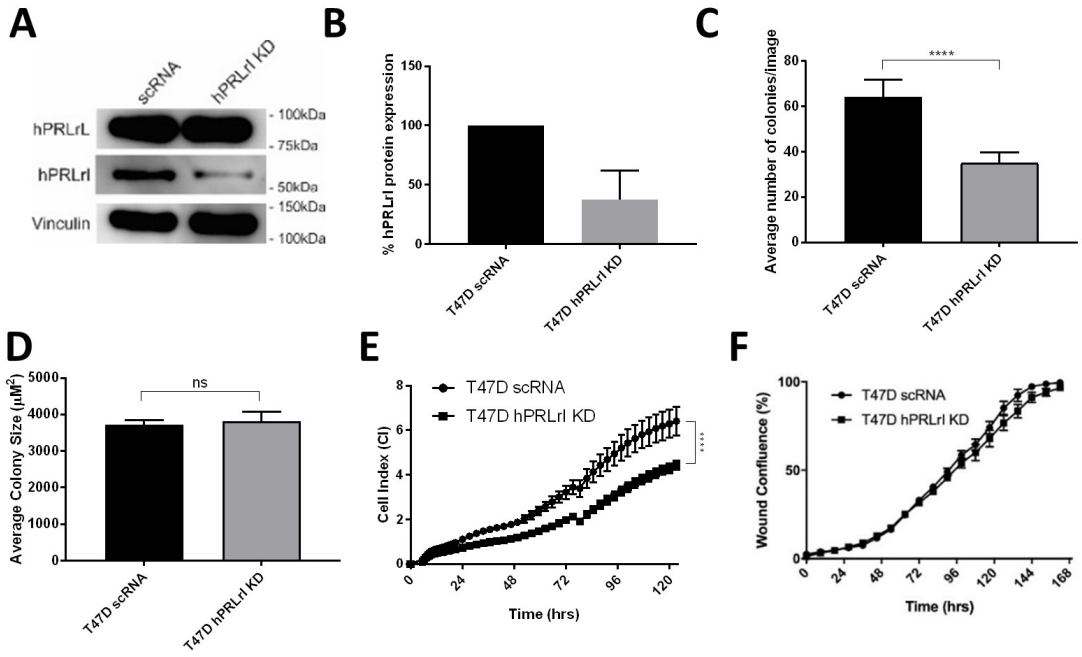

Fig. 16. T47D hPRLrI KD *in vitro*. **A**. T47D cells were stably transfected with either scrambled RNA (scRNA) negative control or shRNA targeting the hPRLrI splice site. **B**. hPRLrI protein expression was quantified by densitometry. These transfectants were analyzed for differential anchorage-independent growth via soft agar assay, quantifying both **C**. colony number and **D**. colony size, using CellProfiler. Transfectants were further assessed for **E**. proliferative potential and **F**. ability to migrate. ****$p < 0.001$, n=3.

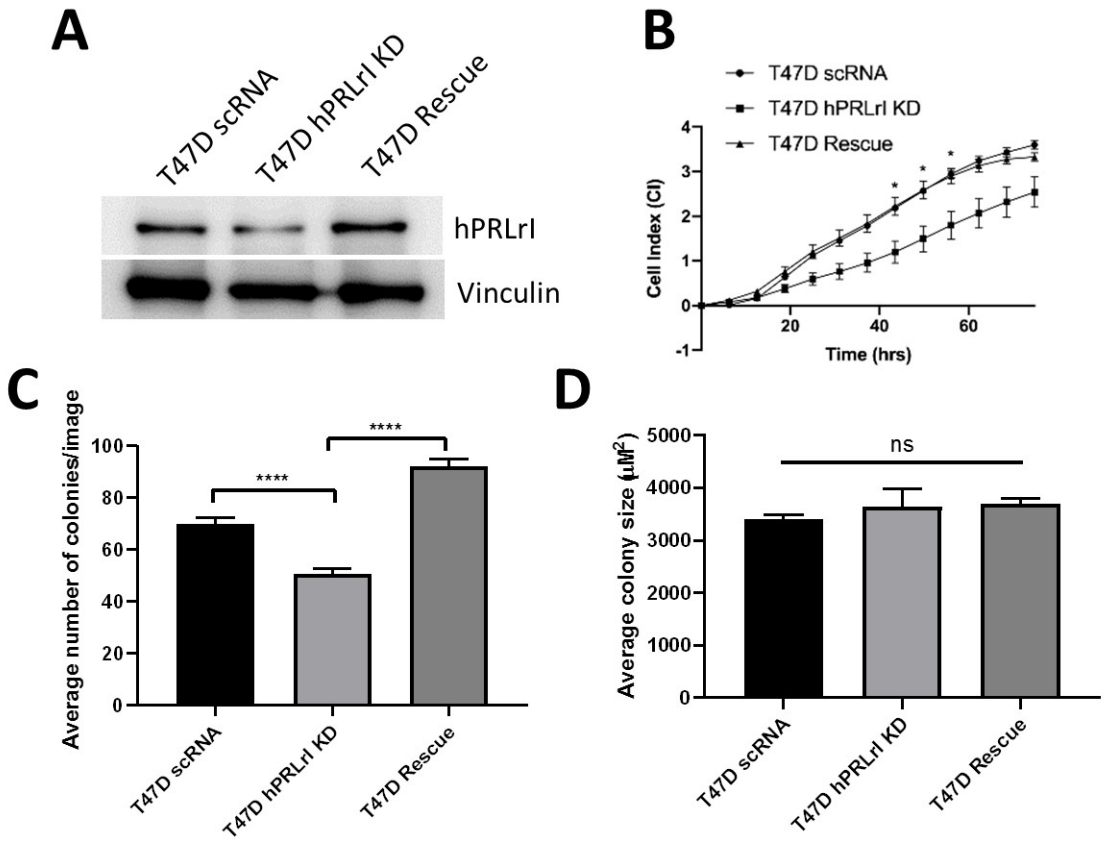

Fig. 17. T47D hPRLrI over-expression rescue of KD cells. T47D hPRLrI KD cells were stably transfected with hPRLrI cDNA. **A**. Protein expression was evaluated by IB. **B**. Proliferation was assessed using an xCELLigence apparatus, and rescue of anchorage-independent colony formation was assessed by soft agar, quantifying both C. colony number and **D**. colony size. *$p < 0.05$, ****$p < 0.001$. n=3.

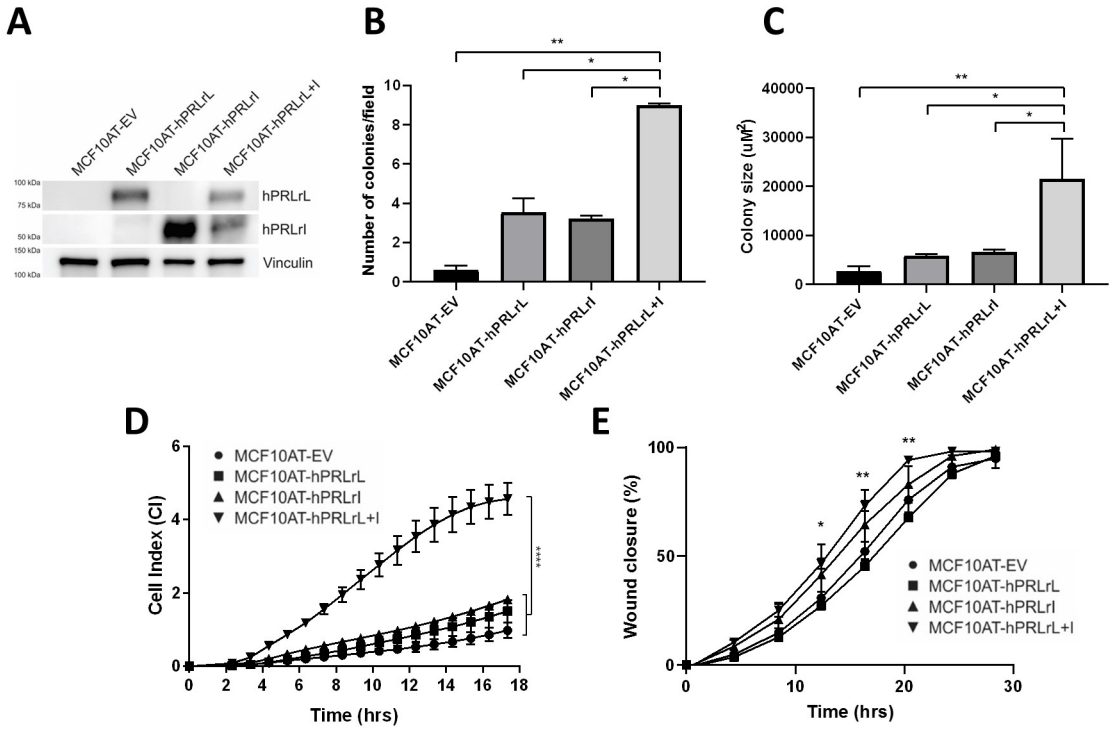

Fig. 18. hPRLrL+I co-overexpression in MCF10AT cells *in vitro*. hPRLrL (MCF10AT-hPRLrL), hPRLrI (MCF10AT-hPRLrI), both isofoms concurrently (0.5:0.5; MCF10AT-hPRLrL+I), or empty vector (MCF10AT-EV) were stably trasfected and expression was confirmed by **A**. IB. MCF10AT over-expression transfectants were grown in soft agar and both **B**. colony number and **C**. colony size were quantified using CellProfiler. **D**. Proliferation was measured using an xCELLigence apparatus, and **E**. migration was assayed for via wound closure using an Incucyte®system. *$p < 0.05$, **$p < 0.01$, ****$p < 0.001$, n=3.

potential, in examining both colony number and size (Figure 18B, C). However, following hPRLrL+I co-overexpression, robust colony forming capacity was observed, which was significantly over that of EV, hPRLrL, or hPRLrI individual expression (Figure 18B, C). Similarly, in examining proliferation (Figure 18D) and migration (Figure 18E), it was uncovered that hPRLrL+I co-overexpression provided a significant proliferative and migratory advantage over that of the other isoforms expression on their own.

To corroborate the results with MCF10AT, we used the parental MCF10A cell line. This is a fully non-transformed yet immortalized cell line, which will not form tumors *in vivo* nor colonies in soft agar. Following confirmation of hPRLr isoform overexpression via IB (Figure 19A), proliferation (Figure 19B), migration (Figure 19C), and anchorange-independent growth (Figure 19D, E) were all assessed. Similar to what was observed with MCF10AT (Figure 18), hPRLrL or hPRLrI individual overexpression was sufficient to elevate both proliferative (Figure 19B) and migratory (Figure 19C) potential above that of MCF10A-EV. However, hPRLrL+I co-overexpression significantly increased both proliferation and migration above individual isoform expression. Similarly, in examining hPRLr-mediated growth in soft agar, hPRLrL overexpression alone significantly increased the average number of colonies that formed (Figure 19D), but the number of colonies was not different from MCF10A-EV or MCF10A-hPRLrI (Figure 19E). Yet similar to what was observed with MCF10AT, hPRLrL+I co-overexpression significantly increased colony forming potential over that of individual isoform expression. Not only did MCF10A-hPRLrL+I grow more colonies (Figure 19D), but those that did form were significantly larger (Figure 19E) than the other three assayed transfectants. These results further bolster the hypothesis that hPRLrL+I co-overexpression contributes significantly to mammary transformation *in vitro*.

We were next interested in understanding possible mechanisms of hPRLrL+I-driven mammary transformation. Considering that hPRLrI lacks the majority of the hPRLr-ICD, including the phosphodegron S349, our focus was two-fold: differential 1) hPRLr complex stability and 2) signal transduction. To assess hPRLr homodimeric versus heterodimeric stability, CHO cells were transfected with either isoform on its own (CHO-hPRLrL, CHO-hPRLrI respectively) or both together (CHO-hPRLrL+I), co-treated with PRL (250ng/mL) and cycloheximide (CHX; 100μg/mL), and protein

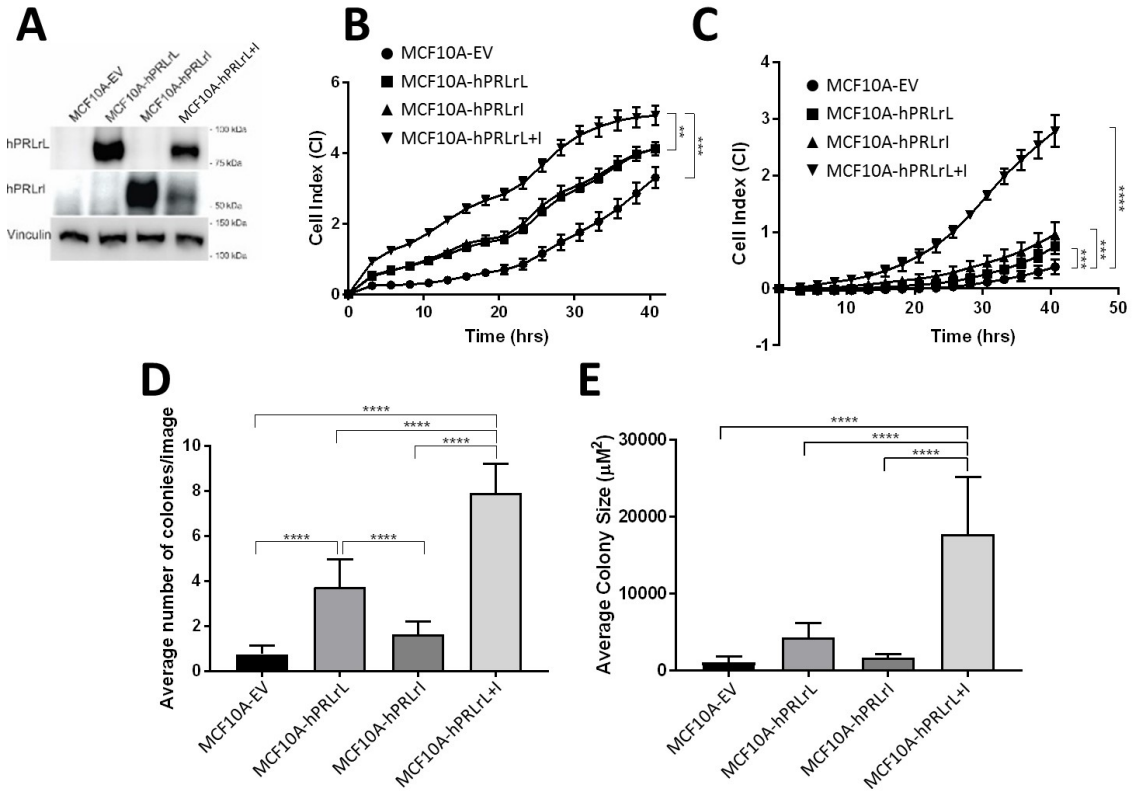

Fig. 19. MCF10A hPRLrL+I overexpression *in vitro*. **A**. MCF10A cells were stably transfected with empty vector, hPRLrL, hPRLrI, or both isoforms together, and respective isoform expression was confirmed via IB. Transfectants were assayed for the differential ability to **B**. proliferate, **C**. migrate, and **D, E** grow in soft agar. $^{**}p < 0.01$, $^{***}p < 0.005$, $^{****}p < 0.001$, n=3.

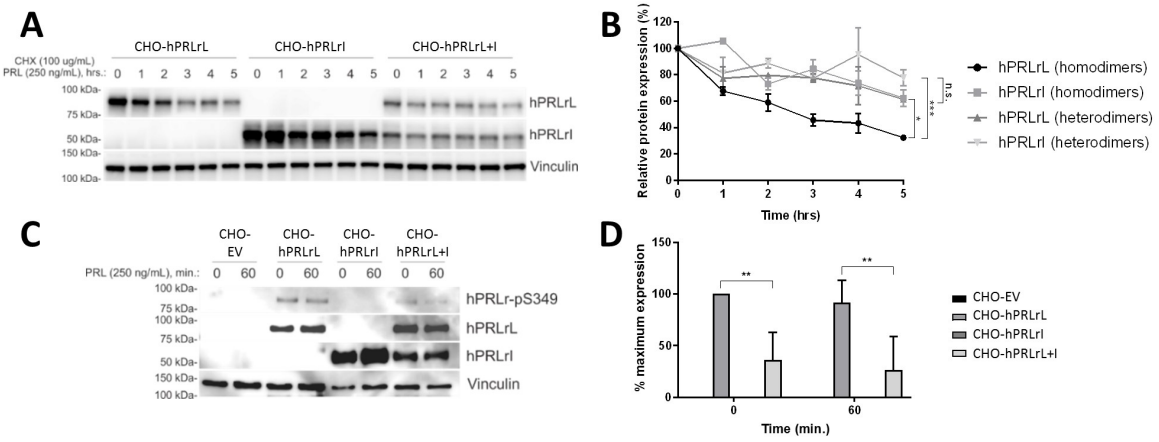

Fig. 20. Differential hPRLr isoform degradation and phospho-degron phosphorylation status. Chinese hamster ovary (CHO) cells (PRLr-null) were transiently-transfected with either hPRLrL, hPRLrI, or both isoforms concurrently. **A**. Transfectants were simultaneously stimulated with cycloheximide (CHX; 100g/mL) and prolactin (PRL; 250ng/mL), and lysates were harvested once per hour for 5 consecutive hours. Protein degradation was quantified, via densitometry, in **B**. and $t_{1/2}$ was extrapolated from each respective slope. **C**. Phosphorylation status of the hPRLr phosphodegron was assessed using a pS349-specific antibody (gift of Dr. Serge Fuchs), and **D**. band intensity was quantified via densitometry. *$p < 0.05$, **$p < 0.01$, ***$p < 0.005$, n=3.

degradation was assessed via IB (Figure 20A). Following co-treatment, hPRLrL homodimers were found to have a half-life of 3 hours, which is consistent with what has been reported in the literature (Figure 20B)[174,175]. Conversely, both hPRLrI homodimers and hPRLrL+I heterodimers were significantly more stable than hPRLrL homodimers, with an estimated half-life of 7.5-9 hours (Figure 20B). As a corollary, we also assessed the phosphorylation status of the phosphodegron in each of these conditions. hPRLrL homodimers carried robust phosphorylation on S349, while none was present on hPRLrI homodimers (Figure 20C, D). Moreoever, hPRLrI heterodimerization with hPRLrL was sufficient to reduce S349 phosphorylation (Figure 20C, D). These data indicate hPRLrI confers stability on its dimerization partner, which is facilitated by hPRLr-S349 phosphodeficiency.

As receptor stability has direct implications for signal transduction, were were

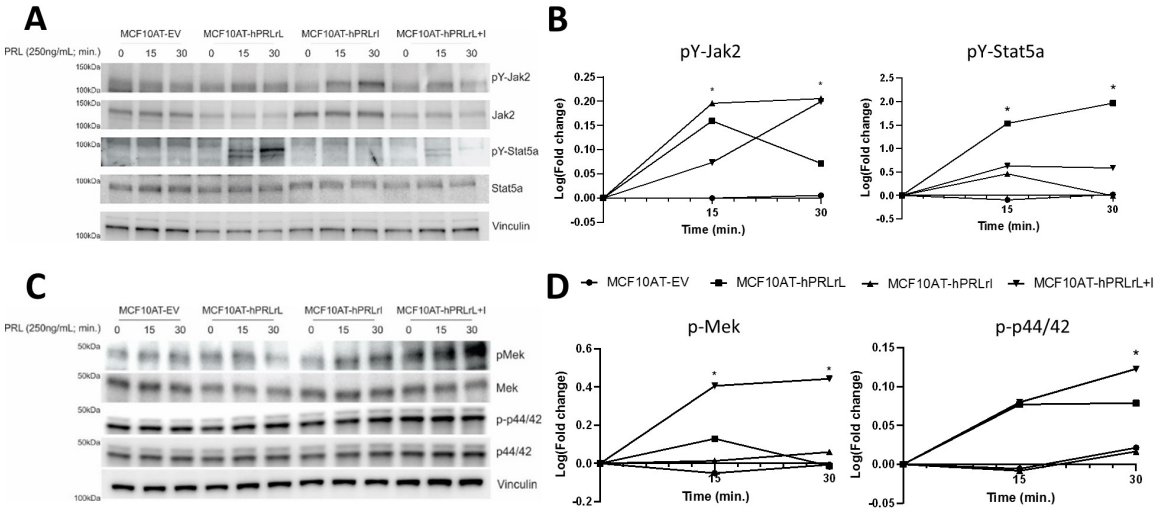

Fig. 21. Differential hPRLr homo- vs. heterodimeric signal transduction. MCF10AT transfectants were PRL (250ng/mL) stimulated for 0, 15, and 30 minutes, and phospho-IB was utilized to assess the activation status of **A, B**. Jak2/Stat5a and **C, D**. Mek/Erk. Band intensities were quantified using densitometry. n=3.

also interested in understanding differential receptor signaling[175]. We first assessed the activation status of Jak2/Stat5a following PRL stimulation of the MCF10AT transfectants utilized above (Figure 21A, B). We found that hPRLrL homodimers, hPRLrI homodimers, and hPRLrL+I heterodimers were capable of stimulating Jak2 phosphorylation/activation (Figure 21A, B). Furthermore, while hPRLrL homodimers were capable of inducing robust Stat5a tyrosine phosphorylation, neither hPRLrI homodimers nor hPRLrL+I heterodimers were capable of such.

We were also interested in examining the activation status of both Erk1/2 (p44/42) and Mek, as both of these proteins are downstream signaling components of Ras activation (Figure 21C, D). Following PRL stimulation, both hPRLrL homodimers and hPRLrL+I heterodimers were capable of phosphorylating both p44/42 and Mek (Figure 21C, D). However, p-Mek expression was significantly greater in hPRLrL+I co-overexpressing MCF10AT cells than those carrying only hPRLrL (Figure 21C, D).

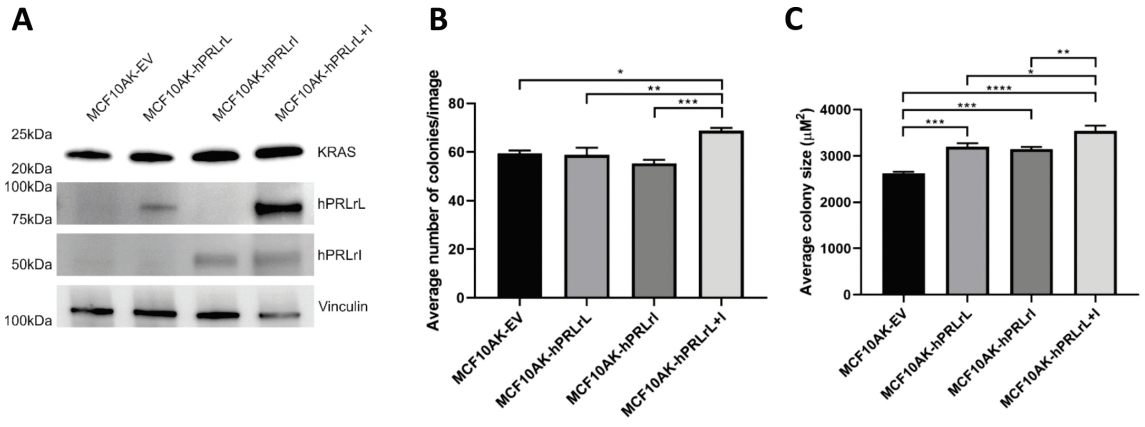

Fig. 22. KRAS G12V overexpression in MCF10A transfectants. **A**. MCF10A hPRLr overexpression transfectants received an additional stable transfection of KRAS-G12V (MCF10AK), and expression was confirmed via IB. Cells were then grown in soft agar, and both **B**. colony number and **C**. colony size were determined. *$p < 0.05$, **$p < 0.01$, ***$p < 0.005$, ****$p < 0.001$. n=3.

hPRLrI homodimers were incapable of stimulating phosphorylation on either of these proteins (Figure 21C, D).

Considering that hPRLrL+I heterodimers are capable of activating Ras, we were interested in the role that Ras would play in the observed transformation. Furthermore, recent literature has indicated that KRAS is critically involved in PRL-mediated tumorigenesis[48]. We therefore over-expressed oncogenic KRAS (G12V) in our MCF10A hPRLr transfectants (hereafter referred to as "MCF10AK"), which was confirmed via IB (Figure 22A). We assessed differential ability to form colonies in soft agar, and we found that oncogenic KRAS conferred a colony-forming advantage to hPRLrL+I co-overexpression over that of individual isoform expression (Figure 22B, C). These results indicate hPRLrL+I heterodimers cooperate with KRAS activity to contribute to *in vitro* mammary transformation.

6.3 Discussion

Initial studies centalized on hPRLrI were quick to realize that this isoform lacks the majority of the hPRLr ICD, and was therefore considered hPRLrI to be, at most, only minimally functional. As shown here, hPRLrI appears to act in a manner similar to Her2: on its own, Her2 is unable to induce cellular transformation, similar to hPRLrI. However, following heterodimerization with a full-length partner (e.g. Her3 or hPRLrL, respectively), the heterodimeric complex is capable of inducing a robust downstream response in signal transduction that ultimately elevates malignant proliferation and anchorage-independent growth. While hPRLr has traditionally been thought of as a driver of exclusively luminal disease, the data presented here implicates a potential broader spectrum of applicability, in being expressed in more cell types than just luminal breast cancer (e.g. T47D, MCF7, HCI-011, HCI-013 versus MDA-MB-231, WHIM2, UCD52).

While hPRLr KD has been shown to significantly abrogate tumorigenic potential of breast cancer cell lines, studies to date have primarily focused on either pan-hPRLr or putative hPRLrL-specific KD[97,302]. This is the first study that has examined the effect of hPRLrI-sepcific KD, confirming the oncogenic effect of this splice variant. Considering that pan-hPRLr antibodies being tested in the clinic have shown little to no efficacy in halting disease progression, these results provides unique insight into a possible explanation on why this may be. Namely, clinical inhibition of hPRLr needs to be performed in an isoform-specific manner: hPRLrL appears to confer pro-differentiative effects, while hPRLrI confers pro-malignancy advantages. Therefore, pan-hPRLr inhibition may be mitigating the positive effects of hPRLrL in breast cancer, thereby abrogating the efficacy of clinical inhibition.

Protein degradation assays revealed hPRLrL+I heterodimers are significantly

more stable than hPRLrL homodimers. These results are of particular relevance given the well-documented oncogenic effects of increased hPRLr stability in breast cancer[174,175,220,268]. Physiologically, greater hPRLr stability results in augmented signal transduction, leading to greater cellular proliferation, anchorage-independent growth, and tumorigenicity[175]. In addition, phospho-immunoblot confirmed that this increase in complex $t_{1/2}$ correlated with a decrease in hPRLr-S349 phosphorylation status. These data suggest that monomeric hPRLr-S349 expression is not sufficient for PRL-induced phosphorylation at the phosphodegron, thereby preventing recruitment of the ubiquitin-ligase machinery to the receptor and subsequent down-regulation of protein turnover[175]. These findings represent a putative mechanism through which hPRLrL+I may contribute to breast cancer pathogenesis.

There are now several reports highlighting a prominent cooperative role for KRAS with hPRLr in breast cancer pathogenesis. For example, in characterizing a PRL-driven mammary cancer mouse line (NRL-PRL), genomic analyses uncovered consistent oncogenic KRAS somatic mutations/amplifications in all primary tumors, which were not found in pre-neoplastic glands[48]. These findings coincided with recent discoveries of significant KRAS involvement in breast cancer metastatic dissemination, mirroring the in vivo results presented herein[298]. One possible mode of interplay between these two pathways may lie in KRAS involvement in hPRLr stability. KRAS is a negative regulator of glycogen synthase kinase-3β (GSK3β), which itself is a negative regulator of hPRLr stability[219]. In this manner, KRAS activity indirectly stabilizes hPRLr, uncovering a possible mechanism for the observed cooperation between these two pathways in in vitro transformation. Given these studies, further characterization is necessary to fully elucidate the interplay between these two oncogenic pathways.

6.4 Limitations and Future Directions

In the studies enumerated here, the greatest hPRLrI KD efficiency achieved in MCF7 cells was approximately 50%, despite extensive efforts to increase the efficiency of this KD. Given the inherent stability of this isoform, this may not have been sufficient to achieve the full phenotypic potential of greater protein KD. Additional experiments that focus on CRISPR-mediated knock-out (KO), rather than shRNA-mediated KD, will be necessary to fully elucidate hPRLrI oncogenic actions in malignancy.

Additionally, an examination of the differential transcriptomic actions of hPRLrI versus hPRLrL would provide unique insight into how this isoform functions. Literature has indicated a clear role of hPRLr nuclear functionality in its transcriptomic actions. Indeed, work from our lab has shown the receptor acts as a scaffold, through its transactivation domain (TAD), to stimulate transcription[96,97]. As preliminary IHC work with our novel hPRLrI pAb was able to show distinct nuclear localization of hPRLrI in certain tissues (Figure 9 and Figure 11), it is reasonable to hypothesize that hPRLrI may have unique sites of genomic recognition and targeting, separate from that of hPRLrL. Therefore, future studies should examine the differential transcriptomic outcome of hPRLrI and hPRLrL+I complex PRL stimulation.

CHAPTER 7

AIM 2: TO ASSESS *IN VIVO* TUMORIGENIC POTENTIAL OF HPRLRL+I CO-OVEREXPRESSION

7.1 Hypothesis

hPRLrL+I co-overexpression contributes to mammary transformation *in vivo*, as determined by both primary tumor growth and metastatic potential.

7.2 Results

Considering the significant degree of *in vitro* transformation demonstrated in Chapter 6, we were interested in examining the *in vivo* transforming potential of hPRLrL+I co-overexpression. We utilized the MCF10AT stable transfectants characterized *in vitro* for our *in vivo* approach. These cells were bilaterally xenografted into the 4th set of mammary glands of female NSG mice. To reiterate, MCF10AT are a partially-transformed mammary cell line which, when engrafted into an immunocompromised host, have a take rate of approximately 25% and do not metastasize[81]. Primary tumor growth was monitored longitudinally, and it was found that following overexpression of either hPRLr isoform individually conferred a slight but non-significant advantage in primary tumor growth (Figure 23A). However, MCF10AT-hPRLrL+I xenografts were found to grow primary tumor more readily than the other three study arms, and these tumors also grew significantly more quickly (Figure 23A). Once the humane endpoint was reached (per IACUC guidelines, one tumor not exceeding $2cm^3$ and/or obvious moribund behavior), all mice were euthanized, and axillary lymph nodes as well as lungs were harvested for FFPE and examination

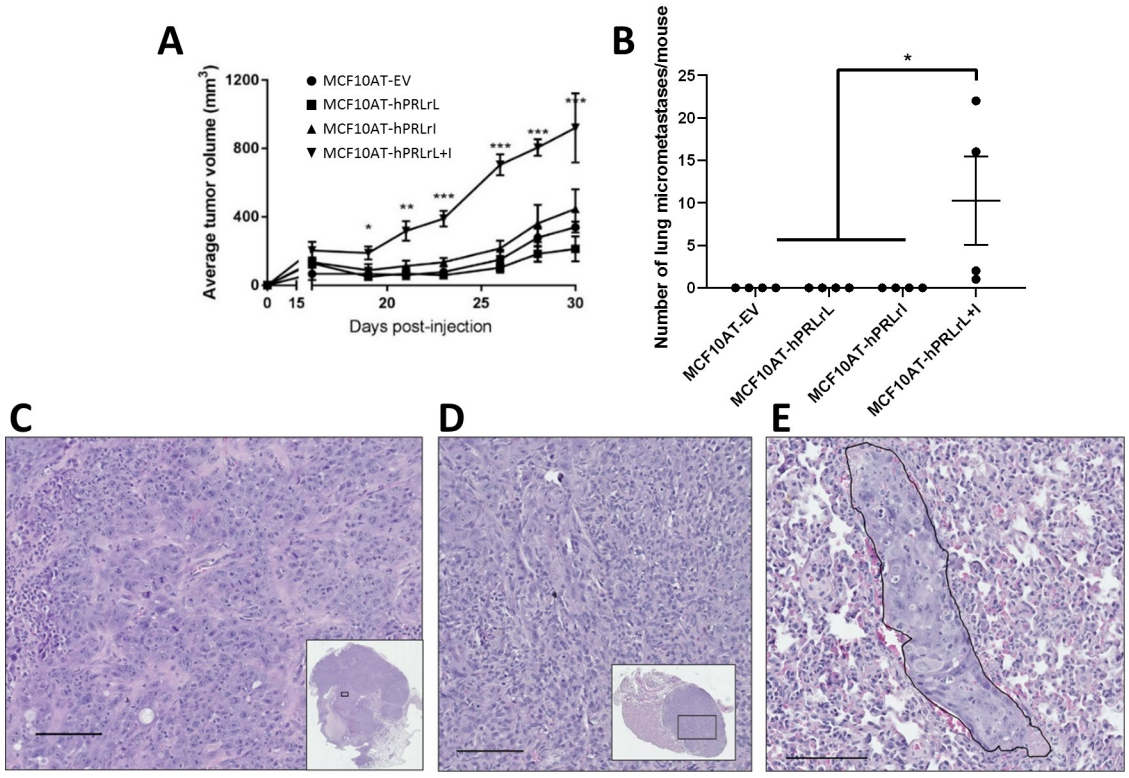

Fig. 23. MCF10AT hPRLrL+I co-overexpression *in vivo*. **A**. MCF10AT transfectants were orthotopically xenografted into female NSG mice, and primary tumor growth was monitored longitudinally. **B**. Lungs were harvested and micrometastatic burden was counted manually. Representative images (scale bar, 100m) of H&E stained **C**. primary tumor, **D**. axillary lymph node, and **E**. lung indicate primary tumors to be high grade adenocarcinoma with nodal infiltration and successful distant metastatic dissemination (outlined; representative image shows metastatic growth long a blood vessel). *$p < 0.05$, **$p < 0.01$, ***$p < 0.005$. n=4 mice/study arm.

for micrometastases (no macrometastases were evident at the time of tissue harvest). Following microscopic examination of the harvested tissues, we found that MCF10AT-hPRLrL+I xenografts harbored a significant number of lung micrometastases, which was not observed in the other three study arms (Figure 23B, E). Histologic examination of the harvested tissues confirmed the MCF10AT-hPRLrL+I primary tumors to be high grade adenocarcinoma (Figure 23C), carrying axillary lymph node metastases (Figure 23D).

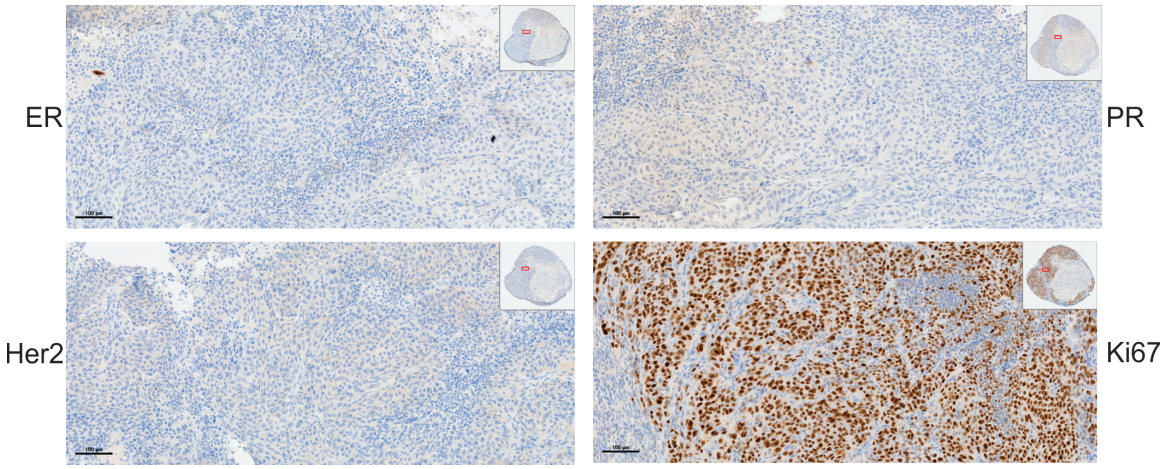

Fig. 24. Hormone receptor and KI67 status of MCF10AT-hPRLrL+I primary tumor. ER, PR, Her2, and KI67 status were assessed by IHC. Scale bar: 100um.

We were additionally interested in assessed the HR status of our MCF10AT-hPRLrL+I xenografts. MCF10AT is a basal cell line that, without exogenous influence, does not express ER, PR, or Her2. However, hPRLr expression has been traditionally associated with HR positive disease. Therefore, we were interested to assess whether or not the HR status of of our MCF10AT-hPRLrL+I xenografts changed during tumorigenesis. As seen in Figure 24, these tumors remained negative for ER, PR, and Her2. Furthermore, these tumors were highly positive for the active proliferation marker KI67 (Figure 24).

Given these results, we were interested to determine if the parental MCF10A tranfectants were also transforming *in vivo*. Therefore, the same experiment outlined above was performed with transfectants generated using MCF10A cells. While the MCF10AT xenografts reached their humane endpoint within 30 days of engraftment (Figure 23A), the MCF10A xenografts did not form palpable tumors within this timeframe. We therefore decided to choose our experimental endpoint based upon the biology of the MMTV-Her2 transgenic mouse, which has an average tumor latency of approximately 30 weeks[101]. Following 30 weeks of observation, no primary

tumors were palpable. At this pre-determined experimental endpoint, the 4th set of presumed normal mammary glands were harvested and subject to FFPE and H&E. Histologic examination of MCF10A-hPRLrL+I mammary gland sections confirmed no microscopic abnormalities (Figure 25).

Next, given our *in vitro* results that confirmed hPRLrI KD was sufficient for abrogation of colony forming potential (Figure 14), we were interested in determining if this mitigation would be observed *in vivo*. MCF7 hPRLrI KD and scRNA control cells were xenografted into the 4th set of mammary glands of female mice, and primary tumor growth was monitored longitudinally. At endpoint, there was no significant difference in primary tumor volume observed in comparing MCF7 scRNA and MCF7 hPRLrI KD xenografts (Figure 26A). IHC of primary tumors confirmed KD of hPRLrI was maintained during tumorigenesis (Figure 26B).

7.3 Discussion

While the co-expression of a truncated mPRLr mutant alongside the wild-type mPRLr was shown to participate in fibroblast transformation, this initial study did not translate their findings into a mammary epithelial model, nor were functional *in vivo* analyses presented utilizing the orthologous hPRLr[114]. Therefore, the studies demonstrated here sought to address this limitation. The data presented here confirm that co-expression of a similarly shortened hPRLr variant (hPRLrI) with the full-length form (hPRLrL) contributes to *in vivo* mammary epithelial transformation, within the context of oncogenic Ras activity. While the Schreiber and Mardis groups focused on the incidence rate of primary tumor only, we assessed both the growth rate of those primary tumors that formed as well as lung and axillary lymph node metastatic incidence[114].

As shown here, hPRLrL+I co-expression resulted in not only rapid primary tu-

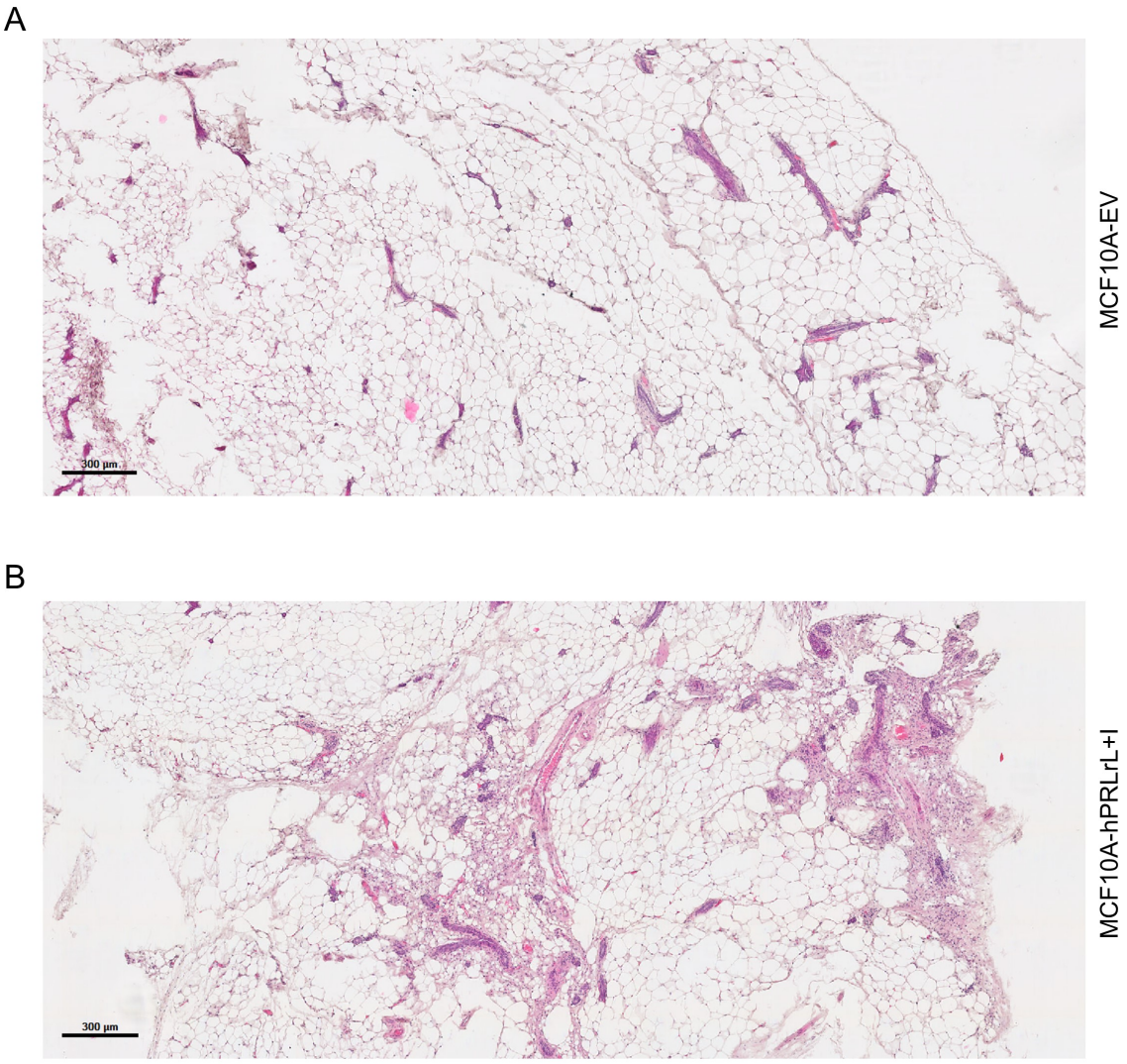

Fig. 25. Mammary glands of MCF10A xenografts. Glands were harvested from MCF10A xenografts 30 weeks post injection and subject to H&E to confirm histology. Both **A**. MCF10A-EV and **B**. MCF10A-hPRLrL+I mice were assessed. Scale bar: 300um.

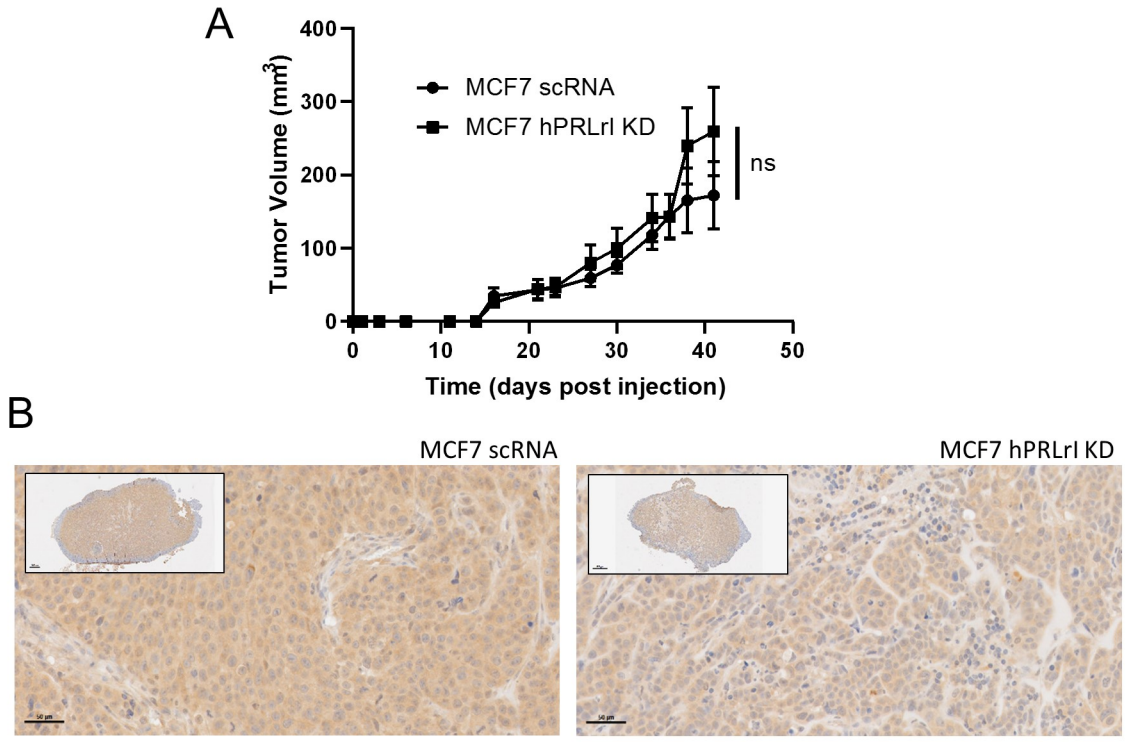

Fig. 26. hPRLrI KD MCF7 growth *in vivo*. MCF7 scRNA and hPRLrI KD cells were orthotopically xenografted into the 4th set of mammary glands of female NSG mice, concurrent with a subcutaneous estrogen pellet. **A**. Primary tumor growth was monitored longitudinally. **B**. Harvested primary tumors were assessed via IHC using the hPRLrI-specific pAb to confirm hPRLrI KD was maintained throughout tumorigenesis. Scale bar: 50um.

mor growth, but also significant lung and axillary lymph node micrometastatic burden. hPRLrL has been implicated in being involved in metastatic colonization of the lung, whereby isoform-specific hPRLrL KD was shown to be sufficient to decrease both lung and liver metastatic infiltrate[302]. Furthermore, research utilizing single-cell RNAseq of an orthotopic prostate cancer mouse line has recently uncovered that hPRLr transcript expression is increased as primary tumor cells extravasate into the lungs and progress to micrometastases[307]. This study uncovered that, following pulmonary colonization, these disseminated tumor cells induced PRL secretion by the adjacent lung stromal tissue, resulting in a paracrine signaling pathway that would inevitably promote metastatic establishment and growth[307]. Though not performed using a breast cancer cell line, these data could explain at least in partiality the significant lung micrometastatic burden observed by our MCF10AT-hPRLrL+I xenografts.

Beyond this, hPRLr has also recently been studied for its potential involvement in metastasis to the bone[264]. In this analysis, higher hPRLr expression in the primary tumor associated with quicker bone metastasis in matched patient samples, which these investigators hypothesized may be a result of PRL-stimulated osteoclast differentiation and osteolysis, the effect of which was mitigated following treatment by the hPRL antagonist Δ1-9-G129R-hPRL[264]. These results were found consistently across multiple breast cancer cell lines, indicating the actions of PRL in promoting bone metastasis are likely not subtype-specific[264]. Additionally, it is worth noting that PRL itself, if measured within 10 years before diagnosis, is a marker for lymph node positive disease[278].

Considering that our MCF10A xenografts were unable for form primary tumors *in vivo*, despite the reciprocal MCF10AT-hPRLrL+I transfectants readily forming both primary tumor and distant metastasis, it is likely that oncogenic Ras activity

is involved in this differential phenotypic outcome. Notably, recent studies involving the NRL-PRL mouse model, which overexpresses rPRL in a mammary-specific manner, uncovered extensive oncogenic KRAS involvement in PRL-driven mammary tumors[48]. While a long primary tumor latency of this particular model certainly dampened assessment of KRAS/PRL/hPRLr synergism in distant metastases, preliminary transcriptomic assays detailing upregulation of genes typically involved in invasion and metastasis (i.e. Itgb4 and Mmp9) would suggest KRAS is likely also involved in metastatic dissemination of PRL-driven tumors[48]. Even more recently, oncogenic KRAS mutations/amplifications were found to be involved in the metastatic progression of two genetically engineered mouse models (i.e. MMTV-PyMT and MMTV-Her2), as well as two PDX models (i.e. HCI01 and WHIM2), contributing further to this hypothesis of KRAS being a critical effector involved in breast cancer metastasis[241].

7.4 Limitations and Future Directions

Similar to the shortcomings enumerated in Chapter 6, a major limitation of our *in vivo* approach is the relative inefficiency of our hPRLrI KD. While approximately 50% hPRLrI protein reduction in MCF7 cells was sufficient to mitigate *in vitro* transforming behavior, it was not sufficient to inhibit primary tumor formation. While this may simply be a result of the elevated stability inherent to hPRLrI protein, our experimental approach utilized transfected pools of MCF7 cells rather than cloned. Therefore, our 50% KD efficiency was an average of those pools. One potential future direction to overcome this discrepancy would be titration xenograft experiments. Only one cell number was utilized for injection ($1.5x10^6$), which may have confounded our results. Therefore, future studies should determine the minimum number of MCF7 scRNA cells needed to form tumors (literature indicates this

may be as low as 1000 cells per gland) and re-perform this assay[290]. Other future analyses should include CRISPR-mediated KO of hPRLrI to ensure complete ablation of hPRLrI protein.

Concerning our MCF10AT overexpression approach, we chose to focus our examination for metastases on the axillary lymph nodes and lungs. The results of this analysis indicate hPRLrL+I co-overexpression facilitates distant metastasis. While studies with the NRL-PRL transgenic mouse model have found PRL-driven tumors metastasize to only these two tissues, a recent review characterized hPRLr as a marker for metastatic risk to both bone and liver as well[48,251]. Future studies should examine hPRLrL+I-mediated metastatic risk to other tissues. An additional potential direction for future study would be assessing the *in vivo* differential tumorigenic potential of our MCF10AK transfectants. We would hypothesize that the co-overexpression of oncogenic KRAS, alongside hPRLrL+I, would be sufficient to overcome the limitations observed with the parental MCF10A strain, similar to what was observed with MCF10AT cells. However, KRAS and HRAS do not exhibit complete overlap in functionality: for example, KRAS is commonly mutated in pancreatic and lung cancers, while HRAS mutations are more commonly observed in skin and bladder cancers, indicative of tissue-specific functionality[53]. Within the context of breast cancer, a recent 2020 study demonstrated that HRAS is more likely to be amplified in patients with large, ER+ breast tumors, while elevated KRAS was associated with node positivity[18]. Therefore, while both KRAS and HRAS are members of the same protein family, our MCF10AK (oncogenic KRAS-overxpressing) and MCF10AT (oncogenic HRAS-overxpressing) transfectants may not necessarily phenocopy one another *in vivo*.

CHAPTER 8

AIM 3: CLINICAL ANALYSES OF HPRLRI IN BREAST CANCER AT THE PROTEIN AND TRANSCRIPT LEVELS

8.1 Hypothesis

hPRLrI mRNA and protein expression correlates positively with aggressive clinocopathologic outcomes.

8.2 Results

The final project aim of this dissertation was focused on the clinical relevance of hPRLrI in breast cancer. To this end, our approach was two-fold: first, we examined hPRLrI protein expression using a breast cancer TMA (n=250; Table 8) and the hPRLrI pAb characterized in Chapter 5; second, we assessed the ratio of hPRLrI:hPRLrL transcript expression using RNAseq data of breast cancer clinical specimens reposited within the TCGA breast cancer (BRCA) cohort (n=67/cohort; Table 10).

Starting with our TMA approach, we were first interested in discerning if hPRLrI protein expression conferred a proliferative advantage in clinical samples. As a marker for active proliferation, we examined KI67 status as a possible correlate to hPRLrI protein expression (Figure 27A). As KI67 status in this TMA was reported as a mix of either percent positive or percent positivity groups (e.g. low, medium, and high), we grouped those samples with KI67 described as a percentage into one of the three groups (low, <25%; medium, 25-35%; high, >35%). There was no statistical difference in hPRLrI expression between $KI67^{lo}$ and $KI67^{med}$ groups. However, hPRLrI

protein expression was significantly higher in the KI67^{hi} group than both the KI67^{lo} and KI67^{med} groups (Figure 27A). Assessment of hPRLrI correlation with tumor grade uncovered similar results, with hPRLrI protein expression being the highest in those samples of the highest grade (3), in comparison to tumors of grade 1 (Figure 27B).

Next, while hPRLrL/PRL are traditionally associated HR+, luminal disease, there has been recent interest in utilizing hPRLr as a marker for TNBC[48,198,239]. Therefore, we assessed hPRLrI protein expression as a function of hormone receptor status. We found that hPRLrI protein was expressed the lowest in samples expressing both ER and PR, and was the highest in the TNBC samples (Figure 27C). Further examination concluded that hPRLrI expression was highest in TNBC samples with high KI67 status, compared to that of low and medium KI67 expression (Figure 27D). Figure 27E consists of representative images of hPRLrI IHC staining from this TMA. These data indicate hPRLrI correlates with breast cancers of high tumor grade, proliferative index, and TNBC.

For our secondary approach to study the clinical implications of hPRLrI, analyses of RNAseq data reposited within the TCGA-BRCA cohort (Table 9) were able to dissect the respective correlates of hPRLrL and hPRLrI transcript expression. Given that our *in vitro* and *in vivo* data indicate that co-expression hPRLrL and hPRLrI is critical for transformation, rather than individual expression, we chose to focus our analysis on the ratio of hPRLrI:hPRLrL transcript expression. To perform these analyses, we first obtained hPRLrL and hPRLrI mRNA expression within the TCGA-BRCA cohort using RNAseq data (normalized read expression values are given as transcripts per million reads, TPM). Every patient sample within the BRCA cohort expressed at least a low level of hPRLrL, and 201 samples were positive for both hPRLrI and hPRLrL. After examining the distribution of our hPRLrI:hPRLrL

		n	% of total
ER Status			
	Positive	65	26%
	Negative	181	72%
PR Status			
	Positive	54	22%
	Negative	192	77%
Her2 Status			
	Positive	24	10%
	Negative	217	87%
	Equivocal	3	1%
KI67 Status			
	Low (<25%)	57	23%
	Intermediate (25-35%)	28	11%
	High (>35%)	119	48%
Tumor Grade			
	1	20	8%
	2	46	18%
	3	173	69%
AJCC Pathologic T			
	T1	99	40%
	T2	69	28%
	T3	24	10%
	T4	9	4%
AJCC Pathologic N			
	N0	92	37%
	N1	57	23%
	N2	22	9%
	N3	15	6%

Table 8. Breast cancer TMA demographics

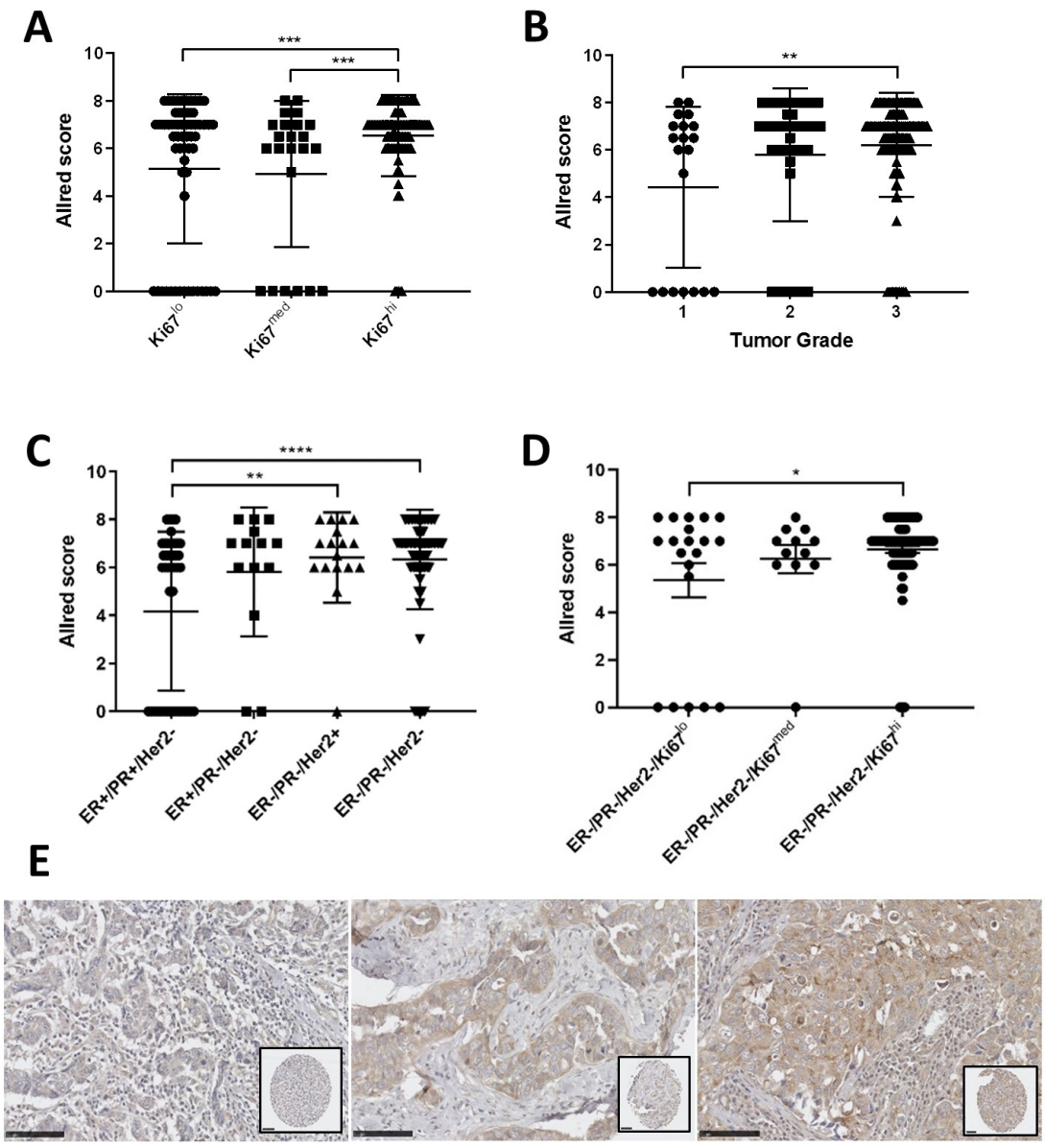

Fig. 27. Breast cancer tissue microarray (TMA). hPRLrI protein in breast cancer clinical samples (n=250) was assessed by TMA analysis. Allred score is reflective of both hPRLrI staining intensity and percent positivity. **A**. Proliferative index, reported via KI67 status, was assessed, as was **B**. tumor grade and **C**. hormone receptor status. **D**. Proliferative index within the ER-/PR-/Her2- cohort was also analyzed. **E**. Representative images of low (left), moderate (center), and high (right) hPRLrI protein expression by IHC. *$p < 0.05$, **$p < 0.01$, ***$p < 0.005$, ****$p < 0.001$.

ratio cohort by breast cancer intrinsic subtype (Figure 28A), it was noted that the approximate lower third of the distribution was enriched in luminal A cases, while that of the upper third was higher in basal-like breast cancers (Figure 28). We therefore chose to stratify our samples by tertiles (i.e. hPRLrI-hi/hPRLrL-lo versus hPRLrI-lo/hPRLrL-hi) for our downstream DEG analyses, hypothesizing this would be the most informative way to analyze these data. Similar to what was observed with our breast cancer TMA, we observed a significant enrichment for basal-like breast cancers in the hPRLrI-hi/hPRLrL-lo cohort (Figure 28B). While intrinsic subtyping was not provided in the patient data of the TMA, basal-like breast cancers tend to be TNBC more often than not[60,217]. Furthermore, in comparing the demographics of the hPRLrI-hi/hPRLrL-lo versus hPRLrI-lo/hPRLrL-hi cohorts, the hPRLrI-hi/hPRLrL-lo cohort was more likely to contain patient samples that were overall larger, higher grade, basal-like breast cancer (Table 10).

Table 9. Demographics of the full TCGA-BRCA cohort

		n	% of total
ER status			
	Positive	758	69.5%
	Negative	224	20.5%
PR status			
	Positive	659	60.4%
	Negative	320	29.3%
Her2 status			
	Positive	153	14.0%
	Negative	526	48.2%
	Equivocal	172	15.8%
HR status			
	ER+/PR+/Her2-	350	32.1%
	ER+/PR-/Her2-	57	5.2%
	ER-/PR-/Her2+	35	3.2%
	ER-/PR-/Her2-	108	9.9%
Intrinsic subtype			
	Luminal A	419	38.4%
	Luminal B	192	17.6%
	Her2-enriched	67	6.1%
	Basal	139	12.7%
	Normal-like	23	2.1%
Gender			
	Female	1078	98.8%
	Male	12	1.1%
Menopause status			
	Pre-menopausal	222	20.6%
	Peri-menopausal	35	3.2%
	Post-menopausal	666	61.8%
Race			

	White	752	68.9%
	Asian	61	5.6%
	African American	182	16.7%
Ethnicity			
	Not Hispanic/Latino	878	80.5%
	Hispanic/Latino	39	3.6%
AJCC Pathologic T			
	T1	279	25.6%
	T2-T4	808	74.1%
AJCC Pathologic N			
	N0	514	47.1%
	N1-N3	556	51.0%
AJCC Pathologic M			
	M0	907	83.1%
	M1	22	2.0%
AJCC Pathologic Stage			
	Stage I	181	16.6%
	Stage II-Stage IV	886	81.2%
Age			
	¡55	431	39.5%
	¿55	644	59.0%
Prior malignancy			
	No	1023	93.8%
	Yes	66	6.0%
hPRLrI status			
	Positive	201	18.4%
	Negative	893	81.9%
hPRLrL status			
	Positive	1091	100.0%
	Negative	0	0.0%

Table 10. Demographics of hPRLrI:L ratio cohort

		hPRLrIhi/hPRLrLlo (n = 67)		hPRLrIlo/hPRLrLhi (n = 67)			
		n	**% of total**	**n**	**% of total**	**z score**	**p**
ER status							
	Positive	48	71.6%	55	82.1%	-1.434	0.152
	Negative	11	16.4%	4	6.0%	1.918	0.055
PR status							
	Positive	41	61.2%	47	70.1%	-1.092	0.275
	Negative	17	25.4%	11	16.4%	1.275	0.202
Her2 status							
	Positive	11	16.4%	10	14.9%	0.238	0.812
	Negative	35	52.2%	36	53.7%	-0.173	0.863
	Equivocal	9	13.4%	11	16.4%	-0.485	0.628
HR status							
	ER+/PR+/Her2-	25	37.3%	31	46.3%	-1.051	0.293
	ER+/PR-/Her2-	5	7.5%	3	4.5%	0.729	0.466
	ER-/PR-/Her2+	2	3.0%	2	3.0%	0.000	1.000
	ER-/PR-/Her2-	4	6.0%	1	1.5%	1.367	0.172
Intrinsic subtype							
	Luminal A	34	50.7%	44	65.7%	-1.752	0.080
	Luminal B	14	20.9%	12	17.9%	0.437	0.662
	Her2-enriched	2	3.0%	5	7.5%	-1.165	0.244
	Basal	11	16.4%	1	1.5%	3.025	**0.002**
	Normal-like	1	1.5%	0	0.0%	1.004	0.315
Gender							
	Female	64	95.5%	66	98.5%	-1.015	0.310
	Male	3	4.5%	1	1.5%	1.015	0.310
Menopause status							
	Pre-menopausal	16	25.0%	15	22.7%	0.304	0.761
	Peri-menopausal	1	1.6%	1	1.5%	0.022	0.983
	Post-menopausal	38	59.4%	44	66.7%	-0.861	0.389

Race							
	White	55	82.1%	58	86.6%	-0.713	0.476
	Asian	1	1.5%	2	3.0%	-0.584	0.559
	African American	4	6.0%	3	4.5%	0.388	0.698
Ethnicity							
	Not Hispanic/Latino	51	76.1%	58	86.6%	-1.552	0.121
	Hispanic/Latino	3	4.5%	2	3.0%	0.456	0.649
AJCC Pathologic T							
	T1	13	19.4%	24	35.8%	-2.125	**0.034**
	T2-T4	54	80.6%	43	64.2%	2.125	**0.034**
AJCC Pathologic N							
	N0	27	40.3%	36	53.7%	-1.558	0.119
	N1-N3	38	56.7%	31	46.3%	1.210	0.226
AJCC Pathologic M							
	M0	55	82.1%	61	91.0%	-1.520	0.129
	M1	2	3.0%	2	3.0%	0.000	1.000
AJCC Pathologic Stage							
	Stage I	8	11.9%	17	25.4%	-1.996	**0.046**
	Stage II-Stage IV	57	85.1%	49	73.1%	1.700	0.089
Age							
	<55	26	38.8%	23	34.3%	0.538	0.591
	>55	41	61.2%	44	65.7%	-0.538	0.591
Prior malignancy							
	No	61	91.0%	65	97.0%	-1.458	0.145
	Yes	6	9.0%	2	3.0%	1.458	0.145

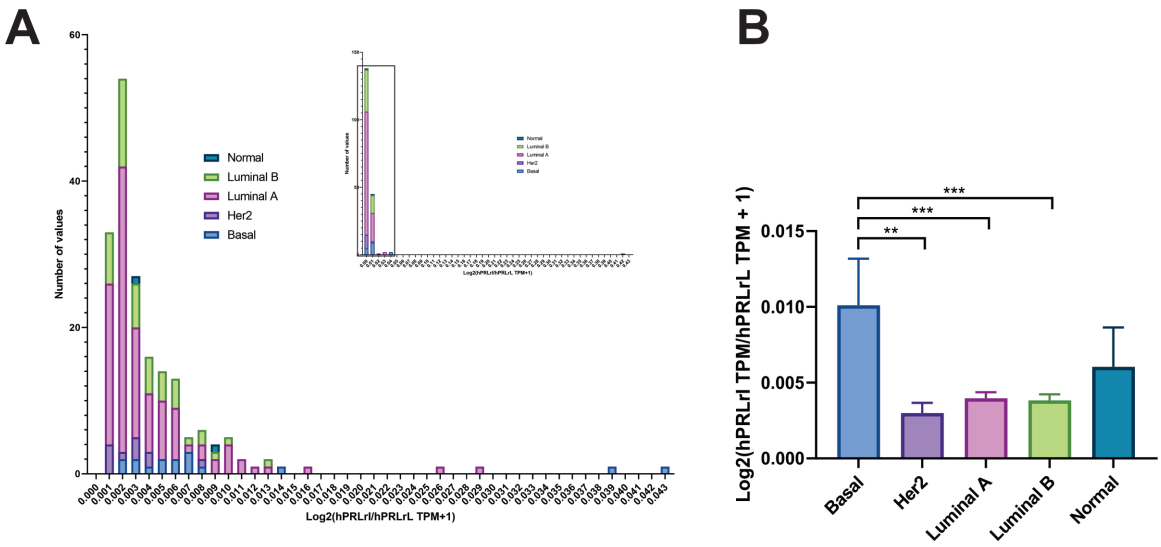

Fig. 28. Distribution of hPRLrI:hPRLrL ratio by breast cancer intrinsic subtype. **A**. The ratio of hPRLrI:hPRLrL transcript expression was distributed by instrinsic subtype status. Inset is the full distribution, including a single outlying value, with the highlighted region of expansion defined by the black box. **B**. hPRLrI transcript expression by intrinsic subtype. **p $<$ 0.01, ***p $<$ 0.005. n=201.

After confirming significantly higher hPRLrI:hPRLrL expression in primary tumor versus normal tissue (Figure 29), we were interested if there was a gene signature that could differentiate between our hPRLrI-hi/hPRLrL-lo and hPRLrI-lo/hPRLrL-hi cohorts. To that end, we performed a differentially-expressed gene (DEG) analysis between the hPRLrI-hi/hPRLrL-lo and hPRLrI-lo/hPRLrL-hi cohorts, using global RNAseq transcriptomics data available from the TCGA. A total of 345 genes were significantly enriched in the hPRLrI-hi/hPRLrL-lo cohort, and 81 genes were concurrently under-represented in this cohort. A full list of these DEGs along with their respective fold-changes and p-values can be found in Appendix H. The top/bottom 50 DEGs, respectively, are found in Figure 30A. Within the enrichment dataset, Gene Set Enrichment Analysis (GSEA; Broad Institute) uncovered expression of 4 *bona fide* oncogenes: BCL11A, ROS1, SSX1, and TLX1. The former two have recent implications in TNBC, lending credence to our hypothesis of hPRLrI involvement in

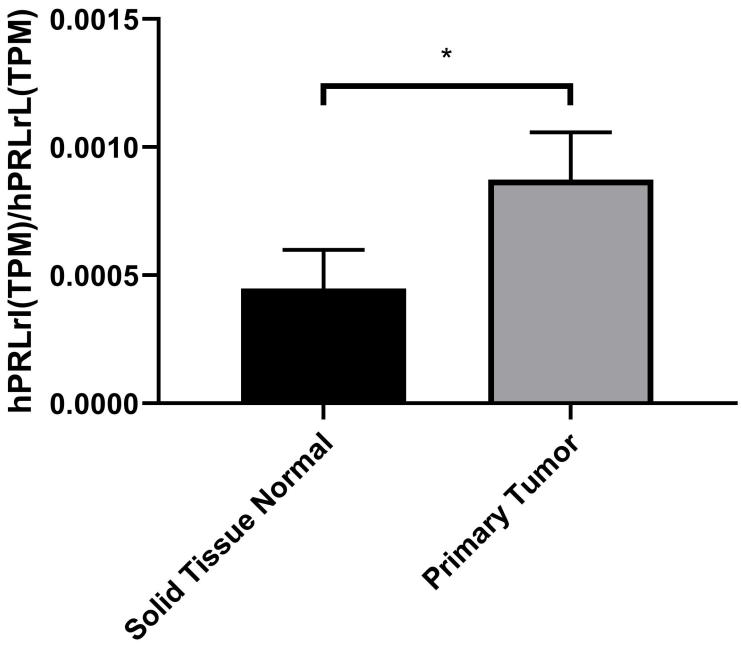

Fig. 29. Ratio in hPRLrI:hPRLrL transcript expression from normal to malignant breast tissue. The ratio of hPRLrI:hPRLrL transcript expression (TPM) was assessed utilizing TCGA RNAseq data, comparing expression values between solid normal breast tissue and that of primary tumor. *$p < 0.05$.

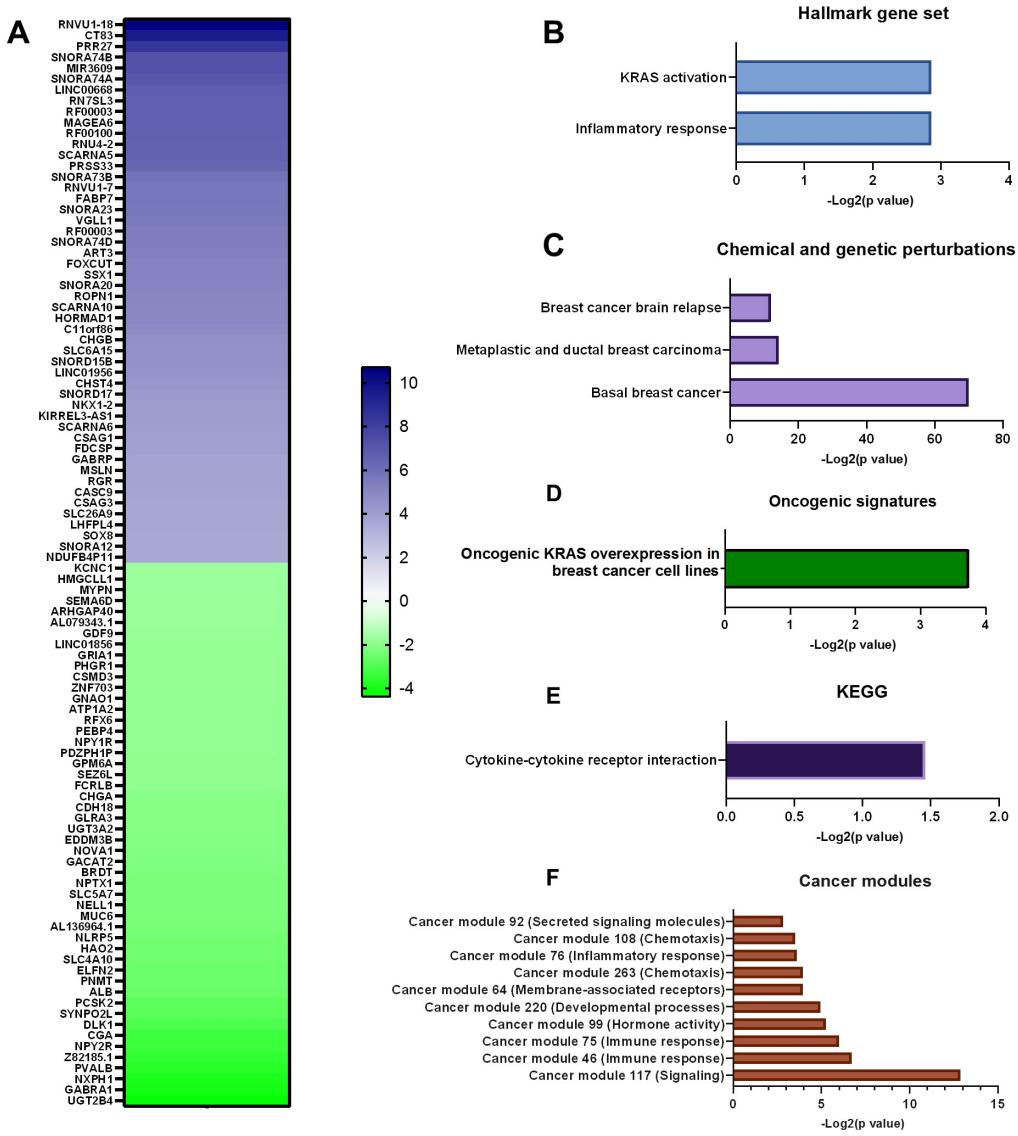

Fig. 30. Ratio of hPRLrI:hPRLrL transcript expression DEG results. The hPRLrI:hPRLrL transcript ratio was examined, using TCGA-reposited RNAseq data. Samples were stratified by tertiles, wherein the top tertile expressed high hPRLrI and low hPRLrL (hPRLrI-hi/hPRLrL-lo) relatively, with the invserse being observed for the hPRLrI-lo/hPRLrL-hi cohort. Differential gene expression patterns were characterized, as demonstrated by **A**. heat map displaying the top/bottom 50 differentially-expressed genes (DEGs), comparing the top/bottom hPRLr isoform ratio tertile. These DEGs were then analyzed via GSEA (Broad), looking within the **B**. Hallmark gene sets, **C**. Chemical and genetic perturbation, **D**. Oncogenic signatures, **E**. Kyoto Encyclopedia of Genes and Genomes (KEGG) gene sets, and **F**. Cancer modules. n=67/cohort.

aggressive TNBC pathogenesis.

We also performed a full GSEA on our 345 enriched gene signature. We assessed a variety of well-annotated gene sets within the MSigDB Collection (e.g. "Hallmark", Chemical and genetic perturbations, etc.; Figure 30B-F) and uncovered a significant association within the hPRLrI-hi/hPRLrL-lo cohort with basal-like breast cancer, metastasis, and oncogenic KRAS actions, along with a number of cancer modules and cytokine signaling effectors.

While these results indicate that high hPRLrI, low hPRLrL expression holds significance in the pathogenesis of TNBC, the majority of studies to date have instead highlighted hPRLr significance in luminal disease. We hypothesized that one possible explanation for this discrepancy is that traditional studies have examined hPRLrL expression specifically, or at least to the greatest extent. We therefore performed GSEA on those genes enriched within the hPRLrI-lo/hPRLrL-hi cohort. Genes within this enrichment set included those which are typically down-regulated in basal-like breast cancer (e.g. PNMT, PVALB, and SLC26A3), as well as genes typically up-regulated in luminal B breast cancer (e.g. CHGA, NPY1R, and CGA).

Given the association observed in our TMA analyses that hPRLrI expression is correlated with high KI67, we assessed the correlation between the hPRLrI:hPRLrL ratio and *MKI67* transcript expression using TCGA data. Regression analysis was unable to find a significant correlation between these two variables (Figure 31A). We also examined hPRLrI:hPRLrL ratio expression by KRAS expression, in consideration of our GSEA results. These results did in fact indicate hPRLrI:hPRLrL ratio expression positively and significantly correlated with KRAS expression (Figure 31B). Considering these results, we assessed for correlation of hPRLrI:hPRLrL expression against a number of oncogenes and effectors of hPRLr signaling (e.g. CCND1, JAK2, SRC, and the MAPK genes; Table 11). Following regression analyses, we found a sig-

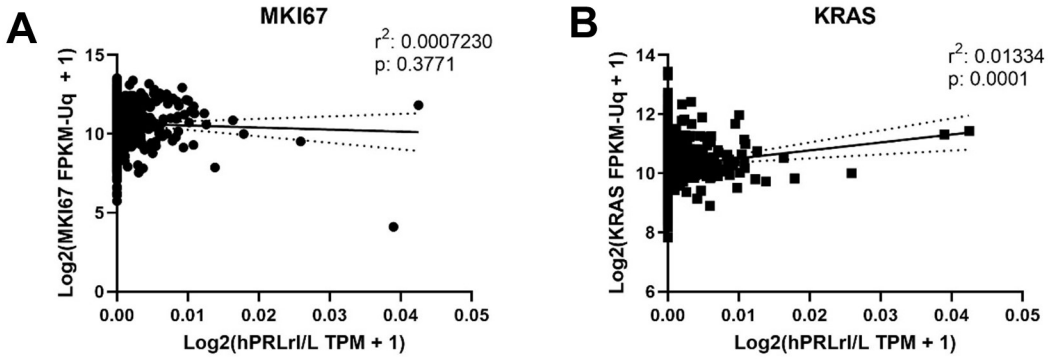

Fig. 31. Expression of MKI67 and KRAS by hPRLrI:hPRLrL transcript ratio. **A**. MKI67 and **B**. KRAS transcript expression, respectively, were compared against the hPRLrI:hPRLrL ratio of transcript expression by regression analysis. n=201.

nificant positive correlation between hPRLrI:hPRLrL expression and CCND1, ERK2, MAPK6, MAPK8, MAPK9, and MAPK14.

8.3 Discussion

These results represent the first study of its kind, encompassing an hPRLr isoform-specific examination of breast cancer clinicopathologies. While there have been a variety of expression analyses, both protein and transcript, that have examined hPRLr expression, these studies have focused on pan-hPRLr expression. In the studies demonstrated here, hPRLrI expression was assessed on both an individual expression level as well as in conjunction with hPRLrL, as a function of hPRLrI:hPRLrL ratio. At the protein level, hPRLrI expression significantly associated with high proliferative index, tumor grade, and TNBC. Similar results were observed at the transcript level, where a high hPRLrI:hPRLrL ratio correlated with larger, late stage, basal-like breast tumors. While a number of recent studies have suggested a role for hPRLr in TNBC, PRL/hPRLr have traditionally been associated with luminal breast cancers[198]. Yet, the assocation with luminal cancers has been restricted to hPRLrL[48,239].

Table 11. hPRLrI:hPRLrL correlation with a number of select oncogenes

Gene name	r [95% CI]	r squared	p value
BCL6	-0.01206 [-0.07164, 0.04760]	0.0001455	0.692
CCND1	0.06824 [0.008651, 0.1273]	0.004657	**0.0249**
CISH	-0.01067 [-0.07025, 0.04898]	0.0001139	0.726
ELF5	-0.07887 [-0.1378, -0.01933]	0.00622	**0.0095**
ERBB2	0.01717 [-0.04250, 0.07671]	0.0002947	0.5729
ERK1	-0.01723 [-0.07677, 0.04244]	0.0002968	0.5715
ERK2	0.1007 [0.04130, 0.1593]	0.01014	**0.0009**
ID1	-0.1562 [-0.2138, -0.09745]	0.02439	<**0.0001**
JAK2	0.02783 [-0.03185, 0.08731]	0.0007743	0.3607
KRAS	0.1155 [0.05628, 0.1739]	0.01334	**0.0001**
MAPK4	-0.07688 [-0.1359, -0.01733]	0.00591	**0.0115**
MAPK6	0.0816 [0.02209, 0.1405]	0.006659	**0.0073**
MAPK7	-0.1191 [-0.1774, -0.05988]	0.01418	<**0.0001**
MAPK8	0.1202 [0.06096, 0.1785]	0.01444	<**0.0001**
MAPK9	0.06887 [0.009287, 0.1280]	0.004744	**0.0235**
MAPK11	-0.1219 [-0.1802, -0.06271]	0.01485	<**0.0001**
MAPK12	-0.08947 [-0.1483, -0.03001]	0.008005	**0.0032**
MAPK14	0.1096 [0.05028, 0.1681]	0.01201	**0.0003**
MKI67	-0.02689 [-0.08637, 0.03279]	0.000723	0.3771
SRC	-0.01421 [-0.07378, 0.04545]	0.000202	0.6406
STAT5A	-0.03953 [-0.09892, 0.02014]	0.001562	0.1941
ZYX	-0.1882 [-0.2450, -0.1300]	0.03541	<**0.0001**

The clinical data presented here highlight a nodel association between the hPRLrI isoform and aggressive TNBC/basal-like breast cancers, corroborating both our *in vivo* and *in vivo* presented herein.

Further analysis into our TCGA findings uncovered that high hPRLrI expression, concurrent with low hPRLrL expression, is associated with its own unique pattern of gene expression. This genetic signature is entirely unique from that exhibited by patient samples with low hPRLrI, high hPRLrL expression. Within our hPRLrI-hi/hPRLrL-lo gene signature, a number of oncogenes were significantly enriched, including BCL11A and ROS1. BCL11A (B-cell CLL/Lymphoma 11A) is a transcription factor with recent implications in cancer stem cell maintenance and TNBC pathogenesis[150,308]. ROS1 is a receptor tyrosine kinase whose inhibition alongside that of E-cadherin exhibited synthetic lethality in breast cancer[15]. These results warrant further investigation into a putative synergistic role between hPRLrI, BCL11A, and/or ROS1. We also examined the correlations between the ratio of hPRLrI:hPRLrL expression and a number of genes typically examined as a function of PRL-stimulated signal transduction and transcription, including BCL6, CCND1, and CISH. While the canonical reporter genes for PRL-mediated transcript up- and down-regulation, CISH and BCL6 respectively, were not found to have a significant correlation with hPRLrI:hPRLrL expression, there was a significant correlation observed with the cell-cycle regulator CCND1. These data in particular corroborate the association observed between hPRLrI:hPRLrL expression and that of MKI67, strongly suggesting hPRLrI is a potent mitogenic agent.

Given this association with hPRLrI-hi/hPRLrL-lo and the above breast cancer oncogenes, we were interested in garnering a more full and global understanding of our gene signature. In performing a GSEA, we uncovered a wide array of pathways enriched in our hPRLrI-hi/hPRLrL-lo gene set. Within the Hallmark gene

sets, which summarizes and represents certain well-defined biological states and/or processes (e.g. angiogenesis, apoptosis, KRAS signaling, p53 activity, etc.), we discovered an association with KRAS activation and inflammatory response. These results were corroborated within the Oncogenic signature gene sets, which is a composite of signatures reflecting cellular pathways which are often dis-regulated in cancer, as well as the Cancer modules gene set. Within the Chemical and genetic perturbations gene sets, we observed significant enrichment in genes associated with breast cancer brain relapse, metaplastic and ductal breast carcinoma, and basal-like breast cancers.

8.4 Limitations and Future Directions

While we were fortunate in our endeavor to create and utilize and hPRLrI-specific antibody, our TMA analyses were limited in that we were unable to perform a concurrent hPRLrL-specific analysis of protein expression in our TMA. While a variety of hPRLr antibodies are commercially available, those that exist target either the hPRLr-ECD (which is 100% retained in all hPRLr isoforms annotated to date except for the ΔS1 form) or the membrane-proximal portion of the hPRLr-ICD. Unfortunately, this indicates that hPRLrL-specific protein analyses for IHC purposes are not currently feasible with commercially-available antibodies. Future studies on this topic should first work to establish an hPRLrL-specific antibody targeting the membrane-distal C-terminal tail, followed by high-throughput protein studies such as the TMA analysis utilized here.

Along with the lack of hPRLrL-specific protein analysis, an additional limitation of our TMA analysis was the limited clinical data available. While we were able to examine hPRLrI expression against ER, PR, Her2, and KI67 status, as well as tumor grade, prior malignancy, etc., reporting on survival and metastasis was limited. In our TMA analysis, 34 of the 250 (13.6%) patients used for study had distant

metastases, and survival outcomes were not reported. Concurrently, only 7 out of the 1091 (0.64%) patients used for study in the TCGA-BRCA cohort had metastatic disease, and only 15% had survival outcomes reported. Unfortunately, these numbers limited our study power, and we were unable to discern a significant association between metastatic burden, survival, and hPRLrI expression in either our TMA or TCGA approaches. Therefore, as outcomes data continues to be reposited within the TCGA, future studies should follow-up these analyses to determine whether or not there is a significant survival disadvantage to high hPRLrI expression. Furthermore, considering that our analyses uncovered a strong association between hPRLrI and TNBC, and considering also that women of West African descent are diagnosed with TNBC significantly more frequently than women of European descent, it would be interesting to determine if hPRLrI is over-expressed in breast cancers of African American patients[138,161]. However, the TCGA-BRCA cohort is neither racially diverse (69% of specimens were obtained from white donors) nor rich in TNBC patient samples (10% of specimens are ER-/PR-/Her2-), significantly limiting any analyses of hPRLrI expression in racial disparities. Therefore, future studies of hPRLrI involvement in TNBC pathogenesis should utilize breast cancer samples obtained primarily from African American patients.

An additional limitation to our study power lies in our approach to studying KI67 status in our TMA sample set. KI67 was reported as a mix of percent positive and three categorical variables: low, intermediate, and high. Ideally we would have kept both variables, KI67 percent positive and hPRLrI expression, as continuous variables. However, we were unable to do so given the format of data as provided. While we were able to keep the KI67 status reported within the TCGA as continuous, transcript expression does not always correlate with protein expression, thereby establishing an additional limitation to our approach.

Considering the degree of similarity between hPRLrI and hPRLrL mRNA, a significant read depth would be required for adequate individual isoform identification. For a standard analysis examining differentially-spliced isoform expression, a minimum of 100M paired-end reads are typically required. For submission of RNAseq data, the TCGA requires a minimum read depth of 60M paired end reads. While it is possible that our approach was sufficient observe hPRLrI expression at 100% efficiency, it is unlikely given the ascribed read depths. Our differential isoform analysis relied exclusively on reads spanning the single splice junction that differentiates hPRLrL from hPRLrI, even further limiting increasing the minimum read depth that would be required for adequate coverage and analysis. Future studies should rely on transcriptomic data of a higher read depth.

CHAPTER 9

GLOBAL DISCUSSION AND FUTURE DIRECTIONS

9.1 Global Discussion

Although a role for PRL/hPRLr in breast cancer has been well-documented, efforts to tease out the functional and clinical significance of PRL in malignancy have largely been displaced by its role in normal physiology. One possible explanation for this dichotomy of milk versus malignancy may lie in the unique functions of the individual hPRLr isoforms, whose respective biological roles in breast cancer remain poorly understood. In the studies presented here, hPRLrI is identified as a novel breast cancer proto-oncogene that is capable of reaching its full oncogenic potential when expressed in concert with hPRLrL. As demonstrated here, hPRLrL+I heterodimers: 1) significantly contribute to distant metastasis formation, 2) exhibit greater complex stability than their full-length counterpart, 3) display unique signal transduction, and 4) cooperate with KRAS signal transduction. Given these results, the data presented here support the role of hPRLrI as a novel oncogenic mechanism. Furthermore, these data suggest that hPRLrI oncogenicity acts in a manner similar to that of Her2: meaning, the full-length receptor partner (e.g. hPRLrL versus Her1/3/4), containing those residues, subdomains, and structures critical for robust signal transduction, is necessary to achieve hPRLrI's full oncogenic potential[122].

Similar to the studies presented here with hPRLrI, the homologous intermediate form in rats (rPRLrI) has also been implicated in tumorigenesis, having initially been studied as a potential oncogene in the rat pre-T lymphoma cell line Nb2[7]. While the overall sizes of the rPRLrI and hPRLrI ORFs (1179 bp and 1297 bp, respectively),

as well as their respective truncation points (rPRLrI, bp 1024; hPRLrI, bp 1009), are incredibly similar, there are significant ways in which they differ, confounding any efforts to over-simplify the relationship between the two. For example, while hPRLrI is generated by an alternative splicing event, rPRLrI appears to be the result of genetic deletion[7,157]. Additionally, while hPRLrI and hPRLrL have similar ligand-binding affinities (K_dhPRLrL, 1.79nM; K_d, 1.64nM), rPRLrI has a three-fold greater affinity for rPRL than rPRLrL (Ka_{rPRLrL}, $8.8x10^9M^{-1}$; Ka_{rPRLrI}, $29.1x10^9M^{-1}$)[7,157]. Considering that Nb2 cells are dependent on lactogenic hormones for both proliferation and viability, this significant elevation in affinity for ligand exhibited by rPRLrI is strong evidence for rPRLrI being significantly involved in the malignant behavior of Nb2 cells[7,112,236]. While there are clear differences between the biologies of rPRLrI and hPRLrI, the work characterizing rPRLrI provided early evidence for the oncogenic potential of a shortened PRLr form.

In that vein, once the Schreiber and Mardis groups uncovered the significance of a truncated mPRLr in mammary neoplasia, they assessed the corroborative significance in human breast cancers. While these investigators did not assess the involvement of hPRLrI in human breast cancers, they chose instead to examine the multiple short forms of hPRLr[114]. Similar to our approach in our TCGA analyses, the Schreiber and Mardis groups examined the ratio of hPRLrL and the short forms of hPRLr. To this end, they uncovered a significant increase in hPRLr short form expression, relative to hPRLrL, in breast tumors[114]. Similar to hPRLrI, minimal investigation has been performed on the short forms of hPRLr (hPRLr-S1a, hPRLr-S1b) since their initial characterization[135]. Curiously, both of these short forms are thought to be dominant-negative, however this conclusion was driven by the results of a luciferase reporter assay, wherein hPRLrL/hPRLr-S1a/S1b co-expression was sufficient to dampen response from the β-casein promoter[135]. However, in direct contradiction to the notion

of the short forms being inhibitory, PRL stimulation following isoform co-expression in 293T cells has been shown to induce Jak2 tyrosine phosphorylation[229]. Furthermore, initial studies confirmed that, similar to hPRLrI, both hPRLr short forms exhibit prolonged stability, in comparison to hPRLrL[135]. These data, though preliminary, would argue that the consideration of the short forms of hPRLr as being dominant negative should be revisited. To this effect, a recent study examining uterine carcinoma uncovered that an unspecified short form of hPRLr is the predominant hPRLr species in uterine cancer, and that G129R-PRL treatment of tumor-harboring PTEN mice is sufficient to significantly reduce tumor growth[295]. These data argue that, not only are shortened forms of the hPRLr functional, they also have the capacity to be significantly oncogenic.

While the co-expression of a truncated mPRLr mutant alongside the wild-type mPRLr was shown to promote fibroblast transformation, the data presented here confirm that co-expression of a similarly shortened PRLr variant (hPRLrI) with the full-length form (hPRLrL) contributes to mammary epithelial transformation[114]. While the study of truncated mPRLr mutants quantified the frequency of primary tumors, metastatic burden was not assessed[114]. As shown here, hPRLrL+I co-expression resulted in not only rapid primary tumor growth, but also significant lung micrometastatic burden. This aggressive transformation was observed when hPRLrL+I acted in concert with Ras, as the parental MCF10A transfectants were unable to form tumors *in vivo*, yet the H-Ras-transformed MCF10AT transfectants were able to achieve such. This observation was corroborated in analyzing TCGA breast cancer cohort DEG data, where a high hPRLrI:hPRLrL ratio associated with a greater likelihood of breast cancer brain relapse, metastais, and KRAS signaling. While studies have demonstrated only minimal association between KRAS activity and primary breast tumor formation, significant evidence exists implicating KRAS

involvement in metastases[48,151,241,298]. This evidence corroborates the significance of our findings, and suggests a potential cooperative relationship between KRAS activity and hPRLrL+I co-expression.

Within this notion, there are now several reports highlighting a prominent co-operative role for KRAS with hPRLr in breast cancer pathogenesis. For example, in characterizing a PRL-driven mammary cancer mouse line (NRL-PRL), genomic analyses uncovered consistent activating oncogenic KRAS somatic mutations/amplifications in all primary tumors, which was not found in pre-neoplastic glands[48]. The NRL-PRL model develops histologically diverse, metastatic carcinomas, and while this 2019 genomic analysis did not examine KRAS involvement in metastasis, likely due to the overall long latency, it is reasonable to hypothesize that KRAS is likely significantly involved in the metastatic dissemination observed in this model[48]. These findings coincided with recent discoveries of the reliance on Ras in breast cancer metastatic dissemination, mirroring the *in vivo* results presented herein[298]. In particular, this dependency was found to be most critical in basal-like and Her2+ breast cancers, in promoting aggressive adenocarcinoma[298]. One possible mode of interplay between KRAS and PRL/hPRLr may lie in KRAS involvement in hPRLr stability. KRAS is a negative regulator of GSK3β, which itself is a negative regulator of hPRLr stability[219]. In this manner, KRAS activity indirectly stabilizes hPRLr, uncovering a possible mechanism for the observed cooperation between these two pathways in *in vitro* transformation. A more obviously connection, however, lies in the signal transduction crosstalk evident in these two oncogenic pathways. Such signaling effectors as PI3K, Erk1/2, and Mek1/2 are key players in the downstream actions of both KRAS and PRL/hPRLr, and may be concurrently involved in the demonstrated cooperativity.

Recently, both PRL and hPRLr themselves implicated in being clinical mark-

ers for metastatic risk[251]. In particular, a strong association between PRL/hPRLr expression and bone metastasis was observed, specifically in the context of ER+ disease[264]. However a limitation of both this review as well as the 2015 study by Sutherland *et al.* was the lack of examination of hPRLr isoform-specific activity and expression[251]. An additional study which examined both high levels of circulating PRL as well as over-expression of hPRLr in a xenograft 4T1 model showed both to be associated with an elevated risk for metastasis to the lungs, liver, and bone[302]. As data regarding metastasis as well as survival outcomes within both the TCGA-BRCA cohort and the breast cancer TMA used are limited, future studies will be necessary to fully parse the unique role of hPRLrI in breast cancer metastasis and survival outcomes.

Similar to the *in vivo results*, hPRLrL+I co-expression promoted *in vitro* transformation. These results were further corroborated following isoform-specific KD using both MCF7 and T47D breast cancer cells. However, unlike the MCF10AT *in vivo* results, hPRLrI KD in MCF7 cells was not sufficient for inhibition of tumorigenic potential. While it is possible that hPRLrI inhibition does not have an effect on *in vivo* transformation, our *in vitro* results would argue that is not the case. The maximum level of hPRLrI KD efficiency we were able to obtain in MCF7 cells was less than 50%, and given the inherent stability of hPRLrI, this may not have been sufficient for our *in vivo* approach to recapitulate our *in vitro* findings. An equally likely possibility for the failure in this approach may in fact lie in the model cell line we employed. As PRL/hPRLr have been traditionally associated with ER+ disease, our approach to hPRLrI KD focused on the two aforementioned luminal cell lines. However, as subsequent examination uncovered, hPRLrI is more significantly associated with ER-, basal-like breast cancer. It therefore may be a result of the differential biology of these two disease types that was ultimately responsible for our lack of sig-

nificant findings *in vivo*. Furthermore, MCF7 cells carry significant aneuploidy, on the order of 60-140 chromosomes, and have a high degree of inherent genomic instability[69]. It therefore equally as likely that, being as significantly mutated as they are, MCF7 cells have acquired other driver mutations and are not reliant on hPRLrI oncogenicity at this stage.

These findings suggest structures within the hPRLrL homodimeric intracellular domain (ICD) contribute to mammary differentiation. Removal of these hPRLr subdomains by differential splicing results in the full realization of hPRLrI oncogenic potential, following heterodimerization with hPRLrL. Studies from our lab utilizing hPRLr-GM-CSFr chimeric receptor constructs further validates this hypothesis. These studies, which utilized both truncation and tyrosine point mutagenesis of the rPRLr ICD, confirmed that PRLr heterodimerization significantly modulates both downstream signaling capabilities as well as physiologic response to stimulus[55,56]. The identification of an oncogenic hPRLr form could resolve many of the unanswered questions regarding the seemingly dichotomous role PRL plays in mammary differentiation versus malignancy. As described here, hPRLrL+I mechanisms that shift the balance away from differentiation toward transformation may include differential complex stability and/or signal transduction.

Protein degradation assays revealed hPRLrL+I heterodimers are significantly more stable than hPRLrL homodimers. These results are of particular relevance given the well-documented oncogenic effects of increased hPRLr stability in breast cancer[174,175,220,268]. Physiologically, greater hPRLr stability results in augmented signal transduction, leading to greater cellular proliferation, anchorage-independent growth, and tumorigenicity[175,220]. Corroborating the significance of hPRLr stability in mammary transformation, hPRLr has been found to be more stable in both breast cancer cell lines as well as patient-derived malignant tissue, when compared to that of normal

mammary epithelia[174]. Furthermore, this elevation in stability was concurrent with a decrease in the phosphorylation status of hPRLr-S349[174]. These results are similar to those uncovered by our studies, wherein phospho-immunoblot confirmed that the increase in hPRLrL+I complex $t_{1/2}$ correlated with a decrease in hPRLr-S349 phosphorylation status. These data suggest that monomeric hPRLr-S349 expression is not sufficient for PRL-induced phosphorylation at the phosphodegron, thereby preventing recruitment of the ubiquitin-ligase machinery to the receptor and subsequent protein turnover[175]. These findings represent a putative mechanism through which hPRLrL+I may contribute to breast cancer pathogenesis.

As hPRLr signal transduction is directly influenced by receptor stability, and as studies with the rPRLr demonstrated that isoform heterodimers signal uniquely from their homodimeric counterparts, it was not surprising to find changes in signaling patterns as a result of hPRLrL+I heterodimerization[56]. Interesting, however, was the observation that hPRLrL+I heterodimers are incapable of inducing Stat5a tyrosine phosphorylation. This phosphorylation event has been long-believed to be the canonical Stat5a activation site, and is required in the normal mammary gland for development and milk production, while unphosphorylated Stat5a (upY-Stat5a) has been dogmatically thought of as functionally inert[115,294]. However, precedent data with upY-Stat3, as well as emerging evidence with upY-Stat5a, has indicated that unphosphorylated Stats are indeed active and function independently from their phosphorylated counterpart[86,134]. Notably, overexpression of phosphodeficient Stat5a-Y694F in HeLa cells was recently shown to promote and stabilize heterochromatin formation, which was sufficient for global transcriptomic downregulation[134]. Many of the genes epigenetically silenced by upY-Stat5a carry tumor suppressive functions (e.g. TIMP4, SH3GL2), suggesting upY-Stat5a itself may be involved in hPRLrL+I-driven mammary transformation[134]. While studies regarding the actions of upY-Stat5a in-

dependent of pY694-Stat5a are gaining traction, the role of Stat5a in breast cancer remains unsettled: elevated pY694-Stat5a in clinical samples associates with more differentiated tumors and better prognosis, yet Stat5a knock-out mice display delayed tumor onset[205,233]. One possible explanation for this discrepancy involves the actions of Stat5a in regulating Jak2 activity. Research has shown pY694-Stat5a may be necessary in attenuating Jak2 promiscuous kinase activity, indicating the apparent Stat5a dichotomy may be the result of unchecked actions of Jak2[271]. These results imply that a paucity of pY694-Stat5a activity, in conjunction with other active hPRLr signaling effectors (e.g. MAPK and Ras) may be contributory mechanistic factors in hPRLrL+I-driven transformation.

While clinical analyses have successfully confirmed the relevance of hPRLr in breast cancer, limited options in reagents have hampered researchers in parsing out the specific effects of differentially-spliced hPRLr isoforms[97]. Accordingly, the approaches utilized in this study were able to successfully focus on those clinical features that associated with both 1) hPRLrI expression, and 2) the hPRLrI:hPRLrL ratio. While a handful of recent studies have suggested a role for this receptor in TNBC, PRL/hPRLr have traditionally been associated with luminal breast cancers, and this association is observed with only hPRLrL[48,198,222,239]. A case study published in March of 2020, for example, discussed the findings of a 27-year-old woman diagnosed with stage III TNBC, which was also deemed pregnancy-associated breast cancer (PABC)[222]. This patient's tumor quickly spread to the bone, and biopsied specimens uncovered an increase in both hPRLr and KI67 expression comparing the primary tumor to the bone metastasis by IHC[222]. The accelerated manner by which this tumor grew and ultimately metastasized was probably a consequence of up-regulated serum PRL that occurs naturally during pregnancy, and provides even further justification of the pressing need for clinically effective hPRLr antagonists. As these clinical data

suggest, and as is supported by the data presented in this dissertation, isoform-specific inhibition of hPRLrI in TNBC/basal-like breast cancers may ultimately serve as an effective therapeutic option for this specific patient population. However, it should be noted that this case study represents an n of 1, and further studies are needed to support this hypothesis[222].

9.2 Future directions

As demonstrated by our TCGA analyses, expression of hPRLrL, hPRLrI, or both concurrently, associates with unique gene expression patterns. While these results established the framework for prognostic indication, they do not provide any insight into the differential transcriptomic response to ligand stimulation of either hPRLrI homodimers or hPRLrL+I heterodimers. Work from our lab has demonstrated that hPRLrL retrotranslocates to the nucleus following PRL stimulation, facilitating target gene transcription[97]. Future studies should examine not only if hPRLrI homodimers/hPRLrL+I heterodimers similarly retrotranslocate, but should also work to determine the transcriptomic response to PRL stimulation of these receptor complexes. Preliminary qRT-PCR studies should first be used to assess differential transcription of such characterized PRL-responsive genes as CISH, CCND1, and ZXN. If a differential response is observed, subsequent RNAseq analyses would be necessary to understand the full global profile of hPRLrI-mediated gene transcription.

As discussed above, one of the major limitations to our studies was the relative inefficiency of our hPRLrI-specific KD. While said KD was sufficient to mitigate colony forming potential *in vitro*, efficacy in mitigating tumorigenic growth *in vivo* was not observed. One possible mechanism to overcome this hurdle may lie in CRISPR-mediated hPRLrI knock-out (KO). Utilizing CRISPR-Cas9 base editing technology, we would establish a synonymous mutation at the 5' hPRLrI cryptic splice donor

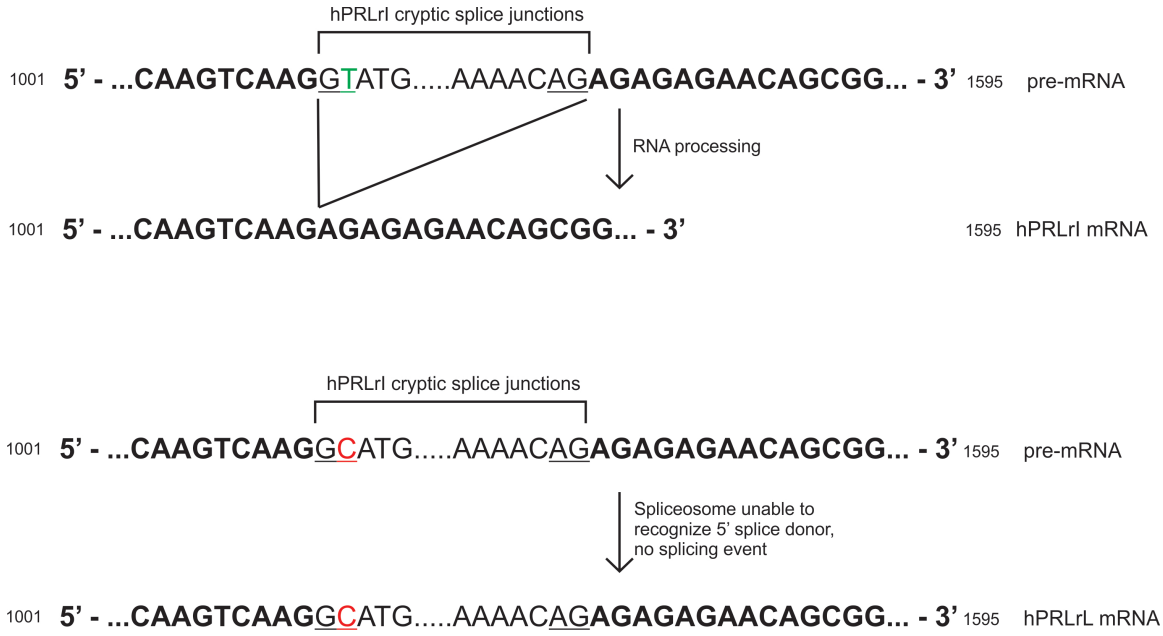

Fig. 32. Proposed approach for CRISPR-mediated hPRLrI KO. CRISPR-mediated homology-directed repair (HDR) would be used to generate a synonymous single point mutation (c.1012T>C), which would suppress the alternative splicing action used to generate hPRLrI while not affecting the remaining hPRLr isoforms.

site of the endogenous hPRLr gene (c.1011T>C). This mutation would prevent the alternative splicing event that generates hPRLrI, while keeping the remaining hPRLr isoforms intact (see Figure 32 for a schematic of this approach). CRISPR construct design and application would be facilitated by VCUs Transgenic/Knockout Mouse Resource Shared Facility[303].

Considering that our studies uncovered a novel association between hPRLrI and TNBC/basal-like breast cancer, we were limited in our approach by using only luminal cell lines (MCF7 and T47D). While these studies provided a relevant preliminary framework for our approach, future analyses should assess the effect of hPRLrI KD/KO in a TNBC and/or basal-like cell line, such as either MDA-MB-436 or SUM190. Similar to the KO approach enumerated above, focusing our hPRLrI loss-of-function studies in a more appropriate cell line could potentially overcome the

confounding factors involved in luminal-focused hPRLrI KD. In this same notion, future studies should also assess the specific actions of hPRLrL loss in both TNBC and luminal disease. Studies to date, aside from that presented here, have focused almost exclusively on pan-hPRLr KD. A single study exists wherein hPRLrL-specific KD was performed using splice-modifying oligomers, however in this manuscript, no IB data was demonstrated to confirm the validity of their approach[302]. Therefore, future studies should examine the effect of hPRLrL-specific KD by targeting the region of hPRLrL that is lost during hPRLrI splicing (i.e. bp 1010-1581). Considering the significant association of hPRLrL with differentiation, we would hypothesize that hPRLrL-specific loss would contribute to malignancy, and could potentially explain why pan-hPRLr inhibitors have failed to show clinical efficacy.

For an additional, and potentially more relevant, approach to modeling hPRLrI loss *in vivo*, we would propose that future studies utilize readily-available PDX models. As depicted in Figure 33 wherein HCI011 cells were transfected with our hPRLrI shRNA constructs, hPRLrI KD is, in fact, possible in this model system. While HCI011-hPRLrI KD transfectants did not grow differently than the scRNA negative control line *in vivo*, follow-up analyses indicated hPRLrI expression was regained during the course of tumorigenesis. While there are a number of rationales as to why this approach failed (e.g. selective pressure, hPRLrI intrinsic stability, and/or HCI011 is an ER+ line, to name only three), it provided a proof-of-principle justification for future studies using PDX models.

As a corollary to the KD approaches described herein, we would also be interested in assessing the functionality in transformation of the individual hPRLr components lost from hPRLrI during differential splicing (e.g. removal of the phosphodegron, the putative Stat5a docking residues, etc.)[157]. Simple point mutagenesis studies removing these residues from hPRLrL, either individually or combined, followed by co-

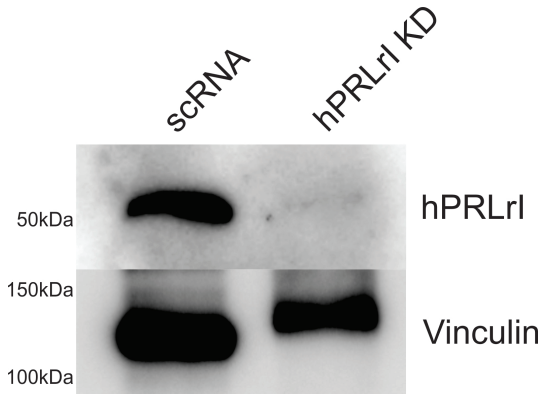

Fig. 33. Pre-injection hPRLrI KD efficiency in HCI011 cells. HCI011 cells were spin-fected with anti-hPRLrI shRNA and subject to puromycin selection for 48 hours before blotting to assess KD efficiency. n=1.

overexpression with the unaltered hPRLrL, would provide insight into the underlying mechanism of hPRLrL+I-mediated transformation. Furthermore, reintroduction of those key residues and subdomains back into hPRLrI could be used to assess for phenotypic rescue.

Another *modus operandi* to study hPRLrL+I involvement in breast cancer etiology would be the establishment of a transgenic mouse model. To date, there have been a number of studies that have established transgenic murine lines, in an effort to study the role of PRL in breast cancer biology[58,188,239]. However, these studies have been limited in their attempts due to the minimal affinity of hPRLr for mouse PRL (mPRL)[282,283]. While a humanized PRL model was developed almost a decade ago, characterization of this model is limited[58]. Given the xenograft data presented herein, generation of an hPRLrL+I transgenic mouse line would be of particular relevance. To date, there has not been an orthologous mPRLrI gene identified. However, three of the manners by which this transgenic model could be achieved are: 1) use the true, respective, hPRLr sequences in the humanized mouse model, against the NSG genotypic background, 2) utilize the mPRLrL and mPRLrT genes, respectively, or 3)

knock-in (KI) the 5' splice recognition sequence into the endogenous mPRLr gene, which would potentially be sufficient for orthologous mPRLrI splicing (c.999T>G; Figure 34)[46,58,114,189,250]. Within these approaches, we would expect hPRLrL+I or mPRLrL+T co-expressing transgenic models to develop spontaneous mammary tumors. Should tumors not arise in this model, we would next assess the functionality of introducing transgenic KRAS.

Fig. 34. Approach to CRISPR-mediated mPRLrI generation. Alignment of the hPRLr and mPRLr ORFs, respectively. The 5' cryptic conserved donor splice sequence is highlighted in green, with the critical GT dinucleotide bolded and underlined. Within the mPRLr 5' region, the site requiring CRISPR-mediated HDR (c.999T) is demonstrated by white text. The downstream 3' cryptic splice-accept site is highlight in orange.

As discussed above in our hPRLrL+I co-overexpression approach, we were only able to achieve primary tumor establishment and growth in the context of oncogenic Ras activity. While we subsequently overexpressed oncogenic KRAS in our MCF10A co-transfectants and performed a soft agar analysis, studies examining other malignant behaviors (e.g. proliferation and/or migration/invasion) were not performed. Assessing these additional behaviors would provide insight into the efficacy of moving forward with a xenograft approach of these MCF10AK transfectants. Within this same line of reasoning, it would be apropos to assess the effect of Ras KD in our MCF7 hPRLrI KD cell lines. Considering that hPRLrI KD alone was sufficient to mitigate *in vitro* colony forming potential, and given both our *in vitro* and *in silico* results that indicate KRAS plays a cooperative role in hPRLrL+I-driven transformation, we would anticipate that concurrent Ras KD would synergize with hPRLrI

KD. In this sense, not only would be expect to observe an even greater reduction in anchorage-independent growth, proliferation, and migration, we would anticipate MCF7 cells with both hPRLrI and KRAS KD would grow significantly less *in vivo* that either KD on its own. Follow-up approaches would involve the pharmacological dual-inhibition of hPRLrI and KRAS; discussions below enumerate the relevant approaches for developing an anti-hPRLrI compound, and while there are currently no FDA-approved KRAS-specific inhibitors (some of those FDA-approved drugs that exhibit non-specific KRAS ihibition include Trifluridine and Regorafenib), clinical trials are underway for the KRAS-specific antagonists MRTX849 and AMG-510[49,50,52,133].

The association of hPRLr and breast cancer has garnered clinical interest, and a variety of pan-hPRLr antibodies have undergone phase I clinical trials[66]. These antibodies, all of which targeted the hPRLr-ECD which is fully conserved among the majority of annotated hPRLr isoforms (i.e. all but the ΔS1 isoform), were found to be safe yet clinically ineffective[66,158]. These agents lacked hPRLr isoform-specificity and, in consideration of the data presented here, would argue that future approaches in drug design may need to target hPRLrI specifically. To this end, three manners by which hPRLrI could be clinically inhibited are: 1) antisense RNA therapy, 2) a monoclonal antibody (mAb) with a covalently-linked antennapedia, and 3) a proteolysis targeting chimera (PROTAC). While the data presented here provide some evidence for the efficacy of an antisense RNA therapeutic approach, both the mAb and PROTAC approaches warrant further explanation, as described below.

PROTACs, conversely, utilize a different approach. PROTACs are comprised of an E3 ubiquitin ligase conjugated to a binding partner of the respective protein of interest, joined by a linker sequence. To this end, a protein of interest is targeted for degradation in an efficient and specific manner. Considering how little still is understood of the biology of hPRLrI, preliminary studies utilizing either yeast

2-hybrid schemes or IP-mass spectrometry would be necessary to uncover binding partners hPRLrI, which could subsequently be utilized in generating a PROTAC. While to date there are no FDA-approved PROTACs used clinically, this is more of a reflection of the youth of the technology rather than a lack of efficacy[249]. Recently, however, the first PROTAC-based therapeutic, ARV-110 (targets the androgen receptor for degradation), was pushed through for phase I clinical trials to treat patients with metastatic castration-resistant prostate cancer[221]. While this study is on-going, preliminary results indicate this approach is likely both safe and potentially efficacious, though further studies are needed. Pending the outcome of this phase I clinical trial, design and application of a PROTAC targeting hPRLrI could be just over the horizon.

In conclusion, and in summation of the data and discussion presented within this dissertation, the human intermediate prolactin receptor in a mammary proto-oncogene, and may ultimately serve as a unique breast cancer therodiagnostic.

CHAPTER 10

CONTRIBUTIONS

nanos gigantum humeris insidentes

Sir Isaac Newton

While this dissertation consists of my (Jacqueline M. Grible) own interpretation of the data presented herein, scientific progress is not achieved in isolation. This work was performed jointly, by both my advisor Dr. Charles V. Clevenger as well as a number of scientific collaborators. The hypothesis for this dissertation, and the research carried out during its course, were made possible under the guidance and mentorship of Dr Charles V. Clevenger. All pathologic scoring was performed by Dr. Patricija Zot, as was the generation of our custom normal tissue TMA. The breast cancer TMAs were provided by Dr. Michael O. Idowu. The bioinformatics work performed to assess TCGA hPRLr expression and gene signature analyses was completed by Amy L. Olex. All protocols regarding tissue acquisition, preparation, and staining, in addition to those regarding cloning, IB, and many of the assays performed during the course of this dissertation, were written by and obtained from Shannon E. Hedrick. IP protocols, mouse surgery, and tissue harvesting was greatly facilitated by Alicia E. Woock. All PDX samples utilized were provided by Dr. J. Chuck Harrell, and prepared by both Tia T. Turner and Mohammad Al-Zubi.

Appendix A

ABBREVIATIONS

aa	amino acid
ab	antibody
ACS	American Cancer Society
ADC	antibody-drug conjugate
BAR	bright, alert, responsive
bp	basepair
BRCA	breast cancer
BSA	bovine serum albumin
β-TrCP	β transducin repeats-containing protein
CCND1	cyclin D1
CDC	Centers for Disease Control and Prevention
CHO	Chinese hamster ovary cell line
CHX	cycloheximide
CI	cell index
CISH	cytokine-inducible SH2-containing protein
coIP	co-immunoprecipitate
CRISPR	clustered regularly interspaced short palindromic repeats
CypA	cyclophilin A
D	aspartate
D_2R	dopamine D_2 receptor
DA	dopamine

Da	Dalton
DCIS	ductal carcinoma *in situ*
DEG	differentially-expressed gene
DMSO	dimethyl sulfoxide
E	glutamate
ECD	extracellular domain
EGF	epidermal growth factor
EMT	epithelial-to-mesenchymal transition
EPOR	erythropoietin receptor
ER	estrogen receptor
ERE	estrogen response element
ExAC	The Exome Aggregation Consortium
FACS	fluorescence-activated cell sorting
FBS	fetal bovine serum
FFPE	formalin-fixation and paraffin-embedding
G	glycin
GDC	Genomic Data Commons
GDP	guanosine diphosphate
GFP	green flourescent protein
GH	growth hormone
GHBP	growth hormone binding protein
GHR	growth hormone receptor
GM-CSF	granulocyte-macrophage colony-stimulating factor
GM-CSFr	granulocyte-macrophage colony-stimulating factor receptor
GSEA	gene set enrichment analysis

GSK3β	glycogen synthase kinase-3β
GTP	guanosine triphosphate
H&E	hematoxylin and eosin
HEK	human embryonic kidney
HER2	human epidermal growth factor receptor 2
HMEC	human mammary epithelial cells
hPRL	human prolactin
hPRLr	human prolactin receptor
hPRLBP	human prolactin-binding protein
hPRLrI	intermediate human prolactin receptor
hPRLrL	long human prolactin receptor
HR	hormone receptor
IACUC	Institutional Animal Care and Use Committee
IB	immunoblot
ICD	intracellular domain
IDC	Invasive ductal carcinoma
IL	interleukin
INF	interferon
INFγ	interferon gamma
IP	immunoprecipitation
Jak2	Janus kinase 2
k	kilo
kb	kilobase
KD	knock-down
K_D	dissociation constant

kDa	kilodalton
KO	knock-out
mAb	monoclonal antibody
MAPK	mitogen-activated protein kinase
MEF	mouse embryonic fibroblast
mPRLr	mouse prolactin receptor
mPRLrL	long form mouse prolactin receptor
mPRLrT	truncated mouse prolactin receptor
MTT	tetrazolium bromide
NA	not applicable
NEB	New England Biolabs
NEP	New England Peptide
NGS	normal goat serum
NHS	Nurses' Health Study
NHSII	Nurses' Health Study II
NRL	neu-related lipocalin
NSG	nod-scid gamma
nt	nucleotide
ORF	open reading frame
OS	overall survival
P	proline
pAb	polyclonal antibody
PABC	pregnancy-associated breast cancer
PAGE	polyacrylamide gel electrophoresis
PBS	Phosphate-buffered saline

PBST	Phosphate-buffered saline with Tween20
PCR	polymerase chain reaction
PDX	patient-derived xenograft
PIAS	peptide inhibitor of activated Stat
P/S	Penicillin/streptomycin
PL	placental lactogen
PR	progesterone receptor
PRL	prolactin
PRLr	prolactin receptor
pS	phospho-serine
PVDF	polyvinylidene difluoride
pY	phospho-tyrosine
Q	glutamine
R	arginine
RFS	relapse-free suurvival
RNAseq	RNA sequencing
rPRLr	rat prolactin receptor
rPRLrI	intermediate rat prolactin receptor
rPRLrL	long rat prolactin receptor
rPRLrS	short rat prolactin receptor
RR	relative risk
rSAP	recombinant shrimp alkaline phosphatase
rt	room temperature
RTK	receptor tyrosine kinase
RT-PCR	reverse transcriptase polymerase chain reaction

RUS	research use statement
S	serine
scRNA	scrambled RNA
sd	standard deviation
SDS	sodium dodecyl sulfate
shRNA	short hairpin loop RNA
SOCS	suppressors of cytokine signaling
SPR	surface plasmon resonance
Stat5a	Signal transducer and activator of transcription 5a
T	threonine
$t_{1/2}$	half-life
TAD	transactivation domain
TBS	Tris-buffered saline
TBST	Tris-buffered saline with Tween20
TCGA	The Cancer Genome Atlas
Tm	melting temperature
TMA	tissue microarray
TMD	transmembrane domain
TNBC	triple-negative breast cancer
TPM	transcripts per million reads
upY	unphosphorylated
V	valine
W	tryptophan
WAP	whey acidic protein
WGS	whole-genome sequencing

Y	tyrosine

Appendix B

HPRLRL ORF

ATGAAGGAAAATGTGGCATCTGCAACCGTTTTCACTCTGCTACTTTTTCTCA
ACACCTGCCTTCTGAATGGACAGTTACCTCCTGGAAAACCTGAGATCTTTAA
ATGTCGTTCTCCCAATAAGGAAACATTCACCTGCTGGTGGAGGCCTGGGACA
GATGGAGGACTTCCTACCAATTATTCACTGACTTACCACAGGGAAGGAGAGA
CACTCATGCATGAATGTCCAGACTACATAACCGGTGGCCCCAACTCCTGCCA
CTTTGGCAAGCAGTACACCTCCATGTGGAGGACATACATCATGATGGTCAAT
GCCACTAACCAGATGGGAAGCAGTTTCTCGGATGAACTTTATGTGGACGTGA
CTTACATAGTTCAGCCAGACCCTCCTTTGGAGCTGGCTGTGGAAGTAAAACA
GCCAGAAGACAGAAAACCCTACCTGTGGATTAAATGGTCTCCACCTACCCTG
ATTGACTTAAAAACTGGTTGGTTCACGCTCCTGTATGAAATTCGATTAAAAC
CCGAGAAAGCAGCTGAGTGGGAGATCCATTTTGCTGGGCAGCAAACAGAGTT
TAAGATTCTCAGCCTACATCCAGGACAGAAATACCTTGTCCAGGTTCGCTGC
AAACCAGACCATGGATACTGGAGTGCATGGAGTCCAGCGACCTTCATTCAGA
TACCTAGTGACTTCACCATGAATGATACAACCGTGTGGATCTCTGTGGCTGT
CCTTTCTGCTGTCATCTGTTTGATTATTGTCTGGGCAGTGGCTTTGAAGGGC
TATAGCATGGTGACCTGCATCTTTCCGCCAGTTCCTGGGCCAAAAATAAAAG
GATTTGATGCTCATCTGTTGGAGAAGGGCAAGTCTGAAGAACTACTGAGTGC
CTTGGGATGCCAAGACTTTCCTCCCACTTCTGACTATGAGGACTTGCTGGTG
GAGTATTTAGAAGTAGATGATAGTGAGGACCAGCATCTAATGTCAGTCCATT
CAAAAGAACACCCAAGTCAAGGTATGAAACCCACATACCTGGATCCTGACAC
TGACTCAGGCCGGGGGAGCTGTGACAGCCCTTCCCTTTTGTCTGAAAAGTGT

GAGGAACCCCAGGCCAATCCCTCCACATTCTATGATCCTGAGGTCATTGAGA

AGCCAGAGAATCCTGAAACAACCCACACCTGGGACCCCCAGTGCATAAGCAT

GGAAGGCAAAATCCCCTATTTTCATGCTGGTGGATCCAAATGTTCAACATGG

CCCTTACCACAGCCCAGCCAGCACAACCCCAGATCCTCTTACCACAATATTA

CTGATGTGTGTGAGCTGGCTGTGGGCCCTGCAGGTGCACCGGCCACTCTGTT

GAATGAAGCAGGTAAAGATGCTTTAAAATCCTCTCAAACCATTAAGTCTAGA

GAAGAGGGAAAGGCAACCCAGCAGAGGGAGGTAGAAAGCTTCCATTCTGAGA

CTGACCAGGATACGCCCTGGCTGCTGCCCCAGGAGAAAACCCCCTTTGGCTC

CGCTAAACCCTTGGATTATGTGGAGATTCACAAGGTCAACAAAGATGGTGCA

TTATCATTGCTACCAAAACAGAGAGAGAACAGCGGCAAGCCCAAGAAGCCCG

GGACTCCTGAGAACAATAAGGAGTATGCCAAGGTGTCCGGGGTCATGGATAA

CAACATCCTGGTGTTGGTGCCAGATCCACATGCTAAAAACGTGGCTTGCTTT

GAAGAATCAGCCAAAGAGGCCCCACCATCACTTGAACAGAATCAAGCTGAGA

AAGCCCTGGCCAACTTCACTGCAACATCAAGCAAGTGCAGGCTCCAGCTGGG

TGGTTTGGATTACCTGGATCCCGCATGTTTTACACACTCCTTTCACTGA

Appendix C

HPRLRI ORF

ATGAAGGAAAATGTGGCATCTGCAACCGTTTTCACTCTGCTACTTTTTCTCA
ACACCTGCCTTCTGAATGGACAGTTACCTCCTGGAAAACCTGAGATCTTTAA
ATGTCGTTCTCCCAATAAGGAAACATTCACCTGCTGGTGGAGGCCTGGGACA
GATGGAGGACTTCCTACCAATTATTCACTGACTTACCACAGGGAAGGAGAGA
CACTCATGCATGAATGTCCAGACTACATAACCGGTGGCCCCAACTCCTGCCA
CTTTGGCAAGCAGTACACCTCCATGTGGAGGACATACATCATGATGGTCAAT
GCCACTAACCAGATGGGAAGCAGTTTCTCGGATGAACTTTATGTGGACGTGA
CTTACATAGTTCAGCCAGACCCTCCTTTGGAGCTGGCTGTGGAAGTAAAACA
GCCAGAAGACAGAAAACCCTACCTGTGGATTAAATGGTCTCCACCTACCCTG
ATTGACTTAAAAACTGGTTGGTTCACGCTCCTGTATGAAATTCGATTAAAAC
CCGAGAAAGCAGCTGAGTGGGAGATCCATTTTGCTGGGCAGCAAACAGAGTT
TAAGATTCTCAGCCTACATCCAGGACAGAAATACCTTGTCCAGGTTCGCTGC
AAACCAGACCATGGATACTGGAGTGCATGGAGTCCAGCGACCTTCATTCAGA
TACCTAGTGACTTCACCATGAATGATACAACCGTGTGGATCTCTGTGGCTGT
CCTTTCTGCTGTCATCTGTTTGATTATTGTCTGGGCAGTGGCTTTGAAGGGC
TATAGCATGGTGACCTGCATCTTTCCGCCAGTTCCTGGGCCAAAAATAAAAG
GATTTGATGCTCATCTGTTGGAGAAGGGCAAGTCTGAAGAACTACTGAGTGC
CTTGGGATGCCAAGACTTTCCTCCCACTTCTGACTATGAGGACTTGCTGGTG
GAGTATTTAGAAGTAGATGATAGTGAGGACCAGCATCTAATGTCAGTCCATT
CAAAAGAACACCCAAGTCAAGAGAGAGAACAGCGGCAAGCCCAAGAAGCCCG
GGACTCCTGAGAACAATAAGGAGTATGCCAAGGTGTCCGGGGTCATGGATAA

CAACATCCTGGTGTTGGTGCCAGATCCACATGCTAAAAACGTGGCTTGCTTT
GAAGAATCAGCCAAAGAGGCCCCACCATCACTTGAACAGAATCAAGCTGAGA
AAGCCCTGGCCAACTTCACTGCAACATCAAGCAAGTGCAGGCTCCAGCTGGG
TGGTTTGGATTACCTGGATCCCGCATGTTTTACACACTCCTTTCACTGA

Appendix D

MPRLR ORF

ATGTCATCTGCACTTGCTTACATGCTGCTTGTCCTCAGCATCAGCCTCCTGA
ATGGACAGTCACCACCTGGAAAACCTGAAATCCACAAATGTCGTTCCCCTGA
CAAGGAAACATTCACCTGCTGGTGGAATCCTGGGTCAGATGGAGGACTCCCC
ACCAATTATTCATTGACATACAGCAAAGAAGGAGAGAAAAACACCTATGAAT
GTCCAGACTACAAAACCAGTGGCCCCAATTCCTGTTTCTTTAGCAAGCAGTA
CACTTCCATATGGAAAATATACATCATCACAGTAAATGCCACGAACGAAATG
GGAAGCAGTACCTCGGATCCACTTTATGTGGATGTGACTTACATTGTTGAAC
CAGAGCCTCCTCGGAACCTGACTTTAGAAGTGAAACAACTAAAAGACAAAAA
AACATATCTGTGGGTAAAATGGTTGCCACCTACCATAACTGATGTAAAAACT
GGTTGGTTTACAATGGAATATGAAATTCGATTAAAGTCTGAAGAAGCAGATG
AGTGGGAGATCCACTTCACAGGTCATCAAACACAATTTAAGGTTTTTGACTT
ATATCCAGGACAAAAGTATCTTGTCCAGACTCGCTGCAAGCCAGACCATGGA
TACTGGAGTAGATGGGGCCAGGAGAAATCTATTGAAATACCAAATGACTTCA
CCTTGAAAGACACAACTGTGTGGATCATTGTGGCCGTTCTCTCTGCTGTCAT
CTGTTTGATTATGGTCTGGGCAGTGGCTTTGAAGGGTTATAGCATGATGACC
TGCATCTTTCCACCAGTTCCGGGGCCAAAAATAAAAGGATTTGATACTCATC
TGCTAGAGAAGGGCAAGTCTGAAGAACTGCTGAGTGCCTTGGGGTGCCAAGA
CTTTCCCCCCCACTTCTGACTGTGAGGACTTGCTGGTGGAGTTCTTGGAAGTG
GATGACAATGAGGACGAGCGGCTAATGCCATCCCATTCCAAAGAGTATCCGG
GTCAAGGTGTTAAACCCACACACCTAGATCCTGACAGTGACTCTGGTCATGG
AAGCTATGACAGCCATTCTCTTTTGTCTGAAAAGTGTGAGGAGCCCCAGGCC

TACCCCCCTGCCTTCCACATCCCTGAGATCACTGAGAAGCCAGAGAATCCTG
AGGCAAATATTCCTCCCACCCCAAATCCCCAAAATAACACCCCCAATTGTCA
TACAGATACATCCAAATCTACAACATGGCCTTTACCACCTGGCCAACACACG
CGCAGATCTCCTTACCACAGCATTGCCGATGTGTGCAAGCTAGCTGGAAGTC
CTGGAGATACACTGGACTCTTTCTTGGACAAAGCAGAGGAAAATGTTCTAAA
GTTGTCTGAAGATGCTGGAGAGGAAGAAGTGGCTGTGCAAGAAGGGGCCAAA
AGCTTCCCTTCTGACAAACAAAACACATCTTGGCCACCACTCCAGGAGAAAG
GCCCCATTGTCTATGCTAAACCCCCAGATTACGTGGAGATTCACAAAGTCAA
CAAAGACGGAGTGCTATCATTACTCCCCAAGCAGAGAGAAAACCACCAGACA
GAAAACCCTGGGGGTTCCTGAAACCAGTAAGGAGTATGCCAAGGTATCTGGGG
TCACGGATAACAACATCCTGGTGTTAGTGCCAGACTCACGAGCCCAGAACAC
AGCTTTGCTTGAGGAATCAGCCAAGAAGGTTCCACCATCGCTTGAACAGAAC
CAATCTGAGAAAGATCTGGCCAGCTTTACTGCAACCTCAAGCAACTGCAGAC
TCCAACTGGGCAGGCTGGATTACCTGGATCCTACGTGCTTCATGCACTCCTT
TCACTGA

Appendix E

VECTORS

Vector name	Manufacturer	Catalog No.
pTracer EF V5 HisA	Addgene	V88720
pBabe GFP	Addgene	10668
psi-U6	GeneCopoeia	NA
pBabe-puro	Addgene	1764

Table 13. Vectors. Used in the course of both protein overexpression and cloning.

Appendix F

CLONING REACTIONS

Component	Volume (uL)
iScript Reaction Mix (5x; Bio-Rad)	4
iScript Reverse Transcriptase (Bio-Rad)	1
Template RNA (1ug)	variable
Water	variable
Total volume	**20**

Table 14. iScript cDNA synthesis reaction components.

Time	Temp.
5 min.	25°C
20 min.	46°C
1 min.	95°C
Hold	4°C

Table 15. cDNA synthesis PCR cycling.

Component	Volume per 50uL
PCR High Fidelity Master Mix (2x; NEB)	25uL
10uM forward primer	2.5uL
10uM reverse primer	2.5uL
template DNA	variable
water	to 50uL

Table 16. PCR amplification components.

Temp.	Time	Cycles
98°C	30 sec.	1
98°C	10 sec.	
See Table 22	30 sec.	35
72°C	30 sec./kb	
72°C	2 min.	1
4°C	hold	1

Table 17. PCR amplification cycling.

Restriction enzyme (NEB)	Restriction site
BamH1	G/GATCC
EcoR1	G/AATTC
Kpn1	GGTAC/C
Not1	GC/GGCCGC
Xho1	C/TCGAG

Table 18. Restriction enzymes.

Component	Volume per 50uL
Restriction enzyme	1uL
DNA	1ug
NEBuffer (10x; NEB)	5uL
water	to 50uL

Table 19. Restriction digest components.

Component	Volume per 20uL
1ug DNA	variable
CutSmart Buffer (10x; NEB)	2uL
rSAP (NEB)	5uL
water	to 20uL

Table 20. rSAP treatment components.

Component	Volume per 20uL
T4 DNA Ligase Buffer (10x; NEB)	2uL
Vector DNA (1x pmol)	variable
Insert DNA (3x pmol)	variable
T4 DNA Ligase (NEB)	1uL
water	10 20uL

Table 21. Ligation components.

Table 23. Sequencing primers.

Label	Sequence	Gene of interest	Annealing locus
PRLR-LF-seq1F-m-S	5' - CCTTGTCCAGGTTCGCTGC - 3'	hPRLrL	hPRLrL bp 606-624
PRLR-LF-seq1F-Mas	5' - GCAGCGAACCTGGACAAGG - 3'	hPRLrL	hPRLrL bp 606-624
PRLR-LF-eq2F-m-S	5' - CGGCAAGCCCAAGAAGCCC - 3'	hPRLrL	hPRLrL bp 1593-1611
PRLR-LF-seq2F-mAS	5' - GGGCTTCTTGGGCTTGCCG - 3'	hPRLrL	hPRLrL bp 1593-1611
PRLR-INT-seq1F-mS	5' - GGGACAGATGGAGGACTTCC - 3'	hPRLrI	hPRLrI bp 151-170
PRLR-INT-seq1F-mAS	5' - GGAAGTCCTCCATCTGTCCC - 3'	hPRLrI	hPRLrI bp 151-17
PRLR-INT-seq2F-mS	5' - GGGCAGTGGCTTTGAAGGG - 3'	hPRLrI	hPRLrI bp 761-779
PRLR-INT-seq2F-mAS	5' - CCCTTCAAAGCCACTGCCC - 3'	hPRLrI	hPRLrI bp 761-779

Table 22. Cloning primers.

Primer name	Abbreviation	Sequence	Tm (C)	Restriction site
PRLR-Kpn1-S2	PRLR3	5' - GGACGGTACCCACCATGAAGG - 5'	51	Kpn1
PRLR-BamH1-Start	PRLR7	5' - CCCCGGATCCACCATGAAGGAAAATGTGGC - 3'	64	BamH1
PRLR-V5-HisEcoR1-STOP	V5 His 1	5' - CCCCGAATTCTCAATGGTGATGGTGATGATGACC - 3'	64	EcoR1
PRLR-Trunc-AS4	T4	5' - GACCGCGGCCGCACTTGACTTGGGTGTTC - 3'	64	Not1
PRLR-Kpn1-S3-TS	PRLR5	5' - GGCCGGTACCCACCATGAAGGAAAATGTGGCA -3'	64	Kpn1
PRLR-Not1-AS3-TS	PRLR6	5' - GAAGCGGCCGCAAGGAGTCCCGGGCTTC - 3'	64	Not1
hPRLr-Start-XhoI	PRLR7	5' - GGACTCGAGATGAAGGAAAATGTGGC - 3'	61	XhoI

Appendix G

BUFFERS

Buffer	Components
RIPA	1% (w/w) NP40, 1% (w/v) sodium deoxycholate, 0.1% SDS, 0.15M NaCl, 0.01M sodium phosphate (pH 7.2), 2mM EDTA, 50mM sodium fluoride
Stripping buffer	1.5% glycine, 0.1% SDS, 1% Tween20, pH 2.2
Laemmli (4x)	250mM TrisCl, 40% (w/v) glycerol, 8.3% (w/v) SDS, 0.04% (w/v) bromophenol blue
IB running buffer	25mM Tris, 190mM glycine, 0.1% SDS
IB transfer buffer	25mM Tris, 190mM glycine, 20% ethanol
IB washing buffer	20mM Tris pH 7.5, 150mM NaCl, 0.1% Tween20
Blocking buffer	5% BSA in TBST or 5% milk in TBST
LB medium	10g/L tryptone, 10g/L NaCl, 5g/L yeast extract
LB agar	LB medium, 15g/L agar

Table 24. Buffers.

Appendix H

HPRLRI:HPRLRL DEG RESULTS

Table 25. All hPRLrI:hPRLrL differentially-expressed genes. Gene expression patterns assessing for enrichment within the hPRLrI-hi/hPRLrL-lo cohort, compared to the hPRLrI-lo/hPRLrL-hi cohort. Gene set enrichment analysis of this dataset is presented in Figure 30.

Gene Symbol	padj	Log2(fold change)
RNVU1-18	5.47E-05	10.70522967
CT83	6.03E-09	9.532522508
PRR27	1.46E-10	8.474067749
SNORA74B	2.11E-26	7.255759124
MIR3609	4.28E-15	7.22928729
SNORA74A	4.18E-19	7.026809283
LINC00668	1.97E-22	6.772341758
RN7SL3	1.41E-37	6.674803977
RF00003	1.67E-14	6.640866684
MAGEA6	6.82E-06	6.606261911
RF00100	1.85E-40	6.592300296
RNU4-2	2.61E-35	6.583634431
SCARNA5	1.03E-32	6.582850303
PRSS33	3.17E-15	6.417309881
SNORA73B	8.43E-35	5.857845815
RNVU1-7	5.86E-18	5.715316843
FABP7	4.76E-22	5.715192445
SNORA23	1.87E-27	5.681456516
VGLL1	5.56E-25	5.569518674
RF00003	2.07E-14	5.40440823
SNORA74D	1.62E-10	5.395345211
ART3	4.95E-27	5.306694275
FOXCUT	4.58E-16	5.180759798
SSX1	0.000563033	5.176846728
SNORA20	5.94E-15	5.088739594
ROPN1	4.05E-15	5.002183111
SCARNA10	2.98E-21	4.990615368
HORMAD1	2.27E-22	4.97681648
C11orf86	2.96E-08	4.783946712

CHGB	9.22E-15	4.605516141
SLC6A15	2.70E-17	4.568935698
SNORD15B	2.37E-22	4.568836894
LINC01956	1.14E-15	4.465626646
CHST4	1.45E-22	4.404228863
SNORD17	1.74E-24	4.222603855
NKX1-2	7.96E-12	4.08974099
KIRREL3-AS1	2.73E-07	4.058340024
SCARNA6	1.62E-19	3.999262866
CSAG1	5.38E-07	3.966106854
FDCSP	1.42E-12	3.956928024
GABRP	4.28E-15	3.803366165
MSLN	1.11E-21	3.798073496
RGR	2.76E-07	3.795820182
CASC9	7.29E-05	3.760696386
CSAG3	2.16E-06	3.680515137
SLC26A9	3.43E-13	3.676732439
LHFPL4	1.62E-14	3.656477857
SOX8	2.62E-20	3.650530137
SNORA12	1.34E-13	3.642874323
NDUFB4P11	3.58E-11	3.639076507
GABRA3	1.15E-07	3.637785305
OLAH	5.05E-14	3.564827952
LINC02188	5.63E-11	3.515769038
ZNF716	0.000557546	3.464701841
ABCA13	4.31E-11	3.451591538
CASC8	1.80E-17	3.388982506
GSTA1	2.52E-11	3.370480809
CALML5	1.80E-12	3.366776272
TLX1	7.03E-08	3.362349325
FGFBP1	1.09E-07	3.361048251
UGT8	3.12E-16	3.345410072
LINC02487	1.14E-17	3.322060982
PPP1R14C	4.90E-15	3.286843174
SNORA2C	3.54E-11	3.267149711
AFAP1-AS1	3.90E-21	3.224588516
AQP5	9.59E-10	3.220142519
EN1	7.23E-20	3.209053032
PRSS3	3.12E-13	3.198890003
HIST1H4B	4.58E-08	3.16866694
A2ML1	4.05E-11	3.142497836
FUT6	7.41E-10	3.098441289

MAGEA12	0.004262687	3.077214117
C1QL4	1.23E-12	3.07651811
AC091078.1	2.77E-09	3.063799596
LINC01446	0.003379055	3.028221566
OCA2	4.25E-08	3.014928974
ROPN1B	1.67E-14	3.01167797
SCARNA21	3.44E-09	2.998231753
POTEC	1.62E-05	2.983273327
GABBR2	7.20E-08	2.971804738
RHOXF1P1	0.000932547	2.964912036
ACE2	4.05E-13	2.949964761
LPO	1.42E-12	2.934705075
LIN28A	5.68E-07	2.913822476
ELF5	3.66E-09	2.905436951
FAM19A3	1.18E-13	2.902361526
BPI	2.28E-13	2.898933881
MUC16	8.82E-10	2.879689524
CDH19	1.02E-05	2.87397286
AC022784.1	2.39E-08	2.861782433
KIF25-AS1	1.33E-06	2.814451737
SCRG1	3.38E-14	2.791991399
LINC01287	2.51E-11	2.779963129
LINC00092	2.54E-11	2.775409876
KLK6	1.47E-07	2.768074392
AC020907.1	6.62E-13	2.754368561
MDGA2	7.64E-06	2.713718147
AC005150.1	0.001535774	2.712467667
C8orf46	2.28E-13	2.705178156
KRT16	6.33E-09	2.688732037
DSG1	1.64E-07	2.681151105
OR2I1P	1.75E-10	2.667855182
SLCO4A1-AS1	1.73E-08	2.661330397
SLC15A1	7.64E-09	2.65152761
CCL7	1.35E-06	2.63483598
IGF2BP3	3.31E-13	2.6346487
SNORA14B	5.36E-12	2.615249171
SPIB	1.29E-09	2.61203599
RAET1L	5.12E-07	2.607290409
ORM2	1.83E-05	2.597419439
RF00003	4.82E-11	2.590476074
SCARNA12	1.17E-10	2.588613179
SIX3	2.08E-06	2.583259642

CHODL	1.80E-12	2.578731331
CXCL5	2.46E-09	2.577093768
LINC00707	3.16E-06	2.569653878
LHX9	1.83E-05	2.569318602
HIST1H1B	2.14E-09	2.542305853
SNORD94	3.17E-12	2.539305765
S100B	6.29E-11	2.523522862
LEMD1	1.55E-06	2.506141976
NCCRP1	1.48E-08	2.504595324
SEC14L4	1.68E-06	2.489704329
RN7SL2	3.17E-12	2.486532739
MIA	5.73E-07	2.48200181
FAR2P4	1.80E-06	2.479699961
KCNK5	3.41E-13	2.46494795
KRT79	4.90E-08	2.448923151
SLC22A16	9.65E-10	2.443655329
IL36RN	6.95E-05	2.430547714
TRPM8	8.82E-10	2.426284311
OFCC1	0.009897532	2.419893631
KIR2DL4	2.59E-07	2.413419778
AC105999.2	0.005992006	2.411577332
DLX6	1.34E-06	2.40792772
UBD	1.61E-09	2.407122239
TTYH1	4.17E-12	2.395996693
BLACAT1	1.40E-06	2.395981097
FZD9	1.48E-08	2.390226205
SBSN	6.22E-05	2.381232998
ERICH5	1.67E-06	2.368962515
PLAC4	4.38E-08	2.334041566
GJB3	2.04E-07	2.331772751
LY6D	0.002030376	2.32361443
ROCR	6.06E-05	2.314816646
ERVV-2	0.005978019	2.302065462
PIGR	1.68E-05	2.286362155
COL9A3	7.41E-10	2.285981268
LINC01133	3.69E-07	2.269196798
PSAT1	1.54E-07	2.267387982
MUC15	6.37E-05	2.266085401
SCARNA13	3.31E-10	2.262003311
SYT8	2.43E-06	2.255358294
CRYAB	1.30E-10	2.236439808
MARCO	7.56E-07	2.230972619

C11orf16	3.40E-08	2.224261383
AC019171.1	5.70E-09	2.222666025
HRCT1	4.65E-09	2.222207829
IL22RA2	1.57E-06	2.221608457
GAD1	8.32E-07	2.212218853
LINC02055	0.00379022	2.209097233
AC010980.2	2.05E-07	2.208789862
IL12RB2	8.17E-08	2.203637428
OPRK1	1.57E-05	2.198393697
FOXA3	2.50E-06	2.198307456
LINC01694	2.52E-11	2.198282738
IGLV3-19	7.44E-07	2.197163145
HIST1H3B	1.42E-06	2.194764716
BCL11A	1.24E-07	2.191593593
SHC4	1.38E-07	2.187891894
GAL	1.39E-07	2.184143684
FGG	0.002874089	2.179541268
AC009041.2	2.11E-10	2.154701561
IDO1	7.89E-09	2.151786794
PRAME	0.002540176	2.136523891
C12orf56	0.000636018	2.12660088
PRSS51	4.90E-11	2.112116431
KLK5	6.56E-05	2.104141949
ORM1	0.000385714	2.091094921
EEF1DP5	0.006226951	2.08428322
C6orf223	1.88E-06	2.081881917
GFRA3	3.13E-06	2.080712271
POLR2F	1.44E-07	2.080056378
IGHV2-26	3.63E-05	2.078507562
AC021683.2	3.88E-08	2.078375414
IGF2BP2	7.53E-11	2.076827347
ATP10B	9.92E-07	2.075443175
TNNI2	2.41E-11	2.072511891
CLDN6	1.54E-06	2.070667324
AC005537.1	0.000120841	2.069037567
SPHKAP	0.000871571	2.067559646
B3GAT1	5.14E-07	2.064388716
CHI3L1	1.47E-07	2.058592391
IGLV3-1	1.37E-05	2.058124756
FOXC1	1.90E-10	2.045416815
CXADRP3	0.001297315	2.042096385
POU6F2	0.000762247	2.041762423

GRB14	3.85E-06	2.039535878
SLC5A12	0.00056112	2.025692544
KCNG1	1.37E-05	2.016244952
IGHV1-18	2.97E-05	2.005065118
KCNQ4	9.65E-10	1.99919856
HRK	6.34E-06	1.997907904
LINC01554	5.17E-07	1.988451228
ODAM	0.000542061	1.979359766
IGKV5-2	0.000262754	1.978515503
LAMP3	1.81E-08	1.975921331
HIST1H4C	4.99E-07	1.973391851
SOX9-AS1	6.61E-08	1.973345744
PICSAR	5.29E-06	1.967885065
CYP27C1	1.68E-07	1.964497298
MATN4	1.25E-06	1.961773747
AC010894.3	4.14E-05	1.953823955
ADAMDEC1	6.68E-09	1.951206217
CASC16	0.000658892	1.948323601
AC011632.1	0.003859269	1.940232088
TRH	8.73E-05	1.938604497
RF00012	0.000931223	1.93179495
SCEL	0.005478298	1.92607258
NLRP7	2.49E-06	1.92374161
L1CAM	1.25E-05	1.913656936
LINC02515	6.09E-06	1.911270103
KLK8	0.000368315	1.911261059
TYRP1	0.000144047	1.910123538
CYP24A1	6.20E-05	1.900233472
AC092821.1	6.82E-08	1.899680821
P2RX2	0.002435205	1.890306557
GBP5	2.79E-08	1.881959381
AL022316.1	2.96E-08	1.875268099
GCNT3	1.16E-07	1.871327678
SLC6A17	4.99E-07	1.85982646
AC015712.4	0.000618872	1.859295831
GZMB	1.22E-06	1.859013627
TLX1NB	0.008827803	1.857271174
RARRES1	1.40E-06	1.855171101
RYR2	7.71E-08	1.854716169
MUC13	0.000401436	1.854311228
MGAM2	5.77E-06	1.850504406
IGLV3-25	8.54E-05	1.84787021

AC008514.1	2.95E-07	1.847615278
LINC02475	0.009767565	1.840077556
LINC02473	0.000538307	1.836869045
CEP295NL	1.43E-07	1.834782877
U62317.2	1.71E-07	1.830470464
AC124248.1	8.79E-05	1.827883958
MT1H	5.13E-05	1.82185909
SLC34A2	0.001181381	1.815950083
AC010980.1	4.27E-06	1.800360659
C6orf15	0.000451823	1.791385679
SLC2A12	1.18E-06	1.786102528
CNTN5	0.009985193	1.785466997
PSORS1C2	0.000976371	1.783445753
HIST1H2BO	7.29E-06	1.779499142
LINC01468	0.000155043	1.778449798
AIM2	7.06E-09	1.77414915
KLHL30	1.79E-07	1.773779676
HAPLN3	7.72E-11	1.769729154
IGHV1-69D	0.000446277	1.769139853
DNER	0.000401436	1.761428353
CXCL10	1.39E-07	1.759845186
KCNMB2-AS1	0.005271239	1.758570946
QRFPR	0.000164625	1.755837424
HLA-DOB	5.10E-09	1.750650837
HSD17B2	1.83E-05	1.748509257
CA9	0.00313654	1.718971539
MELTF	7.12E-09	1.717917375
HIST1H1E	4.89E-07	1.715379309
SOSTDC1	0.000253359	1.714633399
STAC2	0.001852215	1.713444439
IGLV3-21	0.000129409	1.708333247
PRKCQ-AS1	1.12E-06	1.707625731
IGHG1	0.000265229	1.698623938
POPDC3	3.19E-05	1.691967337
FAM181B	0.000241772	1.691114322
WFDC21P	1.07E-07	1.687882132
AC025154.2	0.005681818	1.686438013
IL2RA	1.68E-07	1.679601028
BRINP2	0.003259592	1.679232515
IGHV5-51	0.000450252	1.672796766
SPX	0.000781798	1.665679243
ROS1	0.000120841	1.664954812

FERMT1	3.50E-05	1.662803577
IGHV2-70	0.001161767	1.660939989
AC021683.1	2.55E-06	1.660653156
SCG3	3.82E-05	1.656697281
MKRN3	0.006861242	1.655481205
KRT83	0.002787189	1.643485563
LINC00839	4.41E-05	1.642878486
PI3	0.001535117	1.640785301
AC104964.1	1.64E-07	1.639559125
IGKV1-8	0.000932699	1.638940414
SERPINB7	0.000289814	1.636419085
LCN2	0.002669692	1.634464968
DLX6-AS1	0.0006662	1.633400962
AC139769.2	2.37E-05	1.63307939
TRDV1	0.000257722	1.631203472
C10orf90	4.88E-05	1.63077035
LRRN4	1.67E-06	1.629627594
NOL4	0.000674817	1.627683261
HIST1H3C	0.00057743	1.626450849
PGBD5	1.88E-06	1.624483971
COL22A1	1.16E-06	1.618633758
CCL8	3.53E-07	1.617073028
CALB2	6.70E-06	1.612349346
SLC2A14	0.001110676	1.609050178
POTEE	1.62E-05	1.608500636
AC092198.1	0.000198637	1.607412791
NRTN	5.78E-06	1.602096241
IGHV4-59	0.000418485	1.602080282
IGLC2	0.000178389	1.598034072
AC079949.2	7.33E-06	1.597953719
PCBP3	1.27E-07	1.592801867
PDIA2	0.000213809	1.588321762
HIST1H1D	0.00084015	1.587016417
AC004233.2	0.001469924	1.585938852
GBP1P1	9.41E-07	1.57982194
IGLV9-49	0.001956265	1.578280497
HIST1H2BJ	1.32E-06	1.574388197
PROM1	0.000867399	1.566029922
ANKRD36BP2	6.77E-05	1.565626025
RASGEF1C	2.58E-05	1.562545992
RGMA	1.22E-06	1.561960746
SLC22A31	0.002564443	1.560890429

TNIP3	1.77E-05	1.553279389
AL136366.1	0.000559738	1.551305775
COLEC11	1.98E-06	1.549621278
LINC00689	2.57E-05	1.54422003
RHCG	0.00412463	1.543752829
PKP1	0.00052971	1.540823384
KYNU	1.79E-06	1.539870044
CD38	7.49E-06	1.531922466
TDRD9	0.002341319	1.527402651
CHRM3	2.30E-05	1.525689569
CCL20	1.41E-05	1.521991598
CCL18	0.000430059	1.521166887
AC058791.1	9.36E-05	1.520109432
PCOLCE2	0.000823377	1.514764779
SRSF12	1.42E-07	1.513585797
KCNN4	1.32E-06	1.510162745
PRR26	2.25E-06	1.506589306
TDRD12	0.000127809	1.505787844
SLC6A14	0.004927175	1.505030509
IGHV3-20	0.004095905	1.504787514
Z98257.1	0.000569594	1.501500903
AKR1E2	4.96E-06	1.500782789
PYY	0.000489758	-1.504999508
DNAI1	6.84E-06	-1.505547945
KLHDC7A	0.00200168	-1.513544861
NALCN-AS1	0.000803092	-1.518218808
RPS20P22	0.000480772	-1.529338443
SLC26A3	0.000223501	-1.530953655
DAB1	6.23E-05	-1.541818441
RLN2	0.000127437	-1.551391716
HEPACAM2	0.003505333	-1.554686533
MS4A8	0.005499671	-1.555295745
LINC01016	0.004603225	-1.55583517
FGF10	0.001645906	-1.570833461
DIRAS3	3.12E-06	-1.57181197
EPHA6	0.000317688	-1.579058932
UCP1	0.007213603	-1.583069851
AC069120.1	8.86E-05	-1.583623828
AC114811.2	1.71E-05	-1.584751389
KCNQ5	0.000167242	-1.587905647
NAP1L4P1	1.88E-08	-1.600807687
AGXT2	2.43E-06	-1.610188399

PNLIPRP2	0.003381517	-1.619872073
FAM196A	0.001853841	-1.620228923
AC125603.2	0.001351571	-1.641396788
AC104574.2	0.001721982	-1.648419614
AFP	0.001764435	-1.653192327
DUSP13	0.001969363	-1.655070755
DDC	0.002933085	-1.660767142
AP000439.2	0.000845951	-1.674389635
ENHO	3.12E-05	-1.6822685
PHF21B	0.001701752	-1.692022601
TMEM215	0.000457792	-1.717142477
KCNC1	0.000322816	-1.7229982
HMGCLL1	5.83E-05	-1.72640847
MYPN	0.004807062	-1.739475076
SEMA6D	1.12E-08	-1.749138704
ARHGAP40	0.00288371	-1.760760512
AL079343.1	0.001297315	-1.761268479
GDF9	7.12E-09	-1.767779376
LINC01856	0.003010229	-1.791369654
GRIA1	0.001189873	-1.800447372
PHGR1	0.003500486	-1.810007369
CSMD3	0.00593826	-1.815568325
ZNF703	2.55E-10	-1.829303716
GNAO1	1.04E-07	-1.83559621
ATP1A2	4.81E-06	-1.860793832
RFX6	0.007325426	-1.872063494
PEBP4	3.12E-05	-1.874120588
NPY1R	0.001855712	-1.878556326
PDZPH1P	0.000375196	-1.879561389
GPM6A	1.61E-05	-1.903308702
SEZ6L	0.000162087	-1.915583537
FCRLB	3.16E-05	-1.930769468
CHGA	0.002779067	-2.031689943
CDH18	0.005082496	-2.056380691
GLRA3	0.005524166	-2.100820886
UGT3A2	3.88E-06	-2.105919408
EDDM3B	0.00040929	-2.125332614
NOVA1	3.01E-07	-2.137905672
GACAT2	5.44E-05	-2.157016008
BRDT	4.45E-05	-2.214974502
NPTX1	2.75E-09	-2.263413522
SLC5A7	0.000502731	-2.269204639

NELL1	0.001177524	-2.274666824
MUC6	0.001967426	-2.281128166
AL136964.1	2.59E-07	-2.33194377
NLRP5	0.001266303	-2.424902643
HAO2	3.53E-07	-2.462682333
SLC4A10	2.00E-07	-2.471867538
ELFN2	1.99E-09	-2.539656709
PNMT	7.60E-07	-2.540297424
ALB	1.49E-08	-2.600616584
PCSK2	0.00013155	-2.802146764
SYNPO2L	2.09E-08	-2.826622905
DLK1	0.000480772	-3.0444844
CGA	3.61E-06	-3.331963826
NPY2R	1.12E-05	-3.385595343
Z82185.1	3.98E-06	-3.558209576
PVALB	2.84E-10	-3.689341203
NXPH1	2.54E-09	-3.903412227
GABRA1	9.19E-07	-4.015835889
UGT2B4	2.41E-11	-4.364560652

Appendix I

ADDITIONAL TCGA RESULTS

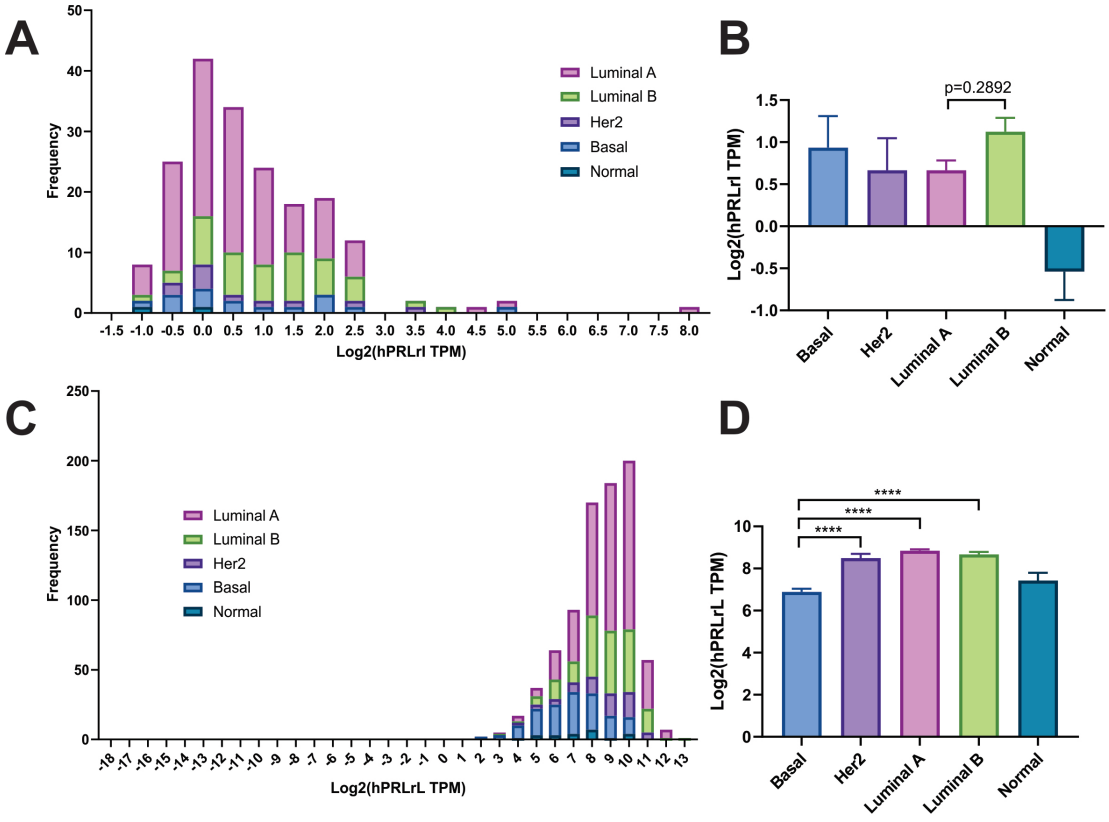

Fig. 35. Distribution of hPRLrI and hPRLrL transcript expression by breast cancer intrinsic subtype. hPRLrI and hPRLrL were individually assessed for association with intrinsic subtype status. **A**. Distribution of intrinsic subtype by hPRLrI transcript status. **B**. hPRLrI transcript enrichment within the breast cancer intrinsic subtypes. **C**. Distribution of intrinsic subtype by hPRLrL transcript status. **D**. hPRLrL transcript enrichment within the breast cancer intrinsic subtypes.

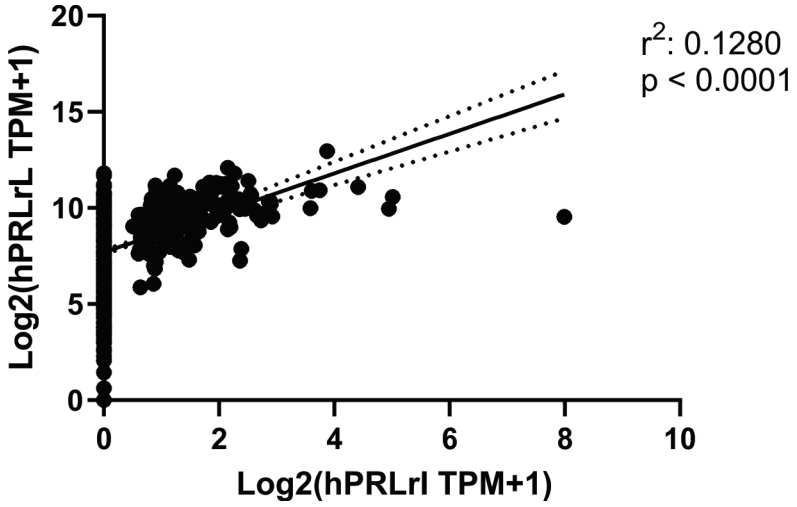

Fig. 36. hPRLrI by hPRLrL expression. Regression analysis demonstrating hPRLrI by hPRLrL transcript expression in TCGA-BRCA RNAseq data.

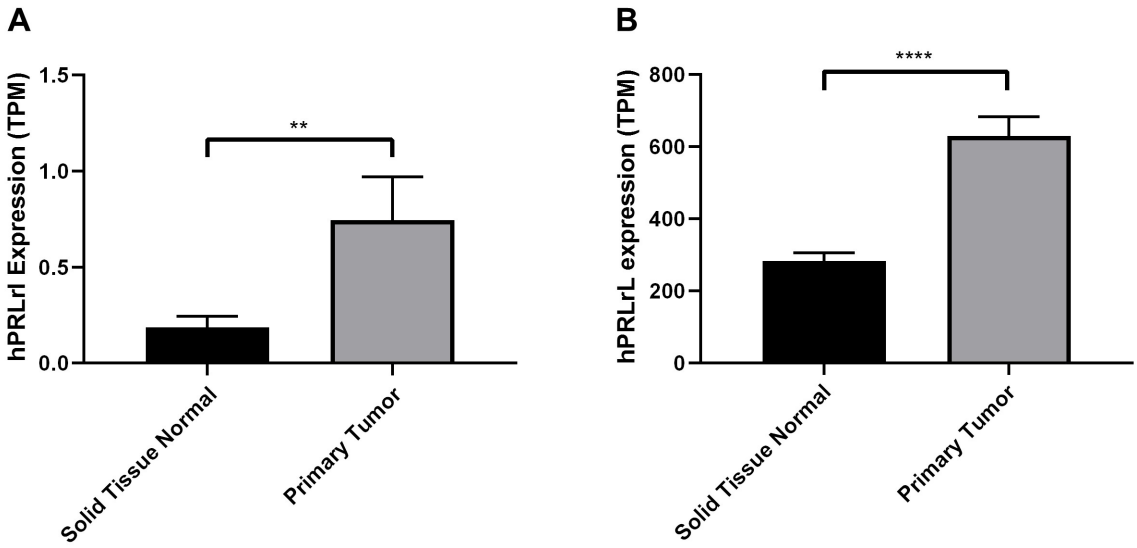

Fig. 37. hPRLr isoform transcript expression in normal and malignant breast tissue. **A**. hPRLrI and **B**. hPRLrL transcript expression levels were assessed in both normal and malignant mammary tissue, using TCGA-BRCA RNAseq data. **$p < 0.01$, ****$p < 0.001$.

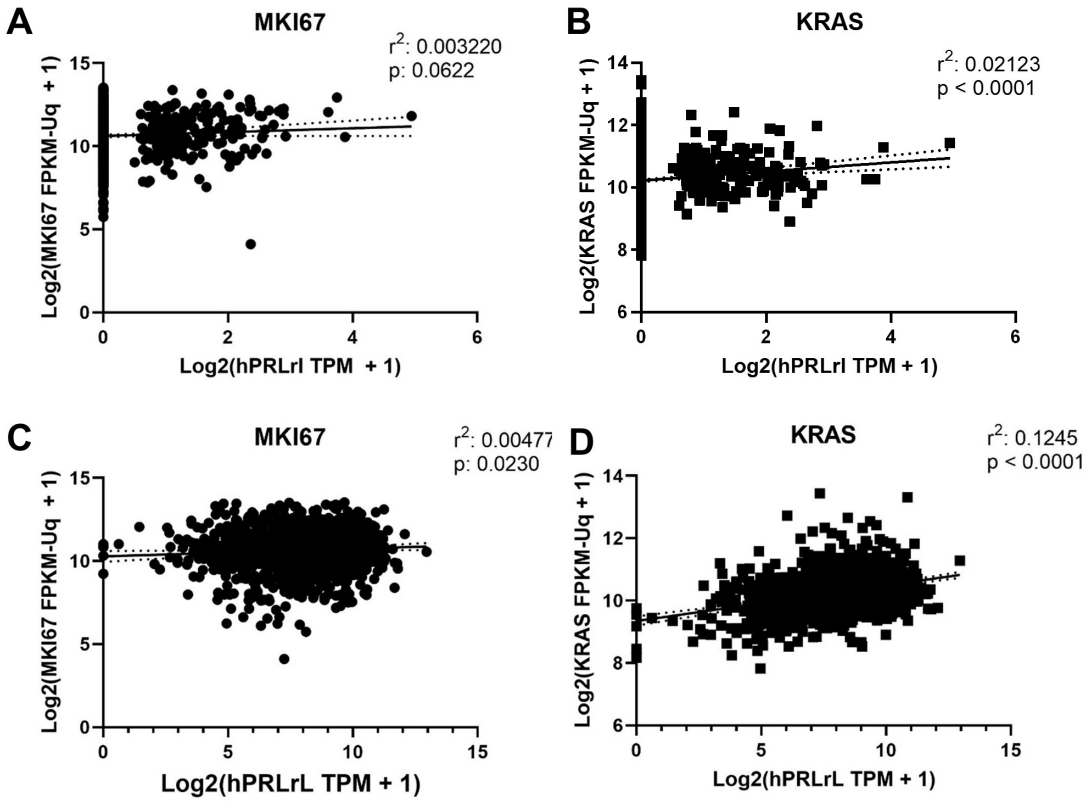

Fig. 38. hPRLrI and hPRLrL transcript correlation with MKI67 and KRAS. hPRLrI transcript expression was correlated with **A**. MKI67 and **B**. KRAS. Regression analyses using hPRLrL (**C, D**) were similarly performed.

Table 26. Demographics of TCGA-BRCA patients, hPRLrI+/-. TCGA-BRCA patients were stratified by hPRLrI status, being positive or negative expressors, as determined by RNAseq analysis.

		hPRLrI+ (n=201)		hPRLrI- (n=890)			
		n	% of total	n	% of total	z score	p
ER status							
	Positive	161	80.1%	593	66.6%	3.73	**0.00019**
	Negative	22	10.9%	202	22.7%	-3.73	**0.00020**
PR status							
	Positive	134	66.7%	521	58.5%	2.12	**0.03361**
	Negative	46	22.9%	274	30.8%	-2.22	**0.02627**
Her2 status							
	Positive	32	15.9%	120	13.5%	0.90	0.36745
	Negative	104	51.7%	421	47.3%	1.14	0.25539
	Equivocal	34	16.9%	137	15.4%	0.54	0.59186
HR status							
	ER+/PR+/Her2-	79	39.3%	270	30.3%	2.46	**0.01383**
	ER+/PR-/Her2-	13	6.5%	44	4.9%	0.88	0.38054
	ER-/PR-/Her2+	5	2.5%	30	3.4%	-0.64	0.52099
	ER-/PR-/Her2-	10	5.0%	98	11.0%	-2.59	**0.00965**
Intrinsic subtype							
	Luminal A	116	57.7%	302	33.9%	6.26	**4.00E-10**
	Luminal B	44	21.9%	146	16.4%	1.85	0.06397
	Her2-enriched	11	5.5%	56	6.3%	-0.44	0.66205
	Basal	16	8.0%	123	13.8%	-2.25	**0.02442**
	Normal-like	2	1.0%	21	2.4%	-1.22	0.22387
Gender							
	Female	197	98.0%	881	99.0%	-1.16	0.24804
	Male	4	2.0%	8	0.9%	1.34	0.18035
Menopause status							

	Pre-menopausal	46	23.4%	174	19.8%	1.13	0.25706
	Peri-menopausal	3	1.5%	32	3.6%	-1.51	0.13101
	Post-menopausal	129	65.5%	533	60.5%	1.30	0.19403
Race							
	White	165	82.1%	587	66.0%	4.46	**0.00001**
	Asian	4	2.0%	57	6.4%	-2.46	**0.01388**
	African American	12	6.0%	170	19.1%	-4.51	**0.00001**
Ethnicity							
	Not Hispanic/Latino	162	80.6%	716	80.4%	0.05	0.96198
	Hispanic/Latino	8	4.0%	31	3.5%	0.34	0.73178
AJCC Pathologic T							
	T1	55	27.4%	224	25.2%	0.64	0.51948
	T2-T4	146	72.6%	662	74.4%	-0.51	0.61015
AJCC Pathologic N							
	N0	92	45.8%	422	47.4%	-0.42	0.67311
	N1-N3	107	53.2%	449	50.4%	0.71	0.47571
AJCC Pathologic M							
	M0	178	88.6%	729	81.9%	2.27	**0.02302**
	M1	4	2.0%	18	2.0%	-0.03	0.97644
AJCC Pathologic Stage							
	Stage I	32	15.9%	149	16.7%	-0.28	0.77743
	Stage II-Stage IV	166	82.6%	720	80.9%	0.55	0.58000
Age							
	<55	72	35.8%	359	40.3%	-1.183	0.23683
	>55	129	64.2%	515	57.9%	1.644	0.10017
Prior malignancy							
	No	185	92.0%	838	94.2%	-1.122	0.26203
	Yes	16	8.0%	50	5.6%	1.2581	0.20837

Table 27. Demographics of TCGA-BRCA patients, hPRLrL hi/lo. TCGA-BRCA patients were stratified by hPRLrL status, being high or low expressors, as determined by RNAseq analysis.

		hPRLrL-hi (n=361)		hPRLrL-lo (n=361)			
		n	**% of total**	**n**	**% of total**	**z score**	**p**
ER status							
	Positive	304	84.2%	209	57.9%	7.80	**1.00E-10**
	Negative	39	10.8%	135	37.4%	-8.35	**1.00E-10**
PR status							
	Positive	265	73.4%	181	50.1%	6.43	**1.00E-10**
	Negative	76	21.1%	163	45.2%	-6.88	**1.00E-10**
Her2 status							
	Positive	58	16.1%	46	12.7%	1.27	0.20342
	Negative	191	52.9%	185	51.2%	0.45	0.65489
	Equivocal	56	15.5%	52	14.4%	0.42	0.67640
HR status							
	ER+/PR+/Her2-	151	41.8%	87	24.1%	5.07	**1.00E-10**
	ER+/PR-/Her2-	20	5.5%	19	5.3%	0.16	0.86923
	ER-/PR-/Her2+	6	1.7%	14	3.9%	-1.81	0.06965
	ER-/PR-/Her2-	15	4.2%	76	21.1%	-6.84	**1.00E-10**
Intrinsic subtype							
	Luminal A	205	56.8%	67	18.6%	10.60	**1.00E-10**
	Luminal B	82	22.7%	36	10.0%	4.63	**3.66E-06**
	Her2-enriched	25	6.9%	16	4.4%	1.45	0.14783
	Basal	20	5.5%	83	23.0%	-6.70	**1.00E-10**
	Normal-like	5	1.4%	11	3.0%	-1.52	0.12929
Gender							
	Female	355	98.3%	357	98.9%	-0.64	0.52420
	Male	5	1.4%	4	1.1%	0.34	0.73730
Menopause status							

	Pre-menopausal	80	22.2%	71	19.7%	0.82	0.41018
	Peri-menopausal	9	2.5%	16	4.4%	-1.42	0.15419
	Post-menopausal	229	63.4%	233	64.5%	-0.31	0.75647
Race							
	White	268	74.2%	218	60.4%	3.97	**0.00007**
	Asian	14	3.9%	25	6.9%	-1.81	0.07014
	African American	23	6.4%	106	29.4%	-8.06	**1.00E-10**
Ethnicity							
	Not Hispanic/Latino	268	74.2%	308	85.3%	-3.71	**0.00021**
	Hispanic/Latino	13	3.6%	12	3.3%	0.20	0.83870
AJCC Pathologic T							
	T1	101	28.0%	80	22.2%	1.80	0.07135
	T2-T4	259	71.7%	280	77.6%	-1.80	0.07239
AJCC Pathologic N							
	N0	151	41.8%	176	48.8%	-1.87	0.06161
	N1-N3	202	56.0%	181	50.1%	1.57	0.11735
AJCC Pathologic M							
	M0	319	88.4%	281	77.8%	3.77	**0.00016**
	M1	6	1.7%	8	2.2%	-0.54	0.58935
AJCC Pathologic Stage							
	Stage I	56	15.5%	56	15.5%	0.00	1.00000
	Stage II-Stage IV	291	80.6%	303	83.9%	-1.17	0.24226
Age							
	<55	138	38.2%	149	41.3%	-0.836518803	0.40286
	>55	219	60.7%	203	56.2%	1.208291523	0.22694
Prior malignancy							
	No	338	93.6%	340	94.2%	-0.311141119	0.75569
	Yes	22	6.1%	21	5.8%	0.157253197	0.87505

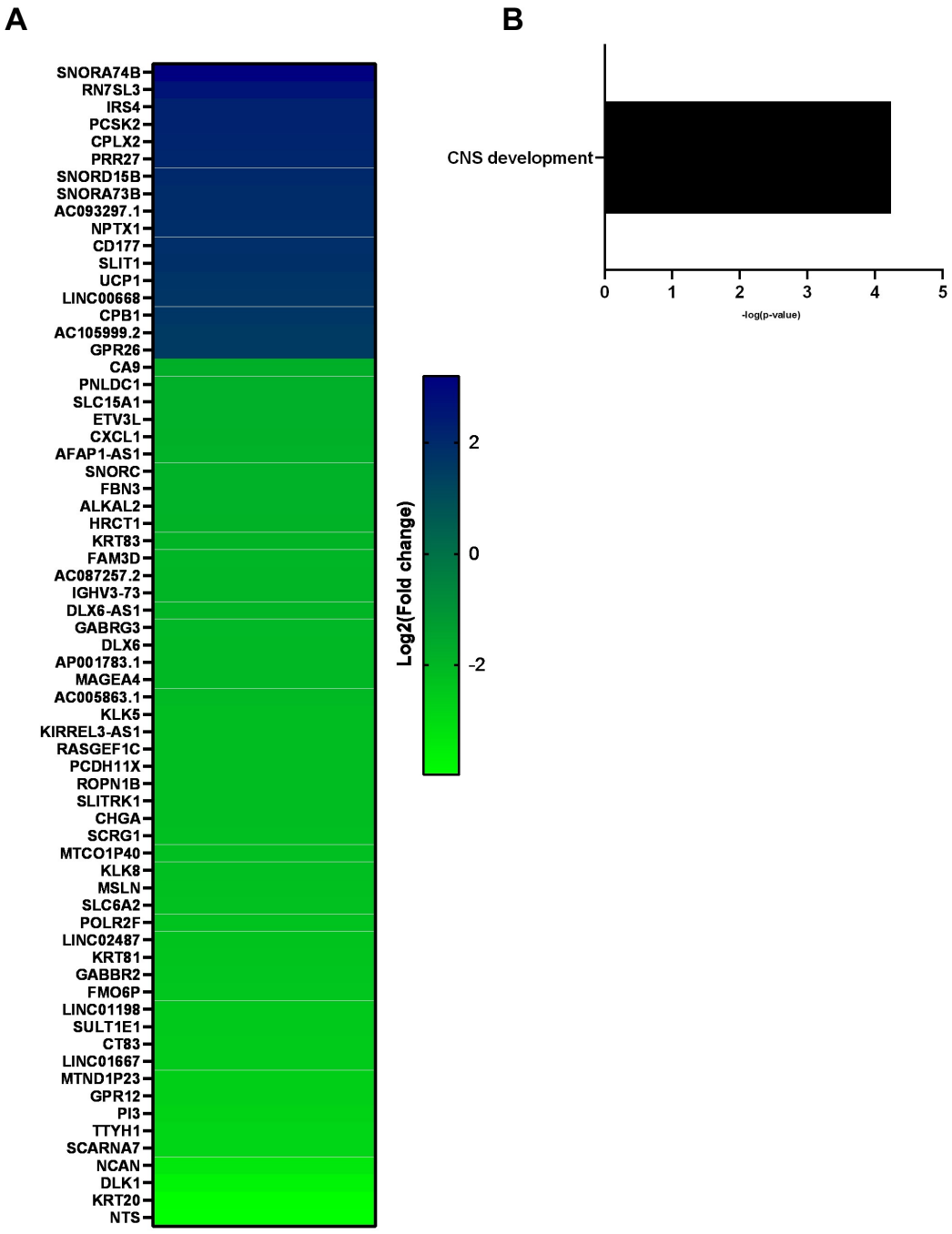

Fig. 39. hPRLrI+/- DEGs. **A**. Top/bottom DEGs as determined by analysis of TCGA-reposited RNAseq data. **B**. Gene set enrichment analysis of the enriched DEGs.

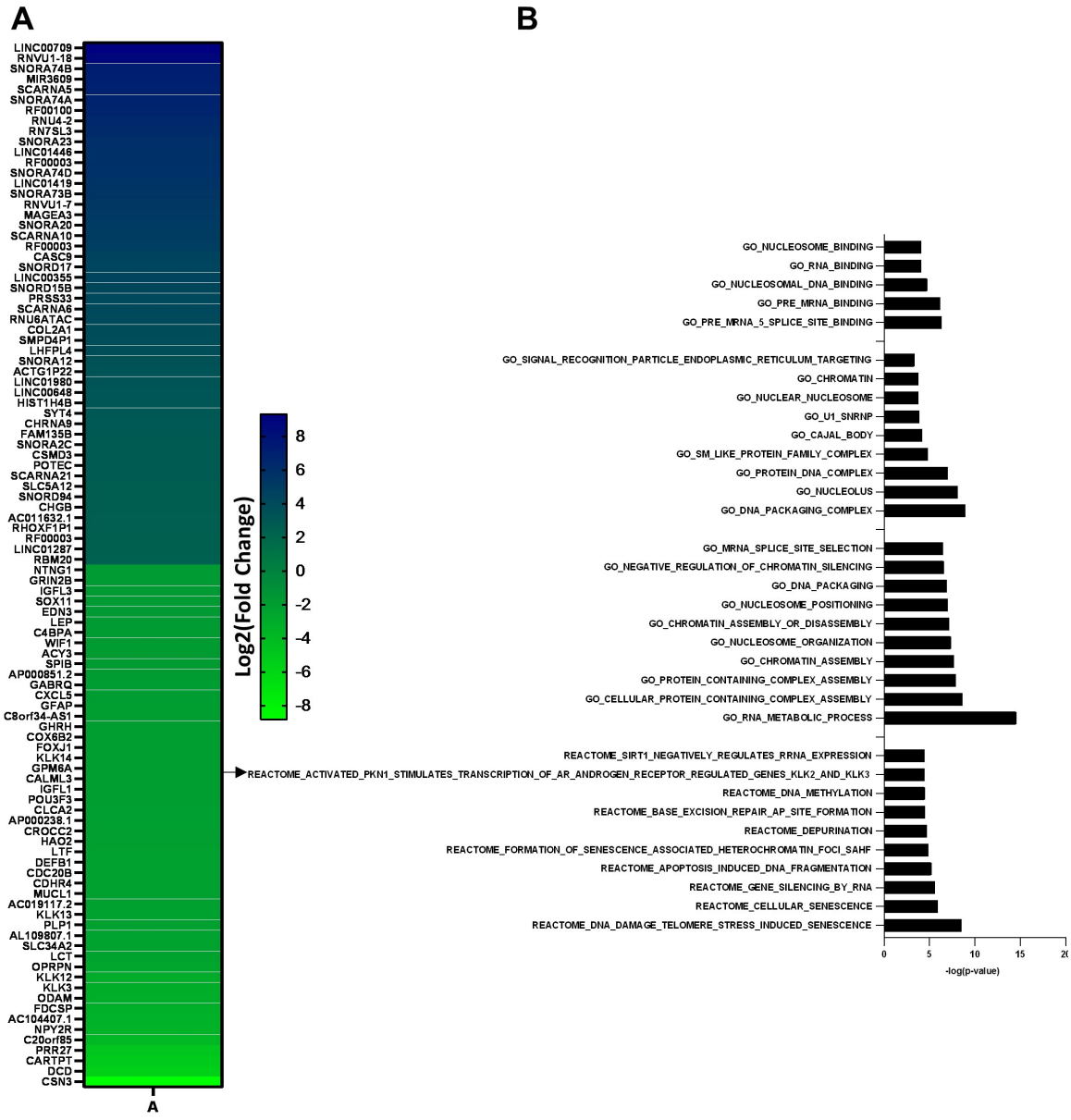

Fig. 40. hPRLrI-hi/lo DEGs. **A**. Top/bottom DEGs as determined by analysis of TCGA-reposited RNAseq data. **B**. Gene set enrichment analysis of the enriched DEGs.

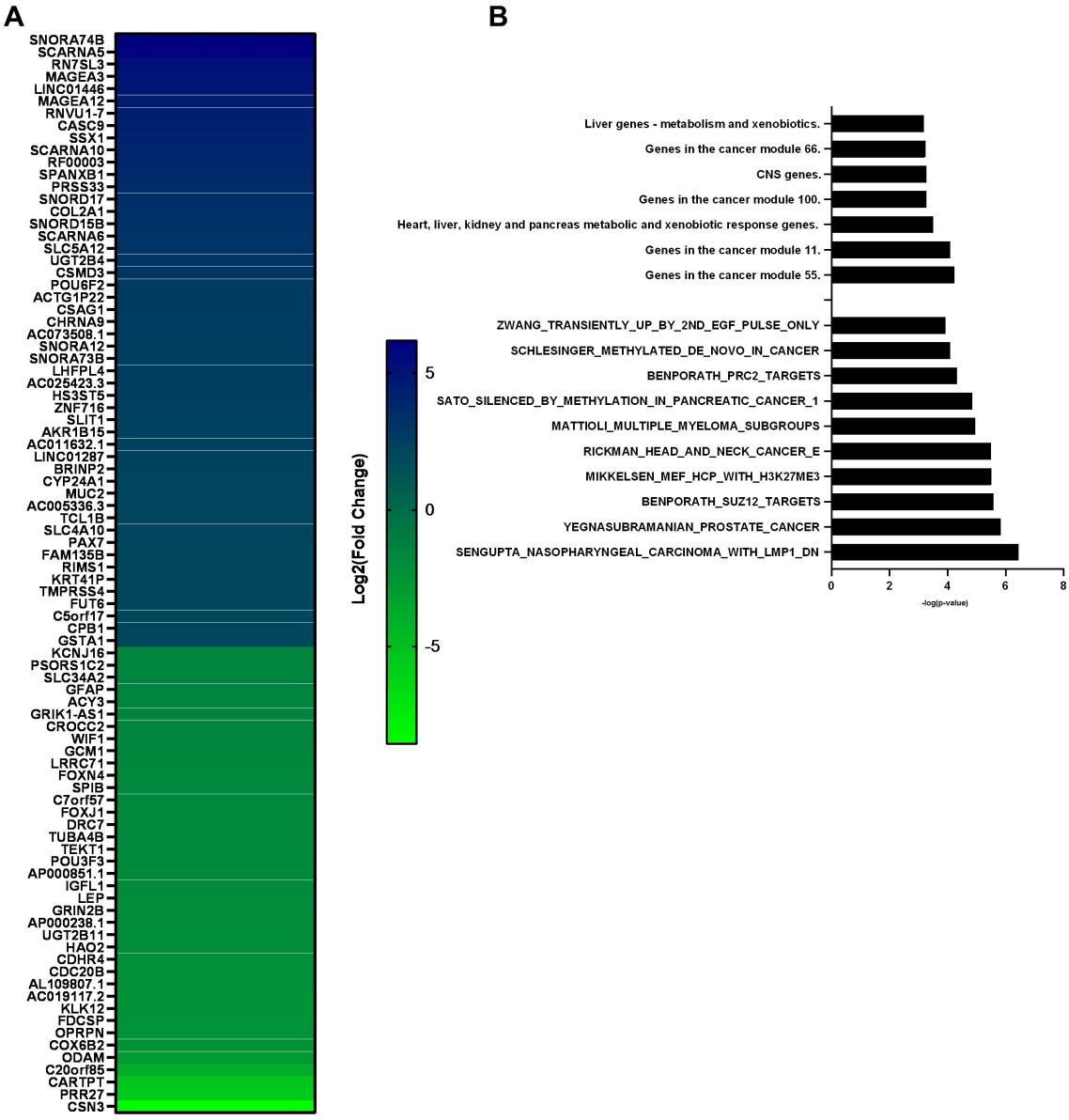

Fig. 41. hPRLrI-hi versus med/lo DEGs. **A**. Top/bottom DEGs as determined by analysis of TCGA-reposited RNAseq data. **B**. Gene set enrichment analysis of the enriched DEGs.

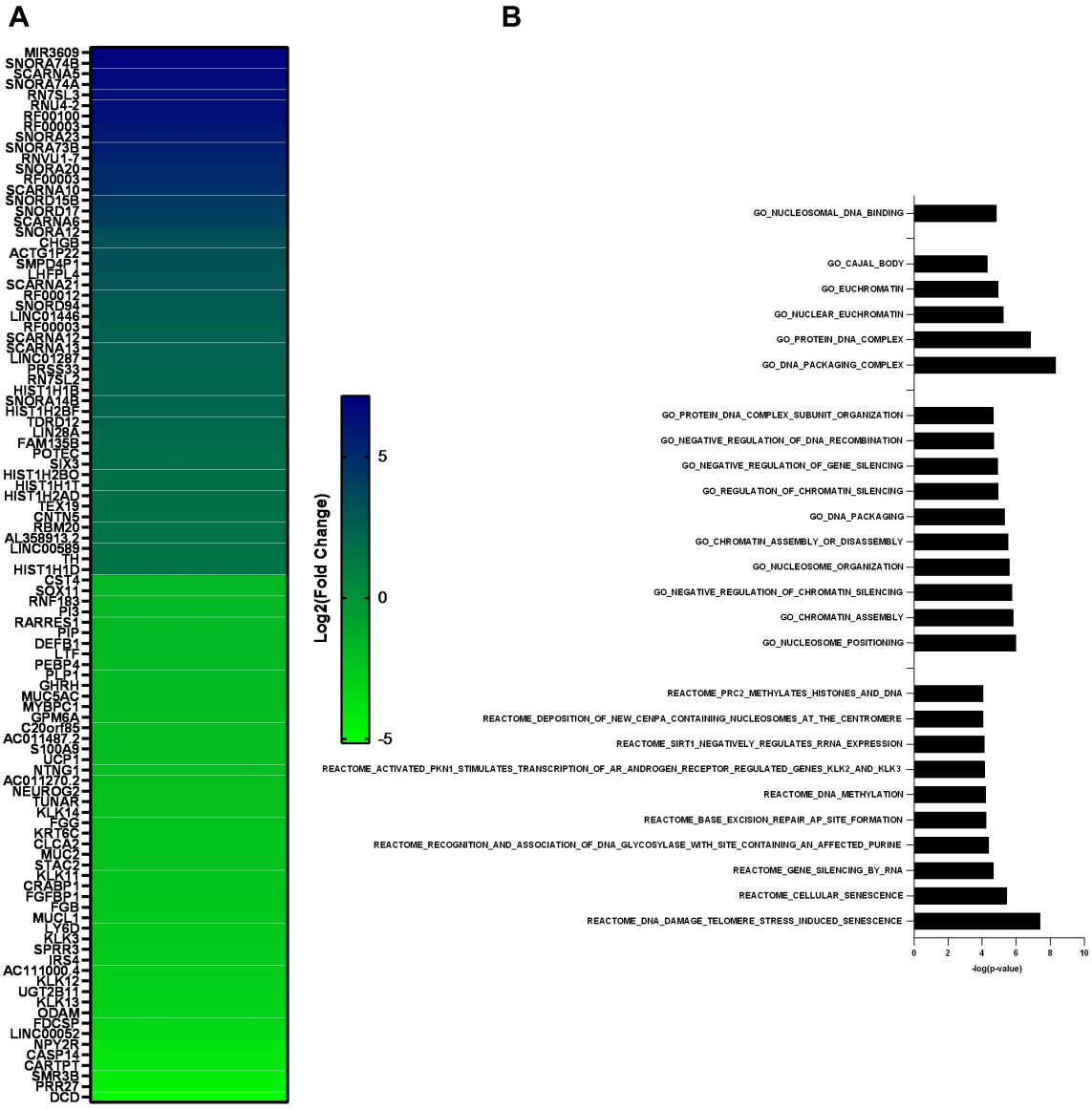

Fig. 42. hPRLrI-hi/med versus lo DEGs. **A**. Top/bottom DEGs as determined by analysis of TCGA-reposited RNAseq data. **B**. Gene set enrichment analysis of the enriched DEGs.

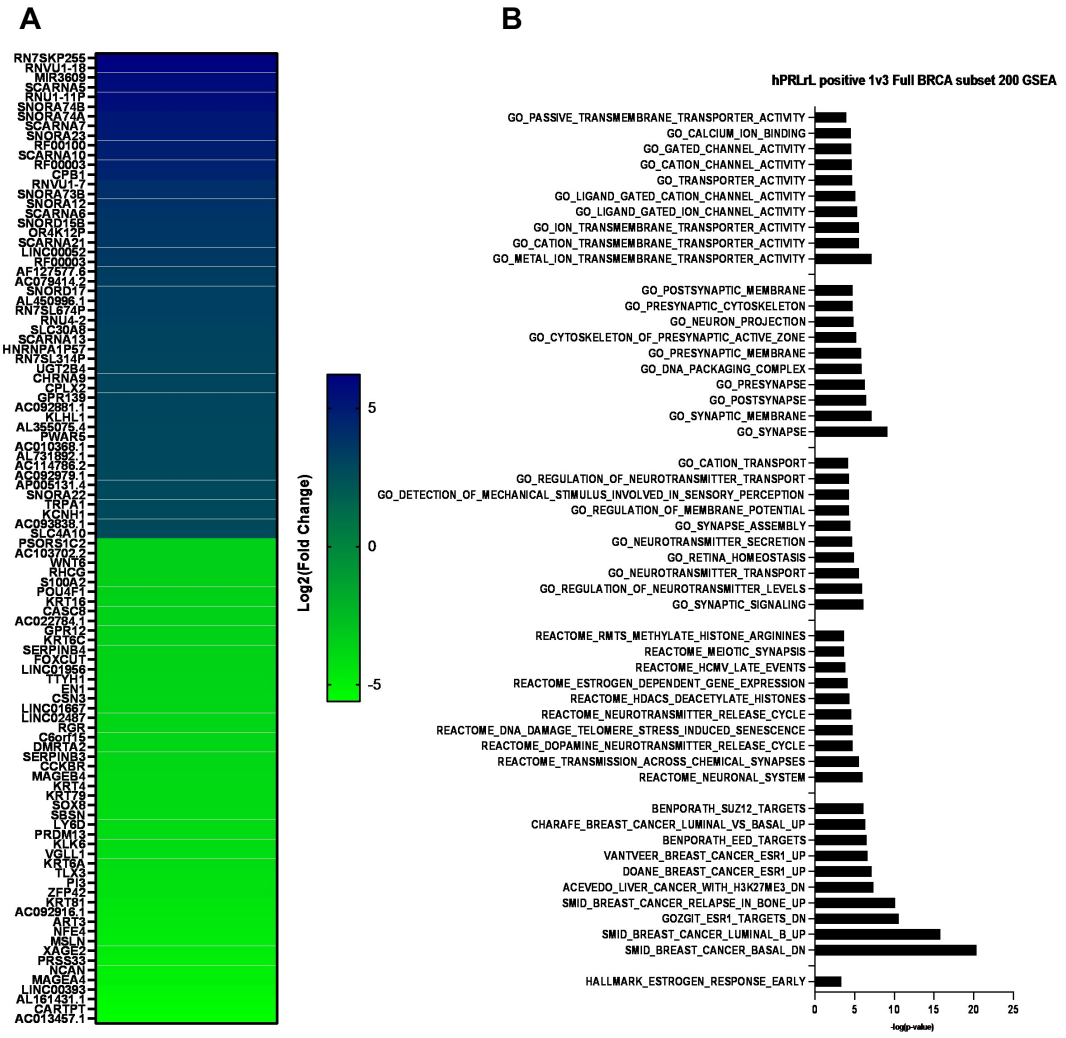

Fig. 43. hPRLrL-hi/lo DEGs. **A**. Top/bottom DEGs as determined by analysis of TCGA-reposited RNAseq data. **B**. Gene set enrichment analysis of the enriched DEGs.

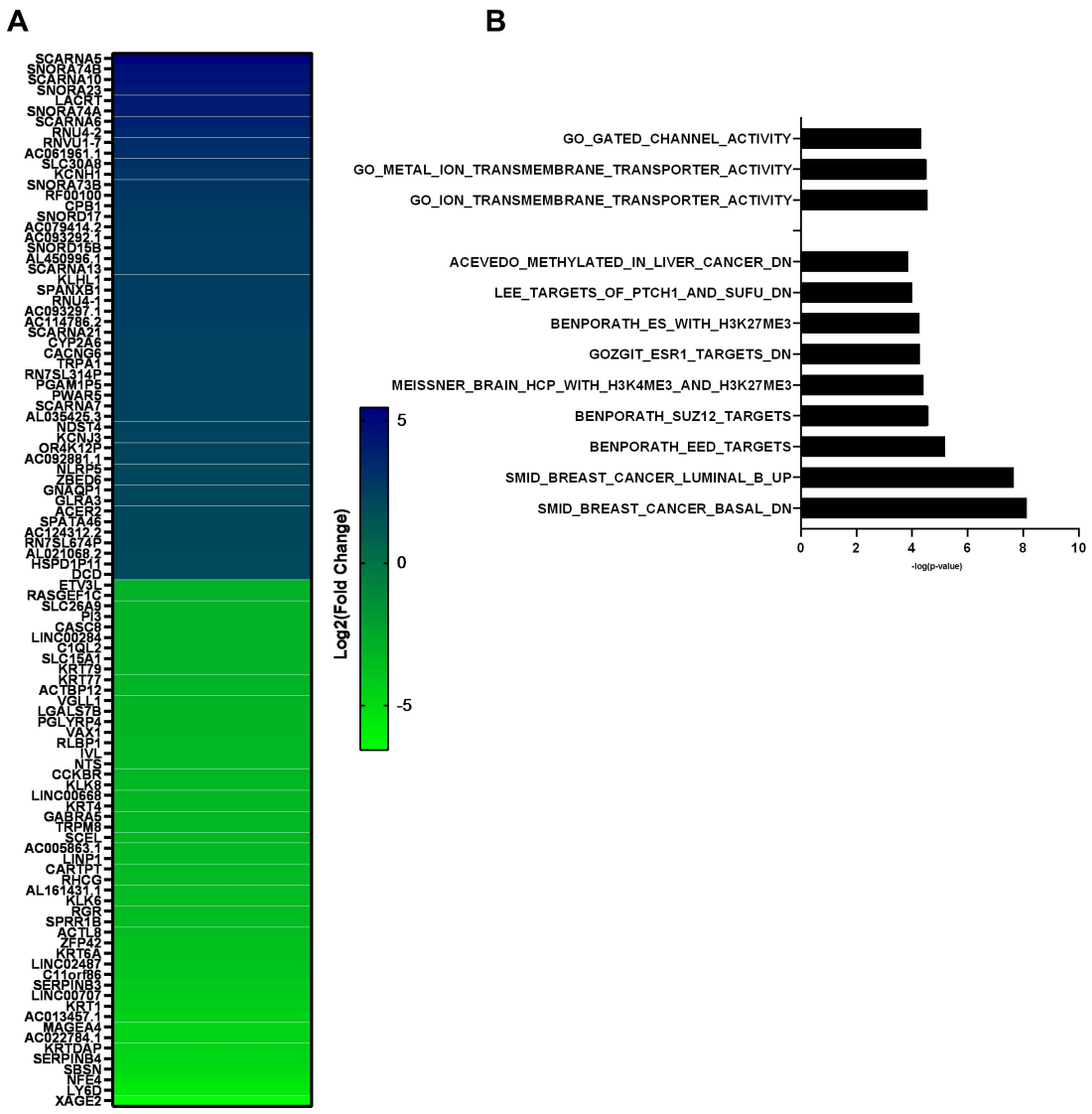

Fig. 44. hPRLrL-hi versus med/low DEGs. **A**. Top/bottom DEGs as determined by analysis of TCGA-reposited RNAseq data. **B**. Gene set enrichment analysis of the enriched DEGs.

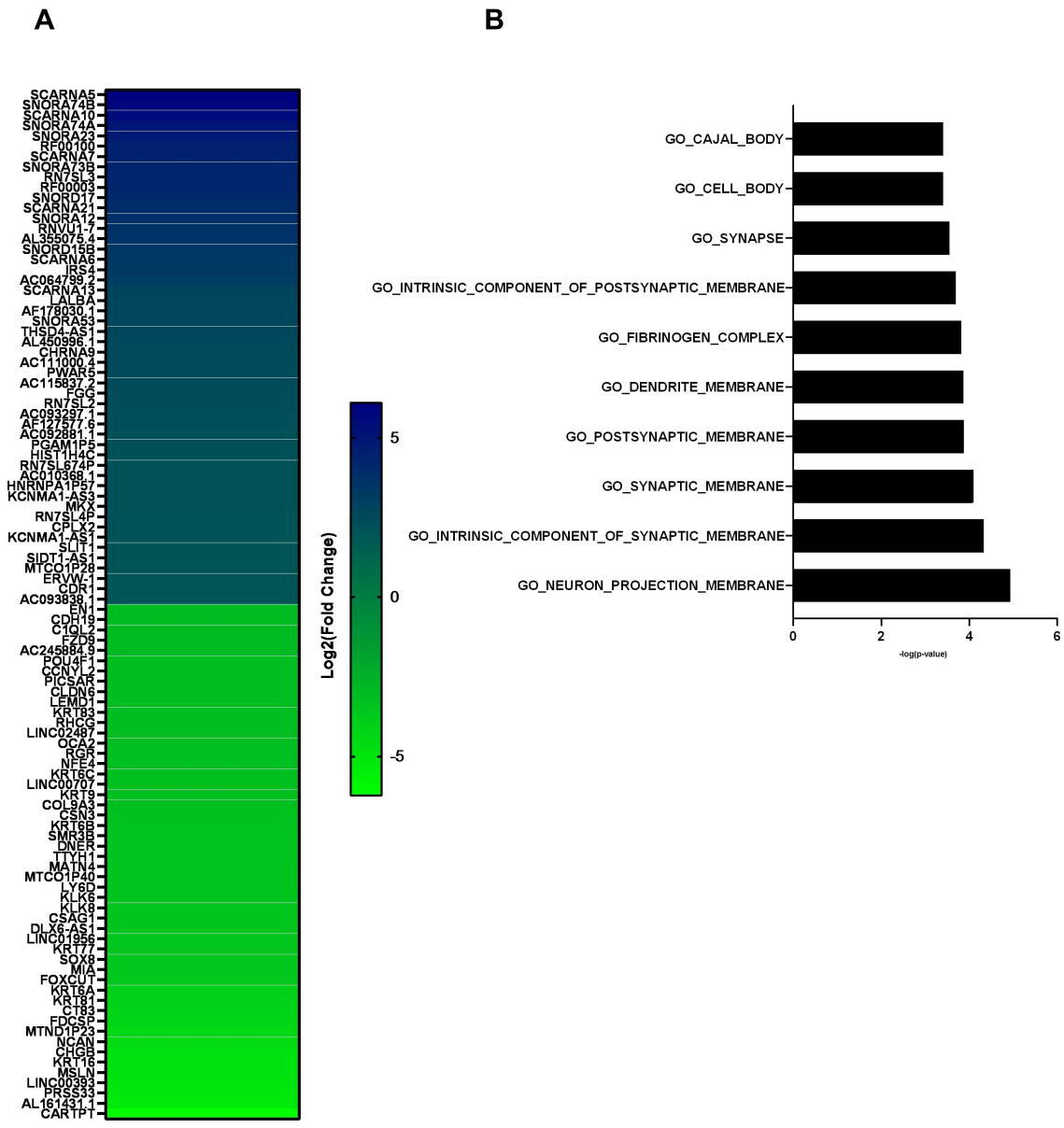

Fig. 45. hPRLrL-hi/med versus lo DEGs. **A**. Top/bottom DEGs as determined by analysis of TCGA-reposited RNAseq data. **B**. Gene set enrichment analysis of the enriched DEGs.

Table 28. hPRLrI+/- DEGs. TCGA-BRCA patients were stratified by hPRLrI status, being positive or negative expressors, as determined by RNAseq analysis.

Gene symbol	Logs(Fold change)	padj
SNORA74B	3.190396314	1.38E-17
RN7SL3	2.637215177	9.46E-17
IRS4	2.211575896	1.21E-08
PCSK2	2.209594651	4.64E-08
CPLX2	2.155369047	4.08E-06
PRR27	2.109130298	0.008106766
SNORD15B	2.031619914	2.13E-15
SNORA73B	1.936512229	1.87E-18
AC093297.1	1.904868804	2.69E-06
NPTX1	1.880634298	6.05E-16
CD177	1.847850958	6.71E-11
SLIT1	1.846602356	6.36E-16
UCP1	1.717850213	3.10E-08
LINC00668	1.678302161	0.000260547
CPB1	1.664167736	3.45E-05
AC105999.2	1.543144892	0.00108115
GPR26	1.534055222	1.30E-06
AC048380.2	-1.500919811	1.17E-14
SLC28A1	-1.502943946	6.04E-10
LINC01819	-1.50599031	4.30E-09
DKK1	-1.508440786	8.62E-09
SMOC1	-1.514860405	6.13E-10
RPRM	-1.521372498	8.79E-10
NKX2-5	-1.521496734	0.000230696
KLK6	-1.542167237	1.38E-07
FOXCUT	-1.54287157	0.000241377
ROPN1	-1.54699662	0.000183769
GDF5	-1.552547616	5.94E-12
LEMD1	-1.566784732	5.75E-07
GACAT2	-1.567750579	6.68E-08
AC015883.1	-1.56889586	4.51E-13
SBSN	-1.570492788	2.81E-07
KRT16	-1.577196442	6.28E-08
OPRK1	-1.580881244	6.58E-06
HSD17B2	-1.589370399	3.04E-10
KLK7	-1.602600445	3.87E-08
SH3GL3	-1.630320594	5.17E-08
MIA	-1.633298999	1.33E-08

ART3	-1.638237447	1.69E-07
PNMA3	-1.649336012	2.29E-12
KRT6B	-1.650630495	5.26E-09
EN1	-1.661453801	1.62E-11
HORMAD1	-1.663187936	2.76E-06
RPL10P6	-1.665384522	2.95E-10
HS3ST4	-1.667891136	4.06E-07
SLC6A15	-1.675677675	3.15E-07
SLC6A14	-1.67689749	5.34E-09
ASAP1-IT2	-1.676969905	2.03E-22
PICSAR	-1.682922432	8.98E-11
SCGB3A1	-1.686152375	1.38E-09
AC022784.1	-1.690830887	1.37E-07
KLK10	-1.692397153	1.50E-08
CRHR1	-1.72901883	6.97E-16
VGLL1	-1.740581731	4.22E-07
CA9	-1.743809391	4.66E-08
PNLDC1	-1.760142895	3.47E-15
SLC15A1	-1.767168328	1.64E-09
ETV3L	-1.780260985	1.65E-10
CXCL1	-1.783163867	1.46E-14
AFAP1-AS1	-1.818538617	1.08E-12
SNORC	-1.821132269	5.63E-23
FBN3	-1.832962191	2.71E-12
ALKAL2	-1.837949548	4.98E-15
HRCT1	-1.847919971	1.04E-16
KRT83	-1.874745901	3.91E-10
FAM3D	-1.899400436	2.42E-16
AC087257.2	-1.910530269	4.68E-12
IGHV3-73	-1.912854943	1.38E-12
DLX6-AS1	-1.923981425	6.51E-13
GABRG3	-1.954551382	3.09E-10
DLX6	-1.98353253	1.16E-11
AP001783.1	-1.986004733	2.95E-07
MAGEA4	-1.998799949	0.001975566
AC005863.1	-2.04625221	6.13E-08
KLK5	-2.120502214	1.55E-12
KIRREL3-AS1	-2.121296262	1.43E-05
RASGEF1C	-2.124437541	2.41E-18
PCDH11X	-2.129782298	4.89E-13
ROPN1B	-2.131603936	5.71E-14
SLITRK1	-2.141967496	1.67E-09

CHGA	-2.171848627	2.60E-09
SCRG1	-2.186947951	3.59E-18
MTCO1P40	-2.199063291	9.19E-28
KLK8	-2.20278699	7.62E-13
MSLN	-2.229263574	6.20E-16
SLC6A2	-2.247055057	2.53E-14
POLR2F	-2.291119613	1.58E-22
LINC02487	-2.314796792	6.84E-20
KRT81	-2.323841059	4.74E-15
GABBR2	-2.34474943	7.48E-13
FMO6P	-2.384981066	2.20E-17
LINC01198	-2.468556262	1.59E-09
SULT1E1	-2.480271958	1.91E-12
CT83	-2.51700155	0.008479585
LINC01667	-2.520537376	8.39E-06
MTND1P23	-2.632296796	2.08E-43
GPR12	-2.65049575	2.08E-16
PI3	-2.76429073	6.43E-21
TTYH1	-2.7946222	1.65E-37
SCARNA7	-2.837501347	1.39E-32
NCAN	-3.339050016	1.25E-26
DLK1	-3.689268323	1.10E-17
KRT20	-3.971455573	1.43E-20
NTS	-3.972936821	9.34E-21

Table 29. hPRLrI-hi/lo DEGs. TCGA-BRCA patients were stratified by hPRLrI status, being high or low expressors (top versus bottom tertiles, respectively), as determined by RNAseq analysis.

Gene symbol	padj	Log2(fold change)
LINC00709	0.00084962	9.326507647
RNVU1-18	0.000745258	8.827820233
SNORA74B	1.25E-26	7.173322727
MIR3609	1.47E-13	7.113740941
SCARNA5	1.36E-38	7.03003461
SNORA74A	5.23E-17	6.803109156
RF00100	3.14E-42	6.678027516
RNU4-2	8.22E-34	6.465505152
RN7SL3	1.99E-34	6.238183447
SNORA23	9.69E-31	5.950593815
LINC01446	4.58E-13	5.907657794
RF00003	1.07E-11	5.858997575
SNORA74D	1.34E-10	5.789272098
LINC01419	0.001566208	5.600552634
SNORA73B	3.78E-30	5.498256491
RNVU1-7	1.78E-14	5.314256538
MAGEA3	0.000519309	5.26392284
SNORA20	4.24E-15	5.082776197
SCARNA10	8.03E-22	4.997213377
RF00003	1.97E-14	4.891838053
CASC9	1.03E-08	4.488820438
SNORD17	1.25E-26	4.402011517
LINC00355	0.000178725	4.376780915
SNORD15B	6.52E-19	4.205662299
PRSS33	7.32E-06	4.180603547
SCARNA6	1.27E-21	4.138884875
RNU6ATAC	3.01E-12	4.053173197
COL2A1	2.79E-10	3.782051699
SMPD4P1	1.59E-11	3.7757351
LHFPL4	3.19E-14	3.650571004
SNORA12	1.51E-11	3.429922889
ACTG1P22	1.03E-08	3.334168736
LINC01980	0.007369603	3.328900653
LINC00648	4.40E-08	3.255682377
HIST1H4B	4.40E-08	3.185903794
SYT4	0.00703374	3.018270184
CHRNA9	9.66E-10	2.956673537

FAM135B	2.67E-10	2.923365008
SNORA2C	3.52E-09	2.85061992
CSMD3	3.24E-06	2.774221864
POTEC	0.000235502	2.746735555
SCARNA21	1.58E-07	2.742974952
SLC5A12	2.03E-06	2.633927305
SNORD94	7.21E-13	2.600667836
CHGB	0.000899446	2.586444893
AC011632.1	1.32E-05	2.558814375
RHOXF1P1	0.008949893	2.529962502
RF00003	8.51E-09	2.476396093
LINC01287	3.20E-08	2.434233162
RBM20	1.35E-10	2.399068595
SCARNA13	4.18E-11	2.368790995
AC017037.4	0.001844606	2.350516525
RN7SL2	3.84E-10	2.339804642
TMPRSS4	5.37E-06	2.315846026
RF00012	2.89E-05	2.286723137
ALB	1.85E-05	2.282107993
SCARNA12	2.79E-08	2.275846509
RIMS1	2.75E-08	2.275358289
SLC4A10	1.97E-06	2.261744612
PSG9	0.000508006	2.184892854
CCDC155	3.16E-05	2.184241518
SNORA14B	4.49E-07	2.174654796
SNORA22	6.52E-08	2.154436296
TDRD12	7.04E-05	2.143962524
CNTN5	0.001381199	2.138398899
LINC01443	0.000334604	2.131360259
S100G	0.003981287	2.113796449
HIST1H1B	4.12E-06	2.106636932
PXDNL	3.97E-06	2.100264704
AC025423.3	0.004026258	2.083009085
TEX19	2.86E-06	2.072237464
KRT41P	0.002176461	2.069313295
AL356311.1	1.62E-05	2.049153738
ALOX15	1.36E-05	2.04269972
DSCAM-AS1	0.004766018	2.019592184
KCNMB2-AS1	0.0017426	1.992533932
HIST1H2BF	2.03E-06	1.985053504
TMEM178B	6.73E-06	1.942397196
PRKACB	2.31E-09	1.929054662

ANKRD34B	0.000885797	1.920018055
OPRK1	0.000881242	1.886601083
DUSP5P1	0.000654502	1.883154636
NSG2	0.000265789	1.879473377
CASC16	0.00128083	1.877146299
HAL	3.85E-08	1.857072106
MIR2052HG	0.004086538	1.854387781
LINC00992	0.000979846	1.838388821
HIST1H1E	2.27E-08	1.798816356
HIST1H1D	5.14E-05	1.798330384
CELF3	0.000342392	1.786705287
MGAT5B	1.66E-06	1.779405471
LINC00707	0.002665552	1.77447147
KCNC1	0.000128294	1.774056637
RTBDN	0.000190705	1.768696539
AC108472.1	5.62E-05	1.764010733
AC026992.2	8.45E-05	1.751608252
RP1	0.000636008	1.726428089
SLIT1	9.07E-05	1.719772225
PEX5L	0.002736848	1.659306241
AC062028.2	0.008743492	1.653581819
HIST1H4C	5.25E-05	1.650081103
LRP1B	0.003624892	1.64828638
IGLV4-60	0.003702531	1.640056673
HIST1H2BO	5.76E-05	1.624191849
KRT31	0.00511856	1.609315171
LINC00589	0.001334985	1.608638533
ABCA12	0.000776745	1.607778775
EML5	4.37E-05	1.590446337
AL160408.3	0.006336683	1.584465066
TDRD9	0.001140793	1.579434385
FAR2P4	0.006407119	1.571312548
HIST1H1T	0.001265724	1.567478892
RN7SL767P	3.57E-05	1.560009807
NCR3LG1	1.04E-08	1.549748731
ADARB2	0.000204232	1.544564538
IGHV1-69D	0.002140819	1.542333391
FREM2	0.00703374	1.508541552
LINC00689	0.000278052	1.503502081
DES	0.00039137	-1.506162867
CPHL1P	0.006343022	-1.517569618
SLC22A31	0.004002352	-1.519303804

WDR38	0.003214829	-1.537161515
PTHLH	8.45E-05	-1.551794105
LINC02551	0.000192424	-1.554424451
WT1-AS	0.005038397	-1.560636926
DLX2	0.006068863	-1.563589736
PI3	0.002294233	-1.593938549
GABRA2	0.002321519	-1.611856416
WNT11	4.42E-05	-1.612883604
CRABP1	0.006496126	-1.614309757
C6orf15	0.00180314	-1.62824158
S100A9	0.000800389	-1.638222778
GABRP	0.004275872	-1.64293864
CLDN6	0.000446618	-1.649703429
DIRAS3	9.47E-06	-1.667243647
FOXN4	0.008122679	-1.671797119
CFAP77	0.000403339	-1.673560293
DRC7	0.000754263	-1.688463551
LRRC71	6.62E-07	-1.700993518
RNF183	0.000104297	-1.722383366
HPSE2	2.60E-05	-1.731527371
NTNG1	0.002733732	-1.740705498
GRIN2B	0.000151859	-1.749918148
IGFL3	0.001218835	-1.754162889
SOX11	2.75E-05	-1.7620739
EDN3	0.007409265	-1.771848896
LEP	0.003733481	-1.773871273
C4BPA	2.26E-05	-1.809210897
WIF1	0.007013658	-1.830123218
ACY3	9.69E-06	-1.839479234
SPIB	2.49E-05	-1.842291281
AP000851.2	0.000526714	-1.844068934
GABRQ	0.00042638	-1.861848854
CXCL5	6.33E-05	-1.862212184
GFAP	2.17E-06	-1.909711614
C8orf34-AS1	0.001498535	-1.910398383
GHRH	0.007409442	-1.913688433
COX6B2	5.37E-06	-1.915809563
FOXJ1	0.000401946	-1.925497146
KLK14	3.06E-06	-1.940116464
GPM6A	4.94E-06	-1.942052997
CALML3	0.000442388	-1.945418503
IGFL1	0.000347981	-1.947911813

POU3F3	0.000817864	-1.984157055
CLCA2	0.000474661	-1.989378058
AP000238.1	1.05E-06	-2.013418577
CROCC2	0.00034585	-2.039733015
HAO2	0.000325496	-2.049591725
LTF	0.000104433	-2.160513682
DEFB1	2.13E-06	-2.160539335
CDC20B	0.002048396	-2.172637523
CDHR4	0.000177498	-2.173831785
MUCL1	0.000207434	-2.175056158
AC019117.2	0.000868915	-2.200988272
KLK13	0.000143173	-2.216357912
PLP1	4.40E-08	-2.223287586
AL109807.1	0.005718419	-2.28407304
SLC34A2	6.08E-05	-2.332054205
LCT	1.11E-05	-2.342925541
OPRPN	0.00467152	-2.589076828
KLK12	0.000232933	-2.984860378
KLK3	2.22E-08	-3.015172021
ODAM	9.72E-08	-3.112188362
FDCSP	1.44E-09	-3.254785618
AC104407.1	0.000634768	-3.401009066
NPY2R	2.75E-05	-3.411246543
C20orf85	3.19E-06	-3.855695571
PRR27	0.004551457	-4.78095904
CARTPT	4.62E-05	-5.056331195
DCD	1.17E-09	-5.520634758
CSN3	3.54E-13	-8.819364527

Table 30. hPRLrI-hi versus med/lo DEGs. TCGA-BRCA patients were stratified by hPRLrI status, being high or medium/low expressors (top versus middle/bottom tertiles, respectively), as determined by RNAseq analysis.

Gene symbol	Log2(Fold change)	padj
SNORA74B	6.188396081	1.35E-23
SCARNA5	6.043256132	1.54E-33
RN7SL3	5.257796497	9.56E-28
MAGEA3	5.066135986	0.000373317
LINC01446	4.861147355	3.65E-10
MAGEA12	4.452005689	6.82E-08
RNVU1-7	4.356363051	3.24E-11
CASC9	4.241477629	5.15E-09
SSX1	4.160920962	0.003230776
SCARNA10	4.064007991	4.27E-17
RF00003	3.935504184	7.23E-10
SPANXB1	3.790832319	6.29E-07
PRSS33	3.588382097	7.48E-06
SNORD17	3.514541261	5.07E-21
COL2A1	3.447098468	1.37E-10
SNORD15B	3.268992471	2.14E-13
SCARNA6	3.221891402	3.74E-16
SLC5A12	3.198896204	3.89E-12
UGT2B4	3.066211634	1.11E-06
CSMD3	3.010630896	1.03E-07
POU6F2	2.767096447	2.05E-09
ACTG1P22	2.700384794	3.81E-06
CSAG1	2.698277377	7.96E-05
CHRNA9	2.652123903	1.20E-09
AC073508.1	2.608674963	1.45E-05
SNORA12	2.5764204	3.07E-08
SNORA73B	2.568630149	3.65E-10
LHFPL4	2.55920889	1.39E-08
AC025423.3	2.543177674	7.93E-05
HS3ST5	2.484495303	8.25E-08
ZNF716	2.482871604	0.006449881
SLIT1	2.43127641	4.57E-10
AKR1B15	2.388276127	5.88E-08
AC011632.1	2.363466857	1.02E-05
LINC01287	2.287925949	2.49E-08
BRINP2	2.258169006	9.98E-07
CYP24A1	2.200588896	5.11E-06

MUC2	2.154933312	0.000480939
AC005336.3	2.146903362	0.000116839
TCL1B	2.143867658	0.003402808
SLC4A10	2.138502564	9.98E-07
PAX7	2.122725966	0.002614179
FAM135B	2.110884913	2.63E-07
RIMS1	2.095898173	3.26E-08
KRT41P	2.092328573	0.000396229
TMPRSS4	2.069559269	5.87E-06
FUT6	2.065585188	9.83E-05
C5orf17	2.039323075	0.000182032
CPB1	2.030915653	0.006598269
GSTA1	2.029624541	0.000147076
LY6D	2.021659081	0.001594199
NTS	2.015980176	0.000725791
FABP7	2.00472145	0.003665108
LGI1	1.999810025	0.000482897
CCDC155	1.982950996	1.34E-05
AC004801.5	1.95829037	0.000571469
LINC01443	1.948952758	0.000430361
KRT31	1.940136135	0.000183406
SCARNA21	1.898799137	8.24E-05
COX6CP1	1.8841474	0.000154738
MS4A18	1.878832768	3.72E-05
DSCAM-AS1	1.870642753	0.003246073
RFX6	1.869333815	0.003125868
NPTX1	1.868632005	2.73E-05
POTEC	1.858746657	0.005323918
ALOX15	1.85721354	1.02E-05
KCNMB2-AS1	1.851653676	0.001222691
AL035425.3	1.843734037	0.000616588
TEX19	1.841844351	6.40E-06
C12orf56	1.83194319	0.000624429
MDGA2	1.825998701	0.002115559
HAL	1.816394851	1.05E-08
GATA4	1.800758249	0.006865404
SNORD94	1.794723458	6.82E-08
KRT24	1.784040094	0.005895702
ANKRD34B	1.779846958	0.000874446
RBM20	1.777102881	2.32E-07
TMEM179	1.755373822	0.00386105
ELF5	1.754392121	0.000367269

ACTN2	1.753353653	0.000150081
SULT1C2P1	1.750262488	0.004649106
ALB	1.749777548	0.000438497
AC026992.2	1.738139577	1.92E-05
PXDNL	1.731093503	5.42E-06
AC062028.2	1.723591416	0.001425738
OPRK1	1.708283877	0.00128122
AC125603.2	1.699436598	7.17E-05
TMEM178B	1.692588075	7.68E-06
CELF3	1.683955397	0.000200233
PRKACB	1.666550094	1.65E-08
VTN	1.637037774	3.78E-08
SCARNA13	1.635308883	4.20E-07
CNTN5	1.632738607	0.009963364
IP6K3	1.621627802	0.001303815
RN7SL2	1.602330841	2.80E-06
LINC00992	1.581142746	0.002445379
PTPRQ	1.575424779	0.000282272
MGAT5B	1.567029102	2.46E-06
PRSS2	1.557207271	0.004033037
RTBDN	1.556495714	0.000462574
MIR2052HG	1.550749226	0.008269936
CD177	1.545971376	0.006583073
KCNC1	1.543694244	0.000208531
SNAP25	1.537501427	1.09E-05
SCARNA12	1.522775136	8.51E-05
SYNPO2L	1.518652356	0.003584855
FAR2P4	1.507998347	0.003736318
CALHM1	1.503445228	7.53E-05
KCNJ16	-1.510407618	0.00091208
PSORS1C2	-1.512300492	0.003529168
SLC34A2	-1.514716648	0.008643598
GFAP	-1.525532846	1.09E-05
ACY3	-1.537864933	1.70E-05
GRIK1-AS1	-1.553707607	0.000540482
CROCC2	-1.575287671	0.002077298
WIF1	-1.619417837	0.007962935
GCM1	-1.620516689	1.98E-05
LRRC71	-1.657205335	5.24E-10
FOXN4	-1.695437392	0.00289648
SPIB	-1.726016928	7.19E-07
C7orf57	-1.740272047	3.16E-05

FOXJ1	-1.743062921	0.000367269
DRC7	-1.755590087	2.74E-05
TUBA4B	-1.763557302	5.02E-05
TEKT1	-1.764510266	7.97E-05
POU3F3	-1.780864054	0.000643315
AP000851.1	-1.824069248	0.000564408
IGFL1	-1.875156152	1.96E-05
LEP	-1.942457808	0.00013337
GRIN2B	-1.967133037	6.82E-08
AP000238.1	-1.982621097	4.60E-10
UGT2B11	-1.989740695	0.008139028
HAO2	-1.991388328	1.69E-05
CDHR4	-2.163306408	6.40E-06
CDC20B	-2.172972242	0.00025388
AL109807.1	-2.175990917	0.002701033
AC019117.2	-2.268425497	2.55E-05
KLK12	-2.296397802	0.001649974
FDCSP	-2.329921521	2.82E-06
OPRPN	-2.330374605	0.003813034
COX6B2	-2.378304126	1.41E-13
ODAM	-2.795430701	2.63E-09
C20orf85	-3.811330251	2.28E-08
CARTPT	-5.233449256	8.60E-08
PRR27	-5.551354433	1.44E-05
CSN3	-8.572254664	1.83E-17

Table 31. hPRLrI hi/med versus lo DEGs. TCGA-BRCA patients were stratified by hPRLrI status, being high/medium or low expressors (top/middle versus bottom tertiles, respectively), as determined by RNAseq analysis.

Gene symbol	log2FoldChange	padj
MIR3609	7.157167667	5.56E-24
SNORA74B	6.910998607	2.58E-46
SCARNA5	6.678779033	5.80E-61
SNORA74A	6.59207504	1.40E-27
RN7SL3	6.450301218	1.95E-66
RNU4-2	6.449387688	1.44E-56
RF00100	6.419985419	1.76E-68
RF00003	5.964354973	5.72E-22
SNORA23	5.798632812	7.09E-50
SNORA73B	5.739204361	4.50E-59
RNVU1-7	5.39431981	7.83E-27
SNORA20	5.090074799	1.24E-27
RF00003	5.080978513	4.50E-26
SCARNA10	4.934737397	1.40E-36
SNORD15B	4.34651787	6.37E-36
SNORD17	4.117108292	8.00E-41
SCARNA6	4.072937422	1.65E-37
SNORA12	3.415646585	1.25E-20
CHGB	3.226728232	2.46E-08
ACTG1P22	3.172393393	9.54E-11
SMPD4P1	3.157213605	3.14E-12
LHFPL4	3.042436738	5.36E-14
SCARNA21	3.007151527	5.84E-16
RF00012	2.912841618	1.12E-12
SNORD94	2.687796405	5.06E-26
LINC01446	2.683526653	0.002257326
RF00003	2.438284398	4.86E-15
SCARNA12	2.38822093	1.42E-15
SCARNA13	2.386891404	5.35E-21
LINC01287	2.36659362	7.53E-14
PRSS33	2.321157964	0.005392314
RN7SL2	2.314741252	5.35E-17
HIST1H1B	2.248546465	1.60E-11
SNORA14B	2.232605139	1.70E-13
HIST1H2BF	2.172180415	7.03E-10
TDRD12	2.170323788	7.71E-07
LIN28A	2.029193824	0.00190591
FAM135B	1.909885247	6.98E-06

POTEC	1.844511202	0.007019057
SIX3	1.797846313	0.000112703
HIST1H2BO	1.728254456	9.11E-09
HIST1H1T	1.704027867	2.46E-05
HIST1H2AD	1.703071099	9.34E-08
TEX19	1.659486049	4.58E-06
CNTN5	1.65221063	0.004832835
RBM20	1.648878247	2.20E-06
AL358913.2	1.647890763	0.003143567
LINC00589	1.63021978	2.20E-05
TH	1.585519684	0.001101088
HIST1H1D	1.523237063	4.92E-05
DUSP5P1	1.513002503	0.00146337
CUX2	-1.527600233	0.000713956
KLK2	-1.538123914	1.90E-05
SLC1A6	-1.541748397	0.004793798
C4BPA	-1.554536912	5.08E-05
SLC34A2	-1.562926504	0.002851286
EDN3	-1.588694139	0.007441472
CLDN6	-1.589623771	0.000160958
SCGB3A1	-1.595283366	0.00025512
C8orf34-AS1	-1.609213923	0.002945696
LCT	-1.65276185	0.000294846
AC004836.1	-1.656497067	8.44E-05
HAO2	-1.67202073	0.000860883
KRT6A	-1.677712745	0.001049012
ROCR	-1.686254207	0.001536906
KRT79	-1.687920842	7.06E-05
OLFM4	-1.704993904	0.000963885
WIF1	-1.721737384	0.001332219
GABRQ	-1.72331682	0.000203524
CST4	-1.750101474	0.000116767
SOX11	-1.755583414	3.39E-07
RNF183	-1.760886015	6.92E-06
PI3	-1.765874688	0.000106568
RARRES1	-1.82975536	2.85E-09
PIP	-1.833936523	0.00049793
DEFB1	-1.84184082	3.27E-06
LTF	-1.846569638	0.000202557
PEBP4	-1.87244596	4.19E-07
PLP1	-1.875572119	9.34E-08
GHRH	-1.880999955	0.003541892

MUC5AC	-1.886935261	0.000444506
MYBPC1	-1.947870144	9.63E-05
GPM6A	-1.996578793	2.56E-07
C20orf85	-2.012400971	0.006743349
AC011487.2	-2.017695199	0.000373334
S100A9	-2.04721218	1.85E-06
UCP1	-2.075428065	8.06E-05
NTNG1	-2.098545592	1.86E-05
AC011270.2	-2.121956663	0.000291367
NEUROG2	-2.179808362	3.74E-05
TUNAR	-2.187024679	0.000209501
KLK14	-2.217766696	1.60E-09
FGG	-2.218322804	0.001148775
KRT6C	-2.223015083	9.19E-05
CLCA2	-2.24814701	1.96E-06
MUC2	-2.300561512	0.000305448
STAC2	-2.310378975	4.65E-07
KLK11	-2.340948885	5.42E-05
CRABP1	-2.366459328	2.39E-06
FGFBP1	-2.387068557	0.000129675
FGB	-2.393120707	0.00272285
MUCL1	-2.525786784	3.17E-07
LY6D	-2.55318488	3.71E-06
KLK3	-2.570755936	6.35E-07
SPRR3	-2.633910979	0.003094011
IRS4	-2.705833843	2.58E-05
AC111000.4	-2.861725603	0.000994201
KLK12	-2.888556683	5.03E-05
UGT2B11	-2.908970761	8.23E-06
KLK13	-3.049944374	1.29E-09
ODAM	-3.120335311	4.09E-09
FDCSP	-3.282969734	6.71E-12
LINC00052	-3.288608364	6.13E-08
NPY2R	-3.862797707	6.04E-08
CASP14	-4.003558384	3.42E-13
CARTPT	-4.084991622	0.000139711
SMR3B	-4.334244256	1.17E-06
PRR27	-4.540019842	0.002037217
DCD	-5.148575026	2.14E-11

Table 32. hPRLrL-hi/lo DEGs. TCGA-BRCA patients were stratified by hPRLrL status, being high or low expressors (top versus bottom tertiles, respectively), as determined by RNAseq analysis

Gene symbol	Log2(fold change)	padj
RN7SKP255	6.222928036	1.11E-13
RNVU1-18	6.040027526	5.45E-07
MIR3609	5.683039062	9.94E-33
SCARNA5	5.63826957	7.79E-72
RNU1-11P	5.621053822	2.20E-11
SNORA74B	5.54095332	2.47E-53
SNORA74A	5.125442091	9.33E-31
SCARNA7	5.052931938	1.02E-58
SNORA23	4.979810961	5.46E-55
RF00100	4.824124047	9.74E-63
SCARNA10	4.749503945	1.71E-50
RF00003	4.649678224	1.37E-32
CPB1	4.578902428	5.35E-37
RNVU1-7	4.052170432	7.03E-30
SNORA73B	4.014231508	1.84E-54
SNORA12	3.993541826	4.91E-43
SCARNA6	3.811827643	3.59E-54
SNORD15B	3.74644697	1.19E-46
OR4K12P	3.704537486	1.22E-22
SCARNA21	3.667454324	4.59E-35
LINC00052	3.619327526	3.75E-22
RF00003	3.495534462	8.95E-16
AF127577.6	3.394612705	3.84E-43
AC079414.2	3.362286685	2.00E-11
SNORD17	3.294344551	2.72E-38
AL450996.1	3.282820283	1.66E-29
RN7SL674P	3.281284786	1.27E-43
RNU4-2	3.23177896	1.95E-27
SLC30A8	3.10180329	7.22E-22
SCARNA13	3.081555079	1.25E-45
HNRNPA1P57	3.074937394	2.19E-19
RN7SL314P	3.065903015	1.89E-25
UGT2B4	3.064851985	1.60E-18
CHRNA9	3.039816735	3.55E-25
CPLX2	3.03042807	4.29E-11
GPR139	3.009281	1.40E-12
AC092881.1	3.008042508	4.31E-60

KLHL1	2.981947818	9.63E-06
AL355075.4	2.97013986	1.94E-15
PWAR5	2.934819167	2.34E-67
AC010368.1	2.930773499	4.37E-65
AL731892.1	2.900298866	3.55E-24
AC114786.2	2.898247547	0.00011131
AC092979.1	2.861302803	2.07E-10
AP005131.4	2.825355143	4.08E-34
SNORA22	2.81277051	1.76E-34
TRPA1	2.806788505	9.88E-31
KCNH1	2.793318432	1.71E-50
AC093838.1	2.791887495	2.02E-21
SLC4A10	2.760839333	2.61E-27
AC093292.1	2.746832937	9.99E-08
VN1R53P	2.729117036	1.30E-20
GRPR	2.728401247	5.89E-31
AC124312.2	2.720919073	3.33E-51
AGXT2	2.71405259	1.96E-48
AC061961.1	2.711855981	4.33E-12
RF00019	2.671539954	4.48E-20
AC093297.1	2.67047343	9.35E-12
AF178030.1	2.649627125	7.14E-27
AL353583.1	2.628303923	6.15E-37
AP003080.1	2.614920214	3.46E-34
TMEM75	2.614786443	4.03E-33
RN7SL2	2.602723128	8.44E-35
NELL1	2.586772963	1.43E-11
RP1	2.561858156	1.61E-30
ANKRD30A	2.53852555	1.30E-19
THSD4-AS1	2.533442868	4.46E-16
GRAMD4P8	2.532767895	2.08E-24
RNU4-1	2.532035927	2.08E-18
FAM135B	2.514149635	4.08E-26
RF00019	2.470901112	5.52E-35
AC115837.2	2.470048158	5.72E-09
CELF3	2.459881035	2.47E-23
RFX6	2.435178243	1.99E-14
AL021068.2	2.420717609	5.48E-54
AP000560.1	2.40798712	2.14E-53
AC062028.2	2.407714322	8.52E-18
AL354733.2	2.405819791	1.77E-46
GNAQP1	2.40156122	1.10E-35

PRLR	2.399288895	5.22E-152
LINC01522	2.38766304	6.14E-19
AL136115.1	2.384562631	3.47E-33
TLK2P2	2.37621758	3.18E-37
SEZ6	2.351786596	4.83E-21
ERVW-1	2.323730575	6.21E-37
MKX	2.319674112	1.44E-21
ZBED6	2.312665552	1.78E-53
HSPD1P11	2.312533076	2.65E-27
CST9	2.301132749	2.30E-08
AC018752.1	2.300891909	7.15E-55
AC090206.1	2.293044345	8.01E-27
SLC6A4	2.286847976	1.38E-18
AC020951.1	2.261539627	4.79E-37
CRYZP1	2.24465247	1.14E-47
RAD17P1	2.243979076	1.70E-19
AC009927.1	2.240968351	2.32E-37
AC002064.2	2.23661043	1.27E-27
SYT1	2.231797772	7.09E-23
PGAM1P5	2.231235789	7.83E-30
AP005131.1	2.229974052	3.22E-37
AL713922.2	2.228694594	6.26E-26
AC096733.2	2.219376292	7.84E-50
GP2	2.21540305	9.67E-14
CST5	2.214918728	2.48E-09
CLSTN2	2.192513715	7.89E-29
AC090181.3	2.187663818	6.86E-40
NDST4	2.184250365	2.73E-07
MIR2052HG	2.178902656	4.11E-14
AC005544.1	2.174516958	4.96E-25
FAM234B	2.170697687	9.32E-43
AC116158.1	2.159307406	1.32E-33
POTEF	2.159087704	2.09E-25
LCMT1-AS2	2.158489953	7.75E-43
SLIT1	2.157451512	7.77E-24
AC008147.2	2.151598935	5.21E-42
CDH7	2.146055485	2.04E-15
AL132708.1	2.13140827	2.65E-13
SLC16A6	2.100999443	1.86E-35
KLHL11	2.091202785	8.01E-74
HIST1H4C	2.089563619	8.62E-20
AL136164.3	2.083882076	6.96E-27

HS6ST3	2.082339525	2.31E-20
AC126564.1	2.078546238	4.72E-11
TRIM58	2.069372629	3.83E-27
KCNJ3	2.062155305	1.26E-09
SPATA46	2.059800852	1.81E-26
AC144450.1	2.056282272	2.84E-35
AC124312.3	2.053553836	1.09E-36
AC006441.1	2.050525204	1.48E-24
AL445187.1	2.043447364	1.30E-37
ACER2	2.041597414	3.39E-66
POTEE	2.030306619	1.44E-22
AL139022.1	2.02365562	2.53E-33
AC094019.1	2.016125186	7.09E-31
KLF7-IT1	2.013653582	2.82E-26
CLEC3A	2.010131101	1.32E-05
AC253536.3	2.009426212	1.16E-34
POTEC	2.001327428	4.25E-06
AL133230.1	2.000485702	1.85E-41
CBLN2	1.999972335	1.84E-10
CDR1	1.989625663	4.67E-15
IPO8P1	1.983472931	1.82E-45
AC079296.1	1.983142835	2.27E-14
AFF3	1.978747615	5.51E-27
NLRP5	1.977499725	8.25E-08
ERVFRD-1	1.977456469	1.79E-21
AC107072.2	1.975372544	6.14E-24
TMEM161BP1	1.974180374	1.71E-13
AC016590.2	1.972274831	3.45E-32
PCSK2	1.968931309	1.01E-07
NADK2-AS1	1.968389253	6.00E-36
HIST4H4	1.96729482	3.83E-42
AC097382.2	1.960740614	6.62E-51
RN7SL3	1.959170861	3.46E-17
AL121578.3	1.957827158	1.57E-11
GLRA3	1.951577559	7.02E-09
LINC01801	1.950876612	2.18E-37
CCDC144A	1.949064011	1.44E-17
LRRC37A9P	1.945843737	5.16E-35
POTEI	1.944513614	3.67E-17
RNU6-1016P	1.931649874	5.57E-31
C8orf86	1.928828368	2.87E-16
AL138878.2	1.927682119	1.66E-16

AC015971.1	1.92153602	4.58E-40
AC010522.1	1.918091286	2.11E-59
ENPP7P10	1.914314842	1.86E-28
ZDHHC22	1.913908031	4.16E-12
AC012531.1	1.907721825	2.97E-31
GTF2IP7	1.907186258	1.19E-34
AP001469.1	1.905818773	2.39E-34
KCNC1	1.905178584	9.16E-16
GUSBP9	1.898528086	2.42E-37
ANKRD20A11P	1.898299837	7.15E-18
ZNF729	1.897284219	6.40E-08
AP001429.1	1.895851626	5.36E-32
AL158847.1	1.893055355	5.85E-17
AC004066.2	1.892519794	3.54E-34
ABCC13	1.891768601	3.58E-08
AC138409.1	1.888215666	5.68E-22
RN7SL381P	1.88241868	3.98E-29
AP000439.2	1.881693222	9.56E-12
RPS20P22	1.881073454	2.55E-19
AC073525.1	1.877167251	4.03E-05
AC087286.2	1.876897501	4.59E-28
AC007114.2	1.874496402	1.43E-30
ZBTB20	1.86994824	5.82E-39
FAM169A	1.867044596	7.34E-38
AL035448.1	1.86658159	6.96E-29
IRS4	1.865673549	3.57E-06
CCDC117	1.865647592	1.40E-62
AC078993.1	1.860947411	3.38E-14
XIST	1.85840292	1.34E-30
ANKRD36C	1.852821431	1.14E-36
AC099677.1	1.849013046	1.89E-32
LINC01344	1.847066148	1.04E-16
MUC19	1.8459149	2.13E-11
CYP4Z1	1.830280288	1.90E-09
ACTG1P22	1.829938277	1.36E-08
LDHAL6A	1.824868564	3.05E-31
HNRNPA1P14	1.822715693	1.40E-29
SYCP3	1.813078187	1.75E-32
AC022336.3	1.8114532	4.34E-25
NOTCH2NL	1.804124147	8.83E-52
ELOVL2	1.797586875	1.25E-16
RPS3AP38	1.795377178	4.75E-26

AL117329.1	1.791702412	1.29E-11
RPL7P57	1.79109567	1.17E-23
NRIP3	1.789525939	7.94E-21
KCNJ13	1.786866475	3.19E-16
CLDN20	1.783811298	7.70E-32
AL356801.1	1.781341673	1.28E-29
ADGRV1	1.778644035	1.14E-20
SCARNA12	1.775384754	1.60E-15
CYP2G1P	1.774593515	2.62E-11
AC091544.2	1.772184705	2.33E-20
KCNMA1-AS1	1.771665474	1.86E-16
AL049869.3	1.769291983	8.05E-37
NPTX1	1.767535824	3.23E-16
LACRT	1.765549993	0.000348406
RBM24	1.764397086	4.79E-15
MIR29B2CHG	1.761263962	2.56E-22
HIST1H2BF	1.757164832	1.90E-17
AF131216.1	1.756771324	4.52E-30
FAM196A	1.753378158	3.38E-12
AC091181.1	1.74890306	4.55E-27
CPHL1P	1.741327602	4.30E-11
AC083806.2	1.735787757	6.79E-28
HIST1H1D	1.733905422	5.81E-15
AC087521.2	1.73336267	1.92E-25
RNU6-813P	1.732137338	9.22E-08
RANBP3L	1.731594282	3.11E-24
DNAH5	1.729697515	1.43E-31
HIST1H4B	1.729316619	6.75E-10
AP001767.4	1.728420051	9.72E-36
RAB11FIP1	1.727790595	1.79E-35
ZNRF2P2	1.726505124	2.17E-42
AL365356.1	1.726247481	2.55E-16
THSD4	1.721095126	8.27E-29
AC093012.1	1.720576635	1.51E-25
HIST2H2AB	1.71955302	1.67E-12
RERG-IT1	1.719262156	1.25E-17
RAPH1	1.718625875	1.72E-60
AC007637.1	1.718089652	1.06E-30
AC109361.2	1.717894943	5.58E-21
AC090114.3	1.71417947	1.16E-32
HIST1H1E	1.712838414	5.05E-17
SLC16A12	1.709758054	1.68E-19

SLC18A2	1.709711497	5.53E-25
ALB	1.706043161	6.90E-12
ANKRD36	1.703772951	2.86E-38
PTPRT	1.701435864	1.02E-13
MKRN5P	1.700828069	1.22E-11
AC131009.4	1.70023915	1.45E-29
LINC02571	1.697706258	6.57E-13
AC012254.3	1.694728388	2.31E-26
NLRP8	1.687506498	6.72E-08
AL136988.2	1.685648976	1.33E-21
PGR	1.683483007	1.36E-11
AC233300.1	1.682796935	9.37E-27
RIMS1	1.680379765	1.28E-13
ACTG1P10	1.675598288	2.77E-29
EEF1DP3	1.674044993	1.15E-25
RIMS4	1.672186936	3.02E-12
SIGLEC6	1.671903491	1.44E-22
AL451064.2	1.665030091	3.76E-21
MYT1	1.664150049	5.18E-12
USP37	1.663401203	1.84E-72
AC131953.1	1.662452021	3.62E-23
ZNF221	1.662115199	1.21E-59
CERS6	1.659844403	8.35E-90
AC036103.1	1.658994579	5.33E-24
C11orf42	1.65792709	1.05E-32
SMG1P1	1.655944486	9.78E-34
SLC1A1	1.653218043	1.19E-15
ASIC2	1.651828381	1.43E-09
AC005480.1	1.651719979	4.55E-25
CCDC144B	1.648268316	1.47E-19
GPM6A	1.648159086	3.99E-13
AC016747.3	1.647777321	5.89E-31
AC063976.2	1.64763989	8.53E-26
NPTN-IT1	1.647627598	1.13E-27
RNU6-531P	1.646198474	1.75E-34
TMEM26-AS1	1.646097409	7.93E-17
HMGB1P14	1.645403382	4.95E-26
POMK	1.643552349	3.60E-31
AC008663.1	1.641260351	8.89E-08
PEX5L	1.639345056	2.13E-12
REPS2	1.638625118	3.29E-30
ADCY1	1.634467379	1.05E-16

AC000120.1	1.633769773	7.81E-27
AC139769.1	1.633629122	2.95E-41
TBC1D9	1.633593168	1.22E-29
STARD13-AS	1.632833824	5.60E-16
AC092162.2	1.632634494	1.78E-17
LINC01087	1.632428001	5.04E-09
KRR1P1	1.631291664	4.86E-22
AC015914.1	1.628602855	5.13E-17
HTR7P1	1.628056574	3.42E-31
AC010761.3	1.626571801	1.95E-29
AL133387.1	1.622245269	1.13E-08
WASF5P	1.621821762	4.94E-10
HIST1H2AI	1.620889345	1.38E-16
CLVS2	1.618512348	3.46E-06
REL	1.616941015	3.81E-61
AC068790.3	1.615525818	7.63E-23
AL132989.2	1.612084652	1.98E-24
AC011498.4	1.610407935	1.17E-12
AC010735.1	1.60812487	1.25E-19
ANKRD36B	1.606740339	1.38E-33
IL6ST	1.606372201	3.03E-40
PCDH19	1.605906128	1.24E-19
PCDHA9	1.602968927	1.67E-14
NRIP1	1.601961186	2.50E-62
AL031009.1	1.599803208	9.02E-29
ELFN2	1.597619729	1.70E-12
AC009812.3	1.597256757	3.60E-28
POTEKP	1.593507454	1.17E-10
LINC00472	1.591393304	2.98E-18
CFAP61	1.589552216	3.88E-25
CNGB3	1.588340911	4.75E-17
GNRHR	1.585821213	1.33E-24
ZNF209P	1.584679695	1.16E-08
NBEAL1	1.583063069	2.68E-53
AC108010.1	1.58168132	5.50E-34
SORCS1	1.579480281	8.02E-09
AC027514.2	1.576957548	1.40E-23
ZNF483	1.576787998	5.89E-28
LDLRAD4-AS1	1.575884872	2.34E-11
DANT2	1.575517373	1.72E-13
ATRNL1	1.575315826	6.02E-11
ITPR1	1.573830459	5.79E-42

AL583832.1	1.573228176	2.90E-23
OCLM	1.570998211	6.45E-29
RN7SL4P	1.568877015	5.45E-13
AC067852.3	1.568756996	2.22E-26
AC108449.2	1.567485904	1.40E-54
AC018462.1	1.567478662	5.42E-29
CGA	1.567338274	3.25E-05
FSIP1	1.561470905	2.14E-14
LIN7A	1.560604184	2.20E-16
AC008895.1	1.560602735	1.28E-36
INPP4B	1.558928246	9.12E-34
AC141930.1	1.555857929	5.47E-23
ERBB4	1.55582924	2.79E-14
NOS1AP	1.554292137	3.49E-32
AC005336.1	1.552647299	8.48E-12
LAMA3	1.551357708	2.42E-24
SAP30L-AS1	1.54956559	1.91E-33
GCSAML	1.548425189	1.48E-19
CCDC150P1	1.546709452	1.69E-23
AL031666.2	1.544595203	2.31E-15
LRRC37A11P	1.542404368	2.28E-17
AC004594.1	1.540459742	1.65E-15
SVOP	1.539711612	2.36E-05
Z68871.1	1.539673726	1.81E-50
AC102945.2	1.539184488	1.16E-30
NCAM2	1.539139774	8.31E-18
CECR2	1.538703908	2.51E-13
HSPA8P15	1.535954491	1.44E-17
AC103702.1	1.532331084	2.69E-08
GCNT7	1.531888366	1.64E-22
Z82185.1	1.530737741	0.000727969
AP000811.1	1.530208858	1.31E-25
LONRF2	1.528621428	5.81E-20
MUM1L1	1.528333374	7.15E-16
CSMD3	1.527791601	0.000122086
PLEKHD1	1.527542553	1.93E-15
KITLG	1.527339598	7.78E-32
ATP1A2	1.526972844	4.31E-13
AC025917.1	1.525802083	7.95E-25
LINC01876	1.525408144	2.18E-08
PSD3	1.524250223	8.45E-26
VWA2	1.524168914	2.54E-20

AC122129.1	1.524056005	2.51E-31
SLC22A10	1.5235429	3.51E-09
IL1RAPL2	1.522309165	2.27E-11
PRTG	1.52198569	1.11E-26
AC092071.1	1.521735365	8.69E-07
PCLO	1.518642517	3.16E-39
CELF2-AS1	1.518641041	3.74E-11
WDR17	1.51791167	6.84E-15
AC118344.1	1.517872171	7.26E-22
GLYATL1P4	1.514285875	1.59E-11
CACNG6	1.513899143	6.37E-06
Z94721.2	1.512437592	8.92E-27
AC012618.2	1.510107715	4.07E-22
SYT13	1.509667005	8.92E-09
AC021087.2	1.507901486	9.13E-31
AL356311.1	1.507301695	3.77E-08
SMG1P3	1.506337912	3.31E-37
ACADSB	1.505852419	1.37E-32
RTL9	1.504962168	2.10E-23
AC108704.2	1.503046344	1.35E-22
CYP4F62P	1.503046246	0.0001769
FLNB-AS1	1.50193894	8.31E-30
AC116533.1	-1.500573564	4.15E-52
ELF5	-1.501109206	1.97E-08
FOXL1	-1.501875518	5.93E-27
TCP11	-1.502278095	4.95E-11
MESP2	-1.50282583	4.23E-17
CAVIN3	-1.50310295	1.60E-49
PPP1R14BP3	-1.503501434	4.27E-62
DOC2GP	-1.504683154	3.11E-20
ATP5F1D	-1.50548636	3.33E-52
TMEM249	-1.507326003	6.56E-19
HSPB2	-1.50979004	2.60E-35
ACTA1	-1.50996061	2.38E-11
CWH43	-1.510493583	7.00E-08
ANGPTL4	-1.511642437	4.70E-21
RPL13AP20	-1.512701068	2.50E-51
NALT1	-1.516098	4.82E-29
ATP5F1EP2	-1.516771068	2.44E-36
SOCS1	-1.516993673	1.32E-35
NMU	-1.517996595	2.64E-12
FUT3	-1.518616752	2.20E-10

TMSB15A	-1.519784545	1.75E-13
LINC01143	-1.520661445	1.81E-10
SAP25	-1.520930398	7.68E-32
AC022784.3	-1.521590408	1.20E-13
GJB5	-1.522170976	7.61E-13
RPL18AP3	-1.525291549	4.74E-51
AL022334.1	-1.526379827	1.10E-10
COL22A1	-1.527270631	1.04E-14
TNNC1	-1.52753011	2.20E-21
ARL6IP4	-1.527975522	1.34E-50
LINC00460	-1.529243269	2.29E-16
CCNE1	-1.533855299	2.70E-21
BBOX1	-1.535229857	1.95E-11
GTF2IRD2P1	-1.53559445	2.65E-18
CPA4	-1.536113877	3.72E-13
DSCR8	-1.538398559	0.000140445
AC112491.1	-1.53878085	2.16E-27
GSTA2	-1.540742585	7.97E-08
CAHM	-1.542615677	7.55E-40
CD7	-1.543047908	1.17E-24
EEF1B2P6	-1.543392058	1.21E-55
AP000851.2	-1.544364968	4.71E-08
KRT13	-1.546154672	2.14E-06
CYBA	-1.546436273	4.06E-47
MRPL12	-1.548988644	2.60E-41
MRGPRX3	-1.549537875	1.04E-08
S100A3	-1.551660377	7.54E-41
CLIC3	-1.553594099	6.90E-21
PRKCQ-AS1	-1.558107773	1.48E-20
LINC00634	-1.558270035	1.08E-23
PHF24	-1.558450429	7.93E-14
EGR4	-1.55935443	3.17E-10
AC074212.1	-1.559962614	4.51E-34
DHDH	-1.560397783	3.02E-29
SMTNL2	-1.563036222	9.14E-14
AC067735.1	-1.563055776	1.44E-23
AL590617.2	-1.56350542	9.24E-51
RPS28P7	-1.564163031	9.92E-22
PRR7	-1.565140679	4.93E-38
LINC00964	-1.566584552	2.45E-12
AC004687.1	-1.566667298	9.92E-22
IGLL5	-1.567625927	2.63E-12

MYOZ1	-1.573430435	9.55E-22
TCF15	-1.576611195	1.50E-24
AC099329.2	-1.578172779	1.43E-12
IGHV3-43	-1.579340009	8.77E-11
LINC00511	-1.580263229	1.32E-18
GZMM	-1.581487711	1.88E-21
TBX10	-1.585625897	2.87E-05
UGT8	-1.585944106	4.98E-11
CHODL	-1.585977891	1.98E-12
IL1R2	-1.58882944	7.54E-19
LINC01781	-1.588926544	1.15E-10
RPL13P12	-1.590212355	1.28E-42
RPS2P32	-1.590764563	2.17E-36
NMB	-1.593852538	5.25E-51
AL138724.1	-1.595863904	7.79E-52
CRLF1	-1.596458953	1.40E-23
IGHV3-20	-1.597534634	1.52E-09
CCL18	-1.59753748	2.35E-14
TNNT2	-1.598276316	1.47E-13
CXCL3	-1.601356568	2.57E-20
PSAT1	-1.604512788	4.22E-14
LINC00461	-1.604897559	3.04E-07
CHRDL2	-1.605320692	1.67E-17
SIX3-AS1	-1.605502693	6.29E-06
FOSL1	-1.605807279	1.75E-22
KBTBD12	-1.607173555	1.55E-08
LGR5	-1.607852309	6.53E-14
HR	-1.609681683	1.72E-22
DCD	-1.613141469	0.000358937
PHGDH	-1.614259136	1.00E-23
TRIM54	-1.617999579	4.20E-12
C8G	-1.618849486	5.41E-47
AC092118.1	-1.620752039	6.81E-12
AC020898.1	-1.62137609	1.42E-38
AC099336.2	-1.622845478	2.85E-36
MT2P1	-1.625402879	9.44E-24
GPR55	-1.625607308	4.70E-22
AC133785.1	-1.628097756	2.47E-08
RNF222	-1.629358822	3.95E-13
IGHV2-70	-1.630179072	7.92E-10
MELTF	-1.634920904	1.11E-24
PLEKHF1	-1.635633721	2.34E-39

TNNT3	-1.637535851	9.16E-17
HAS1	-1.637732758	2.90E-16
MFGE8	-1.638829033	1.20E-34
U62317.2	-1.639865978	8.03E-25
FOXC2	-1.639949701	3.83E-20
CHI3L2	-1.64113494	2.15E-16
ADM5	-1.646465892	3.39E-38
MT1H	-1.647744633	3.80E-13
KRT23	-1.651482622	6.27E-15
AP005233.2	-1.654641801	1.28E-08
RRAD	-1.655722159	4.19E-24
RPL10P9	-1.657363211	7.88E-16
CCDC85B	-1.659943542	1.39E-43
P2RX5	-1.660488665	1.07E-22
CACNA1C-AS2	-1.661472929	6.65E-22
QRFPR	-1.661618455	2.29E-13
LBP	-1.66283325	1.27E-10
AC020659.1	-1.666517173	7.86E-18
POPDC3	-1.666690424	1.38E-13
FAM107A	-1.667934533	3.09E-21
RPL7P9	-1.669250508	3.21E-46
IGKV2D-30	-1.670044136	1.68E-08
RPL3P4	-1.673104219	4.67E-42
MT1M	-1.673923203	3.54E-26
CALML3	-1.674027292	1.90E-10
LINC01356	-1.675783	5.12E-24
HBA2	-1.675890454	3.55E-21
MT1L	-1.677973782	1.23E-26
IL36RN	-1.679095969	3.33E-07
GMPSP1	-1.679425443	2.87E-39
RHEX	-1.679993084	6.42E-17
BAIAP2L2	-1.68092879	1.11E-27
TM4SF4	-1.681079655	2.28E-13
FCAMR	-1.684231842	8.37E-10
IGLV4-69	-1.684900762	4.68E-12
PRSS12	-1.68507193	5.37E-17
IGKV1D-13	-1.689753769	8.89E-09
AC015712.4	-1.691754282	3.13E-12
CALB2	-1.691947838	9.10E-17
GSTP1	-1.694941569	2.41E-35
LINC00839	-1.697087749	4.37E-18
UPK2	-1.698436381	5.76E-23

CLDN10	-1.70446248	4.11E-12
ACE2	-1.705692595	5.17E-13
TMCC2	-1.706559103	2.36E-26
CCL19	-1.707692721	3.17E-15
NCMAP	-1.707815654	3.94E-17
SFN	-1.708143074	1.89E-39
MIMT1	-1.708851859	8.47E-09
CD79A	-1.713494537	2.43E-17
CHRM3	-1.716861395	2.91E-16
LGR6	-1.717154788	5.22E-15
IGLV3-21	-1.725267661	7.00E-14
PART1	-1.727135516	2.24E-14
IGFL1	-1.727234005	3.43E-11
NLRP7	-1.727235555	3.46E-17
STAC2	-1.727591479	4.74E-10
TREX2	-1.727599638	9.88E-44
C9orf170	-1.730437718	8.03E-18
RAPSN	-1.730609806	5.79E-22
AL592429.1	-1.734737599	3.29E-12
AC021087.4	-1.734969513	3.46E-15
WNT11	-1.735818509	5.65E-22
FABP5	-1.737612307	5.60E-33
BX470102.1	-1.740463428	2.59E-30
AC069148.1	-1.74244733	7.74E-23
C4orf48	-1.742741556	3.35E-33
EEF1DP5	-1.744836948	3.06E-08
EDAR	-1.744865099	2.03E-14
RPL21P119	-1.748375868	1.48E-39
TCEAL2	-1.748855028	1.40E-14
C7orf61	-1.749354612	6.62E-32
S100A6	-1.749853384	2.12E-44
TCL1A	-1.750241115	4.69E-12
AC022101.1	-1.753614487	1.30E-10
CCDC129	-1.754611337	7.60E-11
AC034236.1	-1.75706652	1.05E-55
OSR1	-1.757669892	1.68E-19
PCP4L1	-1.760003549	2.25E-17
AC007969.1	-1.762798047	1.63E-51
HPDL	-1.766518898	1.75E-19
SLC1A6	-1.769206104	1.32E-07
HES4	-1.772129391	9.17E-45
CXCL6	-1.774863797	3.94E-12

SOD3	-1.775176216	3.61E-31
LINC02473	-1.776593284	4.03E-14
IGKC	-1.786064988	1.32E-16
SAA2	-1.789015594	4.66E-19
AC023983.2	-1.789560511	6.38E-30
CLDN9	-1.790630649	1.92E-25
AC011247.1	-1.792007316	7.18E-20
RPL13AP25	-1.792707322	1.68E-57
NCCRP1	-1.794161981	7.62E-13
TNFRSF13B	-1.795376228	1.32E-17
FADS6	-1.79564599	1.57E-10
KLF14	-1.795681223	4.07E-25
CD79B	-1.795927968	5.59E-31
AP001024.1	-1.799203248	7.21E-38
MUC5AC	-1.800493341	1.16E-07
KLHDC7B	-1.803964123	7.44E-17
STAC	-1.804929554	1.06E-21
TEX15	-1.805966997	2.34E-06
KRT17P3	-1.806928271	1.64E-09
PSCA	-1.807679473	1.74E-15
TUNAR	-1.808193086	1.23E-07
SLC28A1	-1.810332126	4.08E-18
TNNC2	-1.811046474	1.01E-34
MYLPF	-1.811148001	1.96E-44
SULT1E1	-1.811765048	8.05E-08
ACAN	-1.812493899	2.91E-25
SPAAR	-1.812986719	1.38E-35
GPX1P1	-1.813117068	1.79E-23
AC022424.1	-1.813344132	9.22E-12
RPL10P6	-1.813598909	2.32E-13
TRIM29	-1.81398925	5.54E-20
RGMA	-1.819209215	1.30E-31
NIPAL4	-1.819930956	4.01E-21
AP001505.1	-1.820518027	5.81E-54
AC025154.2	-1.822986379	2.25E-09
AC116614.1	-1.822998266	1.70E-09
UPK1B	-1.823080604	1.11E-07
SLC34A2	-1.823928792	3.80E-12
HS3ST4	-1.82400716	5.04E-09
TLX1NB	-1.826932274	2.76E-09
IGF2BP2	-1.829465511	2.66E-20
AC079922.1	-1.830374094	4.20E-61

AC019171.1	-1.830385273	4.10E-22
PPP1R14A	-1.834119426	3.23E-39
AC107983.1	-1.834324859	2.62E-55
SERPINB5	-1.839290475	2.42E-15
DMRT3	-1.844349732	1.23E-40
HAPLN3	-1.84586341	5.85E-39
AL356417.2	-1.846046821	1.43E-30
CA9	-1.84721505	3.12E-10
MTCO2P22	-1.847390523	9.90E-20
BCL11A	-1.853123806	8.75E-20
SOX9-AS1	-1.855499163	1.68E-20
AC246787.1	-1.856170642	9.12E-78
CCL20	-1.857990254	1.03E-20
AC005912.1	-1.859498113	6.31E-57
IGKV1-8	-1.865968462	1.22E-14
DES	-1.868197994	5.54E-20
NRG2	-1.86855467	1.60E-26
AC090589.1	-1.868960958	1.88E-31
LINC01315	-1.871381388	1.74E-37
NRTN	-1.871388025	9.27E-25
JSRP1	-1.872889052	1.33E-26
AL390729.1	-1.87354646	1.01E-25
VPREB3	-1.875847671	3.25E-25
GPR87	-1.876487177	2.90E-18
IGHG1	-1.878251109	8.59E-15
EXTL1	-1.87951565	1.01E-21
AL109761.1	-1.881522091	5.28E-14
PNMA6A	-1.883258614	4.23E-30
SIX3	-1.883278301	1.65E-11
RETN	-1.88625993	1.63E-19
IGLV8-61	-1.886565687	1.86E-12
CD19	-1.887013454	3.31E-19
DSC3	-1.887734421	9.33E-16
IGKV1D-39	-1.889334494	2.42E-10
LTB	-1.890725235	1.48E-29
TMPRSS5	-1.894788797	5.07E-26
ELFN1-AS1	-1.896670012	4.99E-11
ICAM5	-1.902355122	1.77E-21
ARL9	-1.9097002	8.44E-29
ORM1	-1.913718909	2.49E-09
OLAH	-1.919993644	1.21E-12
SAA4	-1.921198592	2.93E-18

KCNK5	-1.921848346	3.99E-27
IGKV1D-17	-1.924158488	1.78E-11
PGBD5	-1.929355079	1.78E-24
STK33	-1.930206999	1.50E-22
TGM1	-1.932597731	2.75E-43
AC092484.1	-1.935598896	5.32E-11
KCNS1	-1.93932797	8.14E-17
A2ML1	-1.940602009	2.65E-12
SCGB3A2	-1.940710385	5.40E-15
RPS20P14	-1.941965016	4.61E-61
RNF182	-1.946226152	3.31E-23
AC011479.1	-1.949520937	7.88E-26
KCNN4	-1.949647617	2.56E-37
ZIC1	-1.951187325	1.06E-11
AC245041.1	-1.957315625	4.30E-11
EEF1G	-1.963496203	3.88E-64
SLC22A31	-1.964385767	8.35E-16
RAET1L	-1.966106713	3.34E-11
SCX	-1.969967003	1.83E-40
LINC02159	-1.970237253	6.73E-13
FTCD	-1.972683921	9.34E-26
CALCB	-1.972686051	1.01E-11
LINC02538	-1.972788442	9.58E-17
RARRES1	-1.973282915	2.80E-24
GJB3	-1.973596732	3.95E-17
FCER2	-1.97406555	2.07E-14
KCNQ4	-1.976501257	1.03E-30
KCNE5	-1.977431476	4.48E-23
MTCO1P53	-1.980950508	2.36E-20
AC011270.2	-1.987870745	2.59E-10
INA	-1.988468212	7.21E-13
OOEP	-1.992649494	3.55E-12
LMO1	-1.993016977	8.54E-13
BLOC1S5-TXNDC5	-1.995160513	2.39E-42
AP002800.1	-2.005036445	4.15E-26
FAM131C	-2.009065872	1.61E-21
ODAM	-2.010230568	8.12E-10
NKX1-2	-2.015053197	7.50E-08
KRT75	-2.015607804	3.07E-11
FOXC1	-2.021928186	7.71E-26
PRAC2	-2.022986179	2.41E-08
PGPEP1L	-2.025759938	1.61E-14

TCAM1P	-2.030721833	2.97E-13
CDKN2A	-2.032224061	1.03E-34
TDRD12	-2.032662206	2.45E-19
CXCL5	-2.033667779	1.03E-14
AC022509.1	-2.041913776	8.79E-18
AC004233.2	-2.046117719	4.80E-18
NPM2	-2.0476909	3.19E-36
AL033384.1	-2.047741385	1.07E-21
OLIG1	-2.048274932	2.88E-12
POLR2F	-2.048302028	2.56E-21
ANKRD35	-2.049156321	1.39E-40
IGKV1D-27	-2.061093732	3.03E-10
LOXL4	-2.063159017	5.72E-36
SOSTDC1	-2.06357656	2.28E-17
PRKAG3	-2.067865235	6.71E-14
TLX1	-2.070727791	4.25E-11
UCHL1	-2.074167262	6.42E-32
IDO1	-2.079125044	6.20E-26
ACP7	-2.080474718	5.97E-15
MCRIP2P1	-2.081963313	1.79E-21
IGLV9-49	-2.086489465	2.83E-15
AC061975.6	-2.086783394	3.78E-15
ERICH5	-2.089191738	1.03E-16
SLC22A16	-2.09217338	3.70E-22
PRSS3	-2.094607512	3.89E-18
MARCO	-2.095489695	1.87E-18
KLK14	-2.098667776	7.37E-22
SPRR3	-2.099032065	7.73E-07
PRR18	-2.103721351	1.11E-15
IRX1	-2.107109078	9.80E-22
RPL21P16	-2.10712191	1.55E-50
PTX3	-2.107356221	1.88E-22
AL590326.1	-2.107883143	1.14E-33
SLC26A9	-2.110336776	5.00E-15
SAA1	-2.111698836	6.24E-24
AC016735.1	-2.112011198	7.16E-16
LEFTY2	-2.112090255	2.09E-20
NOL4	-2.114280639	2.83E-15
SAA2-SAA4	-2.11431565	3.97E-17
MAGEA3	-2.118333289	0.002436233
NOTUM	-2.120727724	7.15E-28
HTR3A	-2.122494559	1.10E-15

CHI3L1	-2.126046565	7.50E-26
ALX3	-2.127305402	8.62E-14
C5orf66-AS1	-2.128916789	7.98E-16
PKP1	-2.128960652	2.78E-22
NPW	-2.135631042	1.09E-22
IGKV2-29	-2.143262043	8.44E-10
AC026403.1	-2.144688987	3.51E-56
PGLYRP4	-2.144792779	2.78E-12
CDH19	-2.148251956	6.63E-09
ANXA8	-2.153868955	3.35E-19
ANKRD1	-2.154320076	1.76E-22
FOLR1	-2.15472592	3.20E-16
SHC4	-2.155821929	3.75E-21
AC027031.2	-2.15834674	9.75E-45
KRT86	-2.163819569	1.04E-25
AMN	-2.168798425	5.89E-31
AC006058.1	-2.172175332	3.97E-20
OR2S1P	-2.172402497	1.06E-19
IL34	-2.178572301	6.72E-44
ISL2	-2.178803778	9.42E-16
LINC01819	-2.180063979	1.33E-18
CAPN6	-2.192932203	5.16E-18
FMO6P	-2.208856509	3.33E-14
KRTDAP	-2.212373585	2.14E-22
PRR27	-2.213378979	0.00122195
OPRK1	-2.215597816	4.70E-13
PCDH8	-2.216238952	5.41E-15
EPHX3	-2.224799819	2.86E-35
IGLV3-9	-2.227807441	1.50E-19
SERPINB7	-2.22834817	5.02E-19
S100A1	-2.231946913	1.80E-25
DUSP9	-2.233211404	4.11E-21
HORMAD1	-2.238640057	9.80E-12
COL9A1	-2.238888976	1.39E-16
DDN	-2.241409199	1.61E-27
AC245041.2	-2.244309134	6.04E-20
IGSF23	-2.245296156	4.89E-18
IGHV3-73	-2.248356286	3.40E-19
BLACAT1	-2.252707392	5.22E-20
UGT2B7	-2.255555051	2.92E-13
WNT10A	-2.258176607	6.11E-44
CSAG3	-2.268515188	1.50E-07

AL390755.1	-2.269231491	1.40E-21
LINC02437	-2.270320088	2.99E-10
ALDH3A1	-2.27486727	2.24E-31
TRPM8	-2.281201765	7.39E-21
CAMKV	-2.288522874	1.38E-14
KRT5	-2.288614921	8.71E-21
IGF2BP3	-2.291937387	2.62E-22
GATA6-AS1	-2.294870519	2.75E-29
MAL	-2.301426266	7.71E-36
LINC01554	-2.309045635	3.92E-31
DEFB1	-2.315102735	1.33E-23
SERPINB2	-2.316530768	1.44E-18
FABP7	-2.319140047	3.96E-12
LINC02188	-2.319601222	1.85E-15
DLX6-AS1	-2.32116492	1.07E-16
PROK1	-2.325882508	1.61E-19
LINC00092	-2.326135834	6.74E-24
DNAH17-AS1	-2.327933442	1.03E-21
AC020907.1	-2.339877396	1.44E-24
SYCE1L	-2.343142062	1.78E-53
SPIB	-2.346852995	8.31E-31
GAL	-2.347656777	9.19E-26
GABRG3	-2.355783007	1.34E-13
PNMA3	-2.364004721	5.13E-30
NDUFB4P11	-2.366176296	1.44E-14
MTND1P23	-2.366554953	9.73E-14
LINC00668	-2.373123683	4.21E-09
GABBR2	-2.380745192	1.49E-13
NKX2-5	-2.394052608	1.86E-10
GSTA1	-2.3953683	6.64E-16
PCSK1N	-2.398703948	3.51E-20
SCGB3A1	-2.406546747	1.36E-19
ACTG2	-2.413176812	6.65E-29
FGFBP2	-2.416446652	5.10E-31
MPZ	-2.422173507	4.45E-48
ORM2	-2.423692403	5.59E-16
AC024940.2	-2.432146332	6.50E-25
BPI	-2.45334746	5.43E-29
CXCL1	-2.453546374	9.51E-29
SLC6A15	-2.458007715	9.72E-13
FSD1	-2.459297517	1.00E-29
CA6	-2.464315676	6.94E-13

EMILIN3	-2.464361235	6.85E-28
ACTBP12	-2.474517668	1.23E-15
PPP1R14C	-2.493088593	2.00E-25
ANXA8L1	-2.493136547	1.17E-27
DNER	-2.502753892	2.29E-22
C8orf46	-2.504720824	5.12E-35
FBN3	-2.518041137	2.91E-25
KRT16P6	-2.519082008	6.30E-21
SMOC1	-2.525031268	7.58E-31
CHGA	-2.53376521	2.26E-13
MMP7	-2.53451967	1.33E-30
S100B	-2.546580469	3.06E-37
FGFBP1	-2.550334396	8.53E-14
CLEC2L	-2.552411062	2.10E-32
LINC02515	-2.557000497	4.59E-28
CRYAB	-2.557599392	1.95E-46
ABCA13	-2.565643126	3.11E-19
GDF5	-2.565647919	1.72E-32
KRT17	-2.590628516	1.07E-30
HOXD13	-2.591321024	8.23E-30
SCEL	-2.597218664	5.41E-16
OLFM4	-2.602780326	1.91E-20
PICSAR	-2.616189314	1.27E-25
MATN4	-2.616530629	6.48E-37
HILS1	-2.617775065	1.30E-26
IVL	-2.62048324	4.82E-14
IGLVI-70	-2.622284764	1.06E-19
MAPK4	-2.62446974	3.52E-24
C2orf71	-2.636508796	3.31E-18
NTS	-2.646868504	5.69E-11
KLHL34	-2.652807834	5.04E-22
OCA2	-2.662105478	1.77E-20
GFRA3	-2.671927051	1.28E-29
DSG3	-2.685762778	1.17E-21
LGALS7B	-2.687139206	3.04E-26
MMP20	-2.688078052	1.38E-16
ANTXRL	-2.6954346	3.75E-24
DLX5	-2.703316918	1.02E-46
ALX1	-2.721664513	5.05E-22
ALKAL2	-2.729581497	2.58E-30
CMTM5	-2.735625715	7.34E-25
LINC00707	-2.743607517	7.21E-18

SH3GL3	-2.761893445	5.32E-26
POMC	-2.769013842	1.54E-55
CALML5	-2.774344035	1.66E-22
GJB6	-2.77822838	6.31E-22
SLPI	-2.783099418	1.17E-32
MTCO1P40	-2.784172315	5.59E-28
TNNI2	-2.786758617	1.19E-69
SLURP1	-2.787151125	1.64E-20
KIRREL3-AS1	-2.792928493	4.65E-13
ACTL8	-2.794431894	5.46E-17
SLC6A2	-2.802327448	9.68E-21
LCN2	-2.808366236	4.60E-31
CRABP1	-2.821132612	2.27E-21
AMTN	-2.821556896	4.29E-17
GABRA5	-2.833449377	4.23E-17
LEMD1	-2.835295178	2.00E-22
CT83	-2.838612912	2.04E-05
GABRP	-2.838731928	1.26E-25
FAM19A3	-2.841521882	7.28E-39
BARX1	-2.849043929	7.82E-30
SCRG1	-2.858595565	2.75E-35
DSG1	-2.877020616	5.22E-24
CRHR1	-2.883412681	2.35E-40
LINC01436	-2.903745328	1.25E-45
FDCSP	-2.910877112	3.63E-19
ROPN1B	-2.919907726	1.06E-31
ROCR	-2.923173406	1.13E-21
AC008514.1	-2.938103905	1.07E-44
C11orf86	-2.938261328	1.63E-13
AP000851.1	-2.946268496	1.47E-24
AC009041.2	-2.955303815	1.94E-61
FZD9	-2.965568871	2.72E-39
KLK7	-2.978552701	2.16E-26
KLK8	-2.990674834	7.65E-26
LINC01133	-2.993866434	1.45E-33
SMR3B	-3.009282677	4.96E-07
AQP5	-3.014632243	2.39E-25
COL11A2	-3.030609736	2.82E-57
SNORC	-3.046934817	7.52E-58
KRT9	-3.049311619	3.72E-30
C1QL4	-3.049584524	4.33E-39
RASGEF1C	-3.053574066	3.09E-42

LINC00284	-3.05532904	3.42E-35
KRT14	-3.056469287	3.53E-33
KCNG1	-3.066376148	1.20E-37
KLK10	-3.066573589	6.78E-31
PSAPL1	-3.077618714	2.34E-09
DLX6	-3.080246861	8.60E-28
ROPN1	-3.081122207	1.74E-19
SPRR1B	-3.085215448	6.57E-13
FAM3D	-3.126461083	4.33E-44
LINC01198	-3.132543076	7.55E-18
WIF1	-3.141826823	2.13E-23
SYT8	-3.185852435	1.30E-42
AP001783.1	-3.209996149	1.93E-25
AC005863.1	-3.245643374	6.18E-22
CLDN6	-3.252864456	1.04E-46
ETV3L	-3.253951439	4.04E-33
LINC01606	-3.27162096	9.07E-15
VAX1	-3.281943557	2.76E-13
LINP1	-3.282797286	1.77E-18
KRT83	-3.287520129	5.77E-38
LINC00518	-3.309315013	2.06E-18
LIN28B	-3.311532967	1.93E-09
COL9A3	-3.325471684	6.79E-60
SLC15A1	-3.326759367	8.10E-34
AC245884.9	-3.334420824	3.55E-33
HRCT1	-3.334966233	9.07E-66
C1QL2	-3.364584518	1.01E-27
KLK5	-3.376094045	1.57E-33
MIA	-3.3976182	2.02E-38
KRT6B	-3.428078901	7.71E-42
PSORS1C2	-3.434343172	1.68E-44
AC103702.2	-3.442611718	8.80E-41
WNT6	-3.468693837	5.59E-56
RHCG	-3.475724297	2.48E-43
S100A2	-3.490669173	2.02E-55
POU4F1	-3.497103415	1.78E-24
KRT16	-3.519693487	1.13E-38
CASC8	-3.52227807	1.14E-49
AC022784.1	-3.524303942	9.13E-31
GPR12	-3.525432218	3.05E-30
KRT6C	-3.553475612	1.29E-33
SERPINB4	-3.569616318	2.25E-14

FOXCUT	-3.573694585	1.46E-27
LINC01956	-3.601160854	4.04E-33
TTYH1	-3.613413037	2.20E-57
EN1	-3.629408925	6.99E-69
CSN3	-3.658094346	3.29E-08
LINC01667	-3.701925411	1.91E-14
LINC02487	-3.710795152	5.57E-40
RGR	-3.729520973	2.01E-27
C6orf15	-3.733716087	1.21E-41
DMRTA2	-3.77737067	6.61E-32
SERPINB3	-3.784610443	8.21E-13
CCKBR	-3.819045194	1.22E-27
MAGEB4	-3.873900414	6.72E-20
KRT4	-3.881627729	1.74E-31
KRT79	-3.894317354	2.82E-57
SOX8	-3.917237093	1.30E-70
SBSN	-3.944655123	6.38E-40
LY6D	-3.956625942	3.98E-34
PRDM13	-3.96665797	1.67E-16
KLK6	-4.00820086	4.94E-44
VGLL1	-4.032266052	2.17E-39
KRT6A	-4.091676784	3.75E-42
TLX3	-4.146659304	2.99E-15
PI3	-4.221656889	5.03E-53
ZFP42	-4.258088152	6.36E-26
KRT81	-4.438235011	4.58E-59
AC092916.1	-4.523064096	4.41E-09
ART3	-4.548817957	1.17E-51
NFE4	-4.720296758	3.77E-53
MSLN	-4.736845622	4.45E-73
XAGE2	-4.753292691	1.45E-17
PRSS33	-4.940848288	3.40E-35
NCAN	-4.942928184	3.06E-58
MAGEA4	-4.946163533	6.54E-17
LINC00393	-5.212596634	4.04E-28
AL161431.1	-5.374418102	1.11E-27
CARTPT	-5.490622332	3.10E-17
AC013457.1	-5.606366127	1.77E-26

Table 33. hPRLrL hi versus med/lo DEGs. TCGA-BRCA patients were stratified by hPRLrL status, being high or medium/low expressors (top versus middle/bottom tertiles, respectively), as determined by RNAseq analysis.

Gene symbol	Log2(Fold change)	padj
SCARNA5	5.444801	1.98E-67
SNORA74B	4.667222	8.69E-42
SCARNA10	4.626228	6.13E-51
SNORA23	4.233904	9.45E-42
LACRT	4.218039	1.37E-15
SNORA74A	4.042218	1.27E-20
SCARNA6	3.853932	6.69E-57
RNU4-2	3.610939	3.86E-35
RNVU1-7	3.29384	2.10E-22
AC061961.1	3.271079	1.85E-16
SLC30A8	3.099149	1.45E-20
KCNH1	2.915615	5.52E-47
SNORA73B	2.913669	4.86E-36
RF00100	2.908019	1.15E-30
CPB1	2.743423	1.31E-12
SNORD17	2.601085	1.01E-32
AC079414.2	2.594994	2.21E-07
AC093292.1	2.574103	3.13E-06
SNORD15B	2.562731	6.09E-27
AL450996.1	2.549418	4.73E-17
SCARNA13	2.539205	1.06E-34
KLHL1	2.506877	0.0003
SPANXB1	2.502123	1.14E-09
RNU4-1	2.501446	2.27E-17
AC093297.1	2.484107	2.19E-10
AC114786.2	2.44821	0.002592
SCARNA21	2.427873	6.59E-18
CYP2A6	2.358223	2.61E-13
CACNG6	2.342304	1.59E-10
TRPA1	2.334707	6.30E-20
RN7SL314P	2.329359	5.29E-15
PGAM1P5	2.321156	6.30E-31
PWAR5	2.26033	1.19E-39
SCARNA7	2.253239	3.85E-19
AL035425.3	2.249113	1.49E-10
NDST4	2.246636	4.34E-08
KCNJ3	2.23649	4.28E-11

OR4K12P	2.230939	1.06E-07
AC092881.1	2.168663	1.38E-36
NLRP5	2.147251	3.04E-08
ZBED6	2.091917	8.29E-43
GNAQP1	2.083938	2.80E-25
GLRA3	2.078866	1.26E-09
ACER2	2.069122	5.39E-68
SPATA46	2.068076	5.84E-24
AC124312.2	2.06741	1.15E-31
RN7SL674P	2.058273	3.64E-20
AL021068.2	2.056465	2.44E-35
HSPD1P11	2.048776	2.05E-20
DCD	2.034569	2.97E-05
AL132708.1	2.023871	4.37E-12
AC018752.1	2.002868	8.90E-41
CDH7	1.999918	5.56E-12
GPR139	1.997654	3.83E-06
IPO8P1	1.988999	1.00E-36
RAD17P1	1.981856	1.34E-15
AP000560.1	1.976533	1.45E-40
CYP2G1P	1.952715	2.36E-12
GRAMD4P8	1.936052	3.68E-14
AC253536.3	1.932599	1.20E-35
AC073525.1	1.929941	8.78E-05
SLC4A10	1.925441	6.69E-15
ERVW-1	1.910181	1.07E-29
TMC3	1.900225	7.48E-14
AC020951.1	1.890661	3.88E-29
CLSTN2	1.889458	1.89E-20
KLHL11	1.885738	9.32E-53
RF00019	1.883004	2.94E-10
LINC02302	1.869835	1.11E-05
CSN1S1	1.855461	0.000248
ACTG1P22	1.849411	5.21E-09
LRP1B	1.839265	6.98E-12
SORCS1	1.82916	1.60E-11
CLVS2	1.825987	3.99E-08
AC090206.1	1.82414	1.77E-19
PCDHA13	1.806786	6.23E-14
CSMD3	1.802267	2.38E-06
AC096733.2	1.799888	8.10E-33
HNRNPA1P57	1.795817	3.91E-07

AC073508.1	1.789332	1.85E-07
POTEC	1.787762	0.000123
RNU6-813P	1.786594	1.22E-07
AC093838.1	1.771254	1.53E-09
AC144450.1	1.768461	1.12E-24
AL512785.2	1.736275	2.69E-25
ZNF209P	1.733928	5.10E-10
PRLR	1.732258	7.79E-65
NELL1	1.727023	8.44E-06
RP1	1.725162	6.27E-14
AC124312.3	1.723578	7.32E-27
ALB	1.717201	2.56E-12
GRPR	1.712678	1.20E-11
ELOVL2	1.710139	2.35E-14
AC099677.1	1.708443	2.25E-32
PTHLH	1.694637	1.29E-18
ZPLD1	1.685466	4.16E-12
CRYZP1	1.684492	2.21E-31
LRRC37A9P	1.683664	1.69E-23
AC092979.1	1.676903	0.000302
ZNF729	1.671602	1.49E-05
SLC5A7	1.670201	8.25E-06
NOS1AP	1.665998	1.36E-36
HIST1H2AI	1.665138	9.88E-16
AL021068.1	1.65898	1.15E-39
MKX	1.656769	2.62E-12
CYP4Z1	1.650753	7.89E-08
ANKRD30A	1.650673	9.26E-09
HOXB-AS2	1.64848	2.17E-13
SYT1	1.644393	6.50E-13
AC010735.1	1.639816	5.89E-18
LINC00052	1.633958	0.000114
AC087286.2	1.632436	8.34E-21
AC079296.1	1.623672	1.82E-08
ITPR1	1.617912	1.70E-37
ZNRF2P2	1.613441	7.48E-34
AP005131.1	1.608226	8.57E-22
CCDC144A	1.606734	1.49E-12
ESRRG	1.605653	9.17E-17
FER1L6	1.604314	1.40E-13
HTR1F	1.601474	6.78E-24
AC002064.2	1.599839	9.48E-16

AFF3	1.596451	3.29E-18
AC016590.2	1.596104	3.96E-25
TRIM58	1.590898	5.25E-17
SLC16A12	1.589476	1.38E-14
AL136164.3	1.582132	1.53E-17
VN1R53P	1.581579	8.31E-08
GTF2IP7	1.580561	6.03E-22
AC010522.1	1.579941	3.68E-36
AL354984.2	1.57967	0.000263
LINC02197	1.573708	0.000401
LINC01522	1.572398	1.08E-09
RAB11FIP1	1.553058	3.55E-29
CST5	1.526454	0.000366
ACMSD	1.519733	3.90E-11
ADGRV1	1.512912	2.89E-14
STC1	1.512704	3.67E-18
CLEC3A	1.509161	0.001863
EML5	1.508343	3.25E-16
BMPR1B	1.502968	2.11E-08
GALNT4	1.501789	3.46E-29
CALB2	-1.5015	1.07E-11
GABBR2	-1.50559	6.08E-06
OXER1	-1.50836	2.39E-29
AC091078.1	-1.50847	4.88E-08
KISS1	-1.51042	5.62E-16
KIF19	-1.51325	8.34E-16
MUC5AC	-1.51661	5.43E-06
CARD17	-1.51792	3.20E-10
S100A3	-1.52283	2.58E-32
AC021683.1	-1.52427	1.66E-12
TM4SF4	-1.53064	9.20E-12
AC246787.1	-1.53121	2.76E-50
TEX15	-1.53141	9.89E-05
FCAMR	-1.53397	1.71E-08
ELF5	-1.53421	1.94E-08
MSLNL	-1.53642	2.81E-09
LINC00511	-1.53738	1.29E-18
FMO6P	-1.53801	7.79E-08
CRYAB	-1.54025	2.29E-15
AMTN	-1.54146	4.81E-06
FSD1	-1.5421	8.08E-11
AC004687.1	-1.54358	9.60E-20

PCP4L1	-1.54453	7.47E-12
XKR4	-1.54545	9.77E-13
LINC00896	-1.54584	2.53E-16
IGF2BP3	-1.54628	4.93E-10
EEF1G	-1.54828	1.45E-40
SAA2-SAA4	-1.54891	7.27E-10
ODAM	-1.55077	1.57E-06
AC021087.4	-1.55094	9.82E-12
SYT8	-1.55213	3.61E-10
AIM2	-1.55287	6.58E-18
CLDN6	-1.55307	8.13E-10
SCX	-1.55581	2.04E-26
TCEAL2	-1.55621	1.51E-11
KLF14	-1.5563	1.09E-17
NLRP7	-1.55844	7.87E-12
LINC00964	-1.56023	4.90E-13
NPM2	-1.56203	2.84E-20
AC067735.1	-1.56225	5.47E-22
TRPV3	-1.56385	6.23E-17
UCHL1	-1.56468	1.34E-16
LINC00393	-1.56483	0.007731
IRX1	-1.56587	2.08E-12
AC009902.3	-1.56682	1.38E-17
PRKAG3	-1.56716	2.72E-08
PRKCQ-AS1	-1.56743	9.82E-19
SPINK5	-1.56895	1.61E-13
AC009041.2	-1.56978	3.97E-15
TCF15	-1.57088	5.95E-23
CCNE1	-1.57131	6.40E-22
ISL2	-1.57204	7.14E-09
COL22A1	-1.57234	1.06E-15
KRT31	-1.57809	1.11E-07
DPP10-AS1	-1.57857	0.002199
POPDC3	-1.57879	1.86E-11
CASP1P2	-1.5801	4.14E-15
RAET1L	-1.58584	9.25E-08
AC025183.1	-1.58691	1.54E-09
RAPSN	-1.59017	4.78E-20
KLK13	-1.5903	4.77E-09
UGT2B7	-1.59175	5.94E-07
SULT1E1	-1.59286	9.72E-07
SIX3-AS1	-1.59424	1.13E-05

AC239800.2	-1.59446	7.11E-12
PGPEP1L	-1.59614	3.59E-09
KIRREL3-AS1	-1.59912	7.17E-05
BBOX1	-1.60039	8.51E-13
LINC01133	-1.60044	1.18E-08
CD70	-1.60084	1.86E-22
BLOC1S5-TXNDC5	-1.60159	5.01E-25
CD79B	-1.61211	7.46E-22
AC079922.1	-1.6165	9.37E-46
MCRIP2P1	-1.61917	1.86E-14
CRISP2	-1.61921	6.64E-06
CXCL5	-1.61995	2.89E-09
RGS20	-1.62036	1.24E-17
AC023983.2	-1.62182	9.23E-21
CCL18	-1.62393	3.43E-13
S100A7	-1.6249	8.30E-05
DDC	-1.62521	2.15E-09
ARL9	-1.62544	6.25E-19
AC022784.3	-1.6264	6.13E-16
MAGEC2	-1.62662	0.007069
LINC01508	-1.62712	1.89E-10
POU4F1	-1.62724	3.56E-05
LINC02473	-1.62748	8.74E-12
NMU	-1.62993	2.49E-13
GABRE	-1.63142	1.91E-16
BPI	-1.63452	3.43E-11
PNLDC1	-1.63587	3.42E-17
AC011479.1	-1.63859	2.06E-17
RPL21P16	-1.63873	1.99E-29
LINC02532	-1.64004	4.97E-11
LTB	-1.64103	1.63E-19
SOX15	-1.64339	1.30E-19
TMCC2	-1.64358	8.00E-23
SMTNL2	-1.64406	1.01E-15
CTSV	-1.64583	8.79E-24
GATA6-AS1	-1.64738	7.08E-17
HOXD13	-1.65009	7.01E-12
MTCO1P53	-1.6508	1.54E-14
AC020907.1	-1.65149	1.30E-11
GPR87	-1.65192	6.57E-14
RPS20P14	-1.65473	3.43E-42
TMPRSS5	-1.65476	2.53E-17

PLA2G4E	-1.65653	6.04E-08
KRT5	-1.65683	8.31E-11
SCG3	-1.6577	3.12E-11
GAPDHP1	-1.65987	2.54E-19
CHRDL2	-1.66085	1.37E-17
FOXC1	-1.66153	9.32E-17
CD19	-1.66584	1.01E-13
DNER	-1.67202	9.19E-10
BNC1	-1.67404	2.85E-13
DMKN	-1.6754	3.71E-23
CASC9	-1.67645	9.95E-05
CLDN16	-1.67826	4.14E-14
LINC01819	-1.68087	3.25E-11
CCER2	-1.68093	8.96E-26
NOTUM	-1.68176	2.14E-19
IGFL2-AS1	-1.68443	8.11E-11
LINC02515	-1.68641	7.64E-12
MT1H	-1.68665	6.62E-14
AP001505.1	-1.68792	6.09E-44
PSCA	-1.69134	8.61E-13
TLX1NB	-1.69355	2.40E-07
LINC01198	-1.6949	1.60E-05
COL9A1	-1.69502	7.21E-09
KRT83	-1.69619	5.39E-09
NCAN	-1.69733	1.16E-06
AL022334.1	-1.69752	9.14E-12
DLX5	-1.69963	2.23E-16
OR7E62P	-1.70271	1.51E-10
UGT2B28	-1.7042	9.05E-06
CLDN9	-1.70455	8.11E-20
TNNI2	-1.70584	1.40E-21
TLX1	-1.70691	3.23E-07
CCL20	-1.70826	6.14E-18
TTYH1	-1.71099	1.17E-11
TGM1	-1.71135	1.07E-31
SERPINB2	-1.71345	5.81E-10
TMEM171	-1.71385	3.84E-19
CASP14	-1.71792	8.07E-06
AC090589.1	-1.71894	2.49E-24
AC245041.1	-1.72118	1.21E-08
CLLU1OS	-1.72173	1.57E-09
IL34	-1.724	1.62E-28

P2RX5	-1.72501	3.35E-21
CHI3L1	-1.72583	3.63E-18
PRR18	-1.72826	3.44E-11
PPP1R14C	-1.72907	1.85E-12
MMP20	-1.73159	9.90E-09
MTCO3P22	-1.73345	9.72E-15
DLX6	-1.73551	1.35E-08
AC092118.1	-1.73573	2.35E-15
SH3PXD2A-AS1	-1.736	5.62E-18
AC009902.2	-1.73605	8.74E-19
SCRG1	-1.73691	2.66E-11
FOSL1	-1.74182	6.77E-26
EPHX3	-1.74519	1.47E-21
CALCB	-1.74589	1.50E-09
HPDL	-1.7473	1.87E-17
KRT6B	-1.75855	6.88E-10
AC022509.1	-1.75944	1.07E-13
ABCA13	-1.76015	4.29E-09
FAM131C	-1.76083	8.08E-18
ALX3	-1.76151	2.59E-09
RARRES1	-1.76797	5.28E-18
U62317.2	-1.76868	3.31E-25
FTCD	-1.76916	3.42E-20
BCHE	-1.7702	9.90E-18
CPA4	-1.77035	8.50E-17
CRHR1	-1.77176	1.20E-14
SLC6A15	-1.77329	4.07E-07
TSKS	-1.77469	1.44E-24
AC046168.1	-1.77631	1.91E-18
SFN	-1.77661	3.19E-34
SLC22A16	-1.77692	4.36E-16
LINC01781	-1.77734	5.42E-12
ALKAL2	-1.78748	4.77E-14
SIX3	-1.78807	1.82E-10
DDN	-1.79319	1.12E-16
KRT14	-1.79483	6.66E-12
RETN	-1.79626	5.12E-18
AL390729.1	-1.79693	1.30E-24
CERS3	-1.79911	2.63E-17
NPW	-1.79973	3.89E-15
CHI3L2	-1.80128	5.88E-17
SAA4	-1.80393	2.14E-16

SLC28A1	-1.80541	1.65E-17
WNT10A	-1.80594	3.02E-24
CHST4	-1.8168	1.15E-13
VPREB3	-1.82489	8.81E-23
OCA2	-1.82607	1.40E-09
ANXA8L1	-1.82766	3.69E-15
FABP7	-1.82823	7.05E-08
CAPN6	-1.83099	7.39E-13
WFDC21P	-1.83237	1.65E-20
AC021504.1	-1.84103	2.25E-07
MIA	-1.84206	1.32E-12
LINC01554	-1.85037	1.44E-16
S100A1	-1.85608	2.63E-18
KRT9	-1.8601	1.10E-10
C7orf61	-1.86298	6.45E-37
POMC	-1.86691	5.41E-26
CXCL1	-1.86951	2.69E-17
KLK11	-1.87659	1.41E-09
IL1R2	-1.87703	1.12E-24
FGFBP2	-1.8786	1.79E-19
PKP1	-1.8797	3.98E-16
CHODL	-1.88582	1.70E-17
PCDH8	-1.88599	1.78E-11
U62317.1	-1.88804	7.29E-15
FOLR1	-1.88933	1.64E-13
GJB5	-1.89215	8.12E-17
AC027031.2	-1.89566	5.52E-30
ERICH5	-1.89844	1.95E-15
NT5DC4	-1.89911	4.92E-25
HS3ST6	-1.90345	3.53E-10
RSPO4	-1.90424	2.10E-17
BAIAP2L2	-1.90492	1.24E-36
MARCO	-1.90887	1.51E-15
PRR27	-1.91219	0.006175
KLK12	-1.91544	5.78E-08
MIMT1	-1.9173	1.25E-10
DEFB1	-1.92075	1.49E-15
FOXG1	-1.92519	5.42E-07
PGBD5	-1.93226	1.12E-22
ROPN1B	-1.9332	1.00E-12
NKX2-5	-1.94194	3.95E-07
CLEC2L	-1.94231	1.28E-16

FDCSP	-1.94366	9.76E-10
AC026403.1	-1.94472	8.87E-45
SMOC1	-1.94546	5.08E-19
P2RX2	-1.94561	2.30E-12
LINC00092	-1.947	6.15E-17
GSDMC	-1.95022	5.89E-21
MPZ	-1.95088	1.66E-27
AC133785.1	-1.95192	2.18E-12
BCAR4	-1.95197	9.64E-10
AC103702.2	-1.95337	1.79E-12
NKX1-2	-1.95471	3.94E-08
PCSK1N	-1.95731	9.64E-14
TFF2	-1.96696	1.48E-11
HILS1	-1.96993	7.86E-17
MAL	-1.97254	1.97E-24
CDKN2A	-1.97773	1.31E-30
ROCR	-1.98042	1.26E-10
ACE2	-1.9815	2.54E-16
AP002800.1	-1.98829	1.32E-22
AC008592.5	-1.99456	7.34E-16
AMN	-1.99947	1.05E-25
AFAP1-AS1	-2.00043	1.05E-11
HTR3A	-2.00363	1.30E-13
OPRK1	-2.00397	5.56E-09
BLACAT1	-2.01104	9.64E-17
ANXA8	-2.01399	5.67E-17
SYCE1L	-2.01828	6.97E-34
SOX8	-2.01917	3.11E-16
GJB3	-2.02386	1.05E-16
AP005233.2	-2.02838	4.16E-12
UPK1B	-2.03371	2.11E-09
CSAG1	-2.03633	1.43E-08
PNLIPRP3	-2.03697	0.000206
AL109761.1	-2.04141	7.57E-15
LINC02159	-2.04156	8.33E-14
AL592429.1	-2.04655	5.52E-16
PRSS3	-2.04836	9.41E-17
CMTM5	-2.05378	2.79E-14
LMO1	-2.05401	8.17E-14
OLAH	-2.06202	1.42E-14
AC245041.2	-2.0623	1.67E-18
DUSP9	-2.06277	2.25E-16

NDUFB4P11	-2.0711	2.15E-12
FZD9	-2.07397	1.32E-18
PICSAR	-2.07659	5.08E-17
GFRA3	-2.08361	2.39E-16
FABP5	-2.0852	1.52E-41
MTCO1P40	-2.09073	8.59E-16
CRISP3	-2.0918	9.48E-11
CRYBA2	-2.09211	8.12E-15
KLK14	-2.09706	4.00E-22
SLC39A2	-2.09824	2.61E-27
KRT86	-2.09831	1.03E-27
SNORC	-2.0995	5.30E-30
SMR3B	-2.10545	2.57E-05
AC011270.2	-2.10681	1.53E-11
C1QL4	-2.12054	3.30E-17
AC004233.2	-2.12221	4.61E-20
LEMD1	-2.12914	4.20E-13
SPIB	-2.13188	5.24E-23
NIPAL4	-2.1321	2.57E-22
GAL	-2.14821	1.49E-21
ROS1	-2.14888	2.14E-13
SPRR1A	-2.15163	1.89E-07
AC092484.1	-2.16492	8.65E-13
KCNE5	-2.16657	1.32E-24
LCN2	-2.16799	1.94E-18
AC024940.2	-2.17025	8.46E-19
SLC6A2	-2.1757	2.01E-13
ERN2	-2.17884	1.61E-15
AC061975.6	-2.18942	2.89E-14
KLK7	-2.1899	8.03E-14
DNAH17-AS1	-2.19725	3.33E-19
LINC01297	-2.19886	5.79E-06
SLC22A31	-2.20234	5.06E-23
ROPN1	-2.20586	1.45E-10
AC016735.1	-2.20977	1.42E-16
CA6	-2.23139	2.16E-11
CALML5	-2.2581	1.99E-14
ORM1	-2.27256	6.57E-13
MMP7	-2.27368	8.12E-25
KRT16P6	-2.28142	1.34E-15
GABRP	-2.2878	2.77E-17
RIPPLY2	-2.28892	2.13E-07

C8orf46	-2.29425	1.55E-30
ACP7	-2.30384	5.91E-17
TLX3	-2.30739	3.09E-05
LINC02437	-2.31275	1.73E-10
FABP5P7	-2.32661	2.49E-35
SLPI	-2.32859	2.99E-26
A2ML1	-2.33215	2.57E-16
IL36RN	-2.33284	1.69E-11
FGFBP1	-2.33594	9.80E-13
CT83	-2.3438	0.001836
DMRT1	-2.34905	1.67E-11
LINC01436	-2.34946	4.13E-27
AP000851.1	-2.36459	4.48E-17
S100A8	-2.37595	7.64E-20
PHF24	-2.37648	3.54E-32
MAGEB1	-2.37896	8.25E-06
NCCRP1	-2.37962	3.15E-20
KCNG1	-2.38027	5.78E-23
RNF222	-2.38341	1.91E-26
SERPINB7	-2.39116	7.60E-20
HORMAD1	-2.39263	5.61E-13
CCNYL2	-2.40674	2.56E-14
TDRD12	-2.41093	8.39E-29
KLHDC7B	-2.41114	2.75E-31
ALDH3A1	-2.41279	1.03E-31
MATN4	-2.42681	2.28E-29
UPK2	-2.43647	6.59E-42
ORM2	-2.44881	1.61E-18
HRCT1	-2.47447	5.09E-32
KLHL34	-2.47712	1.99E-17
LINC00518	-2.48166	8.29E-12
LINC02538	-2.49894	2.52E-25
EN1	-2.50639	1.37E-27
AP001783.1	-2.5192	2.23E-13
SPRR3	-2.52946	5.72E-09
PSORS1C2	-2.55434	2.61E-27
KLK5	-2.55764	2.22E-18
FADS6	-2.55986	2.34E-19
ALX1	-2.56111	2.27E-18
GPR12	-2.57724	1.62E-18
ANTXRL	-2.58381	1.08E-21
AC008514.1	-2.60067	6.26E-35

LINC01956	-2.6086	1.02E-15
FOXCUT	-2.6102	2.26E-13
KRT81	-2.62864	2.06E-18
INA	-2.64813	4.81E-27
GJB6	-2.64976	2.89E-19
KLK10	-2.65449	2.58E-23
CAPNS2	-2.65486	1.28E-23
KRT16	-2.67445	2.97E-21
CAMKV	-2.67867	1.13E-21
TRIML2	-2.68052	2.65E-23
FAM19A3	-2.68079	1.64E-36
MAGEB4	-2.69065	7.96E-10
OLFM4	-2.69967	8.77E-20
RHEX	-2.70192	1.68E-36
IGSF23	-2.72071	1.51E-26
ART3	-2.7212	1.39E-17
S100A2	-2.7269	1.49E-33
DSG3	-2.73019	1.06E-22
AC245884.9	-2.73768	1.08E-21
MSLN	-2.78731	6.10E-22
PRDM13	-2.79757	6.86E-08
KRT6C	-2.80488	4.71E-19
WNT6	-2.80866	6.90E-37
SLC1A6	-2.82493	1.83E-19
CRABP1	-2.83531	7.60E-22
KRT78	-2.83623	6.82E-16
FAM3D	-2.8563	6.64E-35
LINC01606	-2.86195	8.02E-12
BARX1	-2.87917	3.61E-34
C6orf15	-2.88741	1.41E-24
AC092916.1	-2.88968	0.000179
KRT13	-2.90918	1.70E-21
PRSS33	-2.92052	4.80E-13
LINC01667	-2.94526	7.70E-09
CSN3	-2.94794	2.00E-06
SLURP1	-2.96966	2.45E-22
ETV3L	-2.97176	2.86E-27
RASGEF1C	-2.97199	1.67E-37
SLC26A9	-2.98716	9.19E-29
PI3	-3.00589	1.69E-28
CASC8	-3.01302	2.99E-34
LINC00284	-3.03415	1.91E-35

C1QL2	-3.04251	8.18E-25
SLC15A1	-3.06567	1.72E-27
KRT79	-3.07404	2.39E-31
KRT77	-3.10455	6.69E-15
ACTBP12	-3.10514	1.86E-28
VGLL1	-3.11453	6.89E-23
LGALS7B	-3.12882	1.78E-30
PGLYRP4	-3.13325	9.41E-25
VAX1	-3.15776	2.62E-11
RLBP1	-3.17375	1.15E-24
IVL	-3.18442	1.93E-18
NTS	-3.19588	6.36E-15
CCKBR	-3.19589	1.65E-19
KLK8	-3.20046	3.76E-27
LINC00668	-3.21208	1.64E-17
KRT4	-3.22634	1.47E-24
GABRA5	-3.23384	1.18E-22
TRPM8	-3.28119	1.19E-41
SCEL	-3.29005	5.71E-23
AC005863.1	-3.30098	2.85E-23
LINP1	-3.31669	5.81E-18
CARTPT	-3.34609	1.00E-06
RHCG	-3.35661	1.93E-38
AL161431.1	-3.37416	1.02E-10
KLK6	-3.48329	5.49E-32
RGR	-3.50372	3.30E-26
SPRR1B	-3.51177	4.55E-16
ACTL8	-3.52679	2.10E-28
ZFP42	-3.66597	4.12E-24
KRT6A	-3.72734	4.95E-36
LINC02487	-3.74023	3.00E-41
C11orf86	-3.82434	5.59E-24
SERPINB3	-4.06529	4.20E-16
LINC00707	-4.08422	1.75E-41
KRT1	-4.19559	9.67E-42
AC013457.1	-4.4964	1.13E-16
MAGEA4	-4.5677	3.91E-14
AC022784.1	-4.6129	2.45E-48
KRTDAP	-4.64202	1.50E-63
SERPINB4	-4.64389	9.91E-24
SBSN	-4.81371	4.74E-57
NFE4	-5.31993	1.73E-62

LY6D	-5.64088	2.19E-73
XAGE2	-6.55087	1.08E-30

Table 34. hPRLrL-hi/med versus lo DEGs. TCGA-BRCA patients were stratified by hPRLrL status, being high/medium or low expressors (top/middle versus bottom tertiles, respectively), as determined by RNAseq analysis.

Gene symbol	Log2(Fold change)	padj
SCARNA5	6.098468	1.86E-86
SNORA74B	5.762546	5.00E-61
SCARNA10	5.533184	1.19E-71
SNORA74A	5.062277	2.36E-34
SNORA23	4.860983	8.66E-55
RF00100	4.488428	2.19E-63
SCARNA7	4.460634	2.51E-55
SNORA73B	4.334746	1.35E-66
RN7SL3	4.23798	7.84E-52
RF00003	4.175752	3.11E-22
SNORD17	4.064118	6.19E-62
SCARNA21	3.924622	1.39E-39
SNORA12	3.795977	4.08E-42
RNVU1-7	3.639629	3.60E-25
AL355075.4	3.612377	1.78E-24
SNORD15B	3.433621	4.68E-42
SCARNA6	3.300074	2.19E-48
IRS4	3.268563	5.35E-20
AC064799.2	3.125312	4.09E-28
SCARNA13	2.780756	1.82E-40
LALBA	2.69733	0.000199
AF178030.1	2.695721	3.19E-31
SNORA53	2.642238	4.22E-33
THSD4-AS1	2.624452	2.94E-20
AL450996.1	2.544646	3.10E-20
CHRNA9	2.460841	1.86E-18
AC111000.4	2.450343	2.53E-07
PWAR5	2.447268	6.37E-44
AC115837.2	2.44527	2.37E-08
FGG	2.381333	1.07E-07
RN7SL2	2.365277	8.90E-31
AC093297.1	2.31923	1.64E-09
AF127577.6	2.291698	2.65E-23
AC092881.1	2.156533	6.52E-35
PGAM1P5	2.146528	1.11E-26
HIST1H4C	2.141262	5.43E-21
RN7SL674P	2.119837	2.23E-21

AC010368.1	2.109782	2.65E-42
HNRNPA1P57	2.097126	7.87E-10
KCNMA1-AS3	2.095471	1.44E-22
MKX	2.091134	2.12E-17
RN7SL4P	2.067059	3.78E-22
CPLX2	2.045791	1.88E-06
KCNMA1-AS1	2.025606	1.44E-22
SLIT1	2.02412	8.34E-22
SIDT1-AS1	2.015234	3.09E-21
MTCO1P28	1.999046	4.27E-20
ERVW-1	1.979339	2.68E-27
CDR1	1.977711	4.77E-15
AC093838.1	1.969498	1.18E-12
MIR2052HG	1.966639	8.33E-12
AC020951.1	1.961473	3.40E-29
CELF3	1.959055	8.98E-14
CPHL1P	1.93942	5.36E-15
RN7SL314P	1.937611	5.60E-12
CLVS2	1.929178	1.31E-08
AL136164.3	1.926164	5.24E-26
SLC4A10	1.905332	2.43E-15
STARD13-AS	1.902949	2.90E-20
AC018752.1	1.898455	4.95E-42
TLK2P2	1.897884	3.42E-28
RF00019	1.876344	1.05E-10
AC002064.2	1.86949	8.39E-20
PEX5L	1.864993	1.51E-15
AC093292.1	1.861507	0.0008
AC016590.2	1.860224	7.49E-34
AC124312.2	1.856909	2.44E-25
ANKRD30A	1.854937	4.56E-11
AL390860.1	1.851837	3.79E-18
OR4K12P	1.851668	7.21E-07
AGXT2	1.848401	2.42E-27
AL731892.1	1.846286	1.41E-11
GRIA1	1.840069	8.30E-11
AC008147.2	1.828993	3.12E-32
AP000560.1	1.824367	1.81E-34
AC126564.1	1.804732	2.17E-09
ZBED6	1.799325	3.34E-39
AL354733.2	1.788014	2.66E-28
GRAMD4P8	1.783723	4.06E-13

ANKRD20A11P	1.775831	7.02E-16
AC006441.1	1.77464	9.53E-23
HSPD1P11	1.771606	6.19E-19
AL136115.1	1.765829	2.26E-21
AC090181.3	1.76523	2.49E-27
AL035425.3	1.764435	1.41E-09
TMEM75	1.757914	1.02E-17
AC107072.2	1.744426	5.12E-20
AC083806.2	1.724745	3.46E-25
CYP4Z1	1.720322	9.83E-09
AC090206.1	1.710582	1.10E-16
NDST4	1.702703	2.47E-05
AC062028.2	1.692901	1.70E-08
CCDC144B	1.69173	2.03E-19
GLRA3	1.690639	6.86E-07
KLF7-IT1	1.685305	2.06E-22
EEF1DP3	1.662469	6.13E-28
VN1R53P	1.659999	6.56E-09
AL158847.1	1.659829	1.32E-13
AL392183.1	1.659729	5.66E-13
LINC01876	1.647227	4.09E-09
CLSTN2	1.645461	1.38E-18
RNU4-2	1.644252	4.28E-13
MUC19	1.643849	3.81E-09
ANKRD36C	1.634849	1.24E-30
CLEC3A	1.631378	0.000781
FGA	1.624754	0.003676
KCNH1	1.624266	1.69E-16
SLC30A8	1.619063	4.21E-06
HIST1H1D	1.616966	2.08E-12
PRLR	1.611442	3.66E-61
RF00019	1.609469	4.96E-20
RF00019	1.609225	8.60E-21
GUSBP9	1.606839	1.15E-26
AC015961.1	1.605945	4.61E-18
FAM169A	1.595412	9.55E-28
CSMD3	1.589993	2.02E-05
LCMT1-AS2	1.586745	3.46E-27
ENPP7P10	1.583856	2.32E-20
AC124312.5	1.5754	1.45E-22
AC253536.3	1.57489	1.94E-27
AL139022.1	1.572431	1.35E-25

AC094019.1	1.572078	1.02E-21
TACR3	1.569056	1.63E-09
AL031666.2	1.568645	1.14E-17
AC125603.2	1.568458	1.97E-12
AL445309.1	1.557887	5.38E-28
ADAMTS19	1.555744	1.32E-09
KLHL11	1.555245	1.04E-41
LINC00472	1.544791	9.86E-20
SLC1A2	1.544526	1.22E-15
AC099677.1	1.541621	7.06E-25
NOTCH2NL	1.539723	2.25E-35
AC007114.2	1.538957	1.03E-21
CRYZP1	1.53888	6.18E-22
NADK2-AS1	1.538118	1.54E-24
SNORD94	1.537177	2.07E-20
AC015971.1	1.532762	4.81E-28
AC090114.3	1.531801	9.21E-27
AC012531.1	1.530866	4.10E-21
AL136988.2	1.52989	3.48E-20
AC091544.2	1.529708	2.88E-15
AC036103.1	1.525337	2.75E-25
AC087286.2	1.521113	1.20E-22
CBLN2	1.514313	8.42E-06
AC098829.1	1.511051	2.24E-16
KCNC1	1.510933	7.62E-11
HIST1H1E	1.510499	4.11E-15
AC004066.2	1.505541	1.22E-22
TNNT2	-1.50284	9.50E-12
MYLPF	-1.50418	6.24E-28
IGKV2-24	-1.50444	1.00E-10
STAC	-1.508	2.83E-15
MTCO1P53	-1.51034	4.46E-13
ANKRD1	-1.51114	2.12E-12
PRSS1	-1.51168	2.91E-06
MELTF	-1.51543	2.08E-19
C9orf170	-1.51674	7.91E-14
ZIC1	-1.51697	4.39E-07
CHRDL2	-1.51725	1.43E-15
LINC02159	-1.51818	2.96E-08
KLHDC7B	-1.52617	1.08E-12
CRISP3	-1.52794	1.94E-07
NIPAL4	-1.53118	1.42E-15

SH3GL3	-1.53131	8.08E-09
CTSV	-1.53282	2.67E-21
PCSK1	-1.53282	1.68E-08
JSRP1	-1.5339	1.30E-19
CD1B	-1.53408	2.25E-10
AC015912.3	-1.53444	2.65E-23
SCGB3A1	-1.54157	3.60E-09
ABCA13	-1.54177	1.04E-08
NLRP7	-1.5436	9.61E-13
PCDH8	-1.54382	7.31E-08
MARCO	-1.54692	5.19E-11
PRAC2	-1.5478	7.21E-05
CAPN6	-1.54819	1.31E-10
TGM5	-1.55164	7.54E-12
CNGB1	-1.55348	7.85E-10
ACE2	-1.55361	4.03E-11
KCNQ4	-1.55403	1.65E-20
NTSR1	-1.55518	4.16E-11
CLIC3	-1.55766	1.58E-22
FERMT1	-1.55928	1.48E-12
HOXD13	-1.5595	1.11E-11
NOTUM	-1.55969	2.83E-17
CENPW	-1.56095	2.03E-33
ISL2	-1.56103	2.63E-08
SAA4	-1.5647	2.02E-11
GABRG3	-1.56717	9.00E-07
DCD	-1.56766	0.003315
PSCA	-1.56936	2.83E-11
RPS20P14	-1.5719	2.16E-38
OLIG1	-1.57474	6.33E-08
LTB	-1.57656	5.90E-18
ELF5	-1.57928	1.94E-09
SLC6A14	-1.58183	3.97E-08
CDKN2A	-1.58702	2.07E-20
AC022784.3	-1.5886	1.23E-14
CCDC129	-1.59096	1.36E-08
SERPINB7	-1.59231	2.05E-10
ERICH5	-1.59272	1.99E-09
LINC01315	-1.59284	2.80E-28
BAIAP2L2	-1.5974	2.99E-25
KCNE5	-1.59792	2.53E-14
IGLV1-44	-1.59913	2.26E-12

GTSF1	-1.60111	2.93E-21
DUSP9	-1.60521	2.16E-10
RPL21P16	-1.60773	9.24E-30
IGHV3-33	-1.61168	2.17E-11
GSTA1	-1.61304	1.39E-08
ANTXRL	-1.61623	7.89E-10
LINC00511	-1.61665	1.23E-19
TGM1	-1.61835	6.96E-31
FAM131C	-1.6186	1.66E-15
AP000851.2	-1.61951	1.17E-09
RPL10P9	-1.62286	1.88E-15
CSAG3	-1.62471	0.000297
IL34	-1.62633	8.03E-25
SPAAR	-1.62673	5.09E-28
PHF24	-1.63036	5.82E-19
AC019171.1	-1.63228	1.12E-16
AFAP1-AS1	-1.6374	1.59E-09
CCNA1	-1.64221	5.03E-17
CD19	-1.64227	3.55E-13
SCX	-1.64281	2.52E-28
AL356417.2	-1.64394	2.23E-26
LCT	-1.64457	1.92E-09
OGDHL	-1.64565	1.02E-10
HAPLN3	-1.64891	2.81E-30
MAPK4	-1.64934	2.75E-09
ARL9	-1.65255	2.97E-21
SLC15A1	-1.66154	7.23E-10
FOXQ1	-1.66563	5.35E-18
CCL17	-1.67052	1.06E-18
GATA6-AS1	-1.67653	2.34E-18
AC011247.1	-1.67727	7.20E-17
AC023983.2	-1.68002	7.33E-24
LINC00092	-1.69102	5.55E-12
POPDC3	-1.69203	6.44E-13
UCHL1	-1.69226	2.49E-20
TMEM158	-1.69579	2.08E-22
AC021683.2	-1.69584	1.32E-14
AC005863.1	-1.70206	1.20E-06
MT2P1	-1.70301	3.25E-23
CRISP2	-1.70305	1.14E-06
PCDH11X	-1.70456	7.88E-10
NPW	-1.70709	4.96E-13

AC105914.2	-1.70944	0.004077
RHEX	-1.71191	1.23E-18
ANXA8L1	-1.71194	1.43E-13
ODAM	-1.71727	3.76E-09
PRSS2	-1.71811	1.95E-10
TMPRSS5	-1.71937	2.45E-21
FGFBP2	-1.72409	3.16E-16
LINC00284	-1.72721	1.44E-13
EDAR	-1.73023	1.66E-12
MTND4P24	-1.7305	7.32E-14
IGLV9-49	-1.73073	4.61E-11
SHISA8	-1.73411	1.72E-17
PRSS3	-1.73649	1.22E-12
AC069148.1	-1.73989	6.30E-24
GFRA3	-1.74386	2.67E-13
ANXA8	-1.74772	1.84E-13
NOL4	-1.74904	4.25E-11
RPL10P6	-1.76357	1.74E-12
S100A8	-1.76412	1.08E-11
CASC9	-1.76446	9.58E-06
FOXC1	-1.76805	4.68E-19
VPREB3	-1.76914	8.30E-20
C5orf66-AS1	-1.76969	1.27E-11
SPRR1A	-1.77558	0.000111
LINC02538	-1.78053	9.64E-15
COL22A1	-1.78167	1.26E-22
PNMA6A	-1.78904	3.56E-27
HPDL	-1.79986	9.26E-19
EEF1DP5	-1.80064	3.45E-08
SOX9-AS1	-1.8032	4.22E-19
TCL1A	-1.80408	2.66E-11
POLR2F	-1.80723	6.45E-16
LMO1	-1.80849	2.20E-11
SERPINB2	-1.81741	8.52E-11
AP005233.2	-1.81984	1.14E-09
AC027031.2	-1.82381	5.38E-28
DSG1	-1.82673	4.14E-11
AC103702.2	-1.846	3.48E-12
MUC13	-1.8528	1.74E-10
LINC01554	-1.85367	2.85E-19
AC008514.1	-1.85916	4.95E-22
SHC4	-1.8682	6.92E-16

ACAN	-1.86923	3.97E-24
STRA8	-1.87075	7.68E-06
LINC00839	-1.88037	4.75E-20
FGFBP1	-1.88494	2.24E-07
AP002800.1	-1.88912	7.46E-23
HILS1	-1.89856	6.28E-16
TCP11	-1.90897	6.90E-19
AL162413.1	-1.91115	9.20E-05
CA9	-1.91703	3.18E-10
GPX1P1	-1.9216	1.21E-29
TUBB4A	-1.92432	4.92E-16
PKP1	-1.92707	1.58E-17
IGLVI-70	-1.93742	5.04E-10
KCNK5	-1.94531	3.83E-25
SMOC1	-1.94608	2.75E-17
S100A1	-1.94747	1.24E-20
FOXD1	-1.95383	6.86E-17
FSD1	-1.95625	4.77E-23
CRABP1	-1.95893	4.42E-11
AQP5	-1.96321	2.50E-11
IGKV2D-30	-1.96759	3.64E-10
LINC01287	-1.96918	2.03E-16
SPRR1B	-1.97094	8.97E-05
CLEC2L	-1.97624	6.10E-19
CALML5	-1.98398	4.20E-11
TRPM8	-1.98439	4.96E-18
PSORS1C2	-1.99134	3.29E-18
CRYAB	-1.99694	2.14E-27
KCNS1	-2.00197	2.82E-18
SPDYC	-2.00681	1.84E-08
FOLR1	-2.01037	2.03E-13
TCAM1P	-2.01464	1.18E-12
AC245041.1	-2.01596	6.53E-11
IGKV1D-17	-2.01817	4.97E-13
KLK11	-2.02201	1.29E-09
S100B	-2.02234	3.10E-21
AC021683.1	-2.02309	5.83E-22
NCCRP1	-2.02985	1.29E-15
SLPI	-2.03612	7.38E-20
ICAM5	-2.04392	1.86E-23
AC245041.2	-2.04833	7.50E-17
OR2S1P	-2.05036	5.81E-16

SLCO4A1-AS1	-2.05083	9.10E-16
DNAH17-AS1	-2.05876	5.03E-16
CHODL	-2.06389	1.55E-21
IGKV2-29	-2.06558	1.67E-09
FAM3D	-2.06732	1.61E-21
AMN	-2.08389	1.41E-26
AMTN	-2.08641	3.17E-10
CHGA	-2.08971	7.29E-12
SERPINB5	-2.09221	7.79E-18
MMP7	-2.0944	1.64E-22
CCKBR	-2.10521	2.38E-10
ACP7	-2.10978	2.78E-15
TNNI2	-2.11633	3.73E-41
TMEM213	-2.1222	7.75E-14
BARX1	-2.12466	7.73E-21
KRTDAP	-2.12715	3.65E-16
WNT10A	-2.12947	3.58E-34
SPIB	-2.13212	2.87E-21
SBSN	-2.1397	2.49E-13
IL1R2	-2.14416	2.71E-30
PCSK1N	-2.1476	6.43E-15
OLAH	-2.15441	5.01E-18
FAM19A3	-2.18459	2.41E-27
PI3	-2.19211	5.72E-14
WFDC21P	-2.20844	1.34E-30
KRT5	-2.21913	2.28E-18
LINC02188	-2.22546	6.87E-14
MMP20	-2.22865	4.67E-12
LGALS7B	-2.23463	2.89E-19
ACTBP12	-2.23588	2.13E-13
SNORC	-2.23714	2.36E-34
GJB5	-2.23746	2.52E-24
A2ML1	-2.23936	2.32E-15
PPP1R14C	-2.24167	4.26E-22
CAMKV	-2.2553	6.32E-15
AC061975.6	-2.26248	1.71E-16
KRT4	-2.27415	4.34E-11
KRT17P3	-2.29082	9.02E-16
SLURP1	-2.29436	2.45E-14
KRT17	-2.2947	1.35E-22
PTX3	-2.29768	1.00E-26
LINC02473	-2.30414	1.62E-20

CMTM5	-2.30454	2.36E-17
CASC8	-2.34134	2.84E-24
NKX2-5	-2.34929	2.95E-10
AP000851.1	-2.35693	2.66E-16
COL11A2	-2.36867	3.19E-31
KLK10	-2.36881	3.58E-17
POMC	-2.36925	9.10E-40
CRHR1	-2.37953	5.36E-27
SLC6A2	-2.38111	3.65E-17
C2orf71	-2.39471	3.79E-17
SLC26A9	-2.39596	1.64E-21
FBN3	-2.39965	8.41E-22
KIRREL3-AS1	-2.41932	5.41E-08
PNMA3	-2.43402	1.27E-29
BLACAT1	-2.44947	1.54E-23
AC009041.2	-2.45114	4.04E-34
SCEL	-2.45653	1.72E-14
SYT8	-2.45683	2.96E-25
KRT16P6	-2.4587	1.82E-18
LINC01436	-2.46463	1.98E-32
FABP7	-2.46596	1.15E-13
KLHL34	-2.47733	3.26E-21
PGLYRP4	-2.48503	1.21E-14
SCRG1	-2.49345	2.29E-28
S100A2	-2.49823	2.36E-28
NKX1-2	-2.52124	1.27E-13
LINC02437	-2.52136	2.55E-12
GABRP	-2.52266	1.94E-20
KLK7	-2.53426	1.03E-19
GPR12	-2.56248	6.19E-17
SLC6A15	-2.56767	2.79E-15
ROPN1	-2.57287	1.12E-13
GABBR2	-2.57314	3.60E-17
KLK5	-2.5749	5.86E-21
MAGEA3	-2.58694	0.000201
KCNG1	-2.59452	9.34E-27
MAGEA12	-2.59738	2.01E-06
LINC01198	-2.60044	2.84E-12
RASGEF1C	-2.60961	5.00E-30
DLX5	-2.61203	9.56E-41
GJB6	-2.64574	1.15E-19
NDUFB4P11	-2.64663	3.48E-18

KRT14	-2.65807	3.88E-25
IVL	-2.66185	1.51E-15
DSG3	-2.66547	1.85E-22
RAET1L	-2.67743	2.82E-20
MAGEA6	-2.68457	0.000161
GDF5	-2.68923	3.97E-32
AC020907.1	-2.71326	7.38E-30
WNT6	-2.71484	3.84E-31
OPRK1	-2.72585	2.05E-17
HRCT1	-2.73375	1.13E-37
LINC00518	-2.76796	1.96E-12
AP001783.1	-2.77141	6.13E-17
ROPN1B	-2.78003	3.01E-27
BPI	-2.78324	8.05E-35
HORMAD1	-2.78708	1.23E-17
KRT79	-2.78808	1.13E-29
ETV3L	-2.79055	3.38E-24
GJB3	-2.791	1.24E-30
SERPINB3	-2.80023	1.21E-05
ROCR	-2.81666	5.89E-19
TBX10	-2.84277	6.06E-13
C1QL4	-2.89104	5.75E-35
MAGEA4	-2.92965	4.11E-07
NTS	-2.93555	1.35E-13
C6orf15	-2.95809	1.78E-27
ACTL8	-2.97787	6.17E-19
EN1	-2.98286	1.74E-41
CDH19	-2.99079	4.33E-16
C1QL2	-3.00807	1.36E-21
FZD9	-3.01482	1.82E-38
AC245884.9	-3.01919	1.98E-23
POU4F1	-3.05849	8.62E-17
CCNYL2	-3.09226	1.71E-19
PICSAR	-3.09665	1.71E-34
CLDN6	-3.10844	1.13E-40
LEMD1	-3.10873	6.10E-27
KRT83	-3.11058	4.07E-34
RHCG	-3.11099	1.05E-32
LINC02487	-3.11693	2.70E-38
OCA2	-3.12782	7.03E-26
RGR	-3.17143	3.55E-19
NFE4	-3.17493	6.23E-28

KRT6C	-3.18141	1.30E-21
LINC00707	-3.19763	4.27E-29
KRT9	-3.21169	2.22E-32
COL9A3	-3.21244	3.80E-56
CSN3	-3.24053	2.44E-06
KRT6B	-3.28794	4.82E-33
SMR3B	-3.32463	3.88E-09
DNER	-3.32855	1.36E-34
TTYH1	-3.33065	8.36E-44
MATN4	-3.35178	1.73E-52
MTCO1P40	-3.36631	1.06E-41
LY6D	-3.36787	1.25E-26
KLK6	-3.39518	2.34E-33
KLK8	-3.42058	1.35E-32
CSAG1	-3.45086	6.23E-19
DLX6-AS1	-3.46618	4.46E-43
LINC01956	-3.48859	8.24E-27
KRT77	-3.51405	2.54E-18
SOX8	-3.55507	5.40E-53
MIA	-3.56356	1.16E-40
FOXCUT	-3.58587	1.32E-24
AC022784.1	-3.59265	1.24E-37
ZFP42	-3.67284	6.83E-21
DLX6	-3.67678	1.60E-45
COL9A1	-3.72474	1.89E-37
VGLL1	-3.80004	2.25E-34
ART3	-3.82979	1.28E-39
LINC01667	-3.90329	1.31E-14
KRT6A	-4.00296	3.65E-37
KRT81	-4.08403	2.43E-51
CT83	-4.16165	3.83E-07
FDCSP	-4.28132	6.09E-42
MTND1P23	-4.42595	3.16E-59
NCAN	-4.49491	1.48E-57
CHGB	-4.8407	2.26E-43
KRT16	-4.85559	1.90E-72
MSLN	-4.86367	7.49E-77
LINC00393	-4.9707	2.65E-19
PRSS33	-5.09433	1.27E-43
AL161431.1	-5.27602	1.30E-27
CARTPT	-6.2211	2.94E-26

Bibliography

[1] Abdel-Meguid, S. S., Shieh, H. S., Smith, W. W., Dayringer, H. E., Violand, B. N., and Bentle, L. A. (1987). Three-dimensional structure of a genetically engineered variant of porcine growth hormone. *Proceedings of the National Academy of Sciences of the United States of America*, 84(18):6434–6437.

[2] Acosta, J. J., Muñoz, R. M., González, L., Subtil-Rodríguez, A., Domínguez-Cáceres, M. A., García-Martínez, J. M., Calcabrini, A., Lazaro-Trueba, I., and Martín-Pérez, J. (2003). Src Mediates Prolactin-Dependent Proliferation of T47D and MCF7 Cells via the Activation of Focal Adhesion Kinase/Erk1/2 and Phosphatidylinositol 3-Kinase Pathways. *Molecular Endocrinology*, 17(11):2268–2282.

[3] Adamson, A. D., Friedrichsen, S., Semprini, S., Harper, C. V., Mullins, J. J., White, M. R., and Davis, J. R. (2008). Human prolactin gene promoter regulation by estrogen: Convergence with tumor necrosis factor-α signaling. *Endocrinology*, 149(2):687–694.

[4] Agarwal, N., Machiels, J.-P., Suárez, C., Lewis, N., Higgins, M., Wisinski, K., Awada, A., Maur, M., Stein, M., Hwang, A., Mosher, R., Wasserman, E., Wu, G., Zhang, H., Zieba, R., and Elmeliegy, M. (2016). Phase I Study of the Prolactin Receptor Antagonist LFA102 in Metastatic Breast and Castration-Resistant Prostate Cancer. *The oncologist*, 21(5):535–6.

[5] Aksamitiene, E., Achanta, S., Kolch, W., Kholodenko, B. N., Hoek, J. B., and Kiyatkin, A. (2011). Prolactin-stimulated activation of ERK1/2 mitogen-activated protein kinases is controlled by PI3-kinase/Rac/PAK signaling pathway in breast cancer cells. *Cellular Signalling*, 23(11):1794–1805.

[6] Albrektsen, G., Heuch, I., Hansen, S., and Kvåle, G. (2005). Breast cancer risk by age at birth, time since birth and time intervals between births: exploring interaction effects. *British Journal of Cancer*, 92(1):167–175.

[7] Ali, S., Pellegrini, I., and Kelly, P. A. (1991). A prolactin-dependent immune cell line (Nb2) expresses a mutant form of prolactin receptor. *The Journal of biological chemistry*, 266(30):20110–7.

[8] American Cancer Society (2020). *Breast Cancer Signs and Symptoms.*

[9] Amit, T., Dibner, C., and Barkey, R. J. (1997). Characterization of prolactin- and growth hormone-binding proteins in milk and their diversity among species. *Molecular and Cellular Endocrinology*, 130(1-2):167–180.

[10] Amit, T., Hochberg, Z., Waters, M. J., and Barkey, R. J. (1992). Growth hormone- and prolactin-binding proteins in mammalian serum. *Endocrinology*, 131(4):1793–1803.

[11] Anderson, E., Ferguson, J. E., Morten, H., Shalet, S. M., Robinson, E. L., and Howell, A. (1993). Serum immunoreactive and bioactive lactogenic hormones in advanced breast cancer patients treated with bromocriptine and octreotide. *European Journal of Cancer*, 29(2):209–217.

[12] Anderson, J. (1990). Decidual prolactin. Studies of decidual and amniotic prolactin in normal and pathological pregnancy. *Danish Medical Bulletin*, 37(2):154–165.

[13] Arden, K. C., Boutin, J. M., Djiane, J., Kelly, P. A., and Cavenee, W. K. (1990). The receptors for prolactin and growth hormone are localized in the same region of human chromosome 5. *Cytogenetic and Genome Research*, 53(2-3):161–165.

[14] Ayling, R., Ross, R., Towner, P., Laue, S. V., Finidori, J., Moutoussamy, S., Buchanan, C., Clayton, P., and Norman, M. (1999). New growth hormone receptor exon 9 mutation causes genetic short stature. *Acta Paediatrica*, 88(s428):168–172.

[15] Bajrami, I., Marlow, R., van De Ven, M., Brough, R., Pemberton, H. N., Frankum, J., Song, F., Rafiq, R., Konde, A., Krastev, D. B., Menon, M., Campbell, J., Gulati, A., Kumar, R., Pettitt, S. J., Gurden, M. D., Cardenosa, M. L., Chong, I., Gazinska, P., Wallberg, F., Sawyer, E. J., Martin, L. A., Dowsett, M., Linardopoulos, S., Natrajan, R., Ryan, C. J., Derksen, P. W., Jonkers, J., Tutt, A. N., Ashworth, A., and Lord, C. J. (2018). E-Cadherin/ROS1 inhibitor synthetic lethality in breast cancer. *Cancer Discovery*, 8(4):498–515.

[16] Baker, B. L. and Yu, Y.-Y. (1977). An immunocytochemical study of human pituitary mammotropes from fetal life to old age. *American Journal of Anatomy*, 148(2):217–239.

[17] Bandera, E. V., Chandran, U., Hong, C. C., Troester, M. A., Bethea, T. N., Adams-Campbell, L. L., Haiman, C. A., Park, S. Y., Olshan, A. F., Ambrosone, C. B., Palmer, J. R., and Rosenberg, L. (2015). Obesity, body fat distribution, and risk of breast cancer subtypes in African American women participating in the AMBER Consortium. *Breast Cancer Research and Treatment*, 150(3):655–666.

[18] Banys-Paluchowski, M., Milde-Langosch, K., Fehm, T., Witzel, I., Oliveira-Ferrer, L., Schmalfeldt, B., and Müller, V. (2020). Clinical relevance of H-RAS, K-RAS, and N-RAS mRNA expression in primary breast cancer patients. *Breast Cancer Research and Treatment*, 179(2):403–414.

[19] Barber, D. L., DeMartino, J. C., Showers, M. O., and D'Andrea, A. D. (1994). A dominant negative erythropoietin (EPO) receptor inhibits EPO-dependent growth

and blocks F-gp55-dependent transformation. *Molecular and Cellular Biology*, 14(4):2257–2265.

[20] Baselga, J., Campone, M., Piccart, M., Burris, H. A., Rugo, H. S., Sahmoud, T., Noguchi, S., Gnant, M., Pritchard, K. I., Lebrun, F., Beck, J. T., Ito, Y., Yardley, D., Deleu, I., Perez, A., Bachelot, T., Vittori, L., Xu, Z., Mukhopadhyay, P., Lebwohl, D., and Hortobagyi, G. N. (2012). Everolimus in postmenopausal hormone-receptor-positive advanced breast cancer. *New England Journal of Medicine*, 366(6):520–529.

[21] Baumgartner, J. W., Wells, C. A., Chen, C. M., and Waters, M. J. (1994). The role of the WSXWS equivalent motif in growth hormone receptor function. *The Journal of Biological Chemistry*, 269(46):29094–101.

[22] Bazan, J. F. (1989). A novel family of growth factor receptors: A common binding domain in the growth hormone, prolactin, erythropoietin and IL-6 receptors, and the p75 IL-2 receptor β-chain. *Biochemical and Biophysical Research Communications*, 164(2):788–795.

[23] Bazan, J. F. (1990a). Haemopoietic receptors and helical cytokines. *Immunology Today*, 11(C):350–354.

[24] Bazan, J. F. (1990b). Structural design and molecular evolution of a cytokine receptor superfamily. *Proceedings of the National Academy of Sciences of the United States of America*, 87(18):6934–8.

[25] Ben-Jonathan, N. and Hnasko, R. (2001). Dopamine as a Prolactin (PRL) Inhibitor. *Endocrine Reviews*, 22(6):724–763.

[26] Ben-Jonathan, N., LaPensee, C. R., and LaPensee, E. W. (2008). What can we learn from rodents about prolactin in humans?

[27] Ben-Levy, R., Paterson, H., Marshall, C., and Yarden, Y. (1994). A single autophosphorylation site confers oncogenicity to the Neu/ErbB-2 receptor and enables coupling to the MAP kinase pathway. *The EMBO Journal*, 13(14):3302–3311.

[28] Benitah, S. A., Valerón, P. F., Rui, H., and Lacal, J. C. (2003). STAT5a activation mediates the epithelial to mesenchymal transition induced by oncogenic RhoA. *Molecular Biology of the Cell*, 14(1):40–53.

[29] Berwaer, M., Martial, J. A., and Davis, J. R. (1994). Characterization of an upstream promoter directing extrapituitary expression of the human prolactin gene. *Molecular Endocrinology*, 8(5):635–642.

[30] Berwaer, M., Monget, P., Peers, B., Mathy-Hartert, M., Bellefroid, E., Davis, J. R., Belayew, A., and Martial, J. A. (1991). Multihormonal regulation of the human prolactin gene expression from 5000 bp of its upstream sequence. *Molecular and Cellular Endocrinology*, 80(1-3):53–64.

[31] Bewley, T. A. and Li, C. H. (1972). Circular Dichroism Studies on Human Pituitary Growth Hormone and Ovine Pituitary Lactogenic Hormone. *Biochemistry*, 11(5):884–888.

[32] Biener, E., Martin, C., Daniel, N., Frank, S. J., Centonze, V. E., Herman, B., Djiane, J., and Gertler, A. (2003). Ovine Placental Lactogen-Induced Heterodimerization of Ovine Growth Hormone and Prolactin Receptors in Living Cells Is Demonstrated by Fluorescence Resonance Energy Transfer Microscopy and Leads to Prolonged Phosphorylation of Signal Transducer and Activator of Transcription (STAT)1 and STAT3. *Endocrinology*, 144(8):3532–3540.

[33] Binart, N., Imbert-Bolloré, P., Baran, N., Viglietta, C., and Kelly, P. A. (2003). A Short Form of the Prolactin (PRL) Receptor Is Able to Rescue Mammopoiesis in Heterozygous PRL Receptor Mice. *Molecular Endocrinology*, 17(6):1066–1074.

[34] Biswas, R. and Vonderhaar1, B. K. (1987). Role of Serum in the Prolactin Responsiveness of MCF-7 Human Breast Cancer Cells in Long-Term Tissue Culture. Technical report.

[35] Boeke, C. E., Eliassen, A. H., Oh, H., Spiegelman, D., Willett, W. C., and Tamimi, R. M. (2014). Adolescent physical activity in relation to breast cancer risk. *Breast Cancer Research and Treatment*, 145(3):715–724.

[36] Bole-Feysot, C., Goffin, V., Edery, M., Binart, N., and Kelly, P. A. (1998). Prolactin (PRL) and its receptor: Actions, signal transduction pathways and phenotypes observed in PRL receptor knockout mice.

[37] Bonneterre, J., Mauriac, L., Weber, B., Roche, H., Fargeot, P., Tubiana-Hulin, M., Sevin, M., Chollet, P., and Cappelaere, P. (1988). Tamoxifen plus bromocriptine versus tamoxifen plus placebo in advanced breast cancer: Results of a double blind multicentre clinical trial. *European Journal of Cancer and Clinical Oncology*, 24(12):1851–1853.

[38] Booms, A., Coetzee, G. A., and Pierce, S. E. (2019). MCF-7 as a model for functional analysis of breast cancer risk variants. *Cancer Epidemiology Biomarkers and Prevention*, 28(10):1735–1745.

[39] Bos, J. L. (1989). ras Oncogenes in Human Cancer: A Review. *Cancer Research*, 49(17).

[40] Boutin, J.-M., Jolicoeur, C., Okamura, H., Gagnon, J., Edery, M., Shirota, M.,

Banville, D., Dusanter-Fourt, L., Djiane, J., and Kelly', P. A. (1988). Cloning and Expression of the Rat Prolactin Receptor, a Member of the Receptor Gene Family Growth Hormone/Prolactin. 53:69–77.

[41] Bratthauer, G., Stamatakos, M., and Vinh, T. (2009). Cells with Minimal Expression of the JAK/STAT Pathway Related Proteins STAT5a and the Prolactin Receptor: Evidence of an Alternate Prolactin Receptor Isoform in Breast Disease. *Protein & Peptide Letters*, 17(1):104–108.

[42] Brockman, J. L., Schroeder, M. D., and Schuler, L. A. (2002). PRL activates the cyclin D1 promoter via the Jak2/Stat pathway. *Molecular endocrinology (Baltimore, Md.)*, 16(4):774–84.

[43] Brooks, A. J., Dai, W., O'Mara, M. L., Abankwa, D., Chhabra, Y., Pelekanos, R. A., Gardon, O., Tunny, K. A., Blucher, K. M., Morton, C. J., Parker, M. W., Sierecki, E., Gambin, Y., Gomez, G. A., Alexandrov, K., Wilson, I. A., Doxastakis, M., Mark, A. E., and Waters, M. J. (2014). Mechanism of activation of protein kinase JAK2 by the growth hormone receptor. *Science*, 344(6185).

[44] Brown, R. J., Adams, J. J., Pelekanos, R. A., Wan, Y., McKinstry, W. J., Palethorpe, K., Seeber, R. M., Monks, T. A., Eidne, K. A., Parke, M. W., and Waters, M. J. (2005). Model for growth hormone receptor activation based on subunit rotation within a receptor dimer. *Nature Structural and Molecular Biology*, 12(9):814–821.

[45] Bugge, K., Papaleo, E., Haxholm, G. W., Hopper, J. T., Robinson, C. V., Olsen, J. G., Lindorff-Larsen, K., and Kragelund, B. B. (2016). A combined computational and structural model of the full-length human prolactin receptor. *Nature Communications*, 7(1):1–11.

[46] Burset, M., Seledtsov, I. A., and Solovyev, V. V. (2001). SpliceDB: database of canonical and non-canonical mammalian splice sites. *Nucleic Acids Research*, 29(1).

[47] Campbell, G. S., Argetsinger, L. S., Ihle, J. N., Kelly, P. A., Rillema, J. A., and Carter-Su, C. (1994). Activation of JAK2 tyrosine kinase by prolactin receptors in Nb2 cells and mouse mammary gland explants. *Proceedings of the National Academy of Sciences of the United States of America*, 91(12):5232–6.

[48] Campbell, K. M., O'Leary, K. A., Rugowski, D. E., Mulligan, W. A., Barnell, E. K., Skidmore, Z. L., Krysiak, K., Griffith, M., Schuler, L. A., and Griffith, O. L. (2019). A Spontaneous Aggressive ERα+ Mammary Tumor Model Is Driven by Kras Activation. *Cell Reports*, 28(6):1526–1537.e4.

[49] Canon, J., Rex, K., Saiki, A. Y., Mohr, C., Cooke, K., Bagal, D., Gaida, K., Holt, T., Knutson, C. G., Koppada, N., Lanman, B. A., Werner, J., Rapaport, A. S., San Miguel, T., Ortiz, R., Osgood, T., Sun, J. R., Zhu, X., McCarter, J. D., Volak, L. P., Houk, B. E., Fakih, M. G., O'Neil, B. H., Price, T. J., Falchook, G. S., Desai, J., Kuo, J., Govindan, R., Hong, D. S., Ouyang, W., Henary, H., Arvedson, T., Cee, V. J., and Lipford, J. R. (2019). The clinical KRAS(G12C) inhibitor AMG 510 drives anti-tumour immunity. *Nature*, 575(7781):217–223.

[50] Carmine, A. A., Brogden, R. N., Heel, R. C., Speight, T. M., and Avery, G. S. (1982). Trifluridine: A Review of its Antiviral Activity and Therapeutic Use in the Topical Treatment of Viral Eye Infections. *Drugs*, 23(5):329–353.

[51] Carraway Ill, K. L. and Cantley, L. C. (1994). A Neu Acquaintance for ErbB3 and ErbB4: A Role for Receptor Heterodimerization in Growth Signaling Minireview. 78:5–8.

[52] Caruso, C. (2019). AMG 510 First to Inhibit "Undruggable" KRAS. *Cancer Discovery News in Brief*, pages 988–999.

[53] Castellano, E. and Santos, E. (2011). Functional specificity of ras isoforms: so similar but so different. *Genes & cancer*, 2(3):216–31.

[54] Chan, S. R., Vermi, W., Luo, J., Lucini, L., Rickert, C., Fowler, A. M., Lonardi, S., Arthur, C., Young, L. J., Levy, D. E., Welch, M. J., Cardiff, R. D., and Schreiber, R. D. (2012). STAT1-deficient mice spontaneously develop estrogen receptor a-positive luminal mammary carcinomas.

[55] Chang, W. P. and Clevenger, C. V. (1996). Modulation of growth factor receptor function by isoform heterodimerization. *Proceedings of the National Academy of Sciences of the United States of America*, 93(12):5947–5952.

[56] Chang, W.-P., Ye, Y., and Clevenger, C. V. (1998). Stoichiometric Structure-Function Analysis of the Prolactin Receptor Signaling Domain by Receptor Chimeras. *Molecular and Cellular Biology*, 18(2):896–905.

[57] Chernecky, C. and Berger, B. (2012). *Laboratory Tests and Diagnostic Procedures*. 6 edition.

[58] Christensen, H. R., Murawsky, M. K., Horseman, N. D., Willson, T. A., and Gregerson, K. A. (2013). Completely Humanizing Prolactin Rescues Infertility in Prolactin Knockout Mice and Leads to Human Prolactin Expression in Extrapituitary Mouse Tissues. *Endocrinology*, 154(12):4777–4789.

[59] Chung, C. D., Liao, J., Liu, B., Rao, X., Jay, P., Berta, P., and Shuai, K. (1997). Specific inhibition of Stat3 signal transduction by PIAS3.

[60] Chung, C. H., Bernard, P. S., and Perou, C. M. (2002). Molecular portraits and the family tree of cancer.

[61] Clandinin, M., Chappell, J., and Mager, D. (1986). Prolactin Binding Protein in Human Milk. *Endocrinologia experimentalis*, 20(2-3):209–215.

[62] Clarke, D. L. and Linzer, D. I. H. (1993). Changes in Prolactin Receptor Expression during Pregnancy in the Mouse Ovary. 133(1).

[63] Clevenger, C. V., Chang, W. P., Ngo, W., Pasha, T. L., Montone, K. T., and Tomaszewski, J. E. (1995). Expression of prolactin and prolactin receptor in human breast carcinoma: Evidence for an autocrine/paracrine loop. *American Journal of Pathology*, 146(3):695–705.

[64] Clevenger, C. V., Furth, P. A., Hankinson, S. E., and Schuler, L. A. (2003). The role of prolactin in mammary carcinoma. *Endocrine reviews*, 24(1):1–27.

[65] Clevenger, C. V., Torigoell, T., and Reed, J. C. (1994). Prolactin Induces Rapid Phosphorylation and Activation of Prolactin Receptor-associated RAF-1 Kinase in a T-cell Line. *The Journal of Biological Chemistry*, 269(8):5559–5565.

[66] Clevenger, C. V., Zheng, J., Jablonski, E. M., Galbaugh, T. L., and Fang, F. (2008). From Bench to Bedside: Future Potential for the Translation of Prolactin Inhibitors as Breast Cancer Therapeutics. *Journal of Mammary Gland Biology and Neoplasia*, 13(1):147–156.

[67] Cohen, H., Guillaumot, P., and Sabbagh, I. (1993). Characterization of a prolactin binding protein in rat serum. *Endocrinology*, 132(6):2601–2606.

[68] Cole, E. N., Sellwood, R. A., England, P. C., and Griffiths, K. (1977). Serum

prolactin concentrations in benign breast disease throughout the menstrual cycle. *European Journal of Cancer (1965)*, 13(6):597–603.

[69] Comsa, S., Cimpean, A. M., and Raica, M. (2015). The Story of MCF-7 Breast Cancer Cell Line: 40 years of Experience in Research. *Anticancer Research*, 35:3147–3145.

[70] Constantinescu, S. N., Keren, T., Socolovsky, M., Nam, H. S., Henis, Y. I., and Lodish, H. F. (2001). Ligand-independent oligomerization of cell-surface erythropoietin receptor is mediated by the transmembrane domain. *Proceedings of the National Academy of Sciences of the United States of America*, 98(8):4379–4384.

[71] Cooke, N. E., Coit, D., Weiner, R. I., Baxter, J. D., and Martial, J. A. (1980). Structure of cloned DNA complementary to rat prolactin messenger RNA. *The Journal of Biological Chemistry*, 255(13):6502–10.

[72] Cookeg, N. E., Coit, D., Shines, J., Baxterj, J. D., and Martial, J. A. (1981). Human Prolactin cDNA structural analysis and evolutionary comparisons. 256(8):4–7.

[73] Cunningham, B. C., Ultsch, M., De Vos, A. M., Mulkerrin, M. G., Clauser, K. R., and Wells, J. A. (1991). Dimerization of the extracellular domain of the human growth hormone receptor by a single hormone molecule. *Science*, 254(5033):821–825.

[74] Cunningham, B. C. and Wells, J. A. (1989). High-resolution epitope mapping of hGH-receptor interactions by alanine-scanning mutagenesis. *Science*, 244(4908):1081–1085.

[75] Cunningham, B. C. and Wells, J. A. (1993). Comparison of a structural and a functional epitope. *Journal of Molecular Biology*, 234(3):554–563.

[76] Dagil, R., Knudsen, M. J., Olsen, J. G., O'Shea, C., Franzmann, M., Goffin, V., Teilum, K., Breinholt, J., and Kragelund, B. B. (2012). The WSXWS motif in cytokine receptors is a molecular switch involved in receptor activation: Insight from structures of the prolactin receptor. *Structure*, 20(2):270–282.

[77] Damiano, J. S., Rendah, K. G., Karim, C., Embry, M. G., Ghoddusi, M., Holash, J., Fanidi, A., Abrams, T. J., and Abraham, J. A. (2013). Neutralization of prolactin receptor function by monoclonal antibody LFA102, a novel potential therapeutic for the treatment of breast cancer. *Molecular Cancer Therapeutics*, 12(3):295–305.

[78] Das, R. and Vonderhaar, B. K. (1996). Activation of raf-L MEK, and MAP kinase in prolactin responsive mammary cells. 40:141–149.

[79] DaSilva, L., Howard, O. M., Rui, H., Kirken, R. A., and Farrar, W. L. (1994). Growth signaling and JAK2 association mediated by membrane-proximal cytoplasmic regions of prolactin receptors. *Journal of Biological Chemistry*, 269(28):18267–18270.

[80] Davis, J. A. and Linzer, D. I. (1989). Expression of multiple forms of the prolactin receptor in mouse liver. *Molecular Endocrinology*, 3(4):674–680.

[81] Dawson, P. J., Wolman, S. R., Tait, L., Heppner, G. H., and Millert, F. R. (1996). MCF10AT: A Model for the Evolution of Cancer from Proliferative Breast Disease. 148(1).

[82] De Vos, A. M., Ultsch, M., and Kossiakoff, A. A. (1992). Human growth hormone and extracellular domain of its receptor: Crystal structure of the complex. *Science*, 255(5042):306–312.

[83] Djiane, J., Clauser, H., and Kelly, P. (1979). Rapid down-regulation of prolactin receptors in mammary gland and liver. *Biochemical and biophysical research communications*, 90(4):1371–1378.

[84] Dobin, A., Davis, C. A., Schlesinger, F., Drenkow, J., Zaleski, C., Jha, S., Batut, P., Chaisson, M., and Gingeras, T. R. (2013). STAR: ultrafast universal RNA-seq aligner. *Bioinformatics*, 29(1):15–21.

[85] Drullinsky, P. R. and Hurvitz, S. A. (2020). Mechanistic basis for PI3K inhibitor antitumor activity and adverse reactions in advanced breast cancer. 181:233–248.

[86] Dutta, P., Zhang, L., Zhang, H., Peng, Q., Montgrain, P. R., Wang, Y., Song, Y., Li, J., and Li, W. X. (2020). Unphosphorylated STAT3 in heterochromatin formation and tumor suppression in lung cancer. *BMC Cancer*, 20(1).

[87] Edery, M., Jolicoeur, C., Levi-Meyrueis, C., Dusanter-Fourt, I., Petridou, B., Boutin, J. M., Lesueur, L., Kelly, P. A., and Djiane, J. (1989). Identification and sequence analysis of a second form of prolactin receptor by molecular cloning of complementary DNA from rabbit mammary gland. *Proceedings of the National Academy of Sciences of the United States of America*, 86(6):2112–2116.

[88] Eliassen, A. H., Tworoger, S. S., and Hankinson, S. E. (2007). Reproductive factors and family history of breast cancer in relation to plasma prolactin levels in premenopausal and postmenopausal women. *International Journal of Cancer*.

[89] Erodogan, M., Inal, A., Ozgu, M., Beksac, M., and Ergurbuz, I. (1980). Effect of Oral Contraceptive (Ethinyl Estradiol and D-Norgestrel) on Serum Prolactin-Oestradiol and Progesterone Levels. *Acta reproductiva Turcica*, 1(3):85–91.

[90] Erwin, R. A., Kirken, R. A., Malabarba, M. G., Farrar, W. L., and Rui, H.

(1995). Prolactin activates Ras via signaling proteins SHC, growth factor receptor bound 2, and son of sevenless. *Endocrinology*, 136(8):3512–8.

[91] Fang, F., Antico, G., Zheng, J., and Clevenger, C. V. (2008). Quantification of PRL/Stat5 signaling with a novel pGL4-CISH reporter. *BMC Biotechnology*, 8.

[92] Farvid, M. S., Chen, W. Y., Michels, K. B., Cho, E., Willett, W. C., and Eliassen, A. H. (2016). Fruit and vegetable consumption in adolescence and early adulthood and risk of breast cancer: Population based cohort study. *BMJ (Online)*, 353.

[93] Farvid, M. S., Cho, E., Chen, W. Y., Eliassen, A. H., and Willett, W. C. (2014). Dietary protein sources in early adulthood and breast cancer incidence: Prospective cohort study. *BMJ (Online)*, 348.

[94] Feng, J., Witthuhn, B. A., Matsuda, T., Kohlhuber, F., Kerr, I. M., and Ihle, J. N. (1997). Activation of Jak2 catalytic activity requires phosphorylation of Y1007 in the kinase activation loop. *Molecular and Cellular Biology*, 17(5):2497–2501.

[95] Ferretti, E., Corcione, A., and Pistoia, V. (2017). The IL31/IL31 receptor axis: general features and role in tumor microenvironment. *Journal of Leukocyte Biology*, 102(3):711–717.

[96] Fiorillo, A. A., Medler, T. R., Feeney, Y. B., Liu, Y., Tommerdahl, K. L., and Clevenger, C. V. (2011). HMGN2 Inducibly Binds a Novel Transactivation Domain in Nuclear PRLr to Coordinate Stat5a-Mediated Transcription. *Molecular Endocrinology*, 25(9):1550–1564.

[97] Fiorillo, A. A., Medler, T. R., Feeney, Y. B., Wetz, S. M., Tommerdahl, K. L., and Clevenger, C. V. (2013). The prolactin receptor transactivation domain is

associated with steroid hormone receptor expression and malignant progression of breast cancer. *American Journal of Pathology*, 182(1):217–233.

[98] Fleming, J. M., Ginsburg, E., McAndrew, C. W., Heger, C. D., Cheston, L., Rodriguez-Canales, J., Vonderhaar, B. K., and Goldsmith, P. (2013). Characterization of $\Delta 7/11$, a functional prolactin-binding protein. *Journal of Molecular Endocrinology*, 50(1):79–90.

[99] Flynn, A., Whittington, H., Goffin, V., Uney, J., and Norman, M. (2004). A mutant receptor with enhanced dominant-negative activity for the blockade of human prolactin signalling. *Journal of Molecular Endocrinology*, 32(2):385–396.

[100] Freeman, M. E., Kanyicska, L. A., Lerant, A., Gyo, G., and Nagy, G. (2000). Prolactin: Structure, Function, and Regulation of Secretion.

[101] Fry, E. A., Taneja, P., and Inoue, K. (2017). Oncogenic and tumor-suppressive mouse models for breast cancer engaging HER2/neu.

[102] Fuh, G., Colosi, P., Wood, W. I., and Wells, J. A. (1993). Mechanism-based design of prolactin receptor antagonists. *The Journal of biological chemistry*, 268(8):5376–5381.

[103] Fuh, G. and Wells, J. A. (1995). Prolactin receptor antagonists that inhibit the growth of breast cancer cell lines. *Journal of Biological Chemistry*, 270(22):13133–13137.

[104] Fulford, L. G., Reis-Filho, J. S., Ryder, K., Jones, C., Gillett, C. E., Hanby, A., Easton, D., and Lakhani, S. R. (2007). Basal-like grade III invasive ductal carcinoma of the breast: Patterns of metastasis and long-term survival. *Breast Cancer Research*, 9(1):R4.

[105] Fuxe, K., Hökfelt, T., Eneroth, P., Gustafsson, J. A., and Skett, P. (1977). Prolactin-like immunoreactivity: localization in nerve terminals of rat hypothalamus. *Science (New York, N.Y.)*, 196(4292):899–900.

[106] Gadd, S. L. and Clevenger, C. V. (2006). Ligand-independent dimerization of the human prolactin receptor isoforms: Functional implications. *Molecular Endocrinology*, 20(11):2734–2746.

[107] Galsgaard, E. D., Nielsen, J. H., and Møldrup, A. (1999). Regulation of prolactin receptor (PRLR) gene expression in insulin- producing cells. Prolactin and growth hormone activate one of the rat PRLR gene promoters via STAT5a and STAT5b. *Journal of Biological Chemistry*, 274(26):18686–18692.

[108] Gascuel, O. and Danchin, A. (1986). Protein export in prokaryotes and eukaryotes: Indications of a difference in the mechanism of exportation. *Journal of Molecular Evolution*, 24(1-2):130–142.

[109] Gent, J., van Kerkhof, P., Roza, M., Bu, G., and Strous, G. J. (2002). Ligand-independent growth hormone receptor dimerization occurs in the endoplasmic reticulum and is required for ubiquitin system-dependent endocytosis. *Proceedings of the National Academy of Sciences of the United States of America*, 99(15):9858–63.

[110] Gertler, A., Grosclaude, J., Strasburger, C. J., Nir, S., and Djiane, J. (1996). Real-time kinetic measurements of the interactions between lactogenic hormones and prolactin-receptor extracellular domains from several species support the model of hormone-induced transient receptor dimerization. *Journal of Biological Chemistry*, 271(40):24482–24491.

[111] Goffin, V., Martial, J. A., and Summers, N. L. (1995). Use of a model to under-

stand prolactin and growth hormone specificities. *Protein engineering*, 8(12):1215–31.

[112] Gout, P., Beer, C., and Noble, R. (1980). Prolactin-stimulated Growth of Cell Cultures Established From Malignant Nb Rat Lymphomas. *Cancer Research*, 40(7):2433–2436.

[113] Greendale, G. A., Huang, M. H., Ursin, G., Ingles, S., Stanczyk, F., Crandall, C., Laughlin, G. A., Barrett-Connor, E., and Karlamangla, A. (2007). Serum prolactin levels are positively associated with mammographic density in postmenopausal women. *Breast Cancer Research and Treatment*, 105(3):337–346.

[114] Griffith, O. L., Chan, S. R., Griffith, M., Krysiak, K., Skidmore, Z. L., Hundal, J., Allen, J. A., Arthur, C. D., Runci, D., Bugatti, M., Miceli, A. P., Schmidt, H., Trani, L., Kanchi, K. L., Miller, C. A., Larson, D. E., Fulton, R. S., Vermi, W., Wilson, R. K., Schreiber, R. D., and Mardis, E. R. (2016). Truncating Prolactin Receptor Mutations Promote Tumor Growth in Murine Estrogen Receptor-Alpha Mammary Carcinomas. *Cell Reports*, 17(1):249–260.

[115] Groner, B. and Gouilleux, F. (1995). Prolactin-mediated gene activation in mammary epithelial cells. *Current Opinion in Genetics and Development*, 5(5):587–594.

[116] Groothuizen, F. S., Poger, D., and Mark, A. E. (2010). Activating the Prolactin Receptor: Effect of the Ligand on the Conformation of the Extracellular Domain. *Journal of chemical theory and computation*, 6:3274–3283.

[117] Grossman, R. L., Heath, A. P., Ferretti, V., Varmus, H. E., Lowy, D. R., Kibbe, W. A., and Staudt, L. M. (2016). Toward a Shared Vision for Cancer Genomic Data. *New England Journal of Medicine*, 375(12):1109–1112.

[118] Guy, P. M., Platko, J. V., Cantley, L. C., Cerione, R. A., and Carraway, K. L. (1994). Insect cell-expressed p180(erbB3) possesses an impaired tyrosine kinase activity. *Proceedings of the National Academy of Sciences of the United States of America*, 91(17):8132–8136.

[119] Haglund, F., Lu, M., Vukojević, V., Nilsson, I. L., Andreasson, A., Džabić, M., Bränström, R., Höög, A., Juhlin, C. C., and Larsson, C. (2012). Prolactin receptor in primary hyperparathyroidism - expression, functionality and clinical correlations. *PLoS ONE*, 7(5).

[120] Hammer, A. and Diakonova, M. (2015). Tyrosyl phosphorylated serine-threonine kinase pak1 is a novel regulator of prolactin-dependent breast cancer cell motility and invasion. *Advances in Experimental Medicine and Biology*, 846:97–137.

[121] Hankinson, S. E., Willett, W. C., Michaud, D. S., Manson, J. E., Colditz, G. A., Longcope, C., Rosner, B., and Speizer, F. E. (1999). Plasma Prolactin Levels and Subsequent Risk of Breast Cancer in Postmenopausal Women. *Journal of the National Cancer Institute*, 91(7):629–634.

[122] Harari, D. and Yarden, Y. (2000). Molecular mechanisms underlying ErbB2/HER2 action in breast cancer.

[123] Harding, P. A., Wang, X., Okada, S., Chen, W. Y., Wan, W., and Kopchick, J. J. (1996). Growth hormone (GH) and a GH antagonist promote GH receptor dimerization and internalization. *Journal of Biological Chemistry*, 271(12):6708–6712.

[124] Harigaya, T. and Smith, W. C. (1988). Hepatic Placental Lactogen Receptors During Pregnancy in the Mouse. 122(4).

[125] Harvey, S., Arámburo, C., and Sanders, E. J. (2012). Extrapituitary production of anterior pituitary hormones: An overview.

[126] Haxholm, G. W., Nikolajsen, L. F., Olsen, J. G., Fredsted, J., Larsen, F. H., Goffin, V., Pedersen, S. F., Brooks, A. J., Waters, M. J., and Kragelund, B. B. (2015). Intrinsically disordered cytoplasmic domains of two cytokine receptors mediate conserved interactions with membranes. *Biochemical Journal*, 468(3):495–506.

[127] Herlant, M. (1964). The Cells of the Adenohypophysis and Their Functional Significance. *International Review of Cytology*, 17(C):299–382.

[128] Herman, A., Bignon, C., Daniel, N., Grosclaude, J., Gertler, A., and Djiane, J. (2000). Functional heterodimerization of prolactin and growth hormone receptors by ovine placental lactogen. *Journal of Biological Chemistry*, 275(9):6295–6301.

[129] Herschkowitz, J. I., Simin, K., Weigman, V. J., Mikaelian, I., Usary, J., Hu, Z., Rasmussen, K. E., Jones, L. P., Assefnia, S., Chandrasekharan, S., Backlund, M. G., Yin, Y., Khramtsov, A. I., Bastein, R., Quackenbush, J., Glazer, R. I., Brown, P. H., Green, J. E., Kopelovich, L., Furth, P. A., Palazzo, J. P., Olopade, O. I., Bernard, P. S., Churchill, G. A., Van Dyke, T., and Perou, C. M. (2007). Identification of conserved gene expression features between murine mammary carcinoma models and human breast tumors. *Genome Biology*, 8(5).

[130] Holliday, D. L. and Speirs, V. (2011). Choosing the right cell line for breast cancer research.

[131] Horseman, N. D. and Yu-lee, L.-y. (1994). Transcriptional Regulation by the Helix Bundle Peptide Hormones: Growth Hormone, Prolactin, and Hematopoietic Cytokines.

[132] Hortobagyi, G. N., Stemmer, S. M., Burris, H. A., Yap, Y. S., Sonke, G. S., Paluch-Shimon, S., Campone, M., Blackwell, K. L., Andre, F., Winer, E. P., Janni, W., Verma, S., Conte, P., Arteaga, C. L., Cameron, D. A., Petrakova, K., Hart, L. L., Villanueva, C., Chan, A., Jakobsen, E., Nusch, A., Burdaeva, O., Grischke, E. M., Alba, E., Wist, E., Marschner, N., Favret, A. M., Yardley, D., Bachelot, T., Tseng, L. M., Blau, S., Xuan, F., Souami, F., Miller, M., Germa, C., Hirawat, S., and O'Shaughnessy, J. (2016). Ribociclib as first-line therapy for HR-positive, advanced breast cancer. *New England Journal of Medicine*, 375(18):1738–1748.

[133] Hotta, K., Ueyama, J., Tatsumi, Y., Tsukiyama, I., Sugiura, Y., Saito, H., Matsuura, K., and Hasegawa, T. (2015). Lack of Contribution of Multidrug Resistance-associated Protein and Organic Anion-transporting Polypeptide to Pharmacokinetics of Regorafenib, a Novel Multi-Kinase Inhibitor, in Rats. *Anticancer Research*, 35(9):4681–4689.

[134] Hu, X., Dutta, P., Tsurumi, A., Li, J., Wang, J., Land, H., and Li, W. X. (2013). Unphosphorylated STAT5A stabilizes heterochromatin and suppresses tumor growth. *Proceedings of the National Academy of Sciences of the United States of America*, 110(25):10213–10218.

[135] Hu, Z. Z., Meng, J., and Dufau, M. L. (2001). Isolation and Characterization of Two Novel Forms of the Human Prolactin Receptor Generated by Alternative Splicing of a Newly Identified Exon 11. *Journal of Biological Chemistry*, 276(44):41086–41094.

[136] Hu, Z. Z., Zhuang, L., Meng, J., and Dufau, M. L. (1998). Transcriptional regulation of the generic promoter III of the rat prolactin receptor gene by C/EBPbeta and Sp1. *The Journal of biological chemistry*, 273(40):26225–35.

[137] Hunter, S., Koch, B. L., and Anderson, S. M. (1997). Phosphorylation of cbl after Stimulation of Nb2 Cells with Prolactin and Its Association with Phosphatidylinositol 3-Kinase. *Molecular Endocrinology*, 11(9):1213–1222.

[138] Huo, D., Hu, H., Rhie, S. K., Gamazon, E. R., Cherniack, A. D., Liu, J., Yoshimatsu, T. F., Pitt, J. J., Hoadley, K. A., Troester, M., Ru, Y., Lichtenberg, T., Sturtz, L. A., Shelley, C. S., Benz, C. C., Mills, G. B., Laird, P. W., Shriver, C. D., Perou, C. M., and Olopade, O. I. (2017). Comparison of Breast Cancer Molecular Features and Survival by African and European Ancestry in The Cancer Genome Atlas. *JAMA oncology*, 3(12):1654–1662.

[139] Huo, S.-f., Shang, W.-l., Yu, M., Ren, X.-p., Wen, H.-x., Chai, C.-y., Sun, L., Hui, K., Liu, L.-h., Wei, S.-h., Wang, X.-x., Wang, Y., and Tian, Y.-x. (2020). STEAP1 facilitates metastasis and epithelialmesenchymal transition of lung adenocarcinoma via the JAK2/STAT3 signaling pathway. *Bioscience Reports*, 40(6).

[140] Hwang, P., Guyda, H., and Friesen, H. (1971). A Radioimmunoassay for Human Prolactin. 68(8):1902–1906.

[141] Ihle, J. N. and Kerr, I. M. (1995). Jaks and Stats in signaling by the cytokine receptor superfamily.

[142] Im, S. A., Lu, Y. S., Bardia, A., Harbeck, N., Colleoni, M., Franke, F., Chow, L., Sohn, J., Lee, K. S., Campos-Gomez, S., Villanueva-Vazquez, R., Jung, K. H., Chakravartty, A., Hughes, G., Gounaris, I., Rodriguez-Lorenc, K., Taran, T., Hurvitz, S., and Tripathy, D. (2019). Overall survival with ribociclib plus endocrine therapy in breast cancer. *New England Journal of Medicine*, 381(4):307–316.

[143] Ingram, D. M., Nottage, E. M., and Roberts, A. N. (1990). Prolactin and breast cancer risk. *Medical Journal of Australia*, 153(8):469–473.

[144] Jackson, L. L., Colosit, P., Talamantest, F., and Linzer, D. I. H. (1986). Molecular cloning of mouse placental lactogen cDNA. 83:8496–8500.

[145] Jaiswal, B. S., Kljavin, N. M., Stawiski, E. W., Chan, E., Parikh, C., Durinck, S., Chaudhuri, S., Pujara, K., Guillory, J., Edgar, K. A., Janakiraman, V., Scholz, R.-P., Bowman, K. K., Lorenzo, M., Li, H., Wu, J., Yuan, W., Peters, B. A., Kan, Z., Stinson, J., Mak, M., Modrusan, Z., Eigenbrot, C., Firestein, R., Stern, H. M., Rajalingam, K., Schaefer, G., Merchant, M. A., Sliwkowski, M. X., de Sauvage, F. J., and Seshagiri, S. (2013). Cancer Cell Oncogenic ERBB3 Mutations in Human Cancers. *Cancer Cell*, 23:603–617.

[146] Karunagaran, D., Tzahar, E., Beerli, R. R., Chen, X., Graus-Porta, D., Ratzkin, B. J., Seger, R., Hynes, N. E., and Yarden, Y. (1996). ErbB-2 is a common auxiliary subunit of NDF and EGF receptors: implications for breast cancer. *The EMBO Journal*, 15(2):254–264.

[147] Kavarthapu, R., Morris, C. H. T., and Dufau, M. L. (2014). Prolactin induces up-regulation of its cognate receptor in breast cancer cells via transcriptional activation of its generic promoter by cross-talk between ERa and STAT5. *Oncotarget*, 5(19):9079–9091.

[148] Keeler, C., Dannies, P. S., and Hodsdon, M. E. (2003). The Tertiary Structure and Backbone Dynamics of Human Prolactin. *Journal of Molecular Biology*, 328(5):1105–1121.

[149] Kelly, P. A., Boutin, J.-M., Jolicoeur, C., Okamura, H., Shirota, M., Edery, M., Dusanter-Fourt, I., and Djiane, J. (1989). Purification, Cloning, and Expression of the Prolactin Receptor1. *Biology of Reproduction*, 40(1):27–32.

[150] Khaled, W. T., Lee, S. C., Stingl, J., Chen, X., Ali, H. R., Rueda, O. M., Hadi, F., Wang, J., Yu, Y., Chin, S. F., Stratton, M., Futreal, A., Jenkins, N. A., Aparicio, S., Copeland, N. G., Watson, C. J., Caldas, C., and Liu, P. (2015). BCL11A is a Triple-negative breast cancer gene with critical functions in stem and progenitor cells. *Nature Communications*, 6.

[151] Kim, R. K., Suh, Y., Yoo, K. C., Cui, Y. H., Kim, H., Kim, M. J., Kim, I. G., and Lee, S. J. (2015). Activation of KRAS promotes the mesenchymal features of Basal-type breast cancer. *Experimental and Molecular Medicine*, 47(1):e137.

[152] Kinet, S., Bernichtein, S., Kelly, P. A., Martial, J. A., and Goffin, V. (1999). Biological properties of human prolactin analogs depend not only on global hormone affinity, but also on the relative affinities of both receptor binding sites. *Journal of Biological Chemistry*, 274(37):26033–26043.

[153] Kitamura, T., Hayashida, K., Sakamaki, K., Yokota, T., Arai, K. I., and Miyajima, A. (1991). Reconstitution of functional receptors for human granulocyte/macrophage colony-stimulating factor (GM-CSF): Evidence that the protein encoded by the AIC2B cDNA is a subunit of the murine GM-CSF receptor. *Proceedings of the National Academy of Sciences of the United States of America*, 88(12):5082–5086.

[154] Klapper, L. N., Vaisman, N., Hurwitz, E., Pinkas-Kramarski, R., Yarden, Y., and Sela, M. (1997). A subclass of tumor-inhibitory monoclonal antibodies to ErbB-2/HER2 blocks crosstalk with growth factor receptors. *Oncogene*, 14(17):2099–2109.

[155] Klapper, L. N., Waterman, H., Sela, M., and Yarden, Y. (2000). Tumor-

inhibitory antibodies to HER-2/ErbB-2 may act by recruiting c-Cbl and enhancing ubiquitination of HER-2. *Cancer Research*, 60(13):3384–3388.

[156] Kline, J. B. and Clevenger, C. V. (2001). Identification and Characterization of the Prolactin-binding Protein in Human Serum and Milk. *Journal of Biological Chemistry*, 276(27):24760–24766.

[157] Kline, J. B., Roehrs, H., and Clevenger, C. V. (1999). Functional characterization of the intermediate isoform of the human prolactin receptor. *Journal of Biological Chemistry*, 274(50):35461–35468.

[158] Kline, J. B., Rycyzyn, M. A., and Clevenger, C. V. (2002). Characterization of a novel and functional human prolactin receptor isoform (δS1PRLr) containing only one extracellular fibronectin-like domain. *Molecular Endocrinology*, 16(10):2310–2322.

[159] KOHMOTO, K., TSUNASAWA, S., and SAKIYAMA, F. (1984). Complete amino acid sequence of mouse prolactin. *European Journal of Biochemistry*, 138(2):227–237.

[160] Kreike, B., van Kouwenhove, M., Horlings, H., Weigelt, B., Peterse, H., Bartelink, H., and van de Vijver, M. J. (2007). Gene expression profiling and histopathological characterization of triple-negative/basal-like breast carcinomas. *Breast Cancer Research*, 9(5):R65.

[161] Kroenke, C. H., Sweeney, C., Kwan, M. L., Quesenberry, C. P., Weltzien, E. K., Habel, L. A., Castillo, A., Bernard, P. S., Factor, R. E., Kushi, L. H., and Caan, B. J. (2014). Race and breast cancer survival by intrinsic subtype based on PAM50 gene expression. *Breast Cancer Research and Treatment*, 144(3):689–699.

[162] Kubatzky, K. F., Ruan, W., Gurezka, R., Cohen, J., Ketteler, R., Watowich, S. S., Neumann, D., Langosch, D., and Klingmüller, U. (2001). Self assembly of the transmembrane domain promotes signal transduction through the erythropoietin receptor. *Current Biology*, 11(2):110–115.

[163] Lai, S. Y., Childs, E. E., Xi, S., Coppelli, F. M., Gooding, W. E., Wells, A., Ferris, R. L., and Grandis, J. R. (2005). Erythropoietin-mediated activation of JAK-STAT signaling contributes to cellular invasion in head and neck squamous cell carcinoma. *Oncogene*, 24(27):4442–4449.

[164] Lambe, M., Hsieh, C.-c., Trichopoulos, D., Ekbom, A., Pavia, M., and Adami, H.-O. (1994). Transient Increase in the Risk of Breast Cancer after Giving Birth. *New England Journal of Medicine*, 331(1):5–9.

[165] Lammert, J., Lubinski, J., Gronwald, J., Huzarski, T., Armel, S., Eisen, A., Meschino, W. S., Lynch, H. T., Snyder, C., Eng, C., Olopade, O. I., Ginsburg, O., Foulkes, W. D., Elser, C., Cohen, S. A., Kiechle, M., Narod, S. A., and Kotsopoulos, J. (2018). Physical activity during adolescence and young adulthood and the risk of breast cancer in BRCA1 and BRCA2 mutation carriers. *Breast Cancer Research and Treatment*, 169(3):561–571.

[166] Langenheim, J. F. and Chen, W. Y. (2009). Development of a novel ligand that activates JAK2/STAT5 signaling through a heterodimer of prolactin receptor and growth hormone receptor. *Journal of Receptors and Signal Transduction*, 29(2):107–112.

[167] Lebrun, J. J., Ali, S., Ullrich, A., and Kelly, P. A. (1995). Proline-rich sequence-mediated Jak2 association to the prolactin receptor is required but not sufficient for signal transduction. *Journal of Biological Chemistry*, 270(18):10664–10670.

[168] Lebrun, J.-J., Alisp, S., Sofers, L., Ullricho, A., and Kellyln, P. A. (1994). Prolactin-induced Proliferation of Nb2 Cells Involves Tyrosine Phosphorylation of the Prolactin Receptor and Its Associated Tyrosine Kinase JAK2. 269(19):14021–14026.

[169] Lemech, C., Woodward, N., Chan, N., Mortimer, J., Naumovski, L., Nuthalapati, S., Tong, B., Jiang, F., Ansell, P., Ratajczak, C. K., and Sachdev, J. (2020). A first-in-human, phase 1, dose-escalation study of ABBV-176, an antibody-drug conjugate targeting the prolactin receptor, in patients with advanced solid tumors. *Investigational New Drugs*.

[170] Lenferink, A. E., Pinkas-Kramarski, R., van de Poll, M. L., Vugt, M. J., Klapper, L. N., Tzahar, E., Waterman, H., Sela, M., van Zoelen, E. J., and Yarden, Y. (1998). Differential endocytic routing of homo and heterodimeric ErbB tyrosine kinases confers signaling superiority to receptor heterodimers. *The EMBO Journal*, 17(12):3385–3397.

[171] Levkowitz, G., Waterman, H., Zamir, E., Kam, Z., Oved, S., Langdon, W. Y., Beguinot, L., Geiger, B., and Yarden, Y. (1998). c-Cbl/Sli-1 regulates endocytic sorting and ubiquitination of the epidermal growth factor receptor.

[172] Lewis, U., Singh, R., and Seavey, B. (1971). Human prolactin: isolation and some properties. *Biochemical and biophysical research communications*, 44(5):1169–1176.

[173] Li, H., Handsaker, B., Wysoker, A., Fennell, T., Ruan, J., Homer, N., Marth, G., Abecasis, G., Durbin, R., Project, G., and Subgroup, D. P. (2009). The Sequence Alignment/Map format and SAMtools. *Bioinformatics*, 25(16):2078–2079.

[174] Li, Y., Clevenger, C. V., Minkovsky, N., Kumar, K., Raghunath, P. N., Tomaszewski, J. E., Spiegelman, V. S., and Fuchs, S. Y. (2006). Stabilization of prolactin receptor in breast cancer cells. *Oncogene*, 25(13):1896–1902.

[175] Li, Y., Suresh Kumar, K. G., Tang, W., Spiegelman, V. S., and Fuchs, S. Y. (2004). Negative Regulation of Prolactin Receptor Stability and Signaling Mediated by SCF-TrCP E3 Ubiquitin Ligase. *Molecular and Cellular Biology*, 24(9):4038–4048.

[176] LIEBELT, A. G. and LIEBELT, R. A. (1961). Effects of single pituitary isograft on mammary tumorigenesis in mice. *Cancer research*, 21(1):86–91.

[177] Ling, C., Svensson, L., Odén, B., Weijdegård, B., Edén, B., Edén, S., and Billig, H. (2003). Identification of Functional Prolactin (PRL) Receptor Gene Expression: PRL Inhibits Lipoprotein Lipase Activity in Human White Adipose Tissue. *The Journal of Clinical Endocrinology & Metabolism*, 88(4):1804–1808.

[178] Liscia, D. S., Alhadi, T., and Vonderhaar, B. K. (1982). Solubilization of active prolactin receptors by a nondenaturing zwitterionic detergent. *The Journal of biological chemistry*, 257(16):9401–5.

[179] Liscia, D. S. and Vonderhaar, B. K. (1982). Purification of a prolactin receptor. *Proceedings of the National Academy of Sciences of the United States of America*, 79(19 I):5930–5934.

[180] Liu, C. R., Li, Q., Hou, C., Li, H., Shuai, P., Zhao, M., Zhong, X. R., Xu, Z. P., and Li, J. Y. (2018). Changes in body mass index, leptin, and leptin receptor polymorphisms and breast cancer risk. *DNA and Cell Biology*, 37(3):182–188.

[181] Liu, X., Robinson, G. W., Gouilleux, F., Groner, B., and Hennighausen, L.

(1995). Cloning and expression of Stat5 and an additional homologue (Stat5b) involved in prolactin signal transduction in mouse mammary tissue. *Proceedings of the National Academy of Sciences of the United States of America*, 92(19):8831–8835.

[182] Liu, Y., Jiang, J., Lepik, B., Zhang, Y., Zinn, K. R., and Frank, S. J. (2017). Subdomain 2, not the transmembrane domain, determines the dimerization partner of growth hormone receptor and prolactin receptor. *Endocrinology*, 158(10):3235–3248.

[183] Livnah, O., Stura, E. A., Middleton, S. A., Johnson, D. L., Jolliffe, L. K., and Wilson, I. A. (1999). Crystallographic evidence for preformed dimers of erythropoietin receptor before ligand activation. *Science (New York, N.Y.)*, 283(5404):987–90.

[184] Llovera, M., Pichard, C., Bernichtein, S., Jeay, S., Touraine, P., Kelly, P. A., and Goffin, V. (2000). Human prolactin (hPRL) antagonists inhibit hPRL-activated signaling pathways involved in breast cancer cell proliferation. *Oncogene*, 19(41):4695–4705.

[185] Love, M. I., Huber, W., and Anders, S. (2014). Moderated estimation of fold change and dispersion for RNA-seq data with DESeq2. *Genome Biology*, 15(12):550.

[186] Lu, J.-C., Piazza, T. M., and Schuler, L. A. (2005). Proteasomes Mediate Prolactin-induced Receptor Down-regulation and Fragment Generation in Breast Cancer Cells.

[187] Malarkey, W. B., Schroeder, L. L., Stevens, V. C., James, A. G., and Lããese, R. R. (1977). Disordered Nocturnal Prolactin Regulation in Women with Breast Cancer1. 37:4650–4654.

[188] Manhès, C., Kayser, C., Bertheau, P., Kelder, B., Kopchick, J. J., Kelly, P. A., Touraine, P., and Goffin, V. (2006). Local over-expression of prolactin in differentiating mouse mammary gland induces functional defects and benign lesions, but no carcinoma. *Journal of Endocrinology*, 190(2):271–285.

[189] Maniatis, T. and Reed, R. (1987). The role of small nuclear ribonucleoprotein particles in pre-mRNA splicing. *Nature*, 325(6106):673–678.

[190] Manni, A., Chambers, M. J., and Pearson, O. H. (1978). Prolactin Induces Its Own Receptors in Rat Liver*. 103(6).

[191] Marcuzzi, F., Zucchelli, S., Bertuzzi, M., Santoro, C., Tell, G., Carninci, P., and Gustincich, S. (2016). Isoforms of the Erythropoietin receptor in dopaminergic neurons of the Substantia Nigra. *Journal of Neurochemistry*, 139(4):596–609.

[192] May, P., Gerhartz, C., Heesel, B., Welte, T., Doppler, W., Graeve, L., Horn, F., and Heinrich, P. C. (1996). Comparative study on the phosphotyrosine motifs of different cytokine receptors involved in STAT5 activation. *FEBS Letters*, 394(2):221–226.

[193] Meng, J., Tsai-Morris, C. H., and Dufau, M. L. (2004). Human prolactin receptor variants in breast cancer: Low ratio of short forms to the long-form human prolactin receptor associated with mammary carcinoma. *Cancer Research*, 64(16):5677–5682.

[194] Mercado, M. and Baumann, G. (1994). A growth hormone/prolactin-binding protein in human milk. *Journal of Clinical Endocrinology and Metabolism*, 79(6):1637–1641.

[195] Minh Hung, H., Dieu Hang, T., and Nguyen, M. T. (2019). Structural Investigation of Human Prolactin Receptor Transmembrane Domain Homodimerization in a Membrane Environment through Multiscale Simulations. *Journal of Physical Chemistry B*, 123(23):4858–4866.

[196] Mitra, S., Ring, A. M., Amarnath, S., Spangler, J. B., Li, P., Ju, W., Fischer, S., Oh, J., Spolski, R., Weiskopf, K., Kohrt, H., Foley, J. E., Rajagopalan, S., Long, E. O., Fowler, D. H., Waldmann, T. A., Garcia, K. C., and Leonard, W. J. (2015). Interleukin-2 Activity Can Be Fine Tuned with Engineered Receptor Signaling Clamps. *Immunity*, 42(5):826–838.

[197] Mormando, M., Chiloiro, S., Bianchi, A., Giampietro, A., Angelini, F., Tartaglione, L., Nasto, L., Milardi, D., Formenti, A., Giustina, A., and De Marinis, L. (2016). Growth hormone receptor isoforms and fracture risk in adult-onset growth hormone-deficient patients. *Clinical Endocrinology*, 85(5):717–724.

[198] Motamedi, B., Rafiee-Pour, H. A., Khosravi, M. R., Kefayat, A., Baradaran, A., Amjadi, E., and Goli, P. (2020). Prolactin receptor expression as a novel prognostic biomarker for triple negative breast cancer patients. *Annals of Diagnostic Pathology*, 46.

[199] Murakami, M., Narazaki, M., Hibi, M., Yawata, H., Yasukawa, K., Hamaguchi, M., Taga, T., and Kishimoto, T. (1991). Critical cytoplasmic region of the interleukin 6 signal transducer gp130 is conserved in the cytokine receptor family. *Proceedings of the National Academy of Sciences of the United States of America*, 88(24):11349–11353.

[200] Nagano, M. and Kelly, P. A. (1994). Tissue distribution and regulation of

rat prolactin receptor gene expression. Quantitative analysis by polymerase chain reaction. *Journal of Biological Chemistry*, 269(18):13337–13345.

[201] Nagrani, R., Mhatre, S., Rajaraman, P., Soerjomataram, I., Boffetta, P., Gupta, S., Parmar, V., Badwe, R., and Dikshit, R. (2016). Central obesity increases risk of breast cancer irrespective of menopausal and hormonal receptor status in women of South Asian Ethnicity. *European Journal of Cancer*, 66.

[202] Narod, S. A., Iqbal, J., Giannakeas, V., Sopik, V., and Sun, P. (2015). Breast cancer mortality after a diagnosis of ductal carcinoma in situ. *JAMA Oncology*, 1(7):888–896.

[203] Neilson, H. K., Farris, M. S., Stone, C. R., Vaska, M. M., Brenner, D. R., and Friedenreich, C. M. (2017). Moderate-vigorous recreational physical activity and breast cancer risk, stratified by menopause status. *Menopause*, 24(3):322–344.

[204] Neilson, L. M., Zhu, J., Xie, J., Malabarba, M. G., Sakamoto, K., Wagner, K. U., Kirken, R. A., and Rui, H. (2007). Coactivation of Janus tyrosine kinase (Jak)1 positively modulates prolactin-Jak2 signaling in breast cancer: Recruitment of ERK and signal transducer and activator of transcription (Stat)3 and enhancement of Akt and Stat5a/b pathways. *Molecular Endocrinology*, 21(9):2218–2232.

[205] Nevalainen, M. T., Xie, J., Torhorst, J., Bubendorf, L., Haas, P., Kononen, J., Sauter, G., and Rui, H. (2004). Signal transducer and activator of transcription-5 activation and breast cancer prognosis. *Journal of Clinical Oncology*, 22(11):2053–2060.

[206] Niall, H. D., Hogan, M. L., Sauer, R., Rosenblum, I. Y., and Greenwood, F. C. (1971). Sequences of pituitary and placental lactogenic and growth hormones:

evolution from a primordial peptide by gene reduplication. *Proceedings of the National Academy of Sciences of the United States of America*, 68(4):866–70.

[207] Nosaka, T., Kawashima, T., Misawa, K., Ikuta, K., Mui, A. L., and Kitamura, T. (1999). STAT5 as a molecular regulator of proliferation, differentiation and apoptosis in hematopoietic cells. *The EMBO Journal*, 18(17):4754–4765.

[208] O'Leary, K. A., Shea, M. P., and Schuler, L. A. (2015). Modeling Prolactin Actions in Breast Cancer In Vivo: Insights from the NRL-PRL Mouse. *Advances in Experimental Medicine and Biology*, 846:201–220.

[209] Olsen, J. G. and Kragelund, B. B. (2014). Who climbs the tryptophan ladder? On the structure and function of the WSXWS motif in cytokine receptors and thrombospondin repeats.

[210] Olsen, S. N., Wronski, A., Castaño, Z., Dake, B., Malone, C., De Raedt, T., Enos, M., Derose, Y. S., Zhou, W., Guerra, S., Loda, M., Welm, A., Partridge, A. H., McAllister, S. S., Kuperwasser, C., and Cichowski, K. (2017). Loss of RasGAP tumor suppressors underlies the aggressive nature of luminal B breast cancers. *Cancer Discovery*, 7(2):202–217.

[211] Ormandy, C. J., Hall, R. E., Manning, D. L., Robertson, J. F. R., Blamey, R. W., Kelly, P. A., Nicholson, R. I., and Sutherland, R. L. (1997). Coexpression and Cross-Regulation of the Prolactin Receptor and Sex Steroid Hormone Receptors in Breast Cancer 1 . *The Journal of Clinical Endocrinology & Metabolism*, 82(11):3692–3699.

[212] Pansini, F., Bianchi, A., Zito, V., Mollica, G., Cavallini, A. R., Candini, G. C., Bagni, B., Bergamini, C., and Bassi, P. (1983). Blood prolactin levels: Influence of age, menstrual cycle and oral contraceptives. *Contraception*, 28(3):201–207.

[213] Parganas, E., Wang, D., Stravopodis, D., Topham, D. J., Marine, J. C., Teglund, S., Vanin, E. F., Bodner, S., Colamonici, O. R., Van Deursen, J. M., Grosveld, G., and Ihle, J. N. (1998). Jak2 is essential for signaling through a variety of cytokine receptors. *Cell*, 93(3):385–395.

[214] Patro, R., Duggal, G., Love, M. I., Irizarry, R. A., and Kingsford, C. (2017). Salmon provides fast and bias-aware quantification of transcript expression. *Nature Methods*, 14(4):417–419.

[215] Peeters, S., Friesen, H. G., and Rodbard, D. (1977). A growth hormone binding factor in the serum of pregnant mice. *Endocrinology*, 101(4):1164–1183.

[216] Peles, E., Lamprecht, R., Ben-Levy, R., Tzahar, E., and Yarden, Y. (1992). T H E JOURNAL OF BIOLOGICAL CHEMISTRY Regulated Coupling of the Neu Receptor to Phosphatidylinositol 3"Kinase and Its Release by Oncogenic Activation*. 267(17):12266–12274.

[217] Perou, C. M., Sørile, T., Eisen, M. B., Van De Rijn, M., Jeffrey, S. S., Ress, C. A., Pollack, J. R., Ross, D. T., Johnsen, H., Akslen, L. A., Fluge, Ø., Pergammenschlkov, A., Williams, C., Zhu, S. X., Lønning, P. E., Børresen-Dale, A. L., Brown, P. O., and Botstein, D. (2000). Molecular portraits of human breast tumours. *Nature*, 406(6797):747–752.

[218] Pezet, A., Buteau, H., Kelly, P. A., and Edery, M. (1997). The last proline of Box 1 is essential for association with JAK2 and functional activation of the prolactin receptor. *Molecular and Cellular Endocrinology*, 129(2):199–208.

[219] Plotnikov, A., Li, Y., Tran, T. H., Tang, W., Palazzo, J. P., Rui, H., and Fuchs, S. Y. (2008). Oncogene-mediated inhibition of glycogen synthase kinase 3β impairs degradation of prolactin receptor. *Cancer Research*, 68(5):1354–1361.

[220] Plotnikov, A., Varghese, B., Tran, T. H., Liu, C., Rui, H., and Fuchs, S. Y. (2009). Impaired turnover of prolactin receptor contributes to transformation of human breast cells. *Cancer Research*, 69(7):3165–3172.

[221] Poh, A. (2020). Proof-of-Concept with PROTACs in Prostate Cancer. *Cancer Discovery News in Brief*, page 1084.

[222] Popnikolov, N., Brzezinska, K., Platoff, R. M., Binnebose, R., Rothstein-Rubin, R., Komarnicky, L. T., and Woodworth, A. (2020). Upregulation of Prolactin Receptor Expression and Activation of Prolactin Signaling in an Aggressive Triple-Negative Breast Carcinoma During Pregnancy: A Case Report. *Clinical Breast Cancer*.

[223] Posner, B. I., Kelly, P. A., and Friesen, H. G. (1975). Prolactin receptors in rat liver: Possible induction by prolactin. *Science*, 188(4183):57–59.

[224] Postel-Vinay, M. C. (1996). Growth Hormone- and Prolactin-Binding Proteins: Soluble Forms of Receptors. *Human Heredity*, 45(3-5):178–181.

[225] Postel-Vinay, M. C., Belair, L., Kayser, C., Kelly, P. A., and Djiane, J. (1991). Identification of prolactin and growth hormone binding proteins in rabbit milk. *Proceedings of the National Academy of Sciences of the United States of America*, 88(15):6687–90.

[226] Prat, A., Parker, J. S., Karginova, O., Fan, C., Livasy, C., Herschkowitz, J. I., He, X., and Perou, C. M. (2010). Phenotypic and molecular characterization of the claudin-low intrinsic subtype of breast cancer.

[227] Prat, A. and Perou, C. M. (2011). Deconstructing the molecular portraits of breast cancer.

[228] Prat, A., Pineda, E., Adamo, B., Galv An, P., Fern Andez, A., Gaba, L., Díez, M., Viladot, M., Arance, A., and Mu ˜ Noz, M. (2015). Clinical implications of the intrinsic molecular subtypes of breast cancer.

[229] Qazi, A. M., Tsai-Morris, C. H., and Dufau, M. L. (2006). Ligand-independent homo- and heterodimerization of human prolactin receptor variants: Inhibitory action of the short forms by heterodimerization. *Molecular Endocrinology*, 20(8):1912–1923.

[230] R Core Team (2017). *R: A Language and Environment for Statistical Computing*. R Foundation for Statistical Computing, Vienna, Austria.

[231] Rahman, T., Clevenger, C. V., Kaklamani, V., Lauriello, J., Campbell, A., Malwitz, K., and Kirkland, R. S. (2014). Antipsychotic treatment in breast cancer patients.

[232] Rane, S. G. and Reddy, E. P. (2000). Janus kinases: Components of multiple signaling pathways. *Oncogene*, 19(49):5662–5679.

[233] Ren, S., Hong, R. C., Li, M., and Furth, P. A. (2002). Loss of Stat5a delays mammary cancer progression in a mouse model. *Oncogene*, 21(27):4335–4339.

[234] Reynolds, C., Montone, K. T., Powell, C. M., Tomaszewski, J. E., and Clevenger, C. V. (1997). Expression of prolactin and its receptor in human breast carcinoma. *Endocrinology*, 138(12):5555–5560.

[235] Rice, M. S., Tworoger, S. S., Bertrand, K. A., Hankinson, S. E., Rosner, B. A., Feeney, Y. B., Clevenger, C. V., and Tamimi, R. M. (2015). Immunoassay and Nb2 lymphoma bioassay prolactin levels and mammographic density in premenopausal

and postmenopausal women the Nurses' Health Studies. *Breast Cancer Research and Treatment*.

[236] Richards, J. F., Beer, C. T., Bourgeault, C., Chen, K., and Gout, P. W. (1982). Biochemical response of lymphoma cells to mitogenic stimulation by prolactin. *Molecular and Cellular Endocrinology*, 26(1-2):41–49.

[237] Riddle, O., Bates, R. W., and Dykshorn, S. W. (1933). The preparation, identification, and assay of prolactin - a hormone of the anterior pituitary. *American Journal of Physiology-Legacy Content*, 105(1):191–216.

[238] Rider, L., Oladimeji, P., and Diakonova, M. (2013). PAK1 Regulates Breast Cancer Cell Invasion through Secretion of Matrix Metalloproteinases in Response to Prolactin and Three-Dimensional Collagen IV. *Molecular Endocrinology*, 27(7):1048–1064.

[239] Rose-Hellekant, T. A., Arendt, L. M., Schroeder, M. D., Gilchrist, K., Sandgren, E. P., and Schuler, L. A. (2003). Prolactin induces ERalpha-positive and ERalpha-negative mammary cancer in transgenic mice. *Oncogene*, 22(30):4664–4674.

[240] Rose-Hellekant, T. A., Schroeder, M. D., Brockman, J. L., Zhdankin, O., Bolstad, R., Chen, K. S., Gould, M. N., Schuler, L. A., and Sandgren, E. P. (2007). Estrogen receptor-positive mammary tumorigenesis in TGFα transgenic mice progresses with progesterone receptor loss. *Oncogene*, 26(36):5238–5246.

[241] Ross, C., Szczepanek, K., Lee, M., Yang, H., Qiu, T., and Sanford, J. (2020). The genomic landscape of metastasis in treatment-naïve breast cancer models. *PLOS Genetics*.

[242] Ross, R. (1999). Truncated growth hormone receptor isoforms. *Acta Paediatrica*, 88(s428):164–166.

[243] Ross, R. J., Leung, K. C., Maamra, M., Bennett, W., Doyle, N., Waters, M. J., and Ho, K. K. (2001). Binding and functional studies with the growth hormone receptor antagonist, B2036-PEG (pegvisomant), reveal effects of pegylation and evidence that it binds to a receptor dimer. *The Journal of clinical endocrinology and metabolism*, 86(4):1716–23.

[244] Rozakis-Adcock, M. and Kelly, P. A. (1991). Mutational analysis of the ligand-binding domain of the prolactin receptor. *The Journal of biological chemistry*, 266(25):16472–7.

[245] Rui, H., Kirken, R. A., and Farrar, W. L. (1994a). Activation of Receptor-associated Tyrosine Kinase JAK2 by Prolactin. *The Journal of Biological Chemistry*, 269(7):5364–5368.

[246] Rui, H., Lebrun, J. J., Kirken, R. A., Kelly, P. A., and Farrar, W. L. (1994b). JAK2 activation and cell proliferation induced by antibody-mediated prolactin receptor dimerization. *Endocrinology*, 135(4):1299–306.

[247] Rui, H., Utama, F., Yanac, A., Xia, G., Peck, A., Liu, C., Rosenberg, A., Wagner, K.-U., and Yang, N. (2012). Abstract S1-8: Prolactin-humanized mice: an improved animal recipient for therapy response-testing of patient-derived breast cancer xenotransplants. pages S1–8–S1–8. American Association for Cancer Research (AACR).

[248] Rycyzyn, M. A. and Clevenger, C. V. (2002). The intranuclear prolactin/cyclophilin B complex as a transcriptional inducer. *Proceedings of the National Academy of Sciences of the United States of America*, 99(10):6790–6795.

[249] Sakamoto, K. M., Kim, K. B., Kumagai, A., Mercurio, F., Crews, C. M., and Deshaies, R. J. (2001). Protacs: Chimeric molecules that target proteins to the Skp1-Cullin-F box complex for ubiquitination and degradation. *Proceedings of the National Academy of Sciences of the United States of America*, 98(15):8554–8559.

[250] Shapiro, M. B. and Senapathy, P. (1987). RNA splice junctions of different classes of eukaryotes: sequence statistics and functional implications in gene expression. *Nucleic Acids Research*, 15(17):7155–7174.

[251] Shemanko, C. S. (2016). Prolactin receptor in breast cancer: marker for metastatic risk. *Journal of molecular endocrinology*, 57(4):R153–R165.

[252] Shi, F., Telesco, S. E., Liu, Y., Radhakrishnan, R., and Lemmona, M. A. (2010). ErbB3/HER3 intracellular domain is competent to bind ATP and catalyze autophosphorylation. *Proceedings of the National Academy of Sciences of the United States of America*, 107(17):7692–7697.

[253] Shirota, M., Banville, D., Ali, S., Jolicoeur, C., Boutin, J. M., Edery, M., Djiane, J., and Kelly, P. A. (1990). Expression of two forms of prolactin receptor in rat ovary and liver. *Molecular Endocrinology*, 4(8):1136–1143.

[254] Shiu, R. P. C. (1979). Prolactin Receptors in Human Breast Cancer Cells in Long-Term Tissue Culture. *Cancer Research*, 39(11).

[255] Shome, B. and Parlow, A. F. (1977). Human pituitary prolactin (hPRL): the entire linear amino acid sequence. *The Journal of clinical endocrinology and metabolism*, 45(5):1112–5.

[256] SHULL, J. D. and GORSKI, J. (1989). Estrogen Regulation of Prolactin Gene

Transcription in Vivo: Paradoxical Effects of 17β-Estradiol Dose. *Endocrinology*, 124(1):279–285.

[257] SINHA, Y. N. (1995). Structural Variants of Prolactin: Occurrence and Physiological Significance. *Endocrine Reviews*, 16(3):354–369.

[258] Somers, W., Ultsch, M., De Vos, A. M., and Kossiakoff, A. A. (1994). The X-ray structure of a growth hormone-prolactin receptor complex. *Nature*, 372(6505):478–481.

[259] Song, J., Ding, F., Li, S., Peng, S., Zhu, Y., and Xue, K. (2018). Prolactin stimulation affects the stem cell-dependent mammary repopulating ability of embryonic mammary anlagen. *International Journal of Developmental Biology*, 62(9-10):623–629.

[260] Sorkin, A., Di Fiore, P., and Carpenter, G. (1993). The Carboxyl Terminus of Epidermal Growth Factor receptor/erbB-2 Chimerae Is Internalization Impaired - PubMed. *Oncogene*, 8(11):3021–3028.

[261] Soule, H. D., Maloney, T. M., Wolman, S. R., Peterson, W. D., Brenz, R., McGrath, C. M., Russo, J., Pauley, R. J., Jones, R. F., and Brooks, S. C. (1990). Isolation and characterization of a spontaneously immortalized human breast epithelial cell line, MCF-10. *Cancer research*, 50(18):6075–86.

[262] Stricker, P. and Grueter, R. (1928). Action du lobe anterieur de l'hypophyse sur la montee laiteuse. *C R Soc Biol*, 99.

[263] Subramanian, A., Tamayo, P., Mootha, V. K., Mukherjee, S., Ebert, B. L., Gillette, M. A., Paulovich, A., Pomeroy, S. L., Golub, T. R., Lander, E. S.,

and Mesirov, J. P. (2005). Gene set enrichment analysis: A knowledge-based approach for interpreting genome-wide expression profiles. *Proceedings of the National Academy of Sciences of the United States of America*, 102(43):15545–15550.

[264] Sutherland, A., Forsyth, A., Cong, Y., Grant, L., Juan, T.-H., Lee, J. K., Klimowicz, A., Petrillo, S. K., Hu, J., Chan, A., Boutillon, F., Goffin, V., Egan, C., Tang, P. A., Cai, L., Morris, D., Magliocco, A., and Shemanko, C. S. (2015). The Role of Prolactin in Bone Metastasis and Breast Cancer Cell-Mediated Osteoclast Differentiation.

[265] Suzuki, R., Iwasaki, M., Hara, A., Inoue, M., Sasazuki, S., Sawada, N., Yamaji, T., Shimazu, T., and Tsugane, S. (2013). Fruit and vegetable intake and breast cancer risk defined by estrogen and progesterone receptor status: The Japan Public Health Center-based Prospective Study. *Cancer Causes and Control*, 24(12):2117–2128.

[266] Svensson, L. A., Bondensgaard, K., Nørskov-Lauritsen, L., Christensen, L., Becker, P., Andersen, M. D., Maltesen, M. J., Rand, K. D., and Breinholt, J. (2008). Crystal Structure of a Prolactin Receptor Antagonist Bound to the Extracellular Domain of the Prolactin Receptor.

[267] Swaminathan, G., Varghese, B., and Fuchs, S. Y. (2008a). Regulation of prolactin receptor levels and activity in breast cancer.

[268] Swaminathan, G., Varghese, B., Thangavel, C., Carbone, C. J., Plotnikov, A., Kumar, K. G., Jablonski, E. M., Clevenger, C. V., Goffin, V., Deng, L., Frank, S. J., and Fuchs, S. Y. (2008b). Prolactin stimulates ubiquitination, initial internalization, and degradation of its receptor via catalytic activation of Janus kinase 2. *Journal of Endocrinology*, 196(2).

[269] Syed, F., Rycyzyn, M. A., Westgate, L., and Clevenger, C. V. (2003). A novel and functional interaction between cyclophilin A and prolactin receptor. *Endocrine*, 20(1-2):83–89.

[270] Syed, R. S., Reid, S. W., Li, C., Cheetham, J. C., Aoki, K. H., Liu, B., Zhan, H., Osslund, T. D., Chirino, A. J., Zhang, J., Finer-Moore, J., Elliott, S., Sitney, K., Katz, B. A., Matthews, D. J., Wendoloski, J. J., Egrie, J., and Stroud, R. M. (1998). Efficiency of signalling through cytokine receptors depends critically on receptor orientation. *Nature*, 395(6701):511–6.

[271] Tamiya, T., Kashiwagi, I., Takahashi, R., Yasukawa, H., and Yoshimura, A. (2011). Suppressors of cytokine signaling (SOCS) proteins and JAK/STAT pathways: Regulation of T-cell inflammation by SOCS1 and SOCS3. *Arteriosclerosis, Thrombosis, and Vascular Biology*, 31(5):980–985.

[272] Tan, D., Huang, K. T., Ueda, E., and Walker, A. M. (2008). S2 deletion variants of human PRL receptors demonstrate that extracellular domain conformation can alter conformation of the intracellular signaling domain. *Biochemistry*, 47(1):479–489.

[273] Trott, J. F., Hovey, R. C., Koduri, S., and Vonderhaar, B. K. (2003). Alternative splicing to exon 11 of human prolactin receptor gene results in multiple isoforms including a secreted prolactin-binding protein.

[274] Trott, J. F., Hovey, R. C., Koduri, S., and Vonderhaar, B. K. (2004). Multiple new isoforms of the human prolactin receptor gene. *Advances in experimental medicine and biology*, 554:495–9.

[275] Truong, A., Duez, C., Belayew, A., Renard, A., Pictet, R., Bell, G., and Martial,

J. (1984). Isolation and characterization of the human prolactin gene. *The EMBO Journal*, 3(2):429–437.

[276] Turner, N. C., Slamon, D. J., Ro, J., Bondarenko, I., Im, S. A., Masuda, N., Colleoni, M., DeMichele, A., Loi, S., Verma, S., Iwata, H., Harbeck, N., Loibl, S., André, F., Theall, K. P., Huang, X., Giorgetti, C., Bartlett, C. H., and Cristofanilli, M. (2018). Overall survival with palbociclib and fulvestrant in advanced breast cancer. *New England Journal of Medicine*, 379(20):1926–1936.

[277] Tworoger, S. S., Eliassen, a. H., Sluss, P., and Hankinson, S. E. (2007). A prospective study of plasma prolactin concentrations and risk of premenopausal and postmenopausal breast cancer. *Journal of clinical oncology : official journal of the American Society of Clinical Oncology*.

[278] Tworoger, S. S., Eliassen, A. H., Zhang, X., Qian, J., Sluss, P. M., Rosner, B. A., and Hankinson, S. E. (2013). A 20-year prospective study of plasma prolactin as a risk marker of breast cancer development. *Cancer Research*.

[279] Tworoger, S. S., Rice, M. S., Rosner, B. A., Feeney, Y. B., Clevenger, C. V., and Hankinson, S. E. (2015). Bioactive prolactin levels and risk of breast cancer: A nested case-control study. *Cancer Epidemiology Biomarkers and Prevention*.

[280] Tworoger, S. S., Sluss, P., and Hankinson, S. E. (2006). Association between plasma prolactin concentrations and risk of breast cancer among predominately premenopausal women. *Cancer Research*.

[281] Urbanski, L. M., Leclair, N., and Anczuków, O. (2018). Alternative-splicing defects in cancer: Splicing regulators and their downstream targets, guiding the way to novel cancer therapeutics.

[282] Utama, F. E., LeBaron, M. J., Neilson, L. M., Sultan, A. S., Parlow, A. F., Wagner, K. U., and Rui, H. (2006). Human prolactin receptors are insensitive to mouse prolactin: Implications for xenotransplant modeling of human breast cancer in mice. *Journal of Endocrinology*, 188(3):589–601.

[283] Utama, F. E., Tran, T. H., Ryder, A., LeBaron, M. J., Parlow, A. F., and Rui, H. (2009). Insensitivity of Human Prolactin Receptors to Nonhuman Prolactins: Relevance for Experimental Modeling of Prolactin Receptor-Expressing Human Cells. *Endocrinology*, 150(4):1782–1790.

[284] van Maaren, M. C., de Munck, L., Strobbe, L. J., Sonke, G. S., Westenend, P. J., Smidt, M. L., Poortmans, P. M., and Siesling, S. (2019). Ten-year recurrence rates for breast cancer subtypes in the Netherlands: A large population-based study. *International Journal of Cancer*, 144(2):263–272.

[285] Varghese, B., Barriere, H., Carbone, C. J., Banerjee, A., Swaminathan, G., Plotnikov, A., Xu, P., Peng, J., Goffin, V., Lukacs, G. L., and Fuchs, S. Y. (2008). Polyubiquitination of Prolactin Receptor Stimulates Its Internalization, Postinternalization Sorting, and Degradation via the Lysosomal Pathway. *Molecular and Cellular Biology*, 28(17):5275–5287.

[286] Vonderhaar, B. and Das, R. (1996). Involvement of SHC, GRB2, SOS and RAS in prolactin signal transduction in mammary epithelial cells. *Oncogene*, 13(6):1139–1145.

[287] Wada, T., Qian, X., and Greene, M. I. (1990). Intermolecular Association of the pl8Wu Protein and EGF Receptor Modulates EGF Receptor Function. 61:1339–1347.

[288] Wagner, K., Couillard-Despres, S., Lehner, B., Brockhoff, G., Rivera, F. J., Blume, A., Neumann, I., and Aigner, L. (2009). Prolactin induces MAPK signaling in neural progenitors without alleviating glucocorticoid-induced inhibition of in vitro neurogenesis. *Cellular Physiology and Biochemistry*, 24(5-6):397–406.

[289] Walker, A., Peabody, C., Ho, T., and Warner, M. (1992). 50 kD Prolactin Binding Protein in Schizophrenics on Neuroleptic Medication. *Journal of psychiatry and neuroscience*, 17(2):61–67.

[290] Wang, R., Lv, Q., Meng, W., Tan, Q., Zhang, S., Mo, X., and Yang, X. (2014). Comparison of mammosphere formation from breast cancer cell lines and primary breast tumors. *Journal of Thoracic Disease*, 6(6):829–837.

[291] Wang, X., Lupardus, P., LaPorte, S. L., and Garcia, K. C. (2009). Structural Biology of Shared Cytokine Receptors. *Annual Review of Immunology*, 27(1):29–60.

[292] Welsch, C. W. and Gribler, C. (1973). Prophylaxis of Spontaneously Developing Mammary Carcinoma in C3H/HeJ Female Mice by Suppression of Prolactin. *Cancer Research*, 33(11).

[293] Welsch, C. W. and Nagasawa, H. (1977). Prolactin and murine mammary tumorigenesis: a review. *Cancer research*, 37(4):951–963.

[294] Welte, T., Garimorth, K., Philipp, S., and Doppler, W. (1994). Prolactin-dependent activation of a tyrosine phosphorylated DNA binding factor in mouse mammary epithelial cells. *Molecular Endocrinology*, 8(8):1091–1102.

[295] Wen, Y., Wang, Y., Chelariu-Raicu, A., Stur, E., Liu, Y., Corvigno, S., Bartsch, F., Redfern, L., Zand, B., Kang, Y., Liu, J., Baggerly, K., and Sood, A. K. (2020).

Blockade of the short-form of prolactin receptor induces FOXO3a/EIF-4EBP1-mediated cell death in uterine cancer. *Molecular Cancer Therapeutics*, page molcanther.1026.2019.

[296] Wennbo, H., Gebre-Medhin, M., Gritli-Linde, A., Ohlsson, C., Isaksson, O. G., and Törnell, J. (1997). Activation of the prolactin receptor but not the growth hormone receptor is important for induction of mammary tumors in transgenic mice. *Journal of Clinical Investigation*, 100(11):2744–2751.

[297] White, A. J., Nichols, H. B., Bradshaw, P. T., and Sandler, D. P. (2015). Overall and central adiposity and breast cancer risk in the sister study.

[298] Wright, K. L., Adams, J. R., Liu, J. C., Loch, A. J., Wong, R. G., Jo, C. E., Beck, L. A., Santhanam, D. R., Weiss, L., Mei, X., Lane, T. F., Koralov, S. B., Done, S. J., Woodgett, J. R., Zacksenhaus, E., Hu, P., and Egan, S. E. (2015). Ras signaling is a key determinant for metastatic dissemination and poor survival of luminal breast cancer patients. *Cancer Research*, 75(22):4960–4972.

[299] Xu, J., Zhang, Y., Berry, P. A., Jiang, J., Lobie, P. E., Langenheim, J. F., Chen, W. Y., and Frank, S. J. (2011). Growth Hormone Signaling in Human T47D Breast Cancer Cells: Potential Role for a Growth Hormone Receptor-Prolactin Receptor Complex. *Molecular Endocrinology*, 25(4):597–610.

[300] Yamaguchi, M., Erdenebaatar, C., Saito, F., Honda, R., Ohba, T., Kyo, S., Tashiro, H., and Katabuchi, H. (2019). Prolactin Enhances the Proliferation of Proliferative Endometrial Glandular Cells and Endometrial Cancer Cells. *Journal of the Endocrine Society*, 4(2).

[301] Yamauchi, T., Yamauchi, N., Ueki, K., Sugiyama, T., Waki, H., Miki, H., Tobe, K., Matsuda, S., Tsushima, T., Yamamoto, T., Fujita, T., Taketani, Y., Fukayama,

M., Kimura, S., Yazaki, Y., Nagai, R., and Kadowaki, T. (2000). Constitutive tyrosine phosphorylation of ErbB-2 via Jak2 by autocrine secretion of prolactin in human breast cancer. *Journal of Biological Chemistry*, 275(43):33937–33944.

[302] Yonezawa, T., Chen, K. H., Ghosh, M. K., Rivera, L., Dill, R., Ma, L., Villa, P. A., Kawaminami, M., and Walker, A. M. (2015). Anti-metastatic outcome of isoform-specific prolactin receptor targeting in breast cancer. *Cancer Letters*, 366(1):84–92.

[303] Yuan, J., Ma, Y., Huang, T., Chen, Y., Peng, Y., Li, B., Li, J., Zhang, Y., Song, B., Sun, X., Ding, Q., Song, Y., and Chang, X. (2018). Genetic Modulation of RNA Splicing with a CRISPR-Guided Cytidine Deaminase. *Molecular Cell*, 72(2):380–394.e7.

[304] Zhang, R., Buczko, E., Tsai-Morris, C.-H., Hu, Z.-Z., and Dufau, M. L. (1990). Isolation and characterization of two novel rat ovarian lactogen receptor cDNA species. *BIOCHEMICAL AND BIOPHYSICAL RESEARCH COMMUNICATIONS*, 168(2):415–422.

[305] Zhang, X., Rice, M., Tworoger, S. S., Rosner, B. A., Eliassen, A. H., Tamimi, R. M., Joshi, A. D., Lindstrom, S., Qian, J., Colditz, G. A., Willett, W. C., Kraft, P., and Hankinson, S. E. (2018). Addition of a polygenic risk score, mammographic density, and endogenous hormones to existing breast cancer risk prediction models: A nested casecontrol study. *PLoS Medicine*, 15(9).

[306] Zheng, J., Koblinski, J. E., Dutson, L. V., Feeney, Y. B., and Clevenger, C. V. (2008). Prolyl isomerase cyclophilin A regulation of Janus-activated kinase 2 and the progression of human breast cancer. *Cancer Research*, 68(19):7769–7778.

[307] Zheng, Y., Comaills, V., Burr, R., Boulay, G., Miyamoto, D. T., Wittner, B. S., Emmons, E., Sil, S., Koulopoulos, M. W., Broderick, K. T., Tai, E., Rengarajan, S., Kulkarni, A. S., Shioda, T., Wu, C. L., Ramaswamy, S., Ting, D. T., Toner, M., Rivera, M. N., Maheswaran, S., and Haber, D. A. (2019). COX-2 mediates tumor-stromal prolactin signaling to initiate tumorigenesis. *Proceedings of the National Academy of Sciences of the United States of America*, 116(12):5223–5232.

[308] Zhu, L., Pan, R., Zhou, D., Ye, G., and Tan, W. (2019). BCL11A enhances stemness and promotes progression by activating Wnt/β-catenin signaling in breast cancer. *Cancer Management and Research*, 11:2997–3007.

[309] Zhu, N., Zhang, J., Du, Y., Qin, X., Miao, R., Nan, J., Chen, X., Sun, J., Zhao, R., Zhang, X., Shi, L., Li, X., Lin, Y., Wei, W., Mao, A., Zhang, Z., Stark, G. R., Wang, Y., and Yang, J. (2020). Loss of ZIP facilitates JAK2-STAT3 activation in tamoxifen-resistant breast cancer. *Proceedings of the National Academy of Sciences*, page 201910278.

VITA

Jacqueline Marie Anne Grible was born in Akron, Ohio on December 10th, 1992. In 2011, she graduated from Archbishop Hoban High School in Akron, Ohio. In 2015 she graduate *cum laude* with a Bachelor of Science degree in Molecular Genetics, with Honors Research Distinction, from The Ohio State University in Columbus, Ohio. Her undergraduate research thesis titled *An investigation into the relationship between intracellular bacteria and Acanthamoeba spp.* assessed the symbiotic nature of the single-celled protist Acanthamoeba and its capacity to harbor intracellular pathogenic bacteria, in both the 2003-2005 Chicago Acanthamoeba keratitis outbreak as well as the 2013 Columbus Legionnaire's disease outbreak. This research was guided by Dr. Gregory Booton. She has presented her graduate research project at both regional and national conferences, and she was a recipient of the 2019 Phi Kappa Phi Susan E. Kennedy Scholarship. She currently lives in Richmond, Virginia, with her fiancé Dan and their dog Samwise (Sammy).